SSC-403

DESIGN GUIDE FOR MARINE APPLICATIONS OF COMPOSITES

This document has been approved
For public release and sale; its
Distribution is unlimited

SHIP STRUCTURE COMMITTEE
1997

December 1, 1997

DESIGN GUIDE FOR MARINE APPLICATIONS OF COMPOSITES

The evolution of composite material boat construction has created the need to evaluate the basic design tools that are used to create safe marine structures. During the 1960s, fiberglass boat building proliferated and with it came the rapid increase in boat ownership. Early fiber reinforced plastic (FRP) boat builders relied on "build and test" or empirical methods to guarantee that their hulls were strong enough for the intended service. Presently in this country, motor-yachts have been built up to 160 feet (49 meters) and minehunters up to 188 feet (57 meters). However, as materials and building practices improve, it is not unreasonable to consider composite construction for vessels up to 100 meters (approximately 330 feet) in length. Although, classification societies generally review FRP construction for vessels up to 200 feet in length, current domestic regulations limit commercial composite ships to 100 gross tons or 149 passengers, with the exception of larger fast ferries as allowed by the International Maritime Organization (IMO) High-Speed Craft Code.

The goal of this Design Guide is to familiarize the user with the methodology and information required to design safe marine composite structures. Emphasis is placed on concepts, methodology, and design equations. Reference sources that provide mathematical derivations for specific geometry and load cases are cited throughout the report. The Guide encourages the understanding of how a composite structure responds to loads in the marine environment.

ROBERT C. NORTH
Rear Admiral, U. S. Coast Guard
Chairman, Ship Structure Committee

1. Report No. SSC-403	2. Government Accession No. **PB98-111651**	3. Recipient's Catalog No.	
4. Title and Subtitle Design Guide for Marine Applications of Composites		5. Report Date November 1997	
		6. Performing Organization Code	
7. Author(s) Eric Greene		8. Performing Organization Report No. SR-1367	
9. Performing Organization Name and Address Eric Greene Associates, Inc. 86 River Drive Annapolis, MD 21403		10. Work Unit No. (TRAIS)	
		11. Contract or Grant No. DTCG23-94-C-E01010	
12. Sponsoring Agency Name and Address Ship Structure Committee C/O US Coast Guard 2100 Second Street, SW Washington, DC 20593		13. Type of Report and Period Covered Final Report	
		14. Sponsoring Agency Code **G-M**	
15. Supplementary Notes Sponsored by the Ship Structure Committee and its member agencies			

16. Abstract

The evolution of composite material boat construction has created the need to evaluate the basic design tools that are used to create safe marine structures. During the 1960s, fiberglass boat building proliferated and with it came the rapid increase in boat ownership. Early fiber reinforced plastic (FRP) boat builders relied on "build and test" or empirical methods to guarantee that their hulls were strong enough for the intended service. Presently in this country, motor-yachts have been built up to 160 feet (49 meters) and minehunters up to 188 feet (57 meters). However, as materials and building practices improve, it is not unreasonable to consider composite construction for vessels up to 100 meters (approximately 330 feet) in length. Although, classification societies generally review FRP construction for vessels up to 200 feet in length, current domestic regulations limit commercial composite ships to 100 gross tons or 149 passengers, with the exception of larger fast ferries as allowed by the International Maritime Organization (IMO) High-Speed Craft Code.

The goal of this Design Guide is to familiarize the user with the methodology and information required to design safe marine composite structures. Emphasis is placed on concepts, methodology, and design equations. Reference sources that provide mathematical derivations for specific geometry and load cases are cited throughout the report. The Guide encourages the understanding of how a composite structure responds to loads in the marine environment.

17. Key Words Fiberglass, Composites, Ship Design, Boat Design, Resin, Reinforcements, Core, Laminate, Sandwich Laminate		18. Distribution Statement Distribution Unlimited, Available From: National Technical Information Service U.S. Department of Commerce Springfield, VA 22151 Ph. (703) 487-4650	
19. Security Classif. (of this report) **Unclassified**	20. Security Classif. (of this page) **Unclassified**	21. No. of Pages **342**	22. Price PC - A16 MF - A03

CONVERSION FACTORS
(Approximate conversions to metric measures)

LENGTH			
inches	meters	divide	39.3701
inches	millimeters	multiply by	25.4000
feet	meters	divide by	3.2808
VOLUME			
cubic feet	cubic meters	divide by	35.3149
cubic inches	cubic meters	divide by	61,024
SECTION MODULUS			
inches^2 feet^2	centimeters^2 meters^2	multiply by	1.9665
inches^2 feet^2	centimeters^3	multiply by	196.6448
inches^4	centimeters^3	multiply by	16.3871
MOMENT OF INERTIA			
inches^2 feet^2	centimeters^2 meters	divide by	1.6684
inches^2 feet^2	centimeters^4	multiply by	5993.73
inches^4	centimeters^4	multiply by	41.623
FORCE OR MASS			
long tons	tonne	multiply by	1.0160
long tons	kilograms	multiply by	1016.047
pounds	tonnes	divide by	2204.62
pounds	kilograms	divide by	2.2046
pounds	Newtons	multiply by	4.4482
PRESSURE OR STRESS			
pounds/inch^2	Newtons/meter^2 (Pascals)	multiply by	6894.757
kilo pounds/inch^2	mega Newtons/meter^2 (mega Pascals)	multiply by	6.8947
BENDING OR TORQUE			
foot tons	meter tons	divide by	3.2291
foot pounds	kilogram meters	divide by	7.23285
foot pounds	Newton meters	multiply by	1.35582
ENERGY			
foot pounds	Joules	multiply by	1.355826
STRESS INTENSITY			
kilo pound/inch^2 inch$^{1/2}$(ksi$\surd$in)	mega Newton MNm$^{3/2}$	multiply by	1.0998
J-INTEGRAL			
kilo pound/inch	Joules/mm^2	multiply by	0.1753
kilo pound/inch	kilo Joules/m^2	multiply by	175.3
TEMPERATURE (exact)			
Degrees Fahrenheit	Degrees Celsius	subtract	32
		& multiply by	0.5555556

Table of Contents

Introduction

The evolution of composite material boat construction has created the need to evaluate the basic design tools that are used to create safe marine structures. As materials and building practices improve, it is not unreasonable to consider composite construction for vessels up to 100 meters (approx 330 feet). Although design principles for ship structures and composite materials used for aerospace structures are mature as individual disciplines, procedures for combining the technologies are at an infancy. This design guide will focus on methodologies to ensure that a composite material marine structure can withstand environmental loads and optimize a vessel's performance.

If a good naval architect is required to be a fine artist and a knowledgeable scientist, then composite marine construction requires a true da Vinci. First, one must know exactly how and where a vessel is going to be constructed if any conclusions are going to be made about the strength of the finished product. Fabrication variables heavily influence how a marine composite structure will perform. Next, it is essential to know loads and load paths throughout the structure. A knowledge of material science as it applies to available marine composite systems is also valuable. The marine composites designer must also have a mastery of proven analytical tools that will facilitate design optimization with confidence. Finally, the designer must be able to act as surveyor to ensure that laminate schedules and detail designs are executed as intended.

The Ship Structure Committee sponsored this Design Guide to specifically meet the needs of the marine industry. To achieve that goal, information on marine composite material systems, analysis principles, available design tools, and failure mechanisms has been assembled and presented as a comprehensive treatise for the designer. The reader is encouraged to seek more detail from references cited throughout the Guide. As the subject of the Guide is truly multidisciplinary, concepts, principles and methodologies will be stressed.

The Project Technical Committee has provided valuable input throughout the duration of the project. In particular, Dr. Robert Sielski, Bill Siekierka, CDR Stephen Sharpe, Elizabeth Weaver, Bill Hayden, Loc Nguyen, Dave Heller, Bill Lind and Ed Kadala have given insight into the design of marine composite structures based on their own experience. Art Wolfe and Dr. Ron Reichard of Structural Composites also contributed to the Guide.

Throughout this Guide, reference is made to specific brand names and products for clarification purposes. The Government does not endorse any of the companies or specific products mentioned. This report represents work supported under provisions of Contract DTCG23-94-C-E01010. This document is disseminated under the sponsorship of the U.S. Department of Transportation in the interest of information exchange. The authors, the United States Government and the Ship Structure Committee assume no liability for the contents or use thereof.

Background

The origins of composite material concepts date back to the builders of primitive mud and straw huts. Modern day composite materials were launched with phenolic resins at the turn of the century. The start of fiberglass boatbuilding began after World War II. The U.S. Navy built a class of 28-foot personnel craft just after the war based on the potential for reduced maintenance and production costs. [1]

During the 1960s, fiberglass boatbuilding proliferated and with it came the rapid increase in boat ownership. The mass appeal of lower cost hulls that required virtually no maintenance launched a new class of boaters in this country. Early FRP boatbuilders relied on "build and test" or empirical methods to guarantee that the hulls they were producing were strong enough. Because fiberglass was a relatively new boatbuilding material, designers tended to be conservative in the amount of material used. Illustrative of this was the ad-hoc testing of a hull laminate for the Block Island 40 yawl that involved repeatedly driving over a test panel with the designer, William Tripp's, family car. Note that in the late 1950s, automobiles were also a lot heavier than today's models.

In 1960, Owens-Corning Fiberglas Corporation sponsored the naval architecture firm, Gibbs & Cox to produce the ***"Marine Design Manual for Fiberglass Reinforced Plastics."*** This book, published by McGraw-Hill, was the first fiberglass design guide targeted directly at the boatbuilding industry.   Design and construction methods were detailed and laminate performance data for commonly used materials were presented in tabular form. The guide proved to be extremely useful for the materials and building techniques that were prevalent at the time.

As the aerospace industry embraced composites for airframe construction, analytical techniques developed for design. The value of composite aerospace structures warrants significant analysis and testing of proposed laminates. Unfortunately for the marine industry, aerospace laminates usually consist of carbon fiber and epoxy made from reinforcements pre-impregnated with resin (prepregs) that are cured in an autoclave. Costs and part size limitations make these systems impractical for the majority of marine structures. Airframe loads also differ from those found with maritime structures. However, in recent times, the two industries are coming closer together. High-end marine manufacturing is looking more to using prepregs, while aircraft manufacturers are looking to more cost-effective fabrication methods.

Marine designers have also relied on classification society rules such as Lloyd's, ABS, and DnV to develop scantlings for composite craft. Classification society rules are developed over a long period of time and have traditionally been based on "base" laminates and rules for developing required thicknesses. New materials and innovative construction methods often do not fit neatly into the design rules. The designer may often view a "rule" as a challenge, with the idea to build a structure as light as possible, while still meeting the rule requirements. This can lead to the abandonment of overall engineering judgment that takes into account how a vessel will be manufactured and used.

The proliferation of desktop computers has brought with it programs to assist the marine composites designer, including laminate analysis programs and finite element software. Very detailed predictions of laminate stiffness and strength are output from these programs. In

practice, the stiffness predictions have been easier to verify. One must also consider the following uncertainties when relying on sophisticated computer design tools:

- limited amount physical property data

- unknown input loads and "end conditions"

- fabrication variability

In recent years, a very valuable source for design guidance has been specialized conferences and courses. Composites oriented conferences, such as those sponsored by the Society of the Plastics Industry (SPI) and the Society for the Advancement of Materials Processing and Engineering (SAMPE), have over the years had a few marine industry papers presented at their annual meetings. Ship design societies, such as the Society of Naval Architects and Marine Engineers (SNAME) and the American Society of Naval Engineers (ASNE) also occasionally address composite construction issues in their conferences and publications, Indeed ASNE devoted an entire conference to the subject in the Fall of 1993 in Savannah. SNAME has an active technical committee, HS-9, that is involved with composite materials. The Composites Education Association, in Melbourne, Florida hosts a biennial conference called Marine Applications of Composite Materials (MACM). The five MACM conferences to date have featured technical presentations specific to the marine composites industry.

Robert J. Scott, of Gibbs & Cox, has prepared course notes for the University of Michigan based on his book, *"Fiberglass Boat Design and Construction,"* published in 1973 by John deGraff. An update of that book is now available through SNAME. In 1990, the Ship Structure Committee published SSC-360, *"Use of Fiber Reinforced Plastics in the Marine Industry"* by the author of this publication. That report serves as a compendium of materials and construction practices through the late 1980s. In the United Kingdom, Elsevier Science Publishers released the late C.S. Smith's work, *"Design of Marine Structures in Composite Materials."* This volume provides an excellent summary of Smith's lifelong work for the British Ministry of Defence with much treatment of hat-stiffened, composite panels.

Relevant information can also be found scattered among professional journals, such as those produced by SNAME, ASNE, the Composite Fabricators Association (CFA), SAMPE and industry publications, such as *Composites Technology*, *Composite Design & Application* and *Reinforced Plastics*, *Professional Boatbuilder* magazine, which is emerging as the focal point for technical issues related to the marine composites field.

Application

Builders continue to push the size limits for FRP craft. Motoryachts have been built up to 160 feet (49 meters) and minehunters to 188 feet (57 meters) in this country. It is not unreasonable to consider building small ships with composites. Classification societies generally consider FRP construction to 200 feet, although larger fast ferries being considered in Scandinavia would make use of advanced composite materials, as allowed by the International Maritime Organization (IMO) High-Speed Craft Code. Current domestic regulations limit commercial, composite ships to 100 gross tons or 149 passengers.

On the lower end of the scale, small recreational boats increasingly rely on rational design to produce optimized structures. Production builders can reduce material and labor costs when the loads and resultant laminate stresses are known. This is particularly true as speeds for recreational craft increase.

Design principles presented will generally apply to boats built using one-off methods, as well as production craft. Although the selection of materials may vary with differing approaches to construction, the underlying loads and structural response will be similar. However, different materials and building techniques do require unique focus on various design aspects. Both solid and sandwich laminates are covered, as are traditional and "exotic" materials.

This Guide is also designed to serve the needs of both recreational and commercial boat builders and designers. Although both types of vessels are being built with an increasing eye towards cost conservation, commercial applications impose harsher service requirements, while cosmetics may not be as important. Recent market trends have produced a demand for yachts that look like trawlers or lobster boats and law enforcement craft that resemble high-speed "fun" boats, so the distinction between commercial and recreational is diminishing somewhat.

The Guide should also serve as a resource for designing military vessels. However, specific requirements associated with combat conditions, such as shock and nuclear air blast, are not addressed here.

The Guide is not intended to be a "how-to" book on boatbuilding with composite materials. These step-by-step mechanics are covered well by other texts, periodicals and material supplier technical notes. Instead, the Guide will provide individuals with a basic understanding of forces that act on a composite marine structure and how that structure responds.

Scope

The goal of this Design Guide is to familiarize the reader with methodology and information required to design safe marine composite structures. Emphasis is placed on concepts, methodology and design equations. Reference sources that provide mathematical derivations for specific geometries and load cases are cited throughout the text. Here, the reader is encouraged to develop an understanding of how a composite structure responds to loads in the marine environment. The Guide is organized into the following sections:

- design methodology for composite material boats/ships

- materials used in marine construction

- loads that influence the design of a composite boat/ship

- micromechanics of marine resin/reinforcement systems

- macromechanics of marine panels and structures

- failure modes of marine composite structures

The Design Guide will not cover in detail methods used for Finite Element Analysis (FEA) of marine structures built with composite materials. Several FEA programs are specifically tailored towards composite materials and a few are written primarily to analyze marine structures. As will be shown in the Guide, many uncertainties exist with load conditions, boundary conditions and the variability in laminate material performance. Therefore, an analyst must first understand the materials, loads and structures associated with marine composites before attempting any finite element modeling.

Chapter One - Design Methodology

Optimization of a ship or even a boat structure is a complex task involving various different parameters. Evans proposed the design spiral shown in Figure 1-1 to visualize the process of refining a ship structural design. Shown here is a diagram for the midship section of a longitudinally-spaced steel ship. Note that stiffener spacing; panel and stiffener sizing; weight; and overall bending moment are calculated in an iterative fashion with interlocking constraints that force a solution satisfying each requirement. The example given is for a specific portion (albeit midship section) of a steel vessel. When we add the variable of material properties and the directional behavior of composites, the design process can indeed get quite complex. Add to this the fact that most composite ships are smaller than steel ships, which in turn means a smaller design budget, and the marine composites designer appears to be faced with a formidable task.
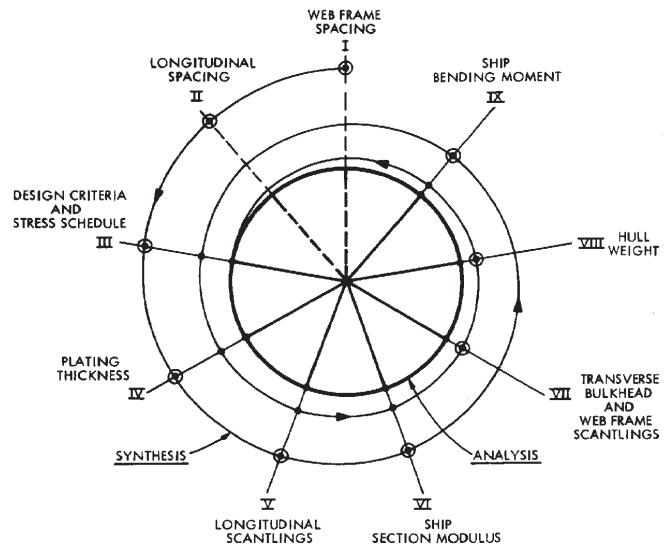
Figure 1-1 Midship Section Structural Design Diagram for Longitudinally Framed Ship [Evans, SSC project SR-200]

The pioneering yacht designer Gary Mull warned in an article titled "Modern Composites in Marine Structures," that:

> "In times gone by, working with traditional materials and on designs less demanding of the last tiny fraction of performance, rules of thumb for structures seldom caused much grief. In those forgiving days, what looked right may not have been right, but it was probably good enough. The apprentice system guaranteed that before a person was given responsibility for designing a frame, he probably had cut, shaped, and fitted hundreds of frames. Today, a desktop PC and a handful of floppy disks quite often confers, at least in the mind of the operator, the notion that an education in engineering is a mere inconvenience which may be avoided in favor of suitable software."

In an effort to avoid the above noted pitfall, some design diagrams for composite marine structures are presented to illustrate design methodology and the "flow" of an evolutionary design process. Depending upon the overriding driving design parameter for a specific project (i.e. cost, weight, durability, etc.), various "branches" of the design path will receive added attention.

Composite Material Concepts

The marine industry has been saturated with the concept that we can build stronger and lighter vehicles through the use of composite materials. This may be true, but only if the designer fully understands how these materials behave. Without this understanding, material systems cannot be optimized and indeed can lead to premature failures. Wood construction requires an understanding of timber properties and joining techniques. Metal construction also involves an understanding of material specific properties and a knowledge of weld geometry and techniques. Composite construction introduces a myriad of new material choices and process variables. This gives the designer more design latitude and avenues for optimization. With this opportunity comes the greater potential for improper design.

Early fiberglass boats featured single-skin construction in laminates that contained a high percentage of resin. Because these laminates were not as strong as those built today and because builders' experience base was limited, laminates tended to be very thick, made from numerous plies of fiberglass reinforcement. These structures were nearly isotropic (properties similar in all directions parallel to the skin) and were very forgiving. In most cases, boats were overbuilt from a strength perspective to minimize deflections. With the emergence of sandwich laminates featuring thinner skins, the need to understand the structural response of laminates and failure mechanisms has increased.

Reinforcement and Matrix Behavior

The broadest definition of a composite material describes filamentary reinforcements supported in a matrix that starts as a liquid and ends up a solid via some cure process. The reinforcement is designed to resist the primary loads that act on the laminate and the resin serves to transmit loads between the plies, primarily via shear. In compression loading scenarios, the resin can serve to "stabilize" the fibers for in-plane loads and transmit loads via direct compression for out-of-plane loads.

Mechanical properties for dry reinforcements and resin systems differ greatly. As an example, E-glass typically has a tensile strength of 500×10^3 psi (3.45 Gpa) and an ultimate elongation of 4.8%. An iso polyester resin typically has a tensile strength of 10×10^3 psi (69 Mpa) and an ultimate elongation of 2%. As laminates are stressed near their ultimate limits, resin systems generally fail first. The designer is thus required the ensure that a sufficient amount of reinforcement is in place to limit overall laminate stress. Contrast this to a steel structure, which may have a tensile yield strength of 70×10^3 psi (0.48 Gpa), an ultimate elongation of 20% and stiffnesses that are an order of magnitude greater that "conventional" composite laminates.

Critical to laminate performance is the bond between fibers and resin, as this is the primary shear stress transfer mechanism. Mechanical and chemical bonds transmit these loads. Resin formulation, reinforcement sizing, processing techniques and laminate void content influence the strength of this bond.

Directional Properties

With the exception of chopped strand mat, reinforcements used in marine composite construction utilize bundles of fibers oriented in distinct directions. Whether the reinforcements are aligned in a single direction or a combination thereof, the strength of the laminate will vary depending on the direction of the applied force. When forces do not align directly with reinforcement fibers, it is necessary for the resin system to transmit a portion of the load.

"Balanced" laminates have a proportion of fibers in 0° and 90° directions. Some newer reinforcement products include ±45° fibers. Triaxial knits have ±45°

Figure 1-2 Comparison of Various Fiber Architectures Using the Hydromat Panel Tester on 3:1 Aspect Ratio Panels [Knytex]

fibers, plus either 0° or 90° fibers. Quadraxial knits have fibers in all four directions. Figure 1-2 illustrates the response of panels made with various knit fabrics subjected to out-of-plane loading.

Design and Performance Comparison with Metallic Structures

A marine designer with experience using steel or aluminum for hull structure will immediately notice that most composite materials have lower strength and stiffness values than the metal alloys used in shipbuilding. Values for strength are typically reported as a function of cross sectional area (ksi or Gpa). Because composite materials are much lighter than metals, thicker plating can be used. Figure 1-3 illustrates a comparison of specific strengths and stiffnesses (normalized for density) for selected structural materials. Because thicker panels are used for composite construction, panel stiffness can match or exceed that of metal hulls. Indeed, frame spacing for composite vessels is often much greater. For a given strength, composite panels may be quite a bit more flexible, which can lead to in-service deflections that are larger than for metal hulls.

The above discussion pertains to panel behavior when resisting hydrostatic and wave slamming loads. If the structure of a large ship in examined, then consideration must be given to the overall hull girder bending stiffness. Because structural material cannot be located farther from the neutral axis (as is the case with thicker panels), the overall stiffness of large ships is limited when quasi-isotropic laminates are used. This has led to concern about main propulsion machinery alignment when considering construction of FRP ships over 300 feet (91 meters)in length. With smaller, high performance vessels, such as racing sailboats, longitudinal stiffness is obtained through the use of longitudinal stringers, 0° unidirectional reinforcements, or high modulus materials, such as carbon fiber.

Damage and failure modes for composites also differ from metals. Whereas a metal grillage will transition from elastic to plastic behavior and collapse in its entirety, composite panels will fail one ply at a time, causing a change in strength and stiffness, leading up to a catastrophic failure. This would be preceded by warning cracks at ply failure points. Crack propagation associated with metals typically does not occur with composites. Interlaminar failures between successive plies is much more common. This scenario has a much better chance of preserving watertight integrity.

Because composite laminates do not exhibit the classic elastic to plastic stress-strain behavior that metals do, safety factors based on ultimate strength are generally higher, especially for compressive failure modes. Properly designed composite structures see very low stress levels in service, which in turn should provide a good safety margin for extreme loading cases.

Figure 1-3 Specific Strength and Stiffness of Various Construction Material [DuPont]

Many design and performance factors make direct comparison between composites and metals difficult. However, it is instructive to compare some physical properties of common shipbuilding materials. Table 1-1 provides a summary of some constituent material characteristics.
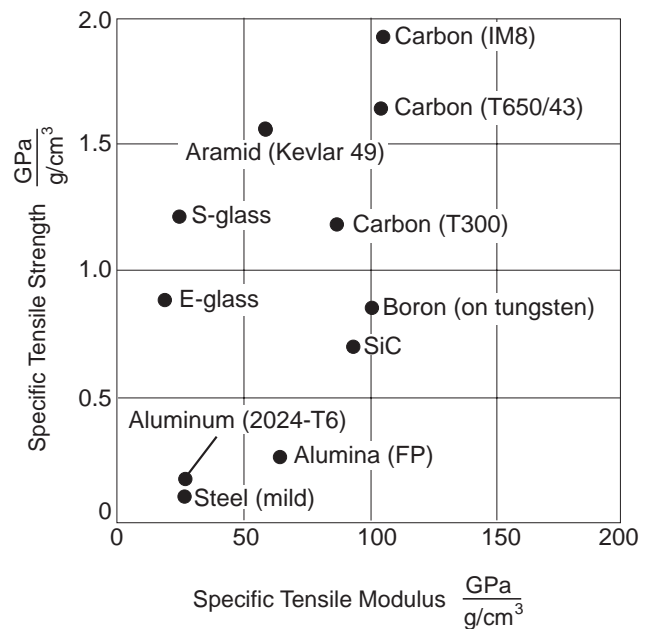
Finite Element Analysis of Marine Composite Structures

The application of FEM techniques to marine composite structures requires the same diligence needed for analysis of steel ships. Care should be given to the selection of element type (shell vs. solid) and definition of the boundary conditions assumed in the analysis. Composite materials do require extra care when specifying material properties for the model. SSC 1364, *Guide for the Evaluation of FEMs and Results*, provides the following material property check list (also see Chapter Four - Micromechanics):

- Are all materials of structural importance to the problem accounted for in the engineering model?

- Are the assumed behaviors valid for each material (e.g.. linear elastic, isotropic, anisotropic, orthotropic)?

- Are the required material parameters defined for the type of analysis (e.g. E, , νetc.)?

- Are orthotropic and/or layered properties defined correctly for non-isotropic materials?

- Are orthotropic properties defined correctly where material orthotropy is used to simulate structural orthotropy (e.g.. stiffened panels)?

- If strain rate effects are expected to be significant for this problem, are they accounted for in the material property data?

- Are the values used for material property data traceable to an acceptable source?

Table 1-1 Overview of Shipbuilding Construction Materials

Material		Density		Tensile Strength		Tensile Modulus		Ultimate Elongation	1995 Cost
		lbs/ft^3	gm/cm^3	psi x 10^3	Mpa	psi x 10^6	Gpa	%	$/lb
Resins	Orthophthalic Polyester	76.7	1.23	7	48.3	.59	4.07	1	1.05
	Isophthalic Polyester	75.5	1.21	10.3	71.1	.57	3.90	2	1.19
	Vinyl Ester	69.9	1.12	11-12	76-83	.49	3.38	4-5	1.74
	Epoxy (Gougen Proset)	74.9	1.20	7-11	48-76	.53	3.66	5-6	3.90
	Phenolic	71.8	1.15	5.1	35.2	.53	3.66	2	1.10
Fibers	E-Glass (24 oz WR)	162.4	2.60	500	3450	10.5	72.45	4.8	1.14
	S- Glass	155.5	2.49	665	4589	12.6	86.94	5.7	5.00
	Kevlar® 49	90	1.44	525	3623	18	124.2	2.9	20.00
	Carbon-PAN	109.7	1.76	350-700	2415-4830	33-57	227-393	0.38-2.0	12.00
Cores	End Grain Balsa	7	0.11	1.320	9.11	.370	2.55	n/a	3.70
	Linear PVC (Airex R62.80)	5-6	.08-.1	0.200	1.38	0.0092	0.06	30	5.20
	Cross-Linked PVC (Diab H-100)	6	0.10	0.450	3.11	0.0174	0.12	n/a	5.95
	Honeycomb (Nomex® HRH-78)	6	0.10	n/a	n/a	0.0600	0.41	n/a	13.25
	Honeycomb (Nidaplast H8PP)	4.8	0.08	n/a	n/a	n/a	n/a	n/a	.80
Laminates	Solid Glass/Polyester *hand lay-up*	96	1.54	20	138	1.4	9.66	n/a	2.50
	Glass/Polyester Balsa Sandwich *vacuum assist*	24	0.38	6	41	0.4	2.76	n/a	4.00
	Glass/Vinyl Ester PVC Sandwich *SCRIMP®*	18	0.29	6	41	0.4	2.76	n/a	5.00
	Solid Carbon/Epoxy *filament wound*	97	1.55	88	607	8.7	60	n/a	10.00
	Carbon/Epoxy Nomex Sandwich *prepreg*	9	0.14	9	62	0.5	3.45	n/a	20.00
Metals	ABS Grd A (ASTM 131)	490.7	7.86	58	400	29.6	204	21	0.29
	ABS Grd AH (ASTM A242)	490.7	7.86	71	490	29.6	204	19	0.34
	Aluminum (6061-T6)	169.3	2.71	45	310	10.0	69	10	2.86
	Aluminum (5086-H34)	165.9	2.66	44	304	10.0	69	9	1.65
Wood	Douglas Fir	24.4	0.39	13.1	90	1.95	13.46	n/a	1.97
	White Oak	39.3	0.63	14.7	101	1.78	12.28	n/a	1.07
	Western Red Cedar	21.2	0.34	7.5	52	1.11	7.66	n/a	2.26
	Sitka Spruce	21.2	0.34	13.0	90	1.57	10.83	n/a	4.48

Note: The values used in this table are for illustration only and should not be used for design purposes. In general, strength is defined as yield strength and modulus will refer to the material's initial modulus. A core thickness of 1" with appropriate skins was assumed for the sandwich laminates listed.

Design Process for Composite Marine Structures

The process for designing marine structures that are to be built with composite materials is unique because of the range of available materials and fabrication methods. Some basic concepts follow good naval architecture procedure, such as initial definition of loads. The remainder of the design process is very interrelated, and does not always flow in a linear fashion. As an example, the selection of an analytical design tool is very dependent on the amount and quality of material property data. Additionally, design optimization is very dependent on fabrication and cost considerations. Because composite materials and fabrication techniques continue to evolve at a rapid pace, there will always be "information gaps" that confront the designer. A prudent approach recognizes the limit of our knowledge and ability to predict performance, while at the same time exploiting emerging design tools and the benefit of four decades of successful fiberglass boat construction.

Definition of Loads and Requirements

Hull structure loading is typically referred to as primary, secondary and tertiary, as noted in Figure 1-4. The magnitude or importance of each load does not necessarily follow this notational hierarchy. Instead, the terms can be thought of as "global," "regional," and "local." Some designers will also add the category called "emergency loads," which don't occur during "normal" vessel operations. Although it is critical to calculate or estimate the magnitude of structural loads, the time history and frequency of the expected load condition must also be considered.
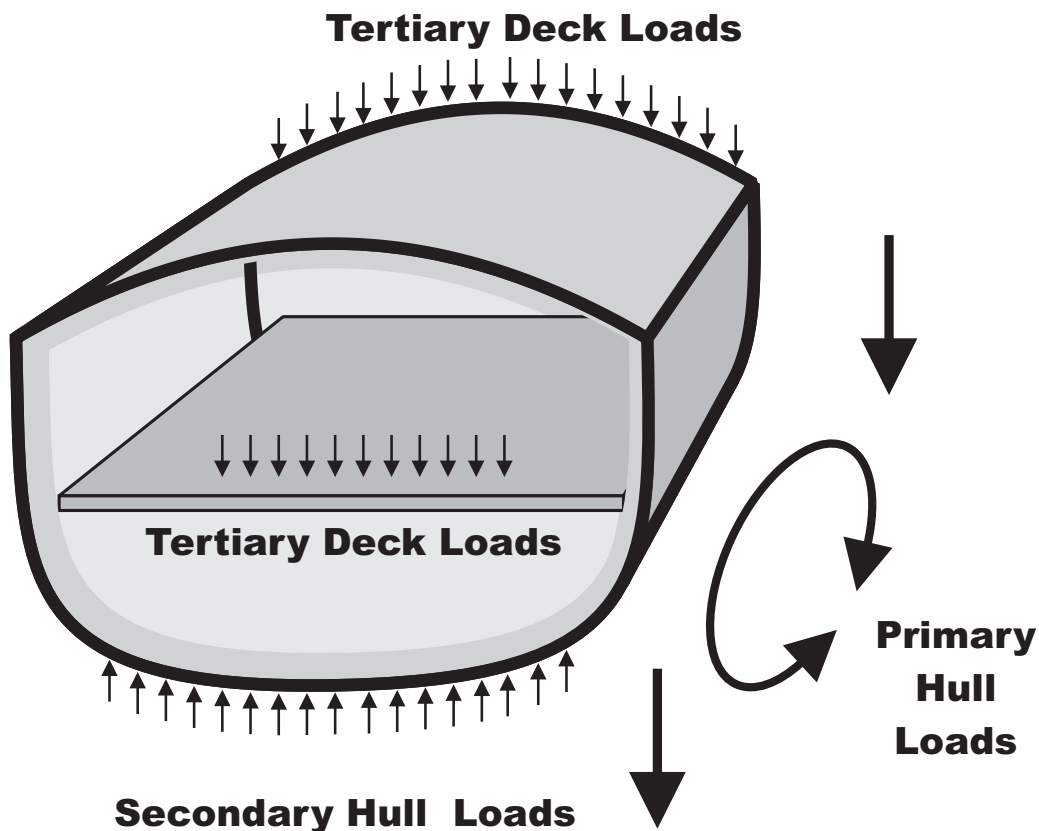
Figure 1-4 Overview of Primary (Overall Hull Bending), Secondary (Hydrostatic and Hydrodynamic Forces Normal to Hull Surface) and Tertiary (Local Forces) Loads

Material Properties and Design Allowables

Although it is often difficult to predict the loads that will act on a structure in the marine environment, it is equally difficult to establish material property data and design allowables that will lead to a well engineered structure. It is first important to note that property data for a reinforcement as presented in Figure 1-5, may apply only to fibers. Designers always need to use data on laminates, which include fibers and resin manufactured in a fashion similar to the final product.

The aerospace design community typically has material property data for unidirectional reinforcements according to the notation in Figure 1-5. Because of extreme safety and weight considerations, the aerospace industry has made considerable investment to characterize relevant composite materials for

Figure 1-5 Notation Typically Used to Describe Properties of Unidirectional Reinforcements

analytical evaluation. Unfortunately, these materials are typically carbon/epoxy prepregs, which are seldom used in marine construction. The best that a marine designer can expect is primary plane (1-2) data. Most available test data is in the primary or "1" axis direction. The type of data that exists, in decreasing order of reliability is: Tensile, Flexural, Compressive, Shear, Poisson's Ratio.

Test data is difficult to get for compression and shear properties because of problems with test fixtures and laminate geometries. Data that is generated usually shows quite a bit of scatter. This must be kept in mind when applying safety factors or when developing design allowable physical property data.

It should be noted that stiffness data or modulus of elasticity values are more repeatable than strength values. As many composite material design problems are governed by deflection rather than stress limits, strength criteria and published material properties should be used with caution.

The type of loading and anticipated type of failure generally determines which safety factors are applied to data derived from laboratory testing of prototype laminates. If the loading and part geometry are such that long term static or fatigue loads can produce a dynamic failure in the structure, a safety factor of 4.0 is generally applied. If loading is transient, such as with slamming, or the geometry is such that gradual failure would occur, then a safety factor of 2.0 is applied. With once-in-a-lifetime occurrences, such as underwater explosions for military vessels, a safety factor of 1.5 is generally applied. Other laminate performance factors, such as moisture, fatigue, impact and the effect of holes influence decisions on design allowables.
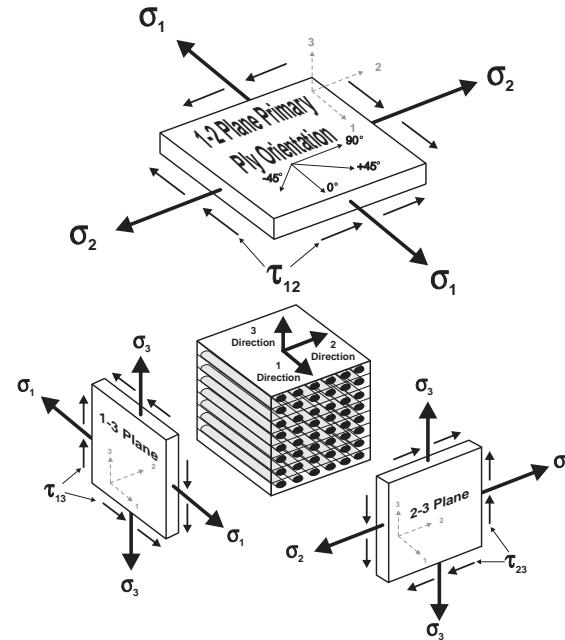
Analytical Tool Selection

The marine composites designer has a number of design tools available that can provide key "pieces" to the design puzzle. After loads are defined, the designer must then choose a specific methodology for predicting the response of a composite material structural system. Different design tools are usually used for modeling structures with varying degrees of detail or complexity. Popular laminate analysis programs work well to define the behavior of composite material beams. These programs are based on laminate plate theory, which assumes that panel spans are much greater than panel thicknesses and that through-thickness shear is linear. Developed surfaces more complicated than panels with curvature are generally modeled with FEA methods. Classification society rules, such as those published by the American Bureau of Shipping, serve well to specify minimum scantlings for major structural elements. The designer is required to understand loads and material behavior in order to perform detail design and design optimization.

Develop Structural Concept

Composite marine vessels are generally constructed using one of the following design concepts:

- Monocoque single-skin construction
- Single-skin construction using bulkheads and stringers
- Monocoque sandwich construction
- Sandwich construction using bulkheads and stringers

Monocoque single-skin construction creates panel structures that span across the turn in the bilge to the hull-to-deck joint and extend from bow to stern. Very thick skins are required to make this construction method feasible for anything but the smallest vessels (canoes). Interestingly enough, the Osprey class minehunter design is also monocoque, because shock criteria drives the scantling development for this class. Single-skin construction is more often combined with a system of bulkheads and stringers to limit the effective panel spans, and thus reduce the laminate strength and stiffness necessary. An example of monocoque sandwich construction is the America's Cup yacht, which have thin, stiff skins on relatively thick cores. These sandwich laminates can resist loads over large spans, while at the same time possess sufficient overall longitudinal stiffness contribution to alleviate the need for added longitudinal stiffeners. Sandwich construction that makes use of bulkheads and stringers permits the use of softer skin and core materials. Panel spans are reduced as with single-skin construction, although stiffener spacing is typically much greater because the thick sandwich laminate have inherently higher moments of inertia. Figure 1-6 illustrates a comparison of relative strengths and stiffnesses for solid and sandwich panels of equal weight.

Design Optimization Through Material Selection

Composite materials afford the opportunity for optimization through combinations of reinforcements, resins, and cores. Engineering optimization always involves tradeoffs among performance variables. Table 1-2 is provided to give an overview of how constituent materials rank against their peers, on a qualitative basis. Combinations of reinforcement, resin and core systems may produce laminates that can either enhance or degrade constituent material properties.
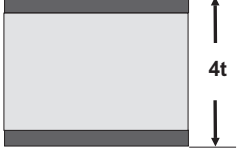
		2t	4t
Relative Stiffness	100	700	3700
Relative Strength	100	350	925
Relative Weight	100	103	106

Figure 1-6 Strength and Stiffness for Cored and Solid Construction [Hexcel, The Basics on Sandwich Construction]

Table 1-2 Qualitative Assessment of Constituent Material Properties

	Fiber			Resin					Core					
	E-Glass	Kevlar	Carbon	Polyester	Vinyl Ester	Epoxy	Phenolic	Thermoplastic	Balsa	Cross Link PVC	Linear PVC	Nomex/Alum Honeycomb	Thermoplastic Honeycomb	Syntactic Foam
Static Tensile Strength	□	■	□	□	□	■	□	□	■	■	■	□	□	□
Static Tensile Stiffness	□	■	■	□	□	□	□	□	■	□	□	■	□	□
Static Compressive Strength	■	□	□	□	□	□	□	□	■	□	■	■	□	□
Static Compressive Stiffness	□	□	■	□	□	□	□	□	■	□	□	■	□	□
Fatigue Performance	□	■	□	□	■	■	□	■	□	□	■	□	■	□
Impact Performance	■	■	□	□	■	■	□	■	□	■	■	□	□	□
Water Resistance	■	□	□	□	■	■	□	■	□	■	■	□	□	□
Fire Resistance	■	□	□	□	□	□	■	□	■	□	□	■	□	■
Workability	■	□	□	□	□	□	□	□	■	□	□	□	□	□
Cost	■	□	□	■	□	□	□	■	■	□	□	□	■	■

■ Good Performance
□ Poor Performance

Cost and Fabrication

Material and production costs for composite marine construction are closely related. Typically, the higher cost materials will require higher-skilled labor and more sophisticated production facilities. The cost of materials will of course vary with market factors.

Material Costs

Table 1-1 provides an overview of material costs associated with marine composite construction. It is difficult to compare composite material cost with conventional homogeneous shipbuilding materials, such as wood or metals, on a pound-for-pound basis. Typically, an optimized structure made with composites will weigh less than a metallic structure, especially if sandwich techniques are used. Data in Table 1-1 is provided to show designers the relative costs for "common" versus "exotic" composite shipbuilding materials.

Production Costs

Production costs will vary greatly with the type of vessel constructed, production quantities and shipyard efficiency. Table 1-3 is compiled from several sources to provide designers with some data for performing preliminary labor cost estimates.

Table 1-3 Marine Composite Construction Productivity Rates

Source	Type of Construction	Application	Lbs/Hour*	Ft²/Hour†	Hours/Ft²‡
Scott Fiberglass Boat Construction	Single Skin with Frames	Recreational	20*	33†	.03‡
		Military	12*	20†	.05‡
	Sandwich Construction	Recreational	10*	17†	.06‡
		Military	6*	10†	.10‡
BLA Combatant Feasibility Study	Single Skin with Frames	Flat panel (Hull)	13**	22**	.05**
		Stiffeners & Frames	5**	9**	.12**
	Core Preparation for Sandwich Construction	Flat panel (Hull)	26**	43**	.02**
		Stiffeners	26**	43**	.02**
	Vacuum Assisted Resin Transfer Molding (VARTM)	Flat panel (Hull)	10§	43§	.02§
		Stiffeners	7§	14§	.07§
	* Based on mat/woven roving laminate ** Based on one WR or UD layer † Single ply of mat/woven roving laminate ‡ Time to laminate one ply of mat/woven roving (reciprocal of Ft²/hr) § Finished single ply based on weight of moderately thick single-skin laminate					

Design Flow Charts for Representative Ship Structures

The following design flow charts are presented to guide the designer through the thought process required to develop sound marine composite laminates. The charts are intended to be conceptual and reflect the methodologies employed by the author. Indeed, there exist numerous other approaches that will produce safe structures and the reader is encouraged to develop methodologies specific to the design problem. Some points common to all the charts include consideration of both materials and structural requirements; stiffness and strength criteria; and cost, cosmetic and manufacturing considerations.

Primary Hull Laminate

The primary hull laminate describes the basic laminate developed to satisfy the design requirements specific to a given project. Development of the primary hull laminate should occur during the first iteration of the design cycle. The flow chart starts with an assessment of how hulls will be constructed and prioritization of design goals. Two consecutive design cycles are illustrated in the chart.
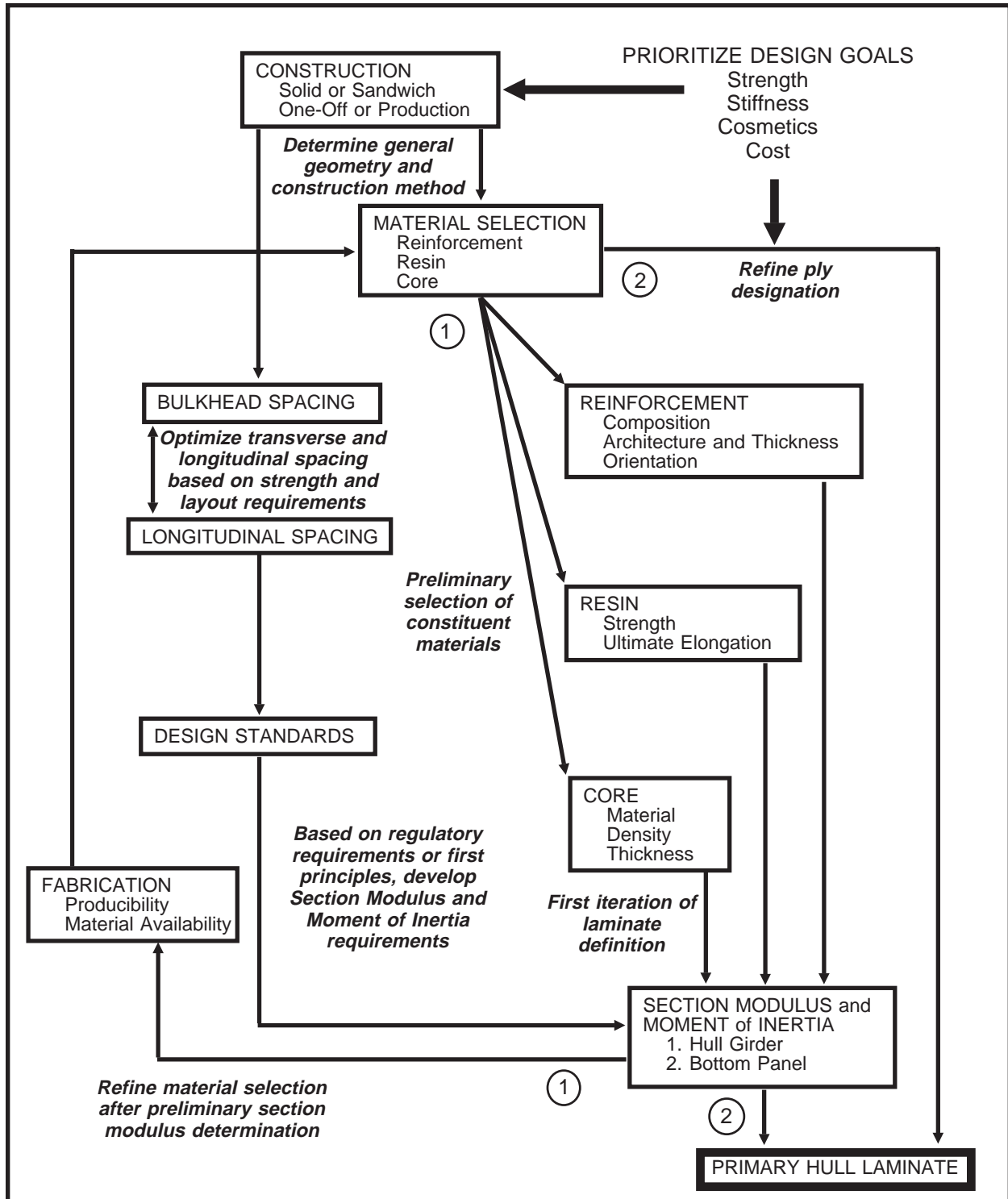
Figure 1-7   Design Flow Chart for Primary Hull Laminate

Bottom Panels Subject to Slamming

Although a bottom panel subject to slamming often dictates the primary laminate, it deserves special attention because of the dynamic nature of loading. The critical aspect of bottom panel laminate development is the determination of design pressures. Material selection, fiber architecture and orientation and shear stress continuity are critical, as dynamic properties of laminates often vary greatly from static test values.
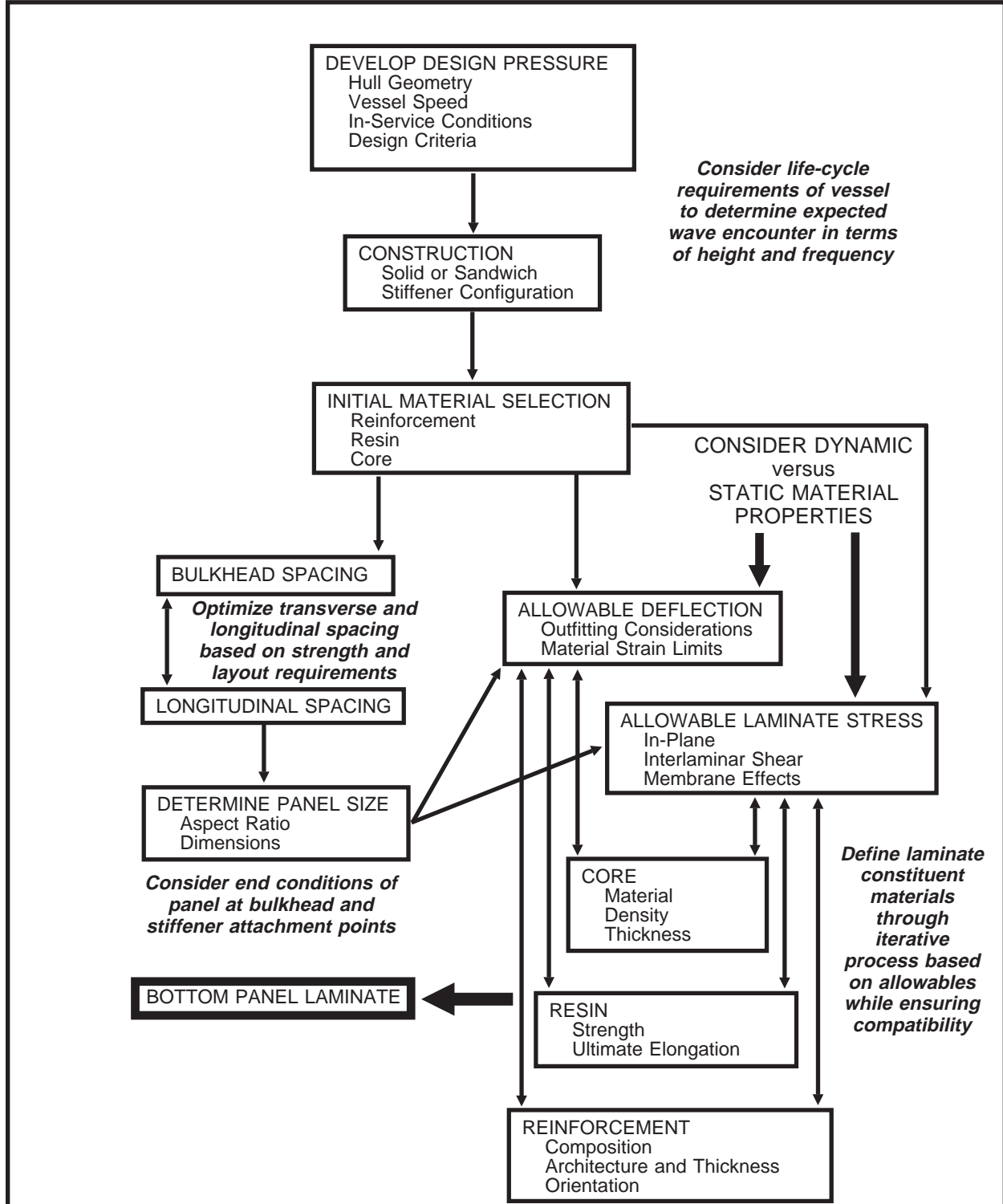
Figure 1-8   Design Flow Chart for Bottom Panels Subject to Slamming

Decks

Development of deck laminates also involves unique considerations. Decks often have numerous openings and require the mounting of hardware. Static stiffness requirements and arrangement considerations can often drive laminate specifications.
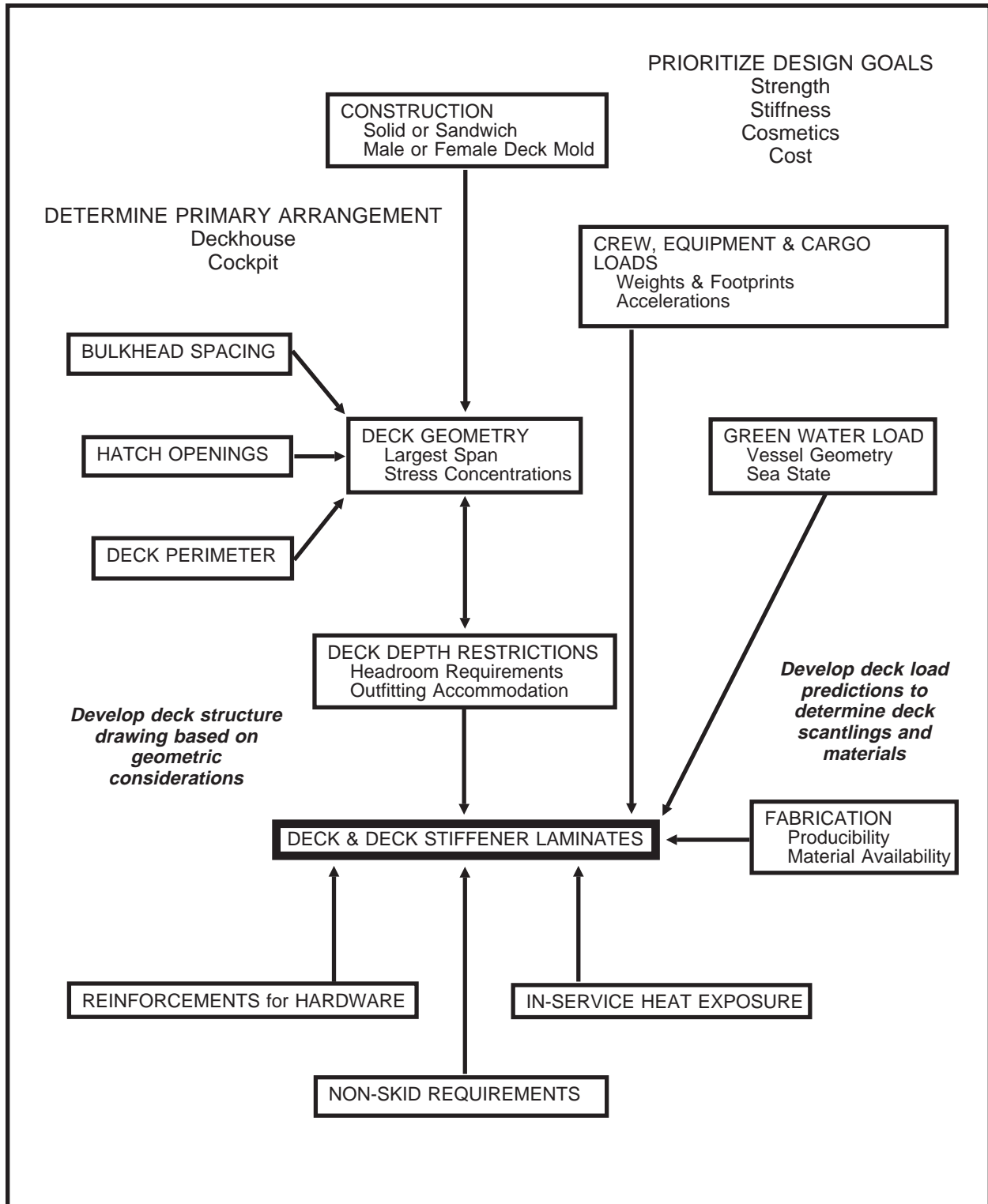
Figure 1-9   Design Flow Chart for Decks

Deckhouses

Design of deckhouse structure can be complicated by styling requirements that can produce geometric shapes that are not inherently strong. As with decks, deckhouses may have numerous openings and can be subjected to extreme thermal loads.
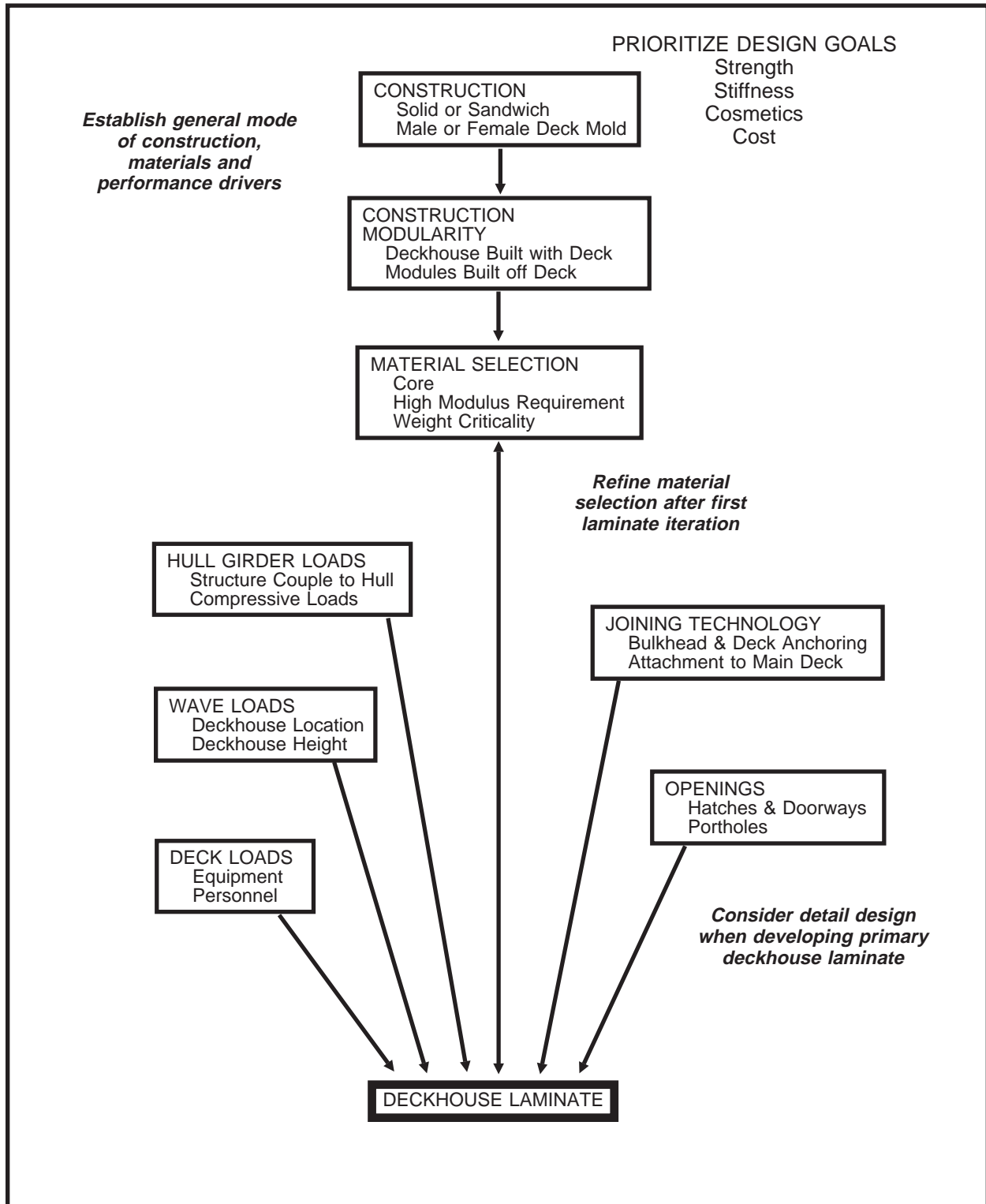
Figure 1-10   Design Flow Chart for Deckhouses

Bulkheads

The design of bulkheads is fairly straightforward, with primary compressive loads from decks and out-of-plane loads from flooding for watertight bulkheads. Particular attention must be paid to hull and deck attachment details.

PRIORITIZE DESIGN GOALS
Strength
Stiffness
Cosmetics
Cost

PRIMARY DESIGN CRITERIA
Out-of-Plane Loading
Compression

CONSTRUCTION
Solid or Sandwich
Prefab or In-Place

COMPARTMENT FLOODING
Design Head
Failure Criteria & Safety Factor

ATTACHMENT TO HULL & DECK
Tape-In Detail
Detail at Longitudinal Intersection

HULL STIFFENER
Panel Strength Contribution
Compression Failure

CONSTRUCTION
CONSIDERATIONS

BULKHEAD LAMINATE

PRIMARY
and
SECONDARY
FUNCTIONAL
REQUIREMENTS

PENETRATIONS
Doorways
HVAC, Plumbing & Electrical

COSMETIC REQUIREMENTS
Veneer Treatment
Paint

Figure 1-11 Design Flow Chart for Bulkheads

Stringers

Stringer or stiffener design is determined very much by geometry, as well as laminate schedule. Care must be given to fiber placement and orientation, as well as attachment detail.
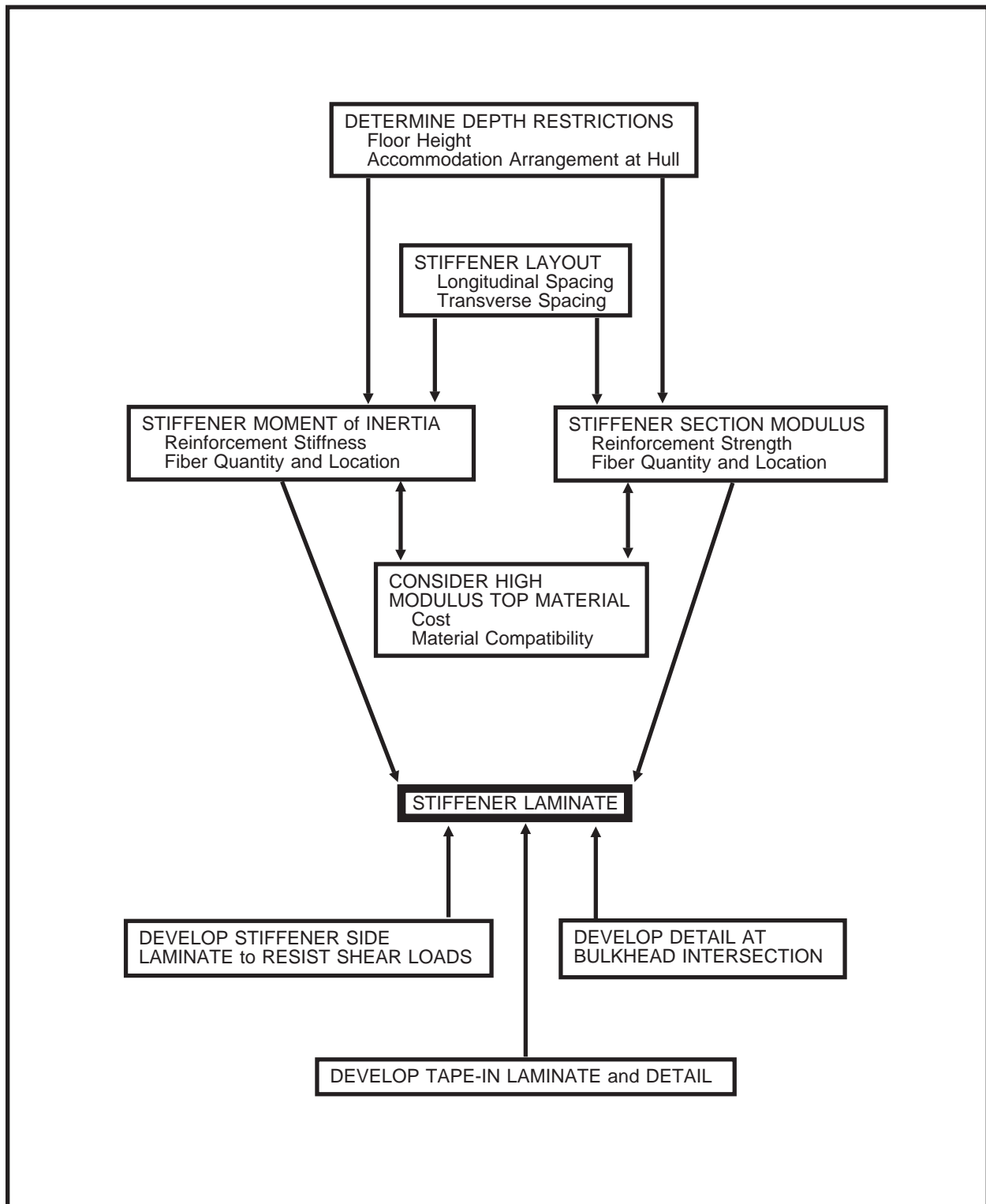
Figure 1-12   Design Flow Chart for Stringers

Joints and Structural Details

Although it is difficult to generalize about a broad class of structures such as "details," composites stand as a testimony to the axiom "the devil is in the details." Stress concentrations can often start at a poorly engineered detail and lead to premature failure. The designer is required to "visualize" load paths and the composite laminate response.

QUANTIFY PRIMARY
LOADS
Strength of Base Member
Functional Loads

IDENTIFY SECONDARY LOADS
Moments from Geometry of Detail
Secondary Load Sources

SECONDARY BOND STRENGTH
Mechanical Surface Preparation
Resin Chemical Bond Strength

STRESS CONCENTRATIONS
Sharp Corners
Laminate Discontinuities

DETAIL LAMINATE

MECHANICAL FASTENERS
Shear Load on Laminate
Compressive Crushing Loads
Pull Out Resistance of Screws

INSPECTION REQUIREMENTS

WATERTIGHT INTEGRITY

Figure 1-13   Design Flow Chart for Joints and Structural Details

Chapter Two - Materials

Materials form an integral part of the way composite structures perform. Because the builder is creating a structural material from diverse constituent compounds, material science concepts are essential to the understanding of how structural composites behave. This chapter encompasses three broad groups of composite materials:

- Reinforcements
- Resins
- Core Materials

Descriptions and physical property data of representative marine materials will be presented. As with all composite material system design, the reader is cautioned not to optimize materials from each group without regard for how a system will perform as a whole. Material suppliers are often a good source of information regarding compatibility with other materials.

Reinforcements for marine composite structures are primarily E-glass due to its cost for strength and workability characteristics. In contrast, the aerospace industry relies on carbon fiber as it's backbone. In general, carbon, aramid fibers and other specialty reinforcements are used in the marine field where structures are highly engineered for optimum efficiency. Architecture and fabric finishes are also critical elements to correct reinforcement selection.

Resin systems are probably the hardest material group for the designer and builder to understand. Fortunately, chemists have been working on formulations since Bakelite in 1905. Although development of new formulations is ongoing, the marine industry has generally based its structures on polyester resin, with trends to vinyl ester and epoxy for structurally demanding projects and highly engineered products. A particular resin system is effected by formulation, additives, catylization and cure conditions. Characteristics of a cured resin system as a structural matrix of a composite material system is therefore somewhat problematic. However certain quantitative and qualitative data about available resin systems exists and is given with the caveat that this is the most important fabrication variable to be verified by the "build and test" method.

Core materials form the basis for sandwich composite structures, which clearly have advantages in marine construction. A core is any material that can physically separate strong, laminated skins and transmit shearing forces across the sandwich. Core materials range from natural species, such as balsa and plywood, to highly engineered honeycomb or foam structures. The dynamic behavior of a composite structure is integrally related to the characteristics of the core material used.

Reinforcements

Fiberglass

Glass fibers account for over 90% of the fibers used in reinforced plastics because they are inexpensive to produce and have relatively good strength to weight characteristics. Additionally, glass fibers exhibit good chemical resistance and processability. The excellent tensile strength of glass fibers, however, is somewhat susceptible to creep (see Chapter Six) and has been shown to deteriorate when loads are applied for long periods of time. [2] Continuous glass fibers are formed by extruding molten glass to filament diameters between 5 and 25 micrometers.

Table 2-1 Glass Composition by Weight for E- and S-Glass [BGF]

	E-Glass	S-Glass
Silicone Dioxide	52 - 56%	64 - 66%
Calcium Oxide	16 - 25%	0 - .3%
Aluminum Oxide	12 - 16%	24 - 26%
Boron Oxide	5 - 10%	—
Sodium & Potassium Oxide	0 - 2%	0 - .3%
Magnesium Oxide	0 - 5%	9 - 11%
Iron Oxide	.05 - .4%	0 - .3%
Titanium Oxide	0 - .8%	—

Individual filaments are coated with a sizing to reduce abrasion and then combined into a strand of either 102 or 204 filaments. The sizing acts as a coupling agent during resin impregnation. E-glass or "electrical glass" was originally developed for the electrical industry because of its high resistivity. S-glass was specifically developed for "structural" applications, with improved tensile strength. The cost for this variety of glass fiber is about three to four times that of E-glass, which precludes a more widespread use of S-glass in the marine construction industry. E-glasss (lime aluminum borosilicate) is the most common reinforcement used in marine laminates because of its good strength properties and resistance to water degradation. S-glass (silicon dioxide, aluminum and magnesium oxides) exhibits about one third better tensile strength, and in general, demonstrates better fatigue resistance. Table 2-1 lists the composition by weight for both E- and S-glass fibers.

Polymer Fibers

The most common aramid fiber is Kevlar® developed by DuPont. This is the predominant organic reinforcing fiber whose use dates to the early 1970s as a replacement for steel belting in tires. The outstanding features of aramids are low weight, high tensile strength and modulus, impact and fatigue resistance, and weaveability. Compressive performance of aramids is not as good as glass, as they show nonlinear ductile behavior at low strain values. Water absorption of un-impregnated Kevlar® 49 is greater than other reinforcements, although ultrahigh modulus Kevlar® 149 absorbs almost two thirds less than Kevlar® 49. The unique characteristics of aramids can best be exploited if appropriate weave style and handling techniques are used.

Polyester and nylon thermoplastic fibers have recently been introduced to the marine industry as primary reinforcements and in a hybrid arrangement with fiberglass. Allied Corporation has developed a fiber called COMPET®, which is the product of applying a finish to PET fibers (polyethylene terephtalate, widely used for blow-molded products, such as bottles) that enhances matrix adhesion properties. Hoechst-Celanese manufactures a product called Treveria®, which is a heat treated polyester fiber fabric designed as a "bulking" material and as a gel coat barrier to reduce "print-through," which occurs when the weave pattern of a reinforcement is

visible at the laminate surface due to resin shrinkage during cure   Although polyester fibers have fairly high strengths, their stiffness is considerably below that of glass. Other attractive features include low density, reasonable cost, good impact and fatigue resistance, and potential for vibration damping and blister resistance.

Carbon Fibers

The terms "carbon" and "graphite" fibers are typically used interchangeably, although graphite technically refers to fibers that are greater than 99% carbon composition versus 93 to 95% for PAN-base (polyacrylonitrile) fibers. All continuous carbon fibers produced to date are made from organic precursors, which in addition to PAN, include rayon and pitches, with the latter two generally used for low modulus fibers.

Carbon fibers offer the highest strength and stiffness of all the common reinforcement fibers. The fibers are not subject to stress rupture or stress corrosion, as with glass and aramids. High temperature performance is particularly outstanding. The major drawback to the PAN-base fibers is their relative cost, which is a function of high precursor costs and an energy intensive manufacturing process. Table 2-2 shows some comparative fiber performance data.

Table 2-2 Mechanical Properties of Reinforcement Fibers

Fiber	Density		Tensile Strength		Tensile Modulus		Ultimate
	lb/in^3	gms/cm^3	psi x 10^3	Mpa	psi x 10^6	Gpa	Elongation
E-Glass	.094	2.60	500	3450	10.5	72	4.8%
S-Glass	.090	2.49	665	4590	12.6	87	5.7%
Aramid-Kevlar® 49	.052	1.44	525	3620	18	124	2.9%
Polyester-COMPET®	.049	1.36	150	1030	1.4	10	22.0%
Carbon-PAN	.062-.065	1.72-1.80	350-700	2400-4800	33-57	228-393	0.38-2.0%

Reinforcement Construction

Reinforcement materials are combined with resin systems in a variety of forms to create structural laminates. Table 2-3 provides definitions for the various forms of reinforcement materials. Some of the lower strength, non-continuous configurations are limited to fiberglass due to processing and economic considerations.

Wovens

Woven composite reinforcements generally fall into the category of cloth or woven roving. The cloths are lighter in weight, typically from 6 to 10 ounces per square yard (200-340 gms/m^2) and require about 40 to 50 plies to achieve a one inch (25 mm) thickness. Their use in marine construction is limited to small parts and repairs. Particular weave patterns include plain weave, which is the most highly interlaced; basket weave, which has warp and fill yarns that are paired up; and satin weaves, which exhibit a minimum of interlacing. The satin weaves are produced in standard four-, five- or eight-harness configurations, which exhibit a corresponding increase in resistance to shear distortion (easily draped). Figure 2-1 shows some commercially available weave patterns. Woven roving reinforcements consist of flattened bundles of continuous strands in a plain weave pattern with slightly more material in the warp direction. This is the most common type of reinforcement used for large marine structures because it is available in fairly heavy weights - 24 ounces per square yard (810 gms/m^2) is the most common, which allows for a rapid buildup of

thickness. Also, directional strength characteristics are possible with a material that is still fairly drapable. Impact resistance is enhanced because the fibers are continuously woven.

Table 2-3 Description of Various Forms of Reinforcements
[Shell, *Epon*® *Resins for Fiberglass Reinforced Plastics*]

Form	Description	Principal Processes
Filaments	Fibers as initially drawn	Processed further before use
Continuous Strands	Basic filaments gathered together in continuous bundles	Processed further before use
Yarns	Twisted strands (treated with after-finish)	Processed further before use
Chopped Strands	Strands chopped $\frac{1}{4}$ to 2 inches	Injection molding; matched die
Rovings	Strands bundled together like rope but not twisted	Filament winding; sheet molding; chopper gun; pultrusion
Milled Fibers	Continuous strands hammermilled into short lengths $\frac{1}{32}$ to $\frac{1}{8}$ inches long	Compounding; casting; reinforced reaction injection molding (RRIM)
Reinforcing Mats	Nonwoven random matting consisting of continuous or chopped strands	Hand lay-up; resin transfer molding (RTM); centrifugal casting
Woven Fabric	Cloth woven from yarns	Hand lay-up; prepreg
Woven Roving	Strands woven like fabric but coarser and heavier	Hand or machine lay-up; resin transfer molding (RTM)
Spun Roving	Continuous single strand looped on itself many times and held with a twist	Processed further before use
Nonwoven Fabrics	Similar to matting but made with unidirectional rovings in sheet form	Hand or machine lay-up; resin transfer molding (RTM)
Surfacing Mats	Random mat of monofilaments	Hand lay-up; die molding; pultrusion

Knits

Knitted reinforcement fabrics were first introduced in 1975 to provide greater strength and stiffness per unit thickness as compared to woven rovings. A knitted reinforcement is constructed using a combination of unidirectional reinforcements that are stitched together with a non-structural synthetic, such as polyester. A layer of mat may also be incorporated into the construction. The process provides the advantage of having the reinforcing fiber lying flat versus the crimped orientation of woven roving fiber.   Additionally, reinforcements can be oriented along any combination of axes. Superior glass to resin ratios are also achieved, which makes overall laminate costs competitive with traditional materials. Figure 2-2 shows a comparison of woven roving and knitted construction.

Omnidirectional

Omnidirectional reinforcements can be applied during hand lay-up as prefabricated mat or via the spray-up process as chopped strand mat. Chopped strand mat consists of randomly oriented glass fiber strands that are held together with a soluble resinous binder. Continuous strand mat is similar to chopped strand mat, except that the fiber is continuous and laid down in a swirl pattern. A chopper gun takes roving and chops it up as it is sprayed with resin to create a structure similar to chopped strand mat. Both hand lay-up and spray-up produce plies with equal properties along the *x* and *y* axes and good interlaminar shear strength. This is a very economical way to build up thickness, especially with complex molds.   In-plane mechanical properties are low because fibers are randomly orientated and plies are resin rich.

Plain weave   Basket weave   Twill

Crowfoot satin   8 harness satin   5 harness satin
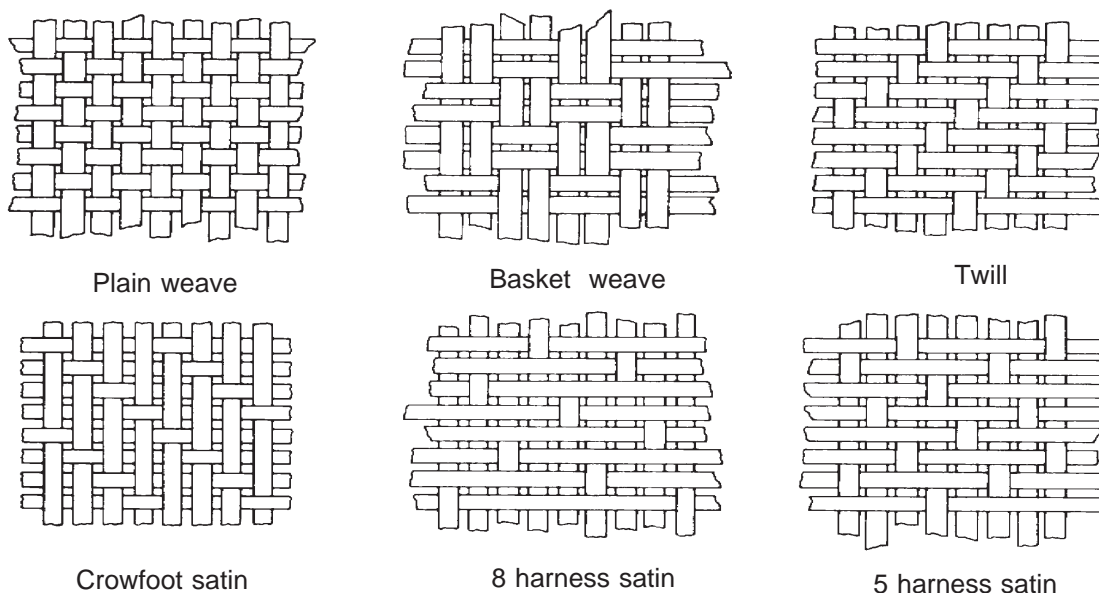
Figure 2-1   Reinforcement Fabric Construction Variations [*ASM **Engineered Materials Handbook***]

Unidirectional

Pure unidirectional construction implies no structural reinforcement in the fill direction. Ultra high strength/modulus material, such as carbon fiber, is sometimes used in this form due to its high cost and specificity of application.   Material widths are generally limited due to the difficulty of handling and wet-out. Some unidirectionals are held together with thermoplastic web binders that are compatible with thermoset resin systems. It is claimed to be easier to handle and cut than traditional pure unidirectional material.   Typical applications for unidirectionals include stem and centerline stiffening as well as the tops of stiffeners. Entire hulls are fabricated from unidirectional reinforcements when an ultra high performance laminate is desired and load paths are well defined.
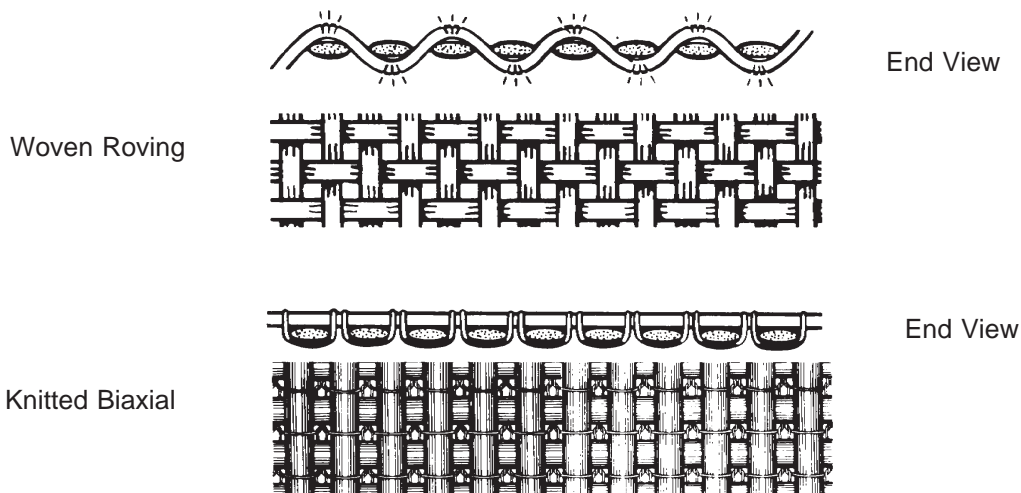
End View

Woven Roving

End View

Knitted Biaxial

Figure 2-2   Comparison of Conventional Woven Roving and a Knitted Biaxial Fabric Showing Theoretical Kink Stress in Woven Roving [Composites Reinforcements, Inc.]

Resins

Polyester

Polyester resins are the simplest, most economical resin systems that are easiest to use and show good chemical resistance. Almost one half million tons of this material are used annually in the United States. Unsaturated polyesters consist of unsaturated material, such as maleic anhydride or fumaric acid, that is dissolved in a reactive monomer, such as styrene. The chemical state of unsaturated polyesters leaves an "unsatisfied" reactive group that is readily available for attachment to other groups via an exothermic process. Saturated polyesters include oil-based paints and polyester fibers and are not considered thermosets. [3] Polyester resins have long been considered the least toxic thermoset to personnel, although recent scrutiny of styrene emissions in the work place has led to the development of alternate formulations.

Most polyesters are air inhibited, meaning they will not cure when exposed to air. Typically, paraffin is added to the resin formulation, which has the effect of sealing the surface during the cure process. However, the wax film on the surface presents a problem for secondary bonding or finishing and must be physically removed. Non-air inhibited resins do not present this problem and are, therefore, more widely accepted in the marine industry where secondary bonding is required. The two basic polyester resins used in the marine industry are orthophthalic and isophthalic. The ortho resins were the original group of polyesters developed and are still in widespread use. They have somewhat limited thermal stability, chemical resistance, and processability characteristics. The iso resins generally have better mechanical properties and show better chemical resistance. Their increased resistance to water permeation has prompted many builders to use this resin as a gel coat or barrier coat in marine laminates.

The rigidity of polyester resins can be lessened by increasing the ratio of saturated to unsaturated acids. Flexible resins may be advantageous for increased impact resistance, however, this comes at the expense of stiffness. Non-structural laminate plies, such as gel coats and barrier veils, are sometimes formulated with more flexible resins to resist local cracking. On the other end of the spectrum are the low-profile resins that are designed to minimize reinforcement print-through. Typically, ultimate elongation values are reduced for these types of resins, which are represented by DCPD in Table 2-4.

Curing of polyester without the addition of heat is accomplished by adding accelerator along with the catalyst. Gel times can be carefully controlled by modifying formulations to match ambient temperature conditions and laminate thickness. Other resin additives can modify the viscosity of the resin if vertical or overhead surfaces are being laminated. This effect is achieved through the addition of silicon dioxide, in which case the resin is called thixotropic. Various other fillers are used to reduce resin shrinkage upon cure, a useful feature for gel coats.

Vinyl Ester

Vinyl ester resins are unsaturated resins prepared by the reaction of a monofunctional unsaturated acid, such as methacrylic or acrylic, with a bisphenol diepoxide. The resulting polymer is mixed with an unsaturated monomer, such as styrene. The handling and performance characteristics of vinyl esters are similar to polyesters. Some advantages of the vinyl esters, which may justify their higher cost, include superior corrosion resistance, hydrolytic stability, and excellent physical properties such as impact and fatigue resistance (failure modes associated with these characteristics are discussed in Chapter Six). It has been shown that a 20 to 60 mil inter-layer with a vinyl ester resin matrix can provide an excellent permeation barrier to resist blistering in marine laminates.

Table 2-4 Comparative Data for Some Thermoset Resin Systems (castings)

Resin	Barcol Hardness	Tensile Strength		Tensile Modulus		Ultimate Elongation
		psi x 10^3	Mpa	psi x 10^5	Gpa	
Orthophthalic	42	7.0	48.3	5.9	4.1	.91%
Dicyclopentadiene (DCPD)	54	11.2	77.3	9.1	6.3	.86%
Isophthalic	46	10.3	77.1	5.65	3.9	2.0%
Vinyl Ester	35	11-12	76-83	4.9	3.4	5-6%
Epoxy	86D*	7.96	54.9	5.3	3.7	7.7%
Phenolic	70	7.0	48.3	5.5	3.8	1.75%
*Hardness values for epoxies are traditionally given on the "Shore D" scale						

Epoxy

Epoxy resins are a broad family of materials that contain a reactive functional group in their molecular structure. Epoxy resins show the best performance characteristics of all the resins used in the marine industry. Additionally, they exhibit the least shrinkage upon cure of all the thermosets.   Aerospace applications use epoxy almost exclusively, except when high temperature performance is critical. The high cost of epoxies and handling difficulties have limited their use for large marine structures. Table 2-4 shows some comparative data for various thermoset resin systems. The mechanical properties of epoxy resins can be influenced by the cure schedule used. Table 2-5 shows some illustrative data on epoxy cure schedule influence.

Table 2-5 Epoxy Resin Mechanical Data [Ness & Whiley, SP Systems]

Cure Schedule	Hardener Used	Flexural Strength		Flexural Modulus		Tensile Strength		Tensile Modulus		Elongation at Break
		ksi	Mpa	ksi	Mpa	ksi	Mpa	ksi	Mpa	
5 hours @ 50° C	Slow	23.4	161	0.46	3.17	11.3	78	0.45	3.10	6.4%
	1:1	23.2	160	0.52	3.59	11.2	77	0.48	3.31	7.2%
	Fast	23.1	159	0.52	3.59	10.7	74	0.48	3.31	7.0%
16 hours @ 45° - 50° C	Slow	23.2	160	0.54	3.72	11.6	80	0.49	3.38	5.6%
	1:1	22.8	157	0.55	3.79	11.6	80	0.49	3.38	5.8%
	Fast	27.1	187	0.54	3.72	12.6	87	0.49	3.38	5.5%
4 weeks @ 18° - 30° C	Slow	14.8	102	0.52	3.59	9.1	63	0.52	3.59	3.3%
	1:1	18.9	130	0.54	3.72	10.0	69	0.52	3.59	3.4%
	Fast	19.6	135	0.54	3.72	11.2	77	0.52	3.59	3.4%

Phenolic

The synthetic resins formed by the condensation of phenols with aldehydes were the first resinous products to be produced commercially entirely from simple compounds of low molecular weight. These thermosetting resins have typically been cured at high temperatures (140 - 180°C) and usually under high pressures. Developments in the late 1970's led to a new range of phenolic resole resins that were designed to cure at lower temperatures and pressures through the use of acid-based catalysts. The processing of these resins has been advanced so that now all the processes normally used for composite production are commercially viable.

Two categories of phenolic resin are novolacs and resoles. Novolacs are thermoplastic materials and are made by heating phenol with formaldehyde in the presence of an acidic catalyst (oxalic or sulphuric acid). Novolacs are often referred to as two-stage resins since they need to be heated with additional formaldehyde in order to crosslink to their final infusible form. Resoles are thermosetting resins often referred to as one-stage resins. They are prepared by heating phenol with formaldehyde using an alkaline catalyst, with the formaldehyde in excess. Resole resins for laminating are usually dissolved in alcohols or water/alcohol mixtures prior to distribution. These resins have a sufficiently high formaldehyde content for them to crosslink on further heating. Curing can also be brought about by the addition of strong acids, in which case the reaction is extremely exothermic.

Phenolic resins perform much better than polyesters and epoxies in fires, showing reduced flame spread characteristics and increased time to ignition (see Chapter Six). Because phenolic resin is very promising for applications where fire is a threat, resin manufacturers have recently devoted effort to improve processability and strength characteristics.

Thermoplastics

Thermoplastics have one- or two-dimensional molecular structures, as opposed to three-dimensional structures for thermosets. The thermoplastics generally come in the form of molding compounds that soften at high temperatures. Polyethylene, polystyrene, polypropylene, polyamides and nylon are examples of thermoplastics. Their use in the marine industry has generally been limited to small boats and recreational items. Reinforced thermoplastic materials have recently been investigated for the large scale production of structural components. Some attractive features include no exotherm upon cure, which has plagued filament winding of extremely thick sections with thermosets, and enhanced damage tolerance. Processability and strengths compatible with reinforcement material are key areas currently under development.

Core Materials

Balsa

End grain balsa's closed-cell structure consists of elongated, prismatic cells with a length (grain direction) that is approximately sixteen times the diameter (see Figure 2-3). In densities between 6 and 16 pounds ft^3 (0.1 and 0.25 gms/cm^3), the material exhibits excellent stiffness and bond strength. Stiffness and strength characteristics are much like aerospace honeycomb cores Although the static strength of balsa panels will generally be higher than the PVC foams, impact energy absorption is lower. Local impact resistance is very good because stress is efficiently transmitted between sandwich skins. End-grain balsa is available in sheet form for flat panel construction or in a scrim-backed block arrangement that conforms to complex curves.
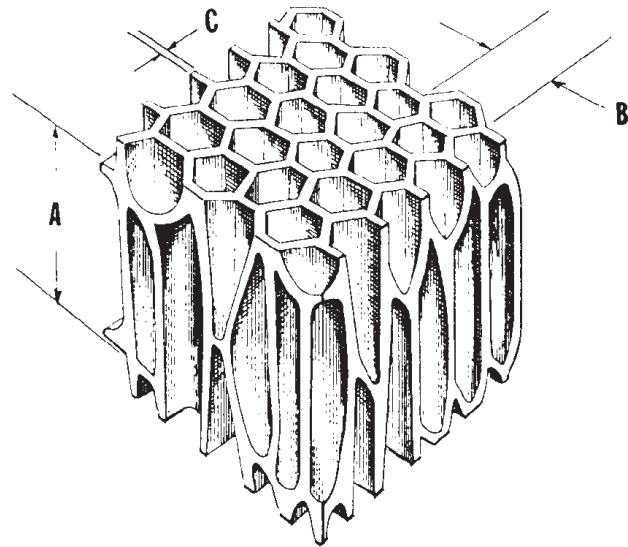
Figure 2-3 Balsa Cell Geometry with **A** = Average Cell Length = .025" (0.64 mm); **B** = Average Cell Diameter = .00126" (0.032 mm); **C** = Average Cell Wall Thickness = .00006" (0.015 mm) [Baltek]

Thermoset Foams

Foamed plastics such as cellular cellulose acetate (CCA), polystyrene, and polyurethane are very light - about 2 lbs/ft^3(55 gms/cm^3) and resist water, fungi and decay. These materials have very low mechanical properties and polystyrene will be attacked by polyester resin. These foams will not conform to complex curves, unless they are blown in place. Use is generally limited to buoyancy rather than structural applications. Polyurethane is often foamed in-place when used as a buoyancy material

Syntactic Foams

Syntactic foams are made by mixing hollow microspheres of glass, epoxy and phenolic into fluid resin with additives and curing agents to form a moldable, curable, lightweight fluid mass. Sprayable syntactic core is available that can be applied in thicknesses up to $\frac{3}{8}$" (9.5 mm) at densities between 30 and 43 lbs/ft^3 (0.48 and 0.69 gms/cm^3). Syntactic cores can be used instead of "laminate bulkers," to build up laminate thickness to increase flexural strength.

Cross Linked PVC Foams

Polyvinyl chloride (PVC) foam cores are manufactured by combining a polyvinyl copolymer with stabilizers, plasticizers, cross-linking compounds and blowing agents. The mixture is heated under pressure to initiate the cross-linking reaction and then submerged in hot water tanks to expand to the desired density. Cell diameters range from .0100 to .100 inches (0.07 to 0.69 mm). [4] The resulting material is thermoplastic, enabling the material to conform to compound curves of a hull. PVC foams have almost exclusively replaced urethane foams as a structural core material, except in configurations where the foam is "blown" in place. A number of manufacturers market cross-linked PVC products to the marine industry in sheet form with densities ranging from 2 to 12 pounds per ft^3 (0.03 and 0.19 gms/cm^3) As with the balsa products, solid sheets or scrim backed block construction configurations are available.

Linear PVC Foam

Linear PVC foam core produced for the marine industry has unique mechanical properties that are a result of a non-connected molecular structure, which allows significant displacements before failure. In comparison to the cross linked (non-linear) PVCs, linear foam will exhibit less favorable static properties and better impact absorption capability. Individual cell diameters range from .020 to .080 inches (0.5 to 2.0 mm). [5] Table 2-6 shows some of the physical properties of the core materials presented here.

Linear Structural Foam

Tom Johannsen of ATC Chemical Corporation has developed a linear polymer foam called Core-Cell®. The aim in developing Core-Cell® was to achieve the impact strength of linear PVC foam and approach the static stiffness of cross-linked foams. ATC claims that Core-Cell® is non-friable (won't crumble), tough and rigid with high shear elongation and good impact strength. Densities range from 3 lbs/ft^3 (55 g/cm^3) to 12 lbs/ft^3 (220 g/cm^3) and thicknesses from ¼ inch (6.35 mm) to 1½ inches (38 mm). Table 2-6 summarizes the physical properties of several Core-Cell® densities.

Honeycomb

Various types of manufactured honeycomb cores are used extensively in the aerospace industry. Constituent materials include aluminum, phenolic resin impregnated fiberglass, polypropylene, and aramid fiber phenolic treated paper. Densities range from 1 to 6 lbs/ft^3 (0.016 to 0.1 gm/cm^3) and cell sizes vary from ⅛ to ⅜ inches (3 to 9.5 mm). [6] Physical properties vary in a near linear fashion with density. Although the fabrication of extremely lightweight panels is possible with honeycomb cores, applications in a marine environment are limited due to the difficulty of bonding to complex face geometries and the potential for significant water absorption.

PMI Foam

Polymrthacrylimide (PMI) foam is targeted primarily at the aerospace industry. The material requires minimum laminating pressures to develop a good bond to face skins (peel strength). The most attractive feature of this material is its ability to withstand curing temperatures in excess of 350°F (175°C). This feature is essential when considering prepreg construction with autoclave cure. Table 2-6 summarizes the physical properties of a common grade of PMI foam.

Table 2-6 Comparative Data for Some Sandwich Core Materials

Core Material		Density		Tensile Strength		Compressive Strength		Shear Strength		Shear Modulus	
		lbs/ft³	g/cm³	psi	Mpa	psi	Mpa	psi	Mpa	psi x 10³	Mpa
End Grain Balsa		7	112	1320	9.12	1190	8.19	314	2.17	17.4	120
		9	145	1790	123	1720	11.9	418	2.81	21.8	151
Cross-Linked PVC Foam	Termanto, C70.75	4.7	75	320	2.21	204	1.41	161	1.11	1.61	11
	Klegecell II	4.7	75	175	1.21	160	1.10			1.64	11
	Divinycell H-80	5.0	80	260	1.79	170	1.17	145	1.00	4.35	30
	Termanto C70.90	5.7	91	320	2.21	258	1.78	168	1.16	2.01	13
	Divinycell H-100	6.0	96	360	2.48	260	1.79	217	1.50	6.52	45
Linear Structural Foam	Core-Cell	3-4	55	118	0.81	58	0.40	81	0.56	1.81	12
		5-5.5	80	201	1.39	115	0.79	142	0.98	2.83	20
		8-9	210	329	2.27	210	1.45	253	1.75	5.10	35
Airex Linear PVC Foam		5-6	80-96	200	1.38	125	0.86	170	1.17	2.9	29
PMI Foam	Rohacell 71	4.7	75	398	2.74	213	1.47	185	1.28	4.3	30
	Rohacell 100	6.9	111	493	3.40	427	2.94	341	2.35	7.1	49
Phenolic Resin Honeycomb		6	96	n/a	n/a	1125	7.76	200	1.38	6.0	41
Polypropylene Honeycomb		4.8	77	n/a	n/a	218	1.50	160	1.10	n/a	n/a

Chapter Three - Loads

The first step in any structural design problem is to define the loads that will act on the structure. For boat and ship design, an exhaustive treatment of this exercise can be truly tedious. Primary loads from operation in a seaway must allow for the variability of the ocean itself. Secondary and tertiary loads resulting from the geometric interaction of structural members may also be critical. In addition to the magnitude and direction of anticipated loads, the frequency of the force is also important to estimate fatigue.

Composite materials allow the designer the flexibility to tailor strength and stiffness in various directions to respond to anticipated loads. This ability brings with it the burden of being able to predict loads and load paths in a structure more accurately than with traditional isotropic metallic building materials.

Stiffness requirements of marine structures are also more acute when composite materials are utilized. In general, strength criteria is easier to meet than stiffness criteria. Variation in laminate stiffness influences load paths within a composite structure. Stiffer elements tend to transfer loads more directly, while softer panels tend to deflect more without transferring loads to adjacent structure. The composites designer must remain aware of directional strength and stiffness characteristics resulting from material selection, thickness, and orientation as this affects load transmission throughout the structure.

Loads to be considered in this chapter include:

- Hull girder bending loads that act over the entire length of a ship
- Wave slamming loads on ships and high speed craft
- Deck and bulkhead loads
- Point loads

The objective for presenting load data is to familiarize the reader with the types of loading one can expect on a boat or ship that may be built with composites. Reference sources for detailed load calculation methodology are cited.

Hull as a Longitudinal Girder

Classical approaches to ship structural design treat the hull structure as a beam for purposes of analytical evaluation. [7] The validity of this approach is related to the vessel's length to beam and length to depth ratios. Consequently, beam analysis is not the primary analytical approach for small craft. Hull girder methods are usually applied to vessels with Length/Depth (L/D) ratios of 12 or more, which usually corresponds to vessels greater than 100 feet (30 meters). Very slender hull forms, such as a canoe or catamaran hull, may have an L/D much greater than 12. Nevertheless, it is always instructive to regard hull structure as a beam when considering forces that act on the vessel's overall length. By determining which elements of the hull are primarily in tension, compression or shear, scantling determination can be approached in a more rational manner. This is particularly important when designing with anisotrophic materials where orientation affects the structure's load carrying capabilities to such a great extent.

A variety of different phenomena contribute to the overall longitudinal bending moments experienced by a ship's hull structure. Analyzing these global loading mechanisms statically is not very realistic with smaller craft. Here, dynamic interaction in a seaway will generally produce loadings in excess of what static theory predicts. However, empirical information has led to the development of accepted safety factors that can be applied to the statically derived stress predictions. Force producers are presented here in an order that corresponds to decreasing vessel size, i.e., ship theory first.

Still Water Bending Moment

Before a ship even goes to sea, some stress distribution profile exists within the structure. Figure 3-1 shows how the summation of buoyancy and weight distribution curves leads to the development of load, shear and moment diagrams. Stresses apparent in the still water condition generally become extreme only in cases where concentrated loads are applied to the structure, which can be the case when holds in a commercial vessel are selectively filled. The still water bending moment (SWBM) is an important concept for composites design because fiberglass can be susceptible to creep or fracture when subjected to long term loads. Static fatigue of glass fibers can reduce their load carrying capability by as much as 70 to 80% depending on load duration, temperature, moisture conditions and other factors. [2]
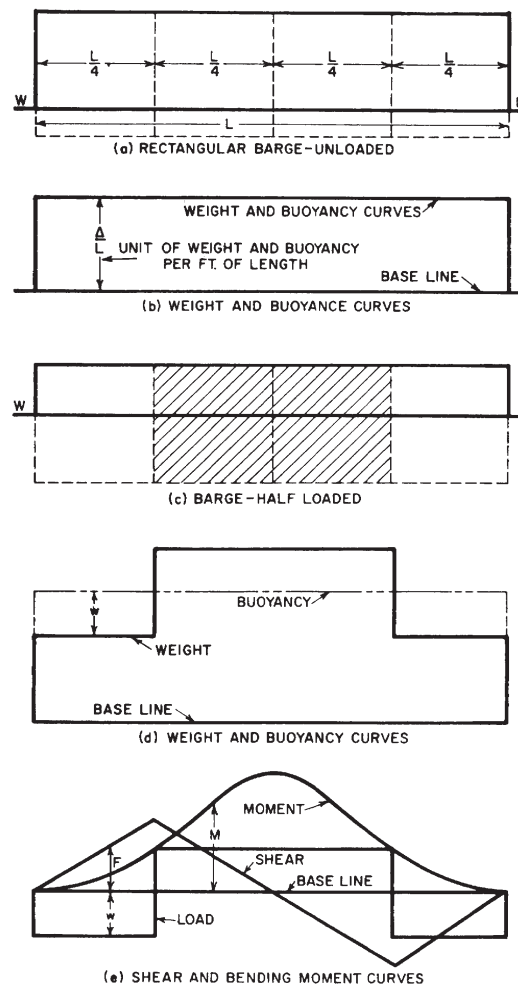
Figure 3-1 Bending Moment Development of Rectangular Barge in Still Water [*Principles of Naval Architecture*]

Wave Bending Moment

A static approach to predicting ship structure stresses in a seaway involves the superposition of a trochoidal wave with a wavelength equal to the vessel's length in a hogging and sagging condition, as shown in Figure 3-2. The trochoidal wave form was originally postulated by Froude as a realistic two-dimensional profile, which was easily defined mathematically. The height of the wave is usually taken as $\frac{1}{9}$ (L < 100 feet or 30 meters), $\frac{1}{20}$ (L > 100 feet or 30 meters) or $1.1L^{\frac{1}{2}}$ (L > 500 feet) or $0.6L^{.6}$ (L > 150 meters). Approximate calculation methods for maximum bending moments and shearing forces have been developed as preliminary design tools for ships over 300 feet (91 meters) long. [8] Except for very slender craft, this method will not apply to smaller vessels.

(a) VESSEL IN STILL WATER

(b) VESSEL IN SAGGING CONDITION

(c) VESSEL IN HOGGING CONDITION
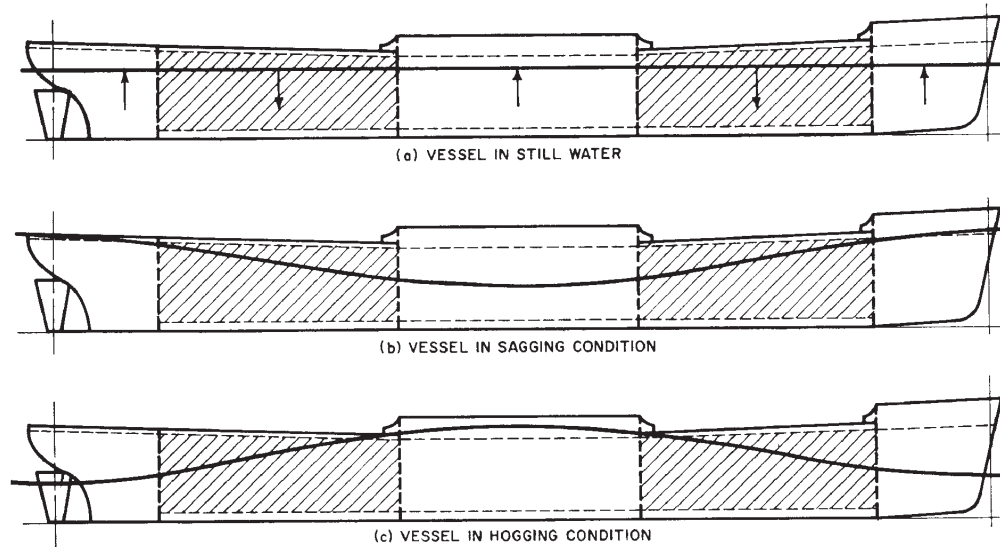
Figure 3-2   Superposition of Static Wave Profile [*Principles of Naval Architecture*]

Ship Oscillation Forces

The dynamic response of a vessel operating in a given sea spectrum is very difficult to predict analytically. Accelerations experienced throughout the vessel vary as a function of vertical, longitudinal and transverse location. These accelerations produce virtual increases of the weight of concentrated masses, hence additional stress. The designer should have a feel for the worst locations and dynamic behavior that can combine to produce extreme load scenarios. Figure 3-3 is presented to define the terms commonly used to describe ship motion. It is generally assumed that combined roll and pitch forces near the deck edge forward represents a "worst case" condition of extreme accelerations for the ship.
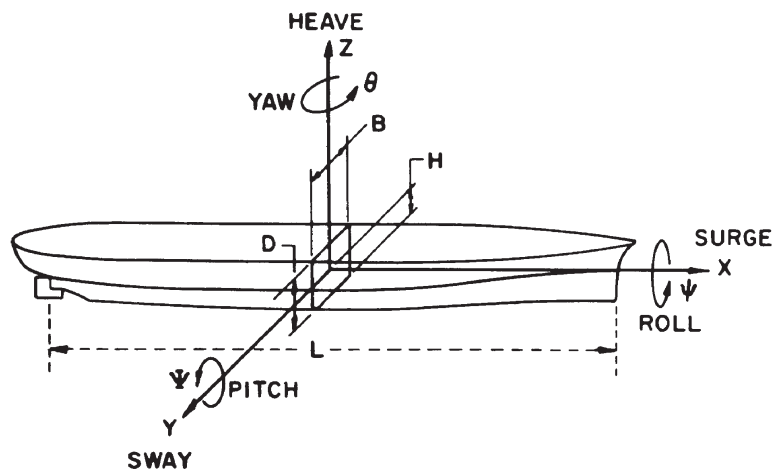
Figure 3-3   Principal Axes and Ship Motion Nomenclature [Evans, *Ship Structural Design Concepts*]

Dynamic Phenomena

Dynamic loading or vibration can be either steady state, as with propulsion system induced phenomena, or transient, such as with slamming through waves. In the former case, load amplitudes are generally within the design limits of hull structural material. However, the fatigue process can lead to premature failures, especially if structural components are in resonance with the forcing frequency. A preliminary vibration analysis of major structural elements (hull girder, engine foundations, deck houses, masts, etc.) is generally prudent to ensure that natural frequencies are not near shaft and blade rate for normal operating speeds. [9] Schlick [10] proposed the following empirical formula to predict the first-mode (2-node) vertical natural frequency for large ships:

$$N_{2v} \;=\; C_1 = \sqrt{\frac{I}{\Delta\, L^3}} \tag{3-1}$$

where:

L = length between perpendiculars, feet
Δ = displacement, tons
I = midship moment of inertia, in^2ft^2
C_1 = constant according to ship type
    = 100,000 for small coastal tankers, 300-350 feet
    = 130,000 for large, fully loaded tankers
    = 143,000 suggested by Noonan for large tankers
    = 156,850 for destroyers

The transient dynamic loading referred to generally describes events that occur at much higher load amplitudes. Slamming in waves is of particular interest when considering the design of high-speed craft. Applying an acceleration factor to the static wave bending analysis outlined above can give some indication of the overall girder stresses produced as a high-speed craft slams into a wave. Other hull girder dynamic phenomena of note include springing and whipping of the hull when wave encounter frequency is coincident with hull natural frequency.

Sailing Vessel Rigging Loads

The major longitudinal load producing element associated with sailing vessels is the mast operating in conjunction with the headstay and backstay. The mast works in compression under the combined action of the aforementioned longitudinal stays and the more heavily loaded athwartship shroud system. Hull deflection is in the sagging mode, which can be additive with wave action response.

Transverse Bending Loads

Transverse loading on a ship's hull is normally of concern only when the hull form is very long and slender. Global forces are the result of beam seas. In the case of sailing vessels, transverse loads can be significant when the vessel is sailing upwind in a heeled condition. Methods for evaluating wave bending moment should be used with a neutral axis that is parallel to the water.

Torsional Loading

Torsional loading of hull structures is often overlooked because there is no convenient analytical approach that has been documented. Quartering seas can produce twisting moments within a hull structure, especially if the hull has considerable beam. In the case of multihulls, this loading phenomena often determines the configuration of cross members. Vessels with large deck openings are particularly susceptible to applied torsional loads. New reinforcement materials are oriented with fibers in the bias direction ($\pm 45°$), which makes them extremely well suited for resisting torsional loading.

Slamming

The loads on ship structures are reasonably well established (e.g. *Principles of Naval Architecture*, etc.), while the loads on small craft structures have received much less attention in the literature. There are some generalizations which can be made concerning these loads, however. The dominant loads on ships are global in-plane loads (loads affecting the entire structure and parallel to the hull plating), while the dominant loads on small craft are local out of plane loads (loads normal to the hull surface over local portions of the hull surface). As a result, structural analysis of ships is traditionally approached by approximating the entire ship as a box beam, while the structural analysis of small craft is approached using local panel analysis. The analysis of large boats (or small ships) must include both global and local loads, as either may be the dominant factor. Since out-of-plane loads are dominant for small craft, the discussion of these loads will center on small craft. However, much of the discussion could be applied to ships or other large marine structures. The American Bureau of Shipping provides empirical expressions for the derivation of design heads for sail and power vessels. [11,12]

Out-of-plane loads can be divided into two categories: distributed loads (such as hydrostatic and hydrodynamic loads) and point loads (such as hauling or keel, rig, and rudder loads on sail boats, or strut, rudder or engine mounts for power boats). The hydrostatic loads on a boat at rest are relatively simple and can be determined from first principles. Hydrodynamic loads are very complex, however, and have not been studied extensively, thus they are usually treated in an extremely simplified manner. The most common approach is to increase the static pressure load by a fixed proportion, called the dynamic load factor. [13] The sources of point loads vary widely, but most can be estimated from first principles by making a few basic assumptions.

Hydrodynamic Loads

There are several approaches to estimating the hydrodynamic loads for planing power boats. However, most are based on the first comprehensive work in this area, performed by Heller and Jasper. The method is based on relating the strain in a structure from a static load to the strain in a structure from a dynamic load of the same magnitude. The ratio of the dynamic strain to the static strain is called the "response factor," and the maximum response factor is called the "dynamic load factor." This approach is summarized here with an example of this type of calculation. Heller and Jasper instrumented and obtained data on an aluminum hull torpedo boat (YP 110) and then used this data as a basis for the empirical aspects of their load calculation. An example of the data is presented in Figure 3-4. The dynamic load factor is a function of the impact pressure rise time, t_o, over the natural period of the structure, T, and is presented in Figure 3-5, where C/C_c is the fraction of critical damping. The theoretical development of the load prediction leads to the following equations:

Maximum Impact Force Per Unit Length:

$$p_0 = \frac{3W}{2L} \times \left(1 + \frac{y_{CG}}{g}\right) \qquad (3\text{-}2)$$

where:

p_0 = maximum impact force per unit length

$$W \;=\; \text{hull weight}$$

$$L \;=\; \text{waterline length}$$

$$y_{CG} \;=\; \text{vertical acceleration of the CG}$$

$$g \;=\; \text{gravitational acceleration}$$

Maximum Effective Pressure at the Keel

$$p_{01} \;=\; \frac{3 p_0}{G} \tag{3-3}$$

where:

$$p_{01} \;=\; \text{maximum effective pressure at the keel}$$

$$G \;=\; \text{half girth}$$

Maximum Effective Pressure

$$\bar{P} \;=\; p_{01} \times DLF \tag{3-4}$$

where:

$$\bar{P} \;=\; \text{the maximum effective pressure for design}$$

$$DLF \;=\; \text{the Dynamic Load Factor from Figure 3-5 (based on known or measured critical damping)}$$

An example of the pressure calculation for the YP110 is also presented by Heller and Jasper:

Maximum Force Per Unit Length:

$$p_0 \;=\; \frac{3 \times 109{,}000}{2 \times 900} \left(1 + 4.7\right) = 1{,}036 \; \text{lbs/in}$$

Maximum Effective Pressure at the Keel:

$$p_{01} \;=\; \frac{1036 \times 3}{96} = 32.4 \; \text{psi}$$

Maximum Effective Pressure:

$$\bar{P} \;=\; 32.4 \times 1.1 = 35.64 \; \text{psi}$$

This work is the foundation for most prediction methods. Other presentations of load calculation, measurement, or design can be found in the classification society publications cited in the reference section of the Guide.
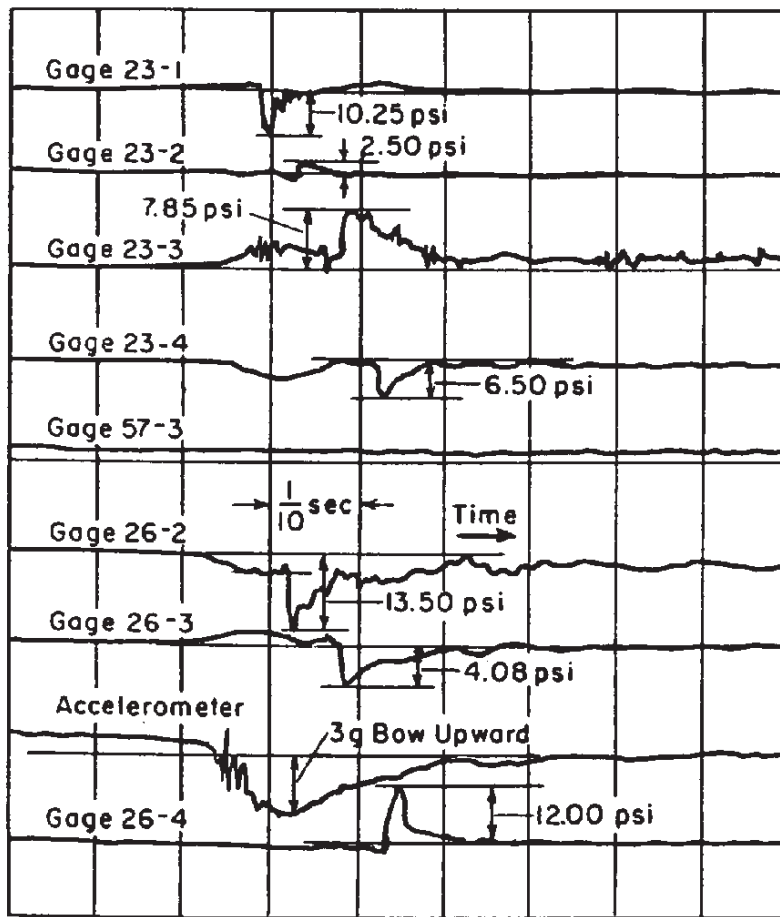
Figure 3-4   Pressures Recorded in Five and Six Foot Waves at a Speed of 28 Knots [Heller and Jasper, *On the Structural Design of Planing Craft*]
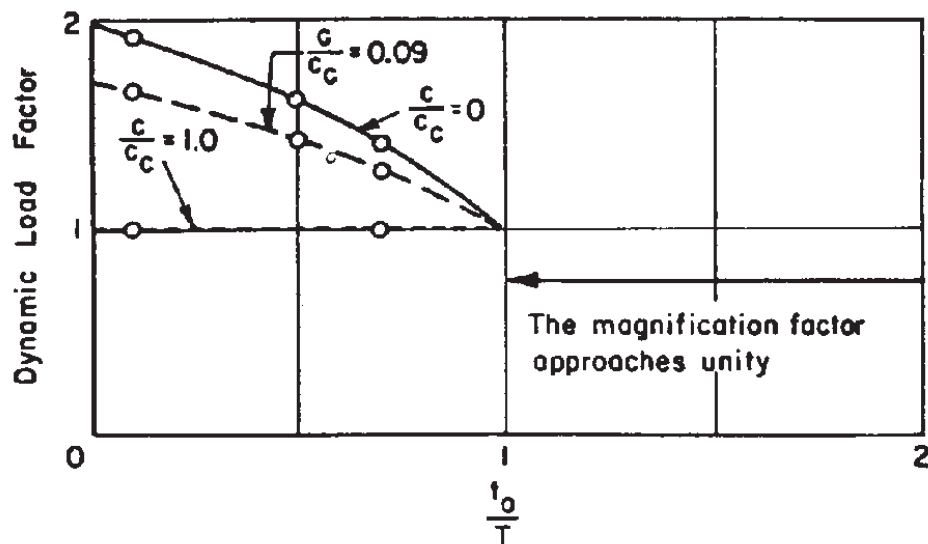
Figure 3-5   Dynamic Load factors for Typical Time Varying Impact Loads [Heller and Jasper, *On the Structural Design of Planing Craft*]

Load Distribution as a Function of Length

Classification society rules, such as the ABS Guide for High-Speed Craft (Oct, 1996 Draft) recognize that slamming loads vary as a function of distance along the waterline. Figures 3-6 and 3-7 show vertical acceleration factors used to calculate dynamic bottom pressures based on hull form and service factors, respectively. The general relationship given by the rules is as follows:
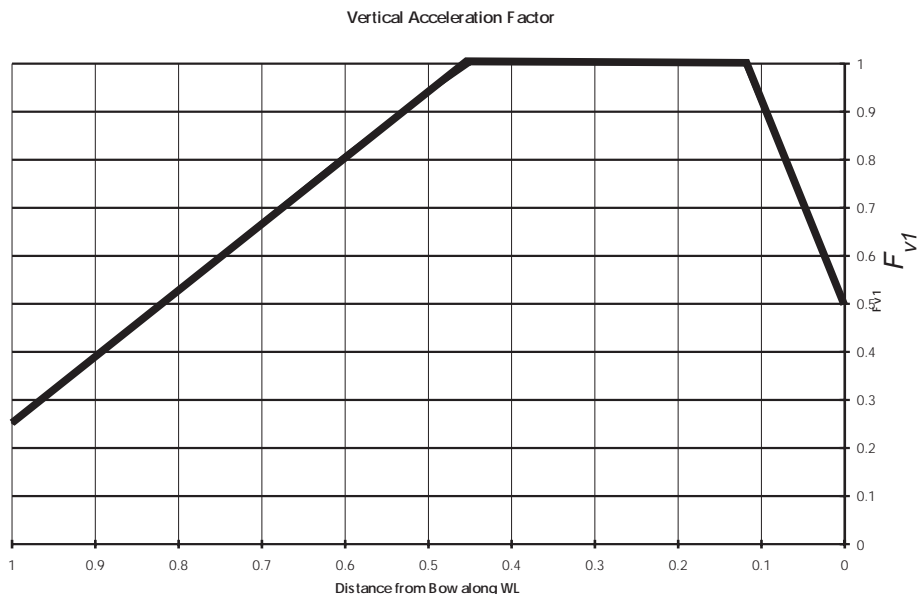
Figure 3-6 Vertical Acceleration Factor as a Function of Distance from Bow, F_{v1}, Used in ABS Calculations

$$Pressure_b \approx \frac{\Delta}{L_{wl} B} F_{v1} \qquad (3\text{-}5)$$

and

$$Pressure_i \approx N \, d \, F_{v2} \qquad (3\text{-}6)$$

where:

Δ = displacement

L_{wl} = waterline length

B = beam

N = service factor

d = draft

The rules require that the higher pressure calculated be used as the design pressure for planing and semi-planing craft. The reader is instructed to consult the published rules to get the exact equations with additional factors to fit hull geometry and engineering units used.
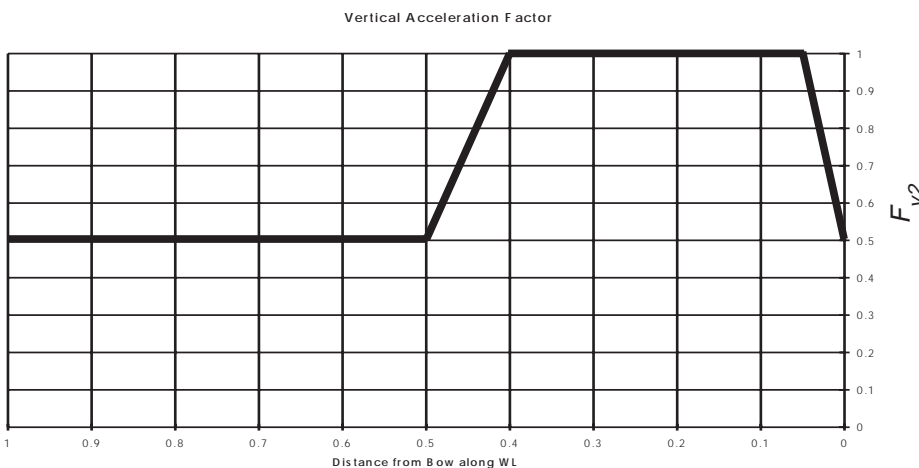
Figure 3-7 Vertical Acceleration Factor as a Function of Distance from Bow, F_{v2}, Used in ABS Calculations

Slamming Area Design Method

NAVSEA's *High Performance Marine Craft Design Manual Hull Structures* [15] prescribes a method for calculating longitudinal shear force and bending moments based on assigning a slamming pressure area extending from the keel to the turn of the bilge and centered at the longitudinal center of gravity (LCG). This area is calculated as follows:

$$A_R = \frac{25\,\Delta}{T} \quad (\text{ft}^2) \tag{3-7a}$$

$$A_R = \frac{0.7\,\Delta}{T} \quad (\text{m}^2) \tag{3-7b}$$

The slamming force is given as:

$$F_{sl} = \Delta\, a_v \tag{3-8}$$

where:

Δ = Full load displacement in tons or tonnes

T = Molded draft in feet or meters

a_v = $\frac{1}{10}$ highest vertical acceleration at the LCG of the vessel

The vertical acceleration, a_v, is calculated for any position along the length of a monohull craft by the following expression:

$$a_v = \frac{k_v\, g_0\, v^{1.5} \left[\dfrac{H_s}{L}\right]}{1.697\,[1.0 + 0.04L]} \left[1 - \frac{\sqrt{L}}{2.6\,V}\right] \quad (\text{ft/sec}^2) \tag{3-9a}$$

$$a_v = \frac{k_v\, g_0\, v^{1.5} \left[\dfrac{H_s}{L}\right]}{1.697\,[1.0 + 0.012L]} \left[1 - \frac{\sqrt{L}}{4.71\,V}\right] \quad (\text{m/sec}^2) \tag{3-9b}$$

where:

H_s = Significant wave height (ft or m)

L = Vessel length (ft or m)

g_0 = Acceleration due to gravity

k_v = Longitudinal impact coefficient from Figure 3-8

V = Maximum vessel speed in knots in a sea state with significant wave height, H_s

The maximum bottom pressure, P_m, is given by:

$$P_m = 0.135\; T\, a_v \quad (\text{psi}) \tag{3-10a}$$

$$P_m = 10\; T\, a_v \quad (\text{Mpa}) \tag{3-10b}$$

The design pressure, P_d, for determining bottom panel scantling requirements is given by the expression:

$$P_d = F_a \times F_l \times P_m \quad (3\text{-}11)$$

with F_a given in Figure 3-9 and F_l given in Figure 3-10. When using P_d to calculate structural members, the following design areas should be used in conjunction with Figure 3-10.

Structural Member	Design Area
Shell Plating	plate area (a × b)
Longitudinal Stiffener	unsupported stiffener length × stringer spacing
Transverse Stiffener	unsupported stiffener length × stiffener spacing
Structural Grillage	unsupported stringer length × unsupported stiffener length

Nonstandard Hull Forms

Hydrofoils, air-cushion vehicles and surface effect ships should be evaluated up on foils or on-cushion, as well as for hullborne operational states. Vertical accelerations for hydrofoils up on foils should not be less than 1.5 g_0.

Transverse bending moments for multihulls and SWATH vessels are the product of displacement, vertical acceleration and beam and often dictate major hull scantlings. Transverse vertical shear forces are the product of displacement and vertical acceleration only.

Model tests are often required to verify primary forces and moments for nonstandard hull forms. [DnV *Rules for Classification of High Speed Light Craft* and NAVSEA *High Performance Craft Design Manual*]
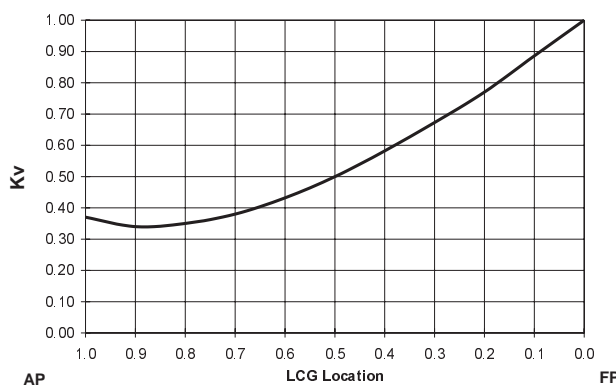
Figure 3-8 Longitudinal Impact Coefficient as a Function of Distance from Bow, k_V, Used in Vertical Acceleration Calculations [NAVSEA High Performance Craft Design Manual]
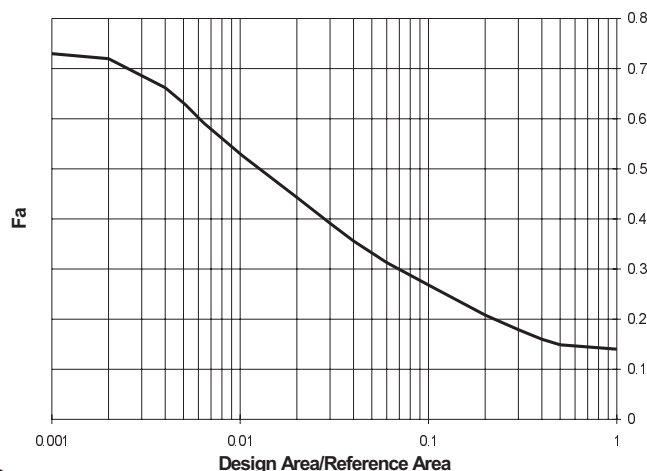
Figure 3-9 Design Area Coefficient Used in Design Pressure Calculations [NAVSEA High Performance Craft Design Manual]
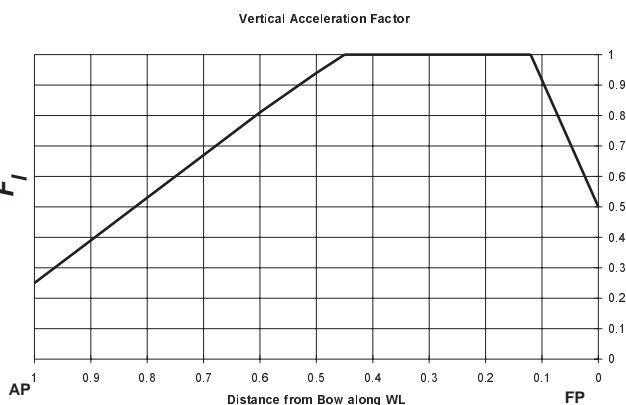
Figure 3-10 Longitudinal Pressure Distribution Used in Design Pressure Calculations [NAVSEA High Performance Craft Design Manual]

Hull Girder Stress Distribution

When the primary load forces act upon the hull structure as a long, slender beam, stress distribution patterns look like Figure 3-11 for the hogging condition with tension and compression interchanged for the sagging case. The magnitude of stress increases with distance from the neutral axis. On the other hand, shear stress is maximum at the neutral axis. Figure 3-12 shows the longitudinal distribution of principal stresses for a long, slender ship.

The relationship between bending moment and hull stress can be estimated from simple beam theory for the purposes of preliminary design. The basic relationship is stated as follows:

$$\sigma = \frac{M}{SM} = \frac{Mc}{I} \qquad (3-12)$$

where:

σ = unit stress

M = bending moment

SM = section modulus

c = distance to neutral axis

I = moment of inertia
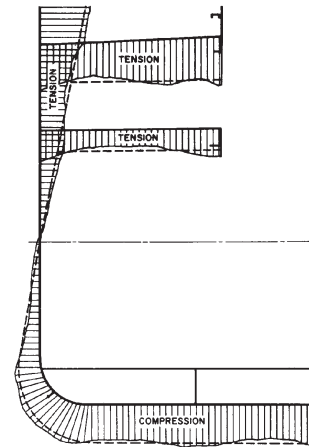
Figure 3-11 Theoretical and Measured Stress Distribution for a Cargo Vessel Midship Section [Principles of Naval Architecture]

The neutral axis is at the centroid of all longitudinal strength members, which for composite construction must take into account specific material properties along the ship's longitudinal axis. The actual neutral axis rarely coincides with the geometric center of the vessel's midship section. Hence, values for σ and c will be different for extreme fibers at the deck and hull bottom.
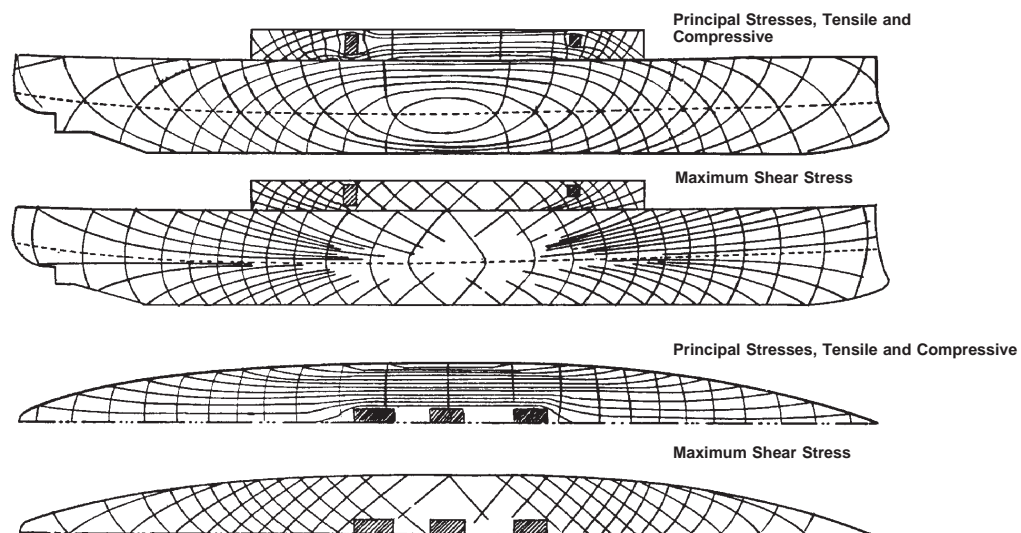
Principal Stresses, Tensile and Compressive

Maximum Shear Stress

Principal Stresses, Tensile and Compressive

Maximum Shear Stress

Figure 3-12 Longitudinal Distribution of Stresses in a Combatant [Hovgaard, *Structural Design of Warships*]

Lu & Jin have reported on an extensive design and test program that took place in China during the 1970's that involved a commercial hull form built using frame-stiffened, single-skin construction. Figure 3-13 shows the distribution of longitudinal strains and the arrangement of bending test strain gages used to verify the predicted hogging and sagging displacements of the 126 feet (38.5 meter) GRP hull studied. This study provided excellent insight into how a moderately-sized composite ship responds to hull girder loadings.
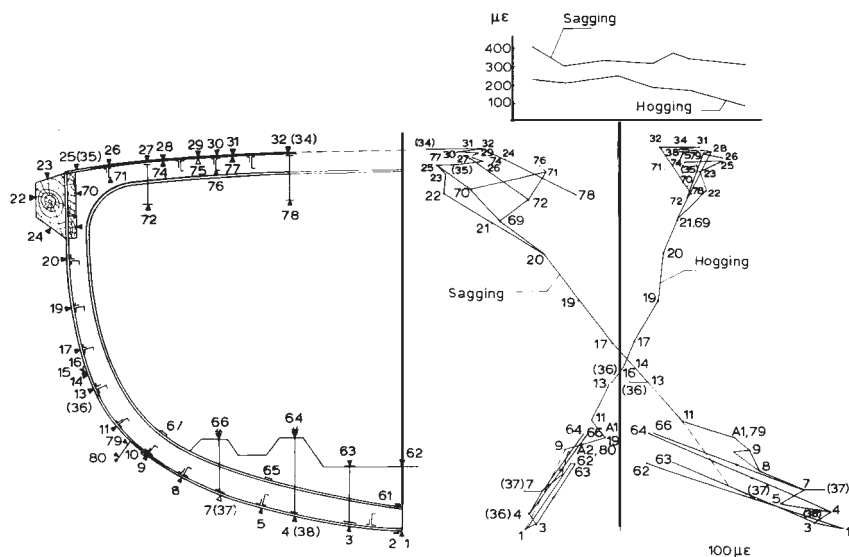
Figure 3-13 Distribution of Longitudinal Strains of a 38.5 Meter GRP Hull (above) and Longitudinal Strain Gage Location (below) [X.S. Lu & X.D. Jin, "*Structural Design and Tests of a Trial GRP Hull*," **Marine Structures**, Elsever, 1990]
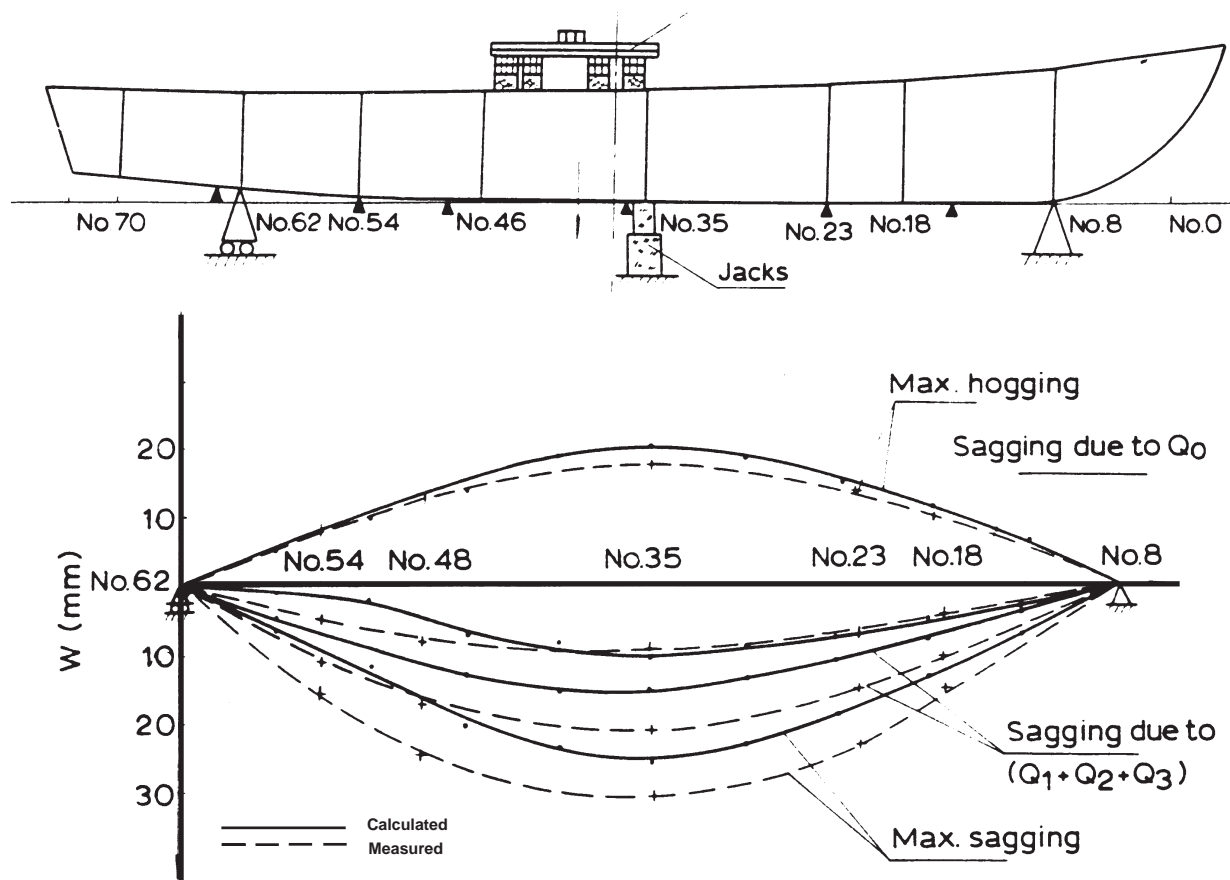
Figure 3-14 Predicted and Measured Vertical Displacements for a 38.5 Meter GRP Hull [X.S. Lu & X.D. Jin, "*Structural Design and Tests of a Trial GRP Hull*," **Marine Structures**, Elsever, 1990]

Other Hull and Deck Loads

Green water loading is used to calculate forces that hull side, topside and deck structure are exposed to in service. Green water loading is dependent on longitudinal vessel location and block coefficient (C_B) as well as the distance that a vessel will be from a safe harbor while in service. This methodology was originally published in the 1985 DnV *Rules for Classification of High Speed Light Craft*.

Hull Side Structure, Topsides and Weather Decks

The design pressure used for designing side shell structure that is above the chine or turn of the bilge but below the designed waterline is given by DnV as:

$$p = 0.44\, h_0 = \left[k_l - \frac{1.5\, h_0}{T} \right] 0.0035\, L \quad \text{(psi)} \qquad (3\text{-}13a)$$

$$p = 10\, h_0 = \left[k_l - \frac{1.5\, h_0}{T} \right] 0.08\, L \quad \text{(Mpa)} \qquad (3\text{-}13b)$$

where:

h_0 = vertical distance from waterline to the load point

k_l = longitudinal factor from Figure 3-15 based on C_B

$C_B = \dfrac{35\,\Delta}{L\,B\,T}$ (English units)

$\quad = \dfrac{\Delta}{1.025\,L\,B\,T}$ (metric units)

B = greatest molded breadth at load waterline

For side shell above the waterline and deck structure, design pressure is given as:

$$p = a\, k_l\, (c\, L - 0.053\, h_0) \qquad (3\text{-}14)$$

where:

for topsides:
a = 0.044 (English)
$\quad$ = 1.00 (metric)

for decks:
a = 0.035 (English)
$\quad$ = 0.80 (metric)

with a minimum pressure of 1 psi (6.5 Mpa) for topeside structure and 0.75 psi (5.0 Mpa) for decks. Service factor, c, is:

c	Nautical Miles Out
0.080	> 45
0.072	≤ 45
0.064	≤ 15
0.056	≤ 5
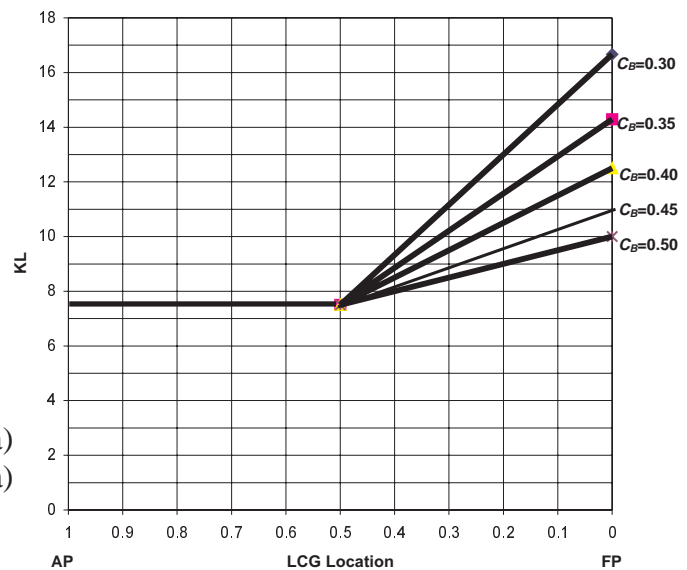
Figure 3-15   Green Water Distribution Factor, K_L [NAVSEA *High Performance Craft Design Manual*]

Deckhouses and Superstructures

For deckhouses and superstructure end bulkheads, the expression for design pressure is the same as for side shell structure above the waterline, where:

for lowest tier of superstructure not protected from weather:

$$a = 0.088 \text{ (English)}$$
$$= 2.00 \text{ (metric)}$$

for other superstructure and deckhouse front bulkheads:

$$a = 0.066 \text{ (English)}$$
$$= 1.50 \text{ (metric)}$$

for deckhouse sides:

$$a = 0.044 \text{ (English)}$$
$$= 1.00 \text{ (metric)}$$

elsewhere:

$$a = 0.035 \text{ (English)}$$
$$= 0.80 \text{ (metric)}$$

with a minimum pressure of $1.45 + 0.024\ L$ psi ($10 + 0.05\ L$ Mpa) for lowest tier of superstructure not protected from weather and $0.725 + 0.012\ L$ psi ($5 + 0.025\ L$ Mpa) elsewhere.

Compartment Flooding

Watertight bulkheads shall be designed to withstand pressures calculated by multiplying the vertical distance from the load point to the bulkhead top by the factor 0.44 (English units) or 10 (metric units) for collision bulkheads and 0.32 (English units) or 7.3 (metric units) for other watertight bulkheads.

Equipment & Cargo Loads

The design pressure from cargo and equipment are given by the expression:

$$p = 2.16 \times 10^{-3} (g_0 + 0.5\ a_v) \quad \text{(psi)} \qquad (3\text{-}15a)$$

$$p = \rho\ H\ (g_0 + 0.5\ a_v) \quad \text{(Mpa)} \qquad (3\text{-}15b)$$

For the metric expression, $\rho\ H = 1.6$ for machinery space; 1.0 for weather decks; and 0.35 for accommodation spaces. ρ shall be 0.7 and H shall be the vertical distance from the load point to the above deck for sheltered decks or inner bottoms. [14,15]

Chapter Four - Micromechanics

Although micromechanic concepts will not be considered every time a designer specifies a laminate schedule, it is instructive to understand how fibers and resin interact on a small scale. Texts on composite materials traditionally build from the concept of a single fiber in a resin matrix to a ply (all fibers in the same direction) and then a laminate, which consists of multiple plies. The distinction between plies and laminates is more acute with aerospace composites, as a greater quantity of thinner plies are used.

Highly engineered marine composite structures will make use of unidirectional reinforcements, and thus data for these products, both on-axis and off-axis, is presented. Engineering data for unidirectionals is very enticing. A designer may be tempted to use a minimum of these reinforcements to resist calculated loads. However, "unknown" loads often appear in large, complex structures and orientation of all reinforcement in a single direction can be fatal. As a rule of thumb, it is good to have at least 12% of the reinforcing fiber in each primary direction (0°, 90° and ± 45°).

Of greater value to the marine composites designer is data on typical marine laminates. A laminate can consist of a single ply of reinforcement that has fibers in various orientations. The simplest of these is woven roving, with fiber in the 0° and 90° directions. Multi-axial marine products can have fibers in the 0°, 90° and ± 45° directions. Available engineering data is presented in Appendix A for typical reinforcements tested in standard marine resin systems. These data are normalized to laminate thickness, which of course can vary as a function of fabrication method. Fiber volumes are noted where available. As will be emphasized throughout this text, as-built performance of marine laminates can vary substantially from published values and fabricators should build sample laminates under shop conditions and test these to verify minimum engineering values.

Mechanics of Composite Materials

The physical behavior of composite materials is quite different from that of most common engineering materials that are homogeneous and isotropic. Metals will generally have similar composition regardless of where or in what orientation a sample is taken. On the other hand, the makeup and physical properties of composites will vary with location and orientation of principal axes. These materials are termed anisotropic, which means they exhibit different properties when tested in different directions. Most composite structures are, however, orthotropic having three mutually perpendicular planes of symmetry.

The mechanical behavior of composites is traditionally evaluated on both microscopic and macroscopic scale to take into account inhomogeneity. Micromechanics attempts to quantify the interactions of fiber and matrix (reinforcement and resin) on a microscopic scale on par with the diameter of a single fiber. Macromechanics treats composites as homogeneous materials with mechanical properties representative of the medium as a whole. The latter analytical approach is more realistic for the study of marine laminates that are often thick and laden with through-laminate inconsistencies. However, it is instructive to understand the concepts of micromechanics as the basis for macromechanic properties. The designer is again cautioned to verify all analytical work by testing builder's specimens.

Micromechanic Theory

General Fiber/Matrix Relationship
The theory of micromechanics was developed to help explain the complex mechanisms of stress and strain transfer between fiber and matrix within a composite. [16] Mathematical relationships have been developed whereby knowledge of constituent material properties can lead to laminate behavior predictions. Theoretical predictions of composite stiffness have traditionally been more accurate than predictions of ultimate strength. Table 4-1 describes the input and output variables associated with micromechanics.

Table 4-1 Micromechanics Concepts
[Chamis, ASM Engineers' Guide to Composite Materials]

Input	Output
Fiber properties	Uniaxial strengths
Matrix properties	Fracture toughness
Environmental conditions	Impact resistance
Fabrication process variables	Hygrothermal effects
Geometric configuration	
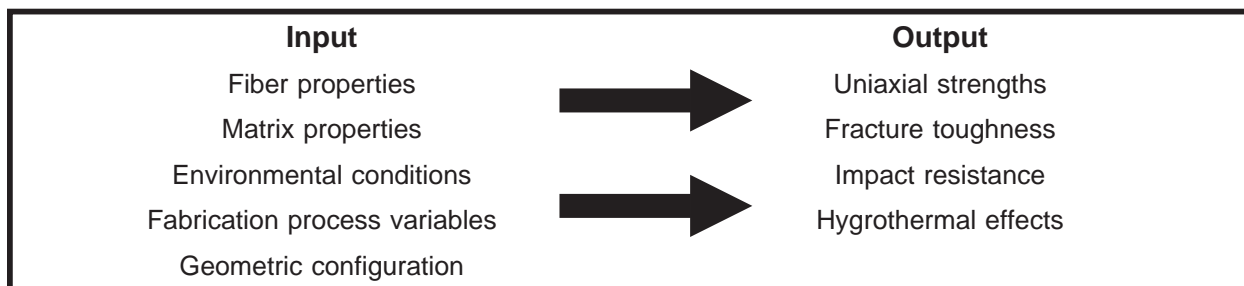
The basic principles of the theory can be illustrated by examining a composite element under a uniaxial force. Figure 4-1 shows the state of stress and transfer mechanisms of fiber and matrix when subjected to pure tension. On a macroscopic scale, the element is in simple tension, while internally a number of stresses can be present. Represented in Figure 4-1 are compressive stresses (vertical arrows pointing inwards) and shear stresses (thinner arrows along the fiber/matrix interface). This combined stress state will determine the failure point of the material. The bottom illustration in Figure 4-1 is representative of a poor fiber/matrix bond or

void within the laminate. The resulting imbalance of stresses between the fiber and matrix can lead to local instability causing the fiber to shift or buckle. A void along 1% of the fiber surface generally reduces interfacial shear strength by 7%. [16]

Fiber Orientation

Orientation of reinforcements in a laminate is widely known to dramatically effect the mechanical performance of composites. Figure 4-2 is presented to understand tension failure mechanisms in unidirectional composites on a microscopic scale. Note that at an angle of 0°, the strength of the composite is almost completely dependent on fiber tensile strength. The following equations refer to the three failure mechanisms shown in Figure 4-2:

Fiber tensile failure:

$$\sigma_c = \sigma \qquad (4\text{-}1)$$

Matrix or interfacial shear:

$$\tau = \sigma \sin\Phi \cos\Phi \quad (4\text{-}2)$$

Composite tensile failure:

$$\sigma_u = \sigma \sin\Phi \qquad (4\text{-}3)$$

where:

σ_c = composite tensile strength

σ = applied stress

Φ = angle between the fibers and tensile axis

τ = shear strength of the matrix or interface

σ_u = tensile strength of the matrix
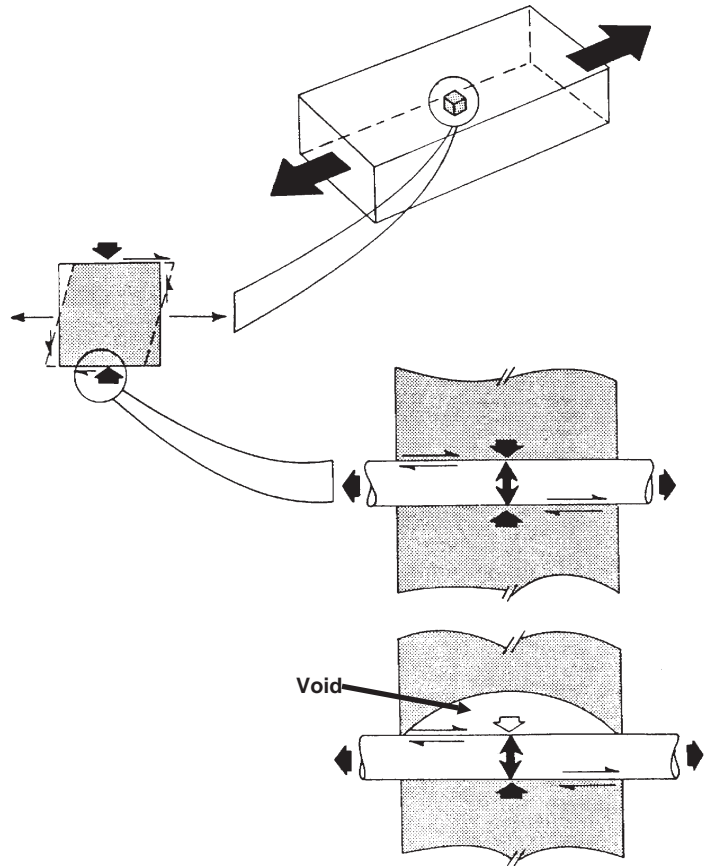
Figure 4-1   State of Stress and Stress Transfer to Reinforcement [*Material Engineering*, May, 1978 p. 29]
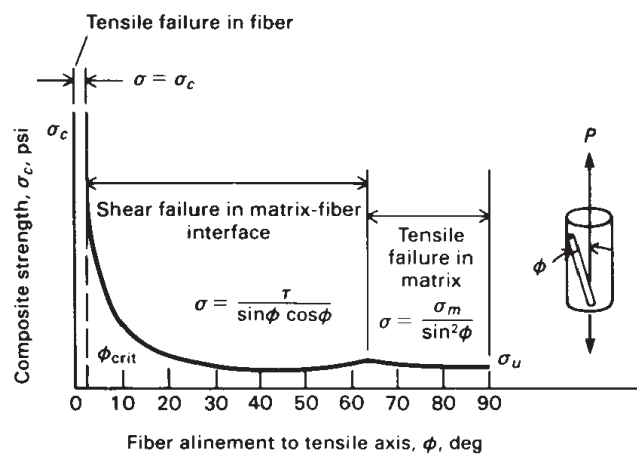
Figure 4-2   Failure Mode as a Function of Fiber Alignment [*ASM Engineers' Guide to Composite Materials*]

Micromechanics Geometry

Figure 4-3 shows the orientation and nomenclature for a typical fiber composite geometry. Properties along the fiber or x direction (1-axis) are called longitudinal; transverse or y (2-axis) are called transverse; and in-plane shear (1-2 plane) is also called intralaminar shear. The through-thickness properties in the z direction (3-axis) are called interlaminar. Ply properties are typically denoted with a letter to describe the property with suitable subscripts to describe the constituent material, plane, direction and sign (with strengths). As an example, $S_{m\,11T}$ indicates matrix longitudinal tensile strength.

The derivation of micromechanics equations is based on the assumption that 1) the ply and its constituents behave linearly elastic until fracture (see Figure 4-4), 2) bonding is complete between fiber and matrix and 3) fracture occurs in one of the following modes: a) longitudinal tension, b) fiber compression, c) delamination, d) fiber microbuckling, e) transverse tension, or f) intralaminar shear. [2] The following equations describe the basic geometric relationships of composite micromechanics:

Partial volumes:

$$k_f + k_m + k_v = 1 \qquad (4\text{-}4)$$

Ply density:

$$\rho_l = k_f\ \rho_f + k_m\ \rho_m \qquad (4\text{-}5)$$

Figure 4-3 Fiber Composite Geometry [Chamis, *ASM Engineers' Guide to Composite Materials*]
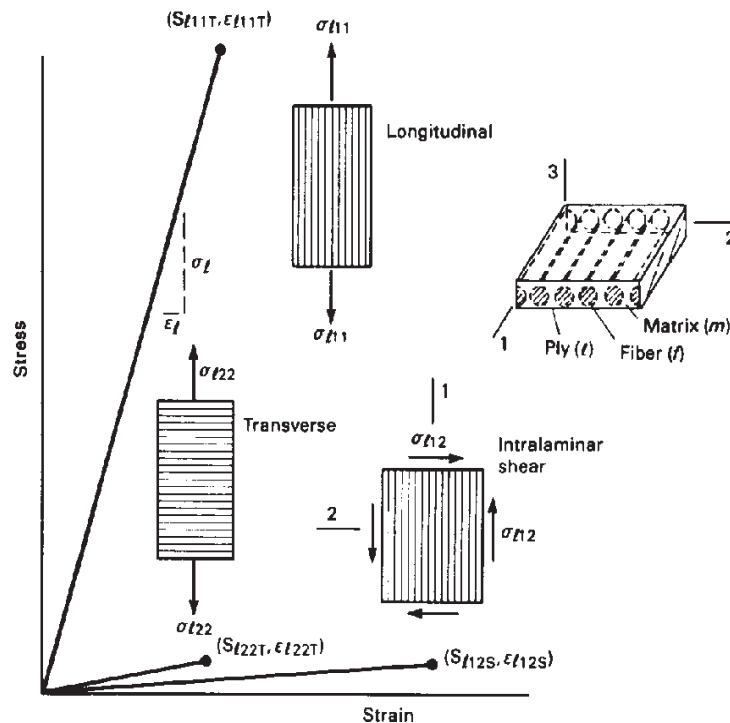
Figure 4-4 Typical Stress-Strain Behavior of Unidirectional Fiber Composites [Chamis, *ASM Engineers' Guide to Composite Materials*]

Resin volume ratio:

$$k_m = \frac{(1 -- k_v)}{\left[1 + \left(\dfrac{\rho_m}{\rho_f}\right)\left(\dfrac{1}{\lambda_m} - 1\right)\right]}$$ (4-6)

Fiber volume ratio:

$$k_f = \frac{(1 -- k_v)}{\left[1 + \left(\dfrac{\rho_f}{\rho_m}\right)\left(\dfrac{1}{\lambda_f} - 1\right)\right]}$$ (4 -7)

Weight ratio:

$$\lambda_f + \lambda_m = 1$$ (4-8)

where:

f = fiber
m = matrix
v = void
l = ply
λ = weight percent
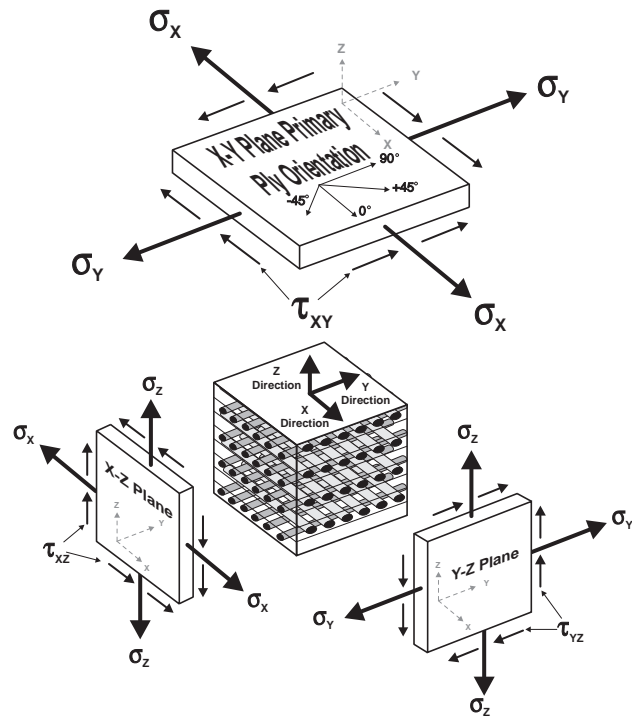
Figure 4-5   Notation Typically Used to Describe Ply Properties

Elastic Constants

The equations for relating elastic moduli and Poisson's ratios are given below. Properties in the 3-axis direction are the same as the 2-axis direction because the ply is assumed transversely isotropic in the 2-3 plane (see bottom illustration of Figure 4-3).

Longitudinal modulus:

$$E_{l\,11} = k_f\,E_{f\,11} + k_m E_m$$ (4-9)

Transverse modulus:

$$E_{l\,22} = \frac{E_m}{1 - \sqrt{k_f}\left(1 - \dfrac{E_m}{E_{f\,22}}\right)} = E_{l\,33}$$ (4-10)

Shear modulus:

$$G_{l\,12} = \frac{G_m}{1 - \sqrt{k_f}\left(1 - \dfrac{G_m}{G_{f\,12}}\right)} = G_{l\,13}$$ (4-11)

$$G_{l\,23} = \frac{G_m}{1 - \sqrt{k_f}\left(1 - \dfrac{G_m}{G_{f\,23}}\right)} = G_{l\,13}$$ (4-12)

Poisson's ratio:

$$\nu_{l\,12} = k_f\,\nu_{l\,12} + k_m\,\nu_m = \nu_{l\,13}$$ (4-13)

In-Plane Uniaxial Strengths

The equations for approximating composite strength properties are based on the fracture mechanisms outlined above under micromechanics geometry. Three of the fracture modes fall under the heading of longitudinal compression. It should be emphasized that prediction of material strength properties is currently beyond the scope of simplified mathematical theory. The following approximations are presented to give insight into which physical properties dominate particular failure modes.

Approximate longitudinal tension:

$$S_{l\,11T} \approx k_f\,S_{f\,T} \tag{4-14}$$

Approximate fiber compression:

$$S_{l\,11C} \approx k_f\,S_{f\,C} \tag{4-15}$$

Approximate delamination/shear:

$$S_{l\,11C} \approx 10\,S_{l\,12S} + 2.5 S_{m\,T} \tag{4-16}$$

Approximate microbuckling:

$$S_{l\,11C} \approx \frac{G_m}{1 - k_f\left(1 - \dfrac{G_m}{G_{f\,12}}\right)} \tag{4-17}$$

Approximate transverse tension:

$$S_{l\,22T} \approx \left[1 - \left(\sqrt{k_f} - k_f\right)\left(1 - \frac{E_m}{E_{f\,22}}\right)\right] S_{m\,T} \tag{4-18}$$

Approximate transverse compression:

$$S_{l\,22C} \approx \left[1 - \left(\sqrt{k_f} - k_f\right)\left(1 - \frac{E_m}{E_{f\,22}}\right)\right] S_{m\,C} \tag{4-19}$$

Approximate intralaminar shear:

$$S_{l\,12S} \approx \left[1 - \left(\sqrt{k_f} - k_f\right)\left(1 - \frac{G_m}{G_{f\,12}}\right)\right] S_{m\,S} \tag{4-20}$$

Approximate void influence on matrix:

$$S_m \approx \left\{1 - \left[\frac{4 k_v}{(1 - k_f)\,\pi}\right]^{1/2}\right\} S_m \tag{4-21}$$

Through-Thickness Uniaxial Strengths

Estimates for properties in the 3-axis direction are given by the equations below. Note that the interlaminar shear equation is the same as that for in-plane. The short beam shear depends heavily on the resin shear strength and is about $1\frac{1}{2}$ times the interlaminar value. Also, the longitudinal flexural strength is fiber dominated while the transverse flexural strength is more sensitive to matrix strength.

Approximate interlaminar shear:

$$S_{l\,13S} \approx \left[1 - \left(\sqrt{k_f} - 1 \right) \left(1 - \frac{G_m}{G_{f\,12}} \right) \right] S_{mS} \tag{4-22}$$

$$S_{l\,23S} \approx \left[\frac{1 - \sqrt{k_f} \left(1 - \frac{G_m}{G_{f\,23}} \right)}{1 - k_f \left(1 - \frac{G_m}{G_{f\,23}} \right)} \right] S_{mS} \tag{4-23}$$

Approximate flexural strength:

$$S_{l\,11F} \approx \frac{3\,k_f\,S_{f\,T}}{1 + \dfrac{S_{f\,T}}{S_{f\,C}}} \tag{4-24}$$

$$S_{l\,22F} \approx \frac{3 \left[1 - \left(\sqrt{k_f} - k_f \right) \left(1 - \frac{E_m}{E_{f\,22}} \right) \right] S_{m\,T}}{1 + \dfrac{S_{m\,T}}{S_{m\,C}}} \tag{4-25}$$

Approximate short-beam shear:

$$S_{l\,13SB} \approx 1.5\,S_{l\,13S} \tag{4-26}$$

$$S_{l\,23SB} \approx 1.5\,S_{l\,23S} \tag{4-27}$$

Uniaxial Fracture Toughness

Fracture toughness is an indication of a composite material's ability to resist defects or discontinuities such as holes and notches. The fracture modes of general interest include: opening mode, in-plane shear and out-of-plane shear. The equations to predict longitudinal, transverse and intralaminar shear fracture toughness are beyond the scope of this text and can be found in the cited reference. [2]

In-Plane Uniaxial Impact Resistance

The impact resistance of unidirectional composites is defined as the in-plane uniaxial impact energy density. The five densities are: longitudinal tension and compression; transverse tension and compression; and intralaminar shear. The reader is again directed to reference [2] for further elaboration.

Through-Thickness Uniaxial Impact Resistance

The through-thickness impact resistance is associated with impacts normal to the surface of the composite, which is generally of particular interest. The energy densities are divided as

follows: longitudinal interlaminar shear, transverse interlaminar shear, longitudinal flexure, and transverse flexure. The derivation of equations and relationships for this and the remaining micromechanics phenomena can be found in reference [2].

Thermal

The following thermal behavior characteristics for a composite are derived from constituent material properties: heat capacity, longitudinal conductivity, and longitudinal and transverse thermal coefficients of expansion.

Hygral Properties

The ply hygral properties predicted by micromechanics equation include diffusivity and moisture expansion. Additional equations have been derived to estimate moisture in the resin and composite as a function of the relative humidity ratio. An estimate for moisture expansion coefficient is also postulated.

Hygrothermal Effects

The combined environmental effect of moisture and temperature is usually termed hygrothermal. All of the resin dominated properties are particularly influenced by hygrothermal influences. The degraded properties that are quantified include: glass transition temperature of wet resin, strength and stiffness mechanical characteristics, and thermal behavior.

Laminate Theory

Laminae or Plies

The most elementary level considered by macromechanic theory is the lamina or ply. This consists of a single layer of reinforcement and associated volume of matrix material. In aerospace applications, all specifications are expressed in terms of ply quantities. Marine applications typically involve thicker laminates and are usually specified according to overall thickness, especially when successive plies are identical.

For most polymer matrix composites, the reinforcement fiber will be the primary load carrying element because it is stronger and stiffer than the matrix. The mechanism for transferring load throughout the reinforcement fiber is the shearing stress developed in the matrix. Thus, care must be exercised to ensure that the matrix material does not become a strain limiting factor. As an extreme example, if a polyester reinforcement with an ultimate elongation of about 20% was combined with a polyester resin with 1.5% elongation to failure, cracking of the resin would occur before the fiber was stressed to a level that was 10% of its ultimate strength.

Laminates

A laminate consists of a series of laminae or plies that are bonded together with a material that is usually the same as the matrix of each ply. Indeed, with contact molding, the wet-out and laminating processes are continuous operations. A potential weak area of laminates is the shear strength between layers of a laminate, especially when the entire lamination process is not continuous.

A major advantage to design and construction with composites is the ability to vary reinforcement material and orientation throughout the plies in a laminate. In this way, the physical properties of each ply can be optimized to resist the loading on the laminate as a whole, as well as the out of plane (through thickness) loads that create unique stress fields in each ply. Figure 4-6 illustrates the concept of stress field discontinuity within a laminate.
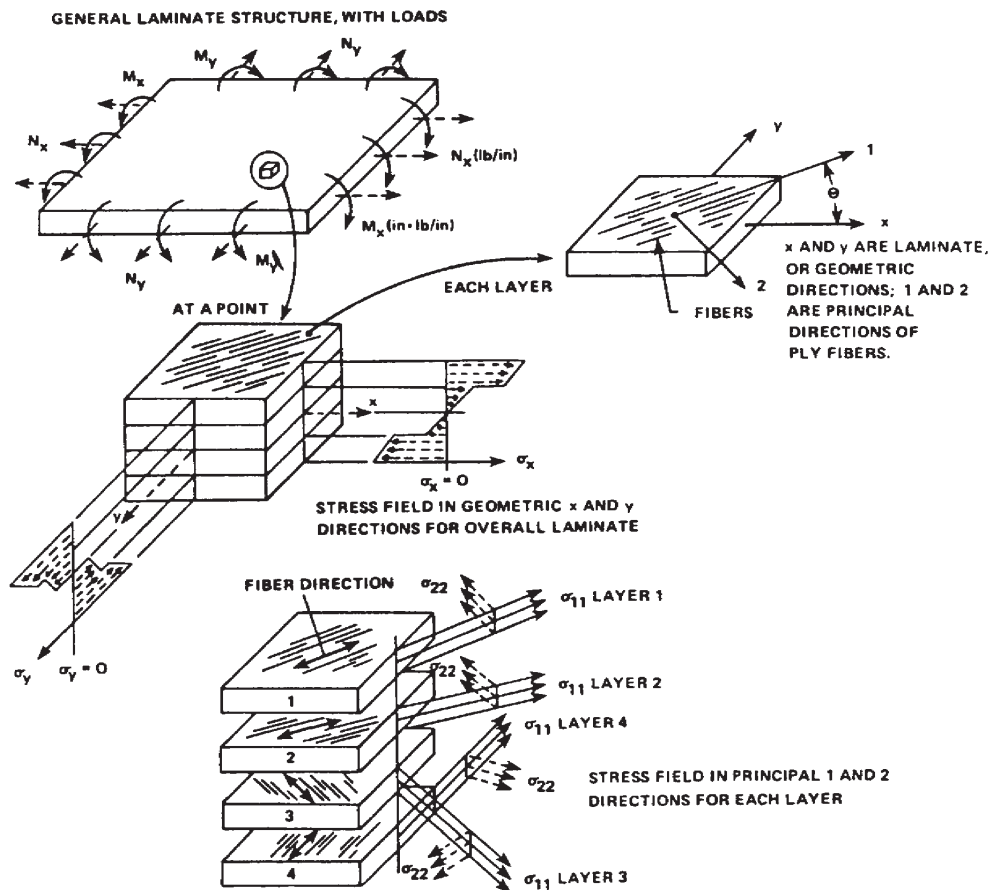
Figure 4-6 Elastic Properties of Plies within a Laminate [Schwartz, *Composite Materials Handbook*]

Laminate Properties

Predicting the physical properties of laminates based on published data for the longitudinal direction (1-axis) is not very useful as this data was probably derived from samples fabricated in a very controlled environment. Conditions under which marine laminates are fabricated can severely limit the resultant mechanical properties. To date, safety factors have generally been sufficiently high to prevent widespread failure. However, instances of stress concentrations, resin-rich areas and voids can negate even large safety factors.

There are essentially three ways in use today to predict the behavior of a laminated structure under a given loading scenario. In all cases, estimates for Elastic properties are more accurate than those for Strength properties. This is in part due to the variety of failure mechanisms involved. The analytical techniques currently in use include:

- Property charts called "Carpet Plots" that provide mechanical performance data based on orientation composition of the laminate;

- Laminate analysis software that allows the user to build a laminate from a materials database and view the stress and strain levels within and between plies in each of the three mutually perpendicular axes;

- Test data based on identical laminates loaded in a similar fashion to the design case.

Carpet Plots

Examples of Carpet Plots based on a Carbon Fiber/Epoxy laminate are shown in Figures 4-7, 4-8 and 4-9 for modulus, Poisson's ratio, and strength respectively. The bottom axis shows the percentage of ±45° reinforcement. "Iso" lines within the graphs correspond to the percentage of 0° and 90° reinforcement. The resultant mechanical properties are based on the assumption of uniaxial loading (hence, values are for longitudinal properties only) and assume a given design temperature and design criterion (such as B-basis where there is 90% confidence that 95% of the failures will exceed the value). [2] Stephen Tsai, an acknowledged authority on composites design, has dismissed this technique as a valid design tool in favor of the more rigorous laminated plate theory. [17]

Carpet plots have been a common preliminary design tool within the aerospace industry where laminates typically consist of a large number of thin plies. Additionally, out of plane loads are not of primary concern as is the case with marine structures. An aerospace designer essentially views a laminate as a homogeneous engineering material with some degraded mechanical properties derived from carpet plots. Typical marine laminates consist of much fewer plies that are primarily not from unidirectional reinforcements. Significant out of plane loading and high aspect ratio structural panels render the unidirectional data from carpet plots somewhat meaningless for designing FRP marine structures.
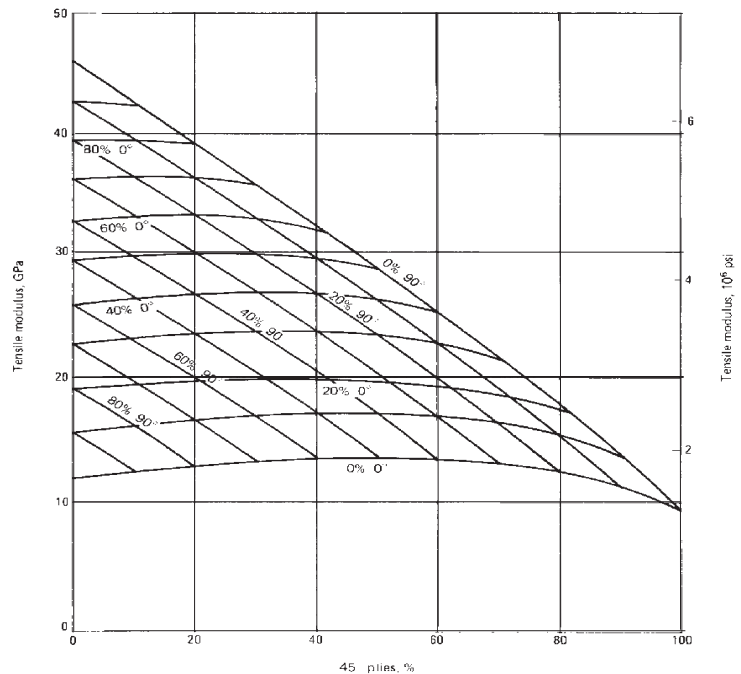
Figure 4-7 Carpet Plot Illustrating Laminate Tensile Modulus [*ASM Engineered Materials Handbook*]
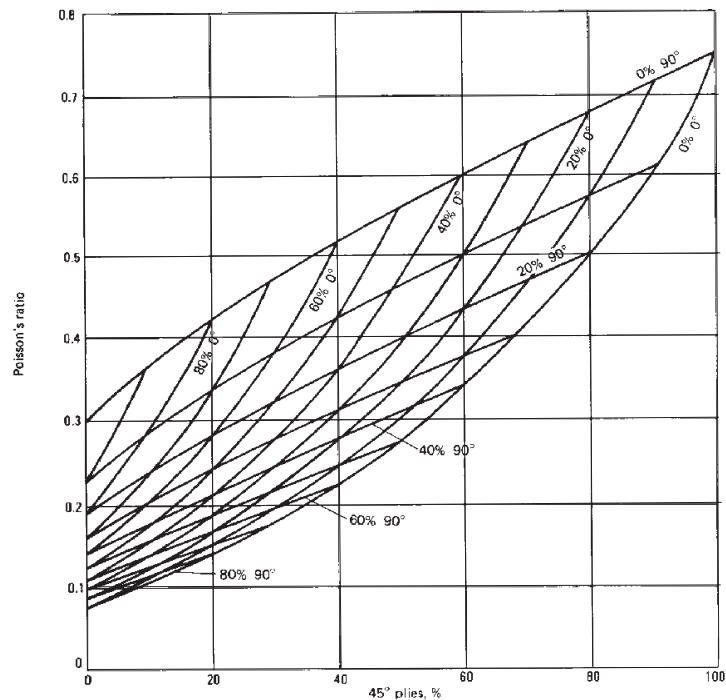
Figure 4-8 Carpet Plot Illustrating Poisson's Ratio [*ASM Engineered Materials Handbook*]

Computer Laminate Analysis

There are a number of structural analysis computer programs available for workstations or advanced PC computers that use finite-element or finite-difference numerical methods and are suitable for evaluating composites. In general, these programs will address:

- Structural response of laminated and multidirectional reinforced composites;

- Changes in material properties with temperature, moisture and ablative decomposition;

- Thin-shelled, thick-shelled, and/or plate structures;

- Thermal-, pressure- traction-, deformation- and vibration-induced load states;

- Failure modes;

- Non-linearity;

- Structural instability; and

- Fracture mechanics.
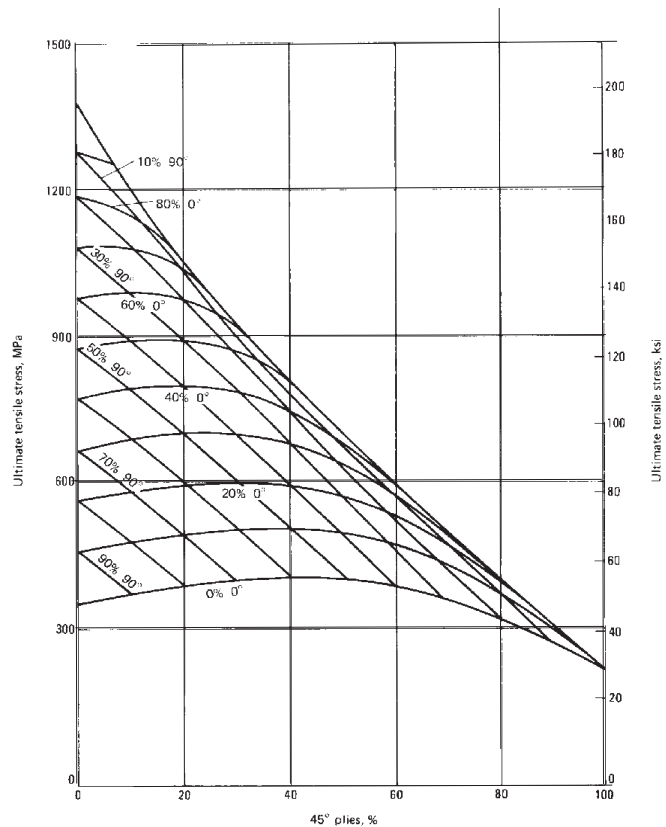
Figure 4-9 Carpet Plot Illustrating Tensile Strength [*ASM Engineered Materials Handbook*]

The majority of these codes for mainframes are quite expensive to acquire and operate, which precludes their use for general marine structures. Specialized military applications such as a pressure hull for a torpedo or a highly stressed weight critical component might justify analysis with these sort of programs. [2]

More useful to the marine designer, are the PC based laminate analysis programs that allow a number of variations to be evaluated at relatively low cost. The software generally costs less than $500 and can run on hardware that is probably already integrated into a design office. The better programs are based on laminated plate theory and do a reasonable job of predicting first ply failure in strain space. Prediction of ultimate strengths with materials that enter non-elastic regions, such as foam cores, will be of limited accuracy. Some other assumptions in laminated plate theory include: [2]

- The thickness of the plate is much smaller than the in-plane dimensions;

- The strains in the deformed are small compared to unity;

- Normal to the undeformed plate surface remain normal to the deformed plate surface;

- Vertical deflection does not vary through the thickness; and

- Stress normal to the plate surface is negligible.

For a detailed description of laminated plate theory, the reader is advised to refer to *Introduction to Composite Materials*, by S.W. Tsai and H.T. Hahn, Technomic, Lancaster, PA (1985).

Table 4-2 illustrates a typical range of input and output variables for computer laminate analysis programs. Some programs are menu driven while others follow a spreadsheet format. Once material properties have been specified, the user can "build" a laminate by selecting materials and orientation. As a minimum, stresses and strains failure levels for each ply will be computed. Some programs will show stress and strain states versus design allowables based on various failure criteria. Most programs will predict which ply will fail first and provide some routine for laminate optimization. In-plane loads can usually be entered to compute predicted states of stress and strain instead of failure envelopes.

Table 4-2 Typical Input and Output Variables for Laminate Analysis Programs

Input		Output	
Load Conditions	**Material Properties**	**Ply Properties**	**Laminate Response**
Longitudinal In-Plane Loads	Modulus of Elasticity	Thicknesses*	Longitudinal Deflection
Transverse In-Plane Loads	Poisson's Ratio	Orientation*	Transverse Deflection
Vertical In-Plane Loads (shear)	Shear Modulus	Fiber Volume*	Vertical Deflection
Longitudinal Bending Moments	Longitudinal Strength	Longitudinal Stiffness	Longitudinal Strain
Transverse Bending Moments	Transverse Strength	Transverse Stiffness	Transverse Strain
Vertical Moments (torsional)	Shear Strength	Longitudinal Poisson's Ratio	Vertical Strain
Failure Criteria	Thermal Expansion Coefficients	Transverse Poisson's Ratio	Longitudinal Stress per Ply
Temperature Change		Longitudinal Shear Modulus	Transverse Stress per Ply
		Transverse Shear Modulus	Vertical Stress (shear) per Ply
			First Ply to Fail
			Safety Factors
*These ply properties are usually treated as input variables			

Failure Criteria

Failure criteria used for analysis of composites structures are similar to those in use for isotropic materials, which include maximum stress, maximum strain and quadratic theories. [17]   These criteria are empirical methods to predict failure when a laminate is subjected to a state of combined stress. The multiplicity of possible failure modes (i.e. fiber vs. laminate level) prohibits the use of a more rigorously derived mathematical formulation.   Specific failure modes are described in Chapter Six.   The basic material data required for two-dimensional failure theory is longitudinal and transverse tensile, and compressive as well as longitudinal shear strengths.

Maximum Stress Criteria

Evaluation of laminated structures using this criteria begins with a calculation of the strength/stress ratio for each stress component.   This quantity expresses the relationship between the maximum, ultimate or allowable strength, and the applied corresponding stress.   The lowest ratio represents the mode that controls ply failure.   This criteria ignores the complexities of composites failure mechanisms and the associated interactive nature of the various stress components.

Maximum Strain Criteria

The maximum strain criteria follows the logic of the maximum stress criteria.   The maximum strain associated with each applied stress field is calculated by dividing strengths by moduli of elasticity when this is known for each ply.   The dominating failure mode is that which produces the highest strain level.   Simply stated, failure is controlled by the ply that first reaches its elastic limit.   This concept is important to consider when designing hybrid laminates that contain low strain materials, such as carbon fiber.   Both the maximum stress and maximum strain criteria can be visualized in two-dimensional space as a box with absolute positive and negative values for longitudinal and transverse axes.   This failure envelope implies no interaction between the stress fields and material response.   Structural design considerations (strength vs. stiffness) will dictate whether stress or strain criteria is more appropriate.

Quadratic Criteria for Stress and Strain Space

One way to include the coupling effects (Poisson phenomena) in a failure criteria is to use a theory based on distortional energy.   The resultant failure envelope is an ellipse which is very oblong.   A constant, called the normalized empirical constant, which relates the coupling of strength factors, generally falls between $-\frac{1}{2}$ (von Mises criteria) and 0 (modified Hill criteria). [17]   A strain space failure envelope is more commonly used for the following reasons:

- Plotted data is less oblong;

- Data does not vary with each laminate;

- Input properties are derived more reliably; and

- Axes are dimensionless.

First- and Last-Ply to Failure Criteria

These criteria are probably more relevant with aerospace structures where laminates may consist of over 50 plies.   The theory of first-ply failure suggests an envelope that describes the failure of the first ply.   Analysis of the laminate continues with the contribution from that and successive plies removed.   With the last ply to failure theory, the envelope is developed that corresponds to failure of the final ply in what is considered analogous to ultimate failure.   Each of these concepts fail to take into account the contribution of a partially failed ply or the geometric coupling effects of adjacent ply failure.

Laminate Testing

Laminates used in the marine industry are typically characterized using standard ASTM tests. Multiple laminates, usually a minimum of $\frac{1}{8}$ inch (3 mm) thick, are used for testing and results are reported as a function of cross-sectional area, i.e. width × thickness. Thus, thickness of the laminate tested is a critical parameter influencing the reported data. High fiber laminates that are consolidated with vacuum pressure will be thinner than standard open mold laminates, given the same amount of reinforcement. Test data for these laminates will be higher, although load carrying capability may not be. The following ASTM tests were used to generate the laminate data presented in Appendix A. Comments regarding the application of these tests to typical marine laminates is also included. Appendix B contains a listing of all current ASTM tests relevant to composite laminates

Tensile Tests

These test methods provide procedures for the evaluation of tensile properties of single-skin laminates. The tests are performed in the axial, or in-plane orientation. Properties obtained can include tensile strength, tensile modulus, elongation at break (strain to failure), and Poisson's ratio.

For most oriented fiber laminates, a rectangular specimen is preferred. Panels fabricated of resin alone (resin casting) or utilizing randomly oriented fibers (such as chopped strand) may be tested using dog-bone (dumbbell) type specimens. Care must be taken when cutting test specimens to assure that the edges are aligned in the axis under test. The test axis or orientation must be specified for all oriented-fiber laminates.
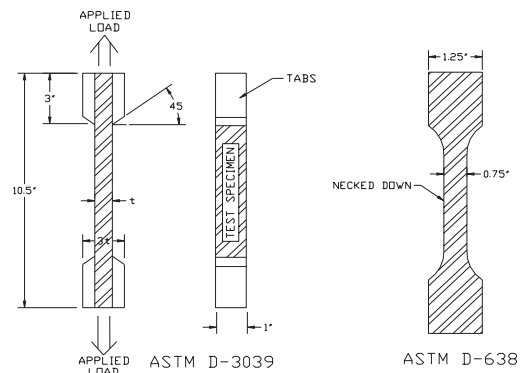
Figure 4-10 Test Specimen Configuration for ASTM D-3039 and D-638 Tensile Tests (Structural Composites, Inc.)

Tensile Test Methods	
ASTM D 3039	Tensile Properties of Polymer Matrix Composite Materials
	Specimen Type: Rectangular, with tabs
ASTM D 638	Tensile Properties of Plastics
	Specimen Type: Dumbbell
ISO 3268	Plastics - Glass-Reinforced Materials - Determination of Tensile Properties
	Specimen Type: Type I Dumbbell
	Type II Rectangular, no tabs
	Type III Rectangular, with tabs
SACMA SRM 4	Tensile Properties of Oriented Fiber-Resin Composites
	Specimen Type: Rectangular, with tabs
SACMA SRM 9	Tensile Properties of Oriented Cross-Plied Fiber-Resin Composites
	Specimen Type: Rectangular, with tabs

Compressive Tests

Several methods are available for determination of the axial (in-plane, edgewise, longitudinal) compression properties. The procedures shown are applicable for single-skin laminates. Other methods are utilized for determination of "edgewise" and "flatwise" compression of sandwich composites. Properties obtained can include compressive strength and compressive modulus.

For most oriented fiber laminates, a rectangular specimen is preferred. Panels fabricated of randomly oriented fibers such as chopped strand may be tested using dog-bone (dumbbell) type specimens.

Compressive Test Methods	
ASTM D 3410	Compressive Properties of Unidirectional or Crossply Fiber-Resin Composites
	Specimen Type: Rectangular, with tabs
ASTM D 695	Compressive Properties of Rigid Plastics
	Specimen Type: Rectangular or dumbbell
ISO 604	Plastics - Determination of Compressive Properties
	Specimen Type: Rectangular
SACMA SRM 1	Compressive Properties of Oriented Fiber-Resin Composites
	Specimen Type: Rectangular, with tabs
SACMA SRM 6	Compressive Properties of Oriented Cross-Plied Fiber-ResinComposites
	Specimen Type: Rectangular, with tabs
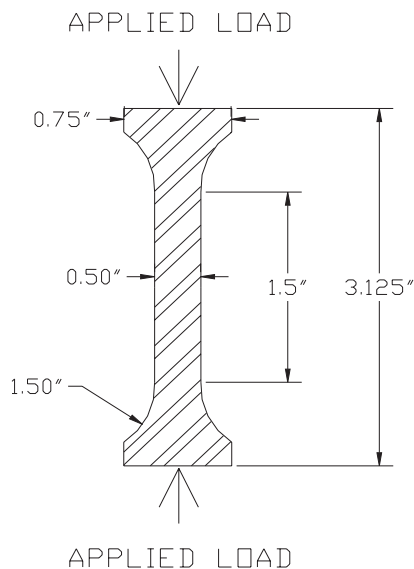
Figure 4-11   Test Specimen Configuration for ASTM D-695 Compression Test
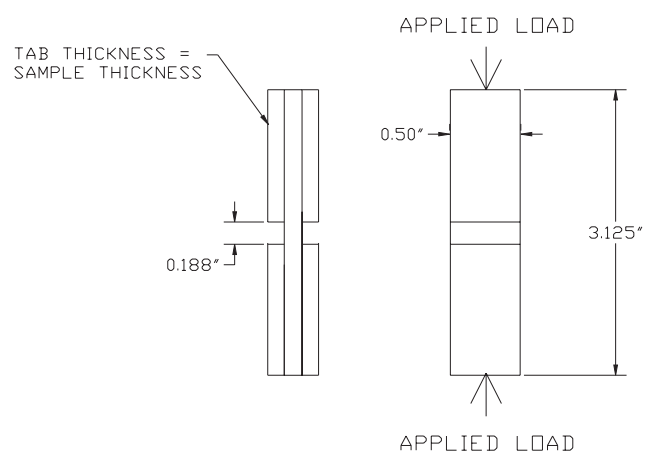
Figure 4-12   Test Specimen Configuration for SACMA SRM-1 Compression Test

Flexural Tests

For evaluation of mechanical properties of flat single-skin laminates under bending (flexural) loading, several standard procedures are available. The methods all involve application of a load which is out-of-plane, or normal to, the flat plane of the laminate. Properties obtained include flexural strength and flexural modulus.

Rectangular specimens are required regardless of reinforcement type. Unreinforced resin castings may also be tested using these procedures. Generally, a support span-to-sample depth ratio of between 14:1 and 20:1 is utilized (support span is 14-20 times the average laminate thickness). Load may be applied at the midpoint of the beam (3-point loading), or a 4-point loading scheme may be used. Flexural tests are excellent for comparing laminates of similar geometry and are often used in Quality Assurance programs.
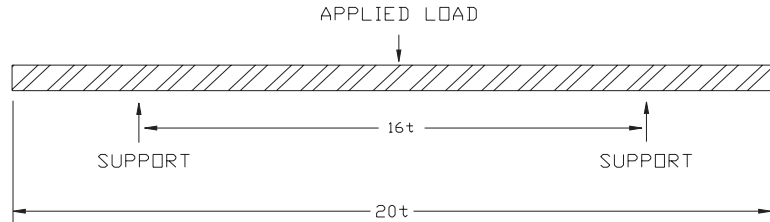

```
                    APPLIED LOAD

|////////////////////////////////////////////////|
       |<------------- 16t ------------->|
    SUPPORT                            SUPPORT
|<----------------------- 20t ----------------------->|


NOTES: 1)   SAMPLE WIDTH = 1"
       2)   LOAD APPLIED IN
            MIDDLE OF SUPPORT
            SPAN
```

Figure 4-13   Test Specimen Configuration for ASTM D-790 Flexural Test, Method I, Procedure A

Flexural Test Methods	
ASTM D 790	Flexural Properties of Unreinforced and Reinforced Plastics and Electrical Insulating Materials
	Method I 3-point bending
	Method II 4-point bending
ISO 178	Plastics - Determination of Flexural Properties
	3-point bending

Shear Tests

Many types of shear tests are available, depending on which plane of the single-skin laminate is to be subjected to the shear force. Various "in-plane" and "interlaminar" shear methods are commonly used. Confusion exists as to what properties are determined by the tests, however. The "short-beam" methods also are used to find "interlaminar" properties.

Through-plane shear tests are utilized for determination of out-of-plane shear properties, such as would be seen when drawing a screw or a bolt out of a panel. The load is applied perpendicular to, or "normal" to, the flat plane of the panel.

Properties obtained by these tests are shear strength, and in some cases, shear modulus.
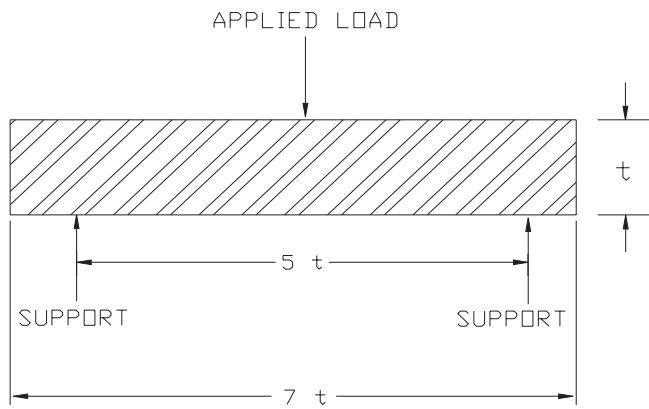
Figure 4-14   Test Specimen Configuration for ASTM D-2344 Short Beam Shear Test
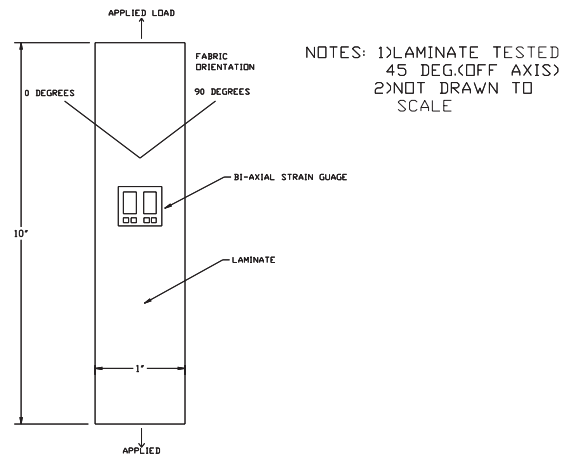
Figure 4-15   Test Specimen Configuration for ASTM D-3518 In-Plane Shear Test
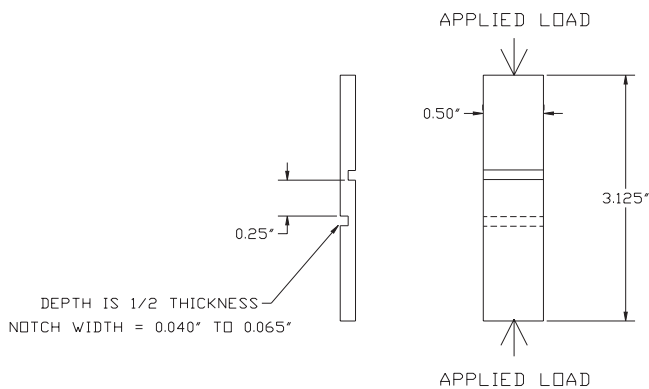
Figure 4-16   Test Specimen Configuration for ASTM D-3846 In-Plane Shear Test
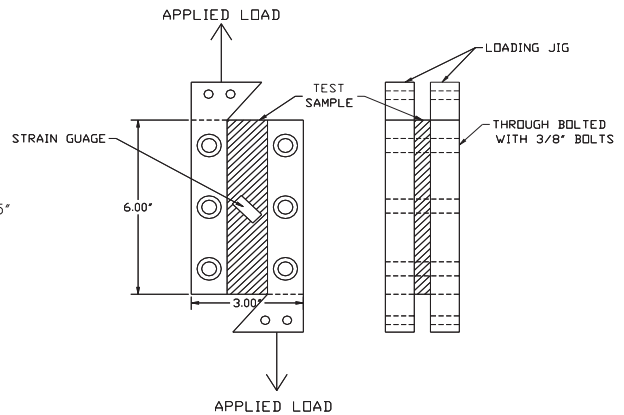
Figure 4-17   Test Specimen Configuration for ASTM D-4255 Rail Shear Test, Method A

Shear Test Methods	
ASTM D 3846	In-Plane Shear Strength of Reinforced Plastics
ASTM D 4255	Inplane Shear Properties of Composites Laminates
ASTM D 2344	Apparent Interlaminar Shear Strength of Parallel Fiber Composites by Short-Beam Method
ASTM D 3518	In-Plane Shear Stress-Strain Response of Unidirectional Polymer Matrix Composites
ASTM D 732	Shear Strength of Plastics by Punch Tool
ISO 4585	Textile Glass Reinforced Plastics - Determination of Apparent Interlaminar Shear Properties by Short-Beam Test
SACMA SRM 7	Inplane Shear Stress-Strain Properties of Oriented Fiber-Resin Composites
SACMA SRM 8	Short Beam Shear Strength of Oriented Fiber-Resin Composites

Impact Tests

Two basic types of impact test are available for single-skin laminates. The "Izod" and "Charpy" tests utilize a pendulum apparatus, in which a swinging hammer or striker impacts a gripped rectangular specimen. The specimen may be notched or unnotched. Also, the specimen may be impacted from an edgewise face or a flatwise face.

Drop weight tests are performed by restraining the edges of a circular or rectangular specimen in a frame. A "tup" or impactor is dropped from a known height, striking the center of the specimen. This test is more commonly used for composite laminates

Impact Test Methods	
ASTM D 256	Impact Resistance of Plastics and Electrical Insulating Materials
ASTM D 3029	Impact Resistance of Flat, Rigid Plastic Specimens by Means of a Tup (Falling Weight)
ISO 179	Plastics - Determination of Charpy Impact Strength
ISO 180	Plastics - Determination of Izod Impact Strength

Resin/Reinforcement Content

The simplest method used to determine the resin content of a single-skin laminate is by a resin burnout method. The procedure is only applicable to laminates containing E-glass or S-glass reinforcement, however. A small specimen is placed in a pre-weighed ceramic crucible, then heated to a temperature where the organic resin decomposes and is burned off, leaving the glass reinforcement intact.

Laminates containing carbon or Kevlar® fibers cannot be analyzed in this way. As carbon and Kevlar® are also organic materials, they burn off together with the resin. More complicated resin "digestion" methods must be used. These methods attempt to chemically dissolve the resin with strong acid or strong base. As the acid or base may also attack the reinforcing fibers, the accuracy of the results may be questionable if suitable precautions are not taken.

Fiber volume (%) may be calculated from the results of these tests, if the dry density of the reinforcement is known.

Resin/Reinforcement Test Methods	
ASTM D 2584	Ignition Loss of Cured Reinforced Resins
ASTM D 3171	Fiber Content of Resin-Matrix Composites by Matrix Digestion
ISO 1172	Textile Glass Reinforced Plastics - Determination of Loss on Ignition

Hardness/Degree of Cure

The surface hardness of cured resin castings or reinforced plastics may be determined using "impressor" methods. A steel needle or cone is pushed into the surface, and the depth of penetration is indicated on a dial gauge.

For cured polyester, vinyl ester, and DCPD type resins, the "Barcol" hardness is generally reported. Epoxy resins may be tested using either the "Barcol" or "Shore" type of test.

Hardness/Degree of Cure Test Methods	
ASTM D 2583	Indentation Hardness of Rigid Plastics by Means of a Barcol Impressor
ASTM D 2240	Rubber Property - Durometer Hardness

Water Absorption

Cured resin castings or laminates may be tested for resistance to water intrusion by simple immersion methods. A rectangular section is placed in a water bath for a specified length of time. The amount of water absorbed is calculated from the original and post-immersion weights. Tests may be performed at ambient or elevated water temperatures.

Water Absorption Test Methods	
ASTM D 570	Water Absorption of Plastics
ISO 62	Plastics - Determination of Water Absorption

Core Flatwise Tensile Tests

The tensile strength of a core material or sandwich structure may be evaluated using a "flatwise" test. Load is applied to the flat faces of a rectangular or circular specimen. This load is perpendicular to, or normal to, the flat plane of the panel.

Test specimens are bonded to steel blocks using a high strength adhesive. The assembly is then placed in a tensile holding fixture, through which load is applied to pull the blocks apart. Failures may be within the core material (cohesive), or between the core and FRP skin (adhesive), or a combination of both.

NOTE: CORE/SANDWICH STRUCTURE BONDED TO STEEL PLATES WITH HIGH STRENGTH ADHESIVE
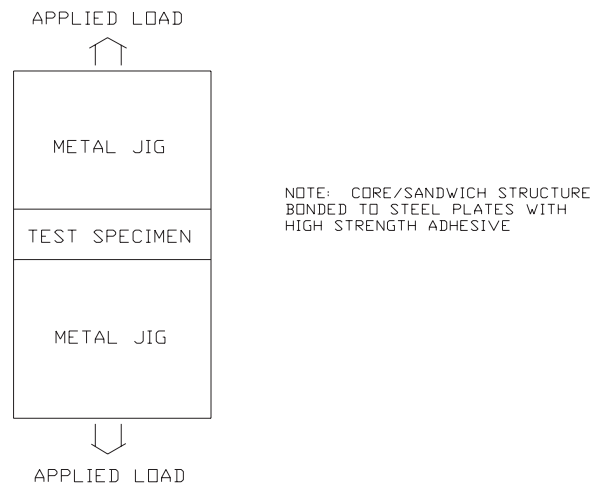
Figure 4-18   Test Specimen Configuration for ASTM C-297 Core Flatwise Tensile Test

Core Flatwise Tensile Test Methods	
ASTM C 297	Tensile Strength of Flat Sandwich Constructions in Flatwise Plane

Core Flatwise Compressive Tests

The compressive properties of core materials and sandwich structures are determined by loading the faces of flat, rectangular specimens. The specimen is crushed between two parallel steel surfaces or plates.

Typically, load is applied until a 10% deformation of the specimen has occurred (1.0" thick core compressed to 0.9", for example). The peak load recorded within this range is used to calculate compressive strength. Deformation data may be used for compressive modulus determination.

Core Flatwise Compressive Test Methods	
ASTM C 365	Flatwise Compressive Strength of Sandwich Cores
ASTM D 1621	Compressive Properties of Rigid Cellular Plastics

Sandwich Flexure Tests

The bending properties of sandwich panels can be evaluated using flexural methods similar to those utilized for single-skin laminates. A 3 or 4-point loading scheme may be used. Generally, the test is set up as a simply-supported beam, loaded at the midpoint (3-point). A 4-point setup can be selected if it is desired to produce higher shear stresses within the core.

Properties obtained from sandwich flexure tests include flexural modulus and panel stiffness, *EI*.

Sandwich Flexure Test Methods	
ASTM C 393	Flexural Properties of Flat Sandwich Constructions

Sandwich Shear Tests

The shear properties of sandwich panels and core materials are determined by a parallel plate test. Steel plates are bonded to the flat faces of rectangular sections. Load is applied to the plates, so as to move them in opposing directions, causing shear stress in the specimen between the plates. Core shear strength is found from the load at failure. Shear modulus may be determined if plate-to-plate displacement is measured during the test.
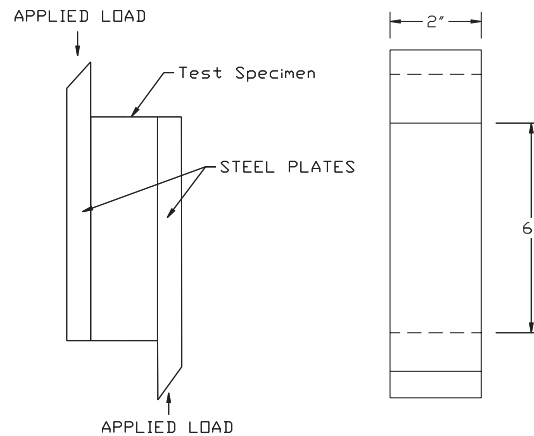
Figure 4-19 Test Specimen Configuration for ASTM C-273 Core Shear Test

Sandwich Shear Test Methods	
ASTM C 273	Shear Properties in Flatwise Plane of Flat Sandwich Constructions or Sandwich Cores

Peel Tests

The adherence of the FRP skins to core in a sandwich structure may be evaluated using peel test methods. One FRP skin is restrained, while the opposite skin is loaded at an angle (starting at one edge of the specimen), to peel the skin away from the core. These methods may be utilized to determine optimum methods of bedding or adhesively bonding skins to sandwich cores.

Peel Test Methods	
ASTM D 1062 (modified)	Cleavage Strength of Metal-to-Metal Adhesive Bonds
ASTM D 1781	Climbing Drum Peel Test for Adhesives

Core Density

The density of core materials used in sandwich constructions is typically determined from a sample of raw material (unlaminated). A rectangular section is weighed, with the density calculated from the mass and volume of the specimen.

Core Density Test Methods	
ASTM D 1622	Apparent Density of Rigid Cellular Plastics
ASTM C 271	Density of Core Materials for Structural Sandwich Constructions

Machining of Test Specimens

A variety of tools are available which are suitable for cutting and machining of test specimens. These methods may be used for both single-skin laminates and sandwich structures. The tools normally utilized for specimen preparation include :

- Milling machine;
- Band saw;
- Wet saw, with abrasive blade (ceramic tile saw);
- Water jet cutter;
- Router, with abrasive bit; and
- Drum sander.

The wet cutting methods are preferred to reduce heating of the sample, and also reduce the amount of airborne dust generated. However, for necking down dumbbell specimens, a drum sander of the proper radius is often employed (with appropriate dust control).

Great care must be taken to assure that the specimens are cut in the correct orientation, when directional fibers are present.

Machining Method	
ISO 2818	Plastics - Preparation of Test Specimens by Machining
ASTM D 4762	Testing Automotive/Industrial Composite Materials (Section 9 - Test Specimen Preparation)

Typical Laminate Test Data

Ideally, all testing should be conducted using standardized test methods. The standardized test procedures described above have been established by the American Society for Testing and Materials (ASTM, 100 Barr Harbor Drive, West Conshohocken, PA   19428-2959) and the Suppliers of Advanced Composite Materials Association (SACMA, 1600 Wilson Blvd., Suite 1008, Arlington, VA   22209). SACMA has developed a set of recommended test methods for oriented fiber resin composites. These tests are similar to ASTM standard tests, and are either improvements on the corresponding ASTM standard tests or are new tests to obtain data not covered by ASTM standard tests. The tests are intended for use with prepreg materials, thus some modifications may be necessary to accommodate common marine laminates. Also, the tolerances on fiber orientations (1°) and specimen size (approximately 0.005 inch) are not realistic for marine laminates. The individual tests have been established for specific purposes and applications. The tests may or may not be applicable to other applications, and must be evaluated on a case by case basis. The test methods for FRP materials have been developed primarily for the aerospace industry, thus they may not be applicable to the marine industry.

There are three major types of testing: 1) tests of the individual FRP components, 2) tests of the FRP laminates, 3) tests of the FRP structure. In general, the tests of individual FRP components tend to be application independent, however, some of the properties may not be useful in certain applications. Tests of the FRP laminates tend to be more application dependent, and tests of FRP structures are heavily application dependent.

Appendix A contains test data on a variety of common marine reinforcements tested with ASTM methods by Art Wolfe at Structural Composites, Inc.; Dave Jones at Sigma; Tom Juska from the Navy's NSWC; and Rick Strand at Comtrex. In limited cases, data was supplied by material suppliers. Laminates were fabricated using a variety of resin systems and fabrication methods, although most were made using hand lay-up techniques. In general, test panels made on flat tables exhibit properties superior to as-built marine structures. Note that higher fiber content laminates will be thinner for the same amount of reinforcement used. This will result in higher mechanical values, which are reported as a function of cross sectional area. However, if the same amount of reinforcement is present in high- and low-fiber content laminates, they may both have the same "strength" in service. Indeed, the low-fiber content may have superior flexural strength as a result of increased thickness. Care must always be exercised in interpreting test data. Additionally, samples should be fabricated by the shop that will produce the final part and tested to verify minimum properties.

As can be seen in Appendix A, complete data sets are not available for most materials. Where available, data is presented for properties measured in 0°, 90° and ±45° directions. Shear data is not presented due to the wide variety in test methods used. Values for Poission's ratio are seldom reported. Lu and Jin reported on materials used for the construction of a 126 foot (38.5 meter) commercial fishing vessel built in China during the 1970's. [18] The mechanical data determined in their test program is presented here as typical of what can be expected using general purpose polyester resin and hand lay-up techniques.

Table 4-2 Ultimate Strengths and Elastic Constants for Polyester Resin Laminates [X.S. Lu & X.D. Jin, "*Structural Design and Tests of a Trial GRP Hull*," Marine Structures, Elsever, 1990]

	Test Angle	Quasi-Isotropic WR & Twill @ 0°/90°		Quasi-Isotropic WR & Twill @ 0°/90°/±45°		Unidirectional		Balanced WR & Twill @ 0°		Mostly WR & Twill @ 0°	
		ksi	MPa	ksi	MPa	ksi	MPa	ksi	MPa	ksi	MPa
Tensile Strength	0°	30.0	207	27.4	189	42.3	292	29.1	201	36.5	252
	90°	25.9	179	26.5	183	10.7	74	28.0	193	n/a	
	±45°	17.5	121	19.6	135	n/a		17.8	123	n/a	
Compress Strength	0°	21.2	146	20.1	139	n/a		23.9	165	21.6	149
	90°	17.8	123	20.3	140	n/a		21.6	149	n/a	
	±45°	n/a		n/a		n/a		n/a		n/a	
Flexural Strength	0°	36.7	253	36.1	249	n/a		39.7	274	40.3	278
	90°	39.6	273	38.4	265	n/a		35.8	247	n/a	
	±45°	n/a		n/a		n/a		n/a		n/a	
In-Plane Shear	0°	n/a		n/a		n/a		n/a		n/a	
	90°	10.4	72	11.4	79	n/a		10.7	74	n/a	
	±45°	n/a		n/a		n/a		n/a		n/a	
Out-of-Plane	0°	14.3	99	14.3	99	n/a		14.6	101	15.1	104
	90°	14.3	99	13.8	95	n/a		13.6	94	n/a	
	±45°	n/a		n/a		n/a		n/a		n/a	
		msi	GPa	msi	GPa	msi	GPa	msi	GPa	msi	GPa
Tensile Modulus	0°	2.22	15.3	1.94	13.4	3.06	21.1	2.26	15.6	2.29	15.8
	90°	2.19	15.1	1.85	12.8	1.35	9.3	2.14	14.8	n/a	
	±45°	1.07	7.4	1.38	9.5	n/a		1.01	7.0	n/a	
Shear Modulus	In-Plane	0.44	3.03	0.65	4.51	n/a		0.36	2.45	n/a	
Poisson's Ratio	0°	0.15		0.23		0.19		0.14		n/a	
	90°	0.13		0.22		0.12		0.12		n/a	
	±45°	0.62		0.50		n/a		0.60		n/a	

Material Testing Conclusions

In the previous text there is a review of ASTM and SACMA test procedures for determining physical and mechanical properties of various laminates.

In order to properly design a boat or a ship, the designer must have accurate mechanical properties. The properties important to the designer are the tensile strength and modulus, the compressive strength and modulus, the shear strength and modulus, the interply shear strength, and the flexural strength and modulus.

The ASTM and SACMA tests are all uniaxial tests. There are some parts of a boat's structure that are loaded uniaxially, however, much of the structure, the hull, parts of the deck and bulkheads, etc., receive multiaxial loads. Multiaxial tests are difficult to conduct and typically are only done with panel "structures," (i.e. sandwich or stiffened panels).

It's going to be very important for the marine industry to develop a set of tests which yield the right type of data for the marine designer. Once this has been accomplished and an industry wide set of accepted tests has been developed, then a comprehensive testing program, testing all the materials that are commonly used in the marine industry, would be very beneficial to the designers to try to yield some common data. Meanwhile, until these tests are developed, there is still a need for some common testing. In particular, the tests recommended to be performed on laminates are the ASTM D3039 tensile test or the appropriate SACMA variation of that, SRM 4-88.

The ASTM compressive tests all leave something to be desired for marine laminates. However, the SACMA compression test looks like it might yield some useful uniaxial compressive load data for marine laminates, and therefore, at this time would probably be the recommended test for compression data. Flexural data should be determined using ASTM D790. This is a fairly good test.

As far as shear is concerned, there is really no good test for determining the inplane shear properties. The ASTM test (D3518) is basically a 3039 tensile test performed on a fabric that has been laid up at a bias so that all the fibers are at 45°. This has a number of problems, since the fibers are not continuous, and the results are heavily dependent on the resin, much more so than would be in a continuous laminate. Some recent investigations at Structural Composites, Inc. has shown that wider samples with associated wider test grips will yield higher test values.

Currently, there is not a test that would yield the right type of data for the inplane shear properties. For the interply shear, about the only test that's available is the short beam shear test (ASTM D2344). The data yielded there is more useful in a quality control situation. It may be, however, that some of the other tests might yield some useful information. There's a shear test where slots are cut half way through the laminate on opposite sides of the laminate (ASTM D3846). This one might yield some useful information, but because the laminate is cut with the inherent variability involved, it difficult to come up with consistent data.

In summary, what is recommended as a comprehensive laminate test program is the ASTM D3039 tensile test, the SACMA compressive test, ASTM D790 flexural test and a panel test that realistically models the edge conditions. This type of test will be discussed further in the Macromechanics chapter. A laminate test program should always address the task objectives, i.e. material screening, preliminary design, detail design and the specific project needs.

Chapter Five - Macromechanics

Our definition of macromechanics as applied to marine composite structures includes analysis of beams, panels and structures. A beam, in its simplest form, consists of one or more laminates supported at each end resisting a load in the middle. The beam usually is longer than it is wide and characteristics are considered to be two dimensional. Much testing of composites is done with beams, which may or may not be representative of typical marine structures.

Analyzing panel structures more closely matches the real world environment. If we consider a portion hull bottom bounded by stiffeners and bulkheads, it is apparent that distinct end conditions exist at each of the panel's four edges. Static and most certainly dynamic response of that panel will not always behave like a beam that was used to generate test data. Unfortunately, testing of panels is expensive and not yet universally accepted, resulting in little comparative data. Geometries of panels, such as aspect ratio and stiffener arrangement, can be used in conjunction with two-dimensional test data to predict the response of panel structures. Reichard and Bertlesen have investigated panel test methods to measure panel response to out-of-plane loads. Preliminary results of those tests are presented at the end of the chapter.

Sandwich panel construction is an extremely efficient way to resist out-of-plane loads that are often dominant in marine structures. The behavior of core materials varies widely and is very much a function of load time history. Static governing equations are presented. Through-thickness stress distribution diagrams serve as illustrations of sandwich panel response.

With larger composite structures, such as deckhouses, masts or rudders, global strength or stiffness characteristics may govern the design. Global characteristics are very much a function of geometry. As composite materials are molded to their final form, the designer should have the ability to specify curved corners and surfaces that minimize stress concentrations.

Not to be overlooked is the important subject of joints and details. Failures in composite vessels tend to occur at some detail design area. The reason for this is twofold. First, unintended stress concentrations tend to occur in detail areas. Secondly, fabrication quality control is more difficult in tight, detail areas.

Beams

Although actual marine structures seldom resemble two-dimensional beams, it is instructive to define moments and deflections for some idealized load and end conditions of statically determinate beams. The generalized relationship of stress in a beam to applied moment is:

$$\sigma = \frac{Mc}{I} \qquad\qquad (5\text{-}1)$$

where:

σ = stress in the beam
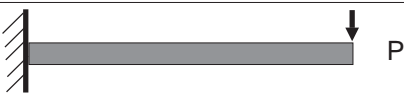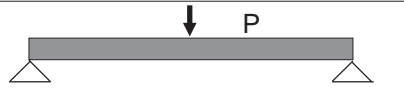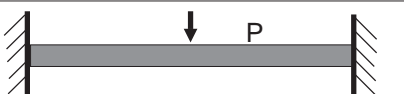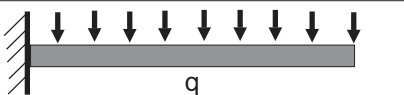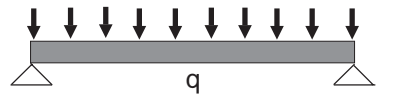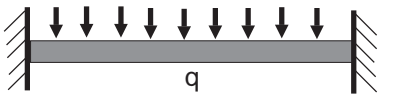
M = bending moment

c = vertical distance from the neutral axis

I = moment of inertia of the beam about the neutral axis

Expressions for moments and displacements for several types of beam loading scenarios are presented in Table 5-1.

Table 5-1 Maximum Moments and Deflections for Some Simple Beams

Load Cases	Maximum Moment	Maximum Deflection
	PL	$\dfrac{PL^3}{3EI}$
	$\dfrac{PL}{4}$	$\dfrac{PL^3}{48EI}$
	$\dfrac{PL}{8}$	$\dfrac{PL^3}{192EI}$
	$\dfrac{qL^2}{2}$	$\dfrac{qL^4}{8EI}$
	$\dfrac{qL^2}{8}$	$\dfrac{5qL^4}{384EI}$
	$\dfrac{qL^2}{12}$	$\dfrac{qL^4}{384EI}$
P = concentrated load L = beam length q = load per unit length E = beam elastic modulus I = beam moment of inertia		

Panels

Throughout our discussion of marine panel structures, formulas will appear that have varying coefficients for "clamped," "pinned," and "free" end conditions. The end condition of a panel is the point where it attaches to either a bulkhead or a stiffener. With composite structures, the actual end condition is usually somewhere between "fixed" and "pinned," depending upon the attachment detail. It is common practice for designers to perform calculations for both condition and choose a solution somewhere in between the two. For truly "fixed" conditions, stress levels near the ends will be greater because of the resisting moment introduced here. For purely "pinned" conditions, deflections in the center of the panel will be greater.

Unstiffened, Single-Skin Panels

Buckling Strength of Flat Panels

The buckling strength of hull, deck and bulkhead panels is critical because buckling failure is often catastrophic, rather than gradual. The following discussion of flat panel buckling strength is contained in the Navy's DDS 9110-9 [19] and is derived from MIL-HDBK 17. [20]

The ultimate compressive stress, F_{ccr}, is given by the formula:

$$F_{ccr} = H_c \frac{\sqrt{E_{fa}E_{fb}}}{\lambda_{fba}} \left(\frac{t}{b}\right)^2 \qquad (5\text{-}2)$$

where:

t = plate thickness

b = length of loaded edge

λ_{fba} = $1 - \mu_{fba}\,\mu_{fab}$

μ_{fba} = Poisson's ratio with primary stress in b direction

μ_{fab} = Poisson's ratio with primary stress in a direction

H_c = $h_c + C_c K_f$

h_c = coefficient from Figures 5-1 through 5-3

C_c = $\dfrac{\pi^2}{3}$ for edges simply supported or loaded edges clamped

$\quad$ = $\dfrac{2\,\pi^2}{3}$ for loaded edges simply supported, other edges clamped, or all edges clamped

K_f = $\dfrac{E_{fb}\,\mu_{fab} + 2\lambda_{fba}\,G_{ba}}{\sqrt{E_{fa}\,E_{fb}}}$

E_{fa} = flexural Young's modulus in a direction

E_{fb} = flexural Young's modulus in b direction

G_{ba} = shear modulus in the ba direction

The edge stiffener factor, r, is computed as follows:

$$r = -\left(\frac{E_{fb}}{E_{fa}}\right)^{\frac{1}{4}}$$ (5-3)

The ultimate shear stress due to buckling loads, F_{scr}, is given by the following formula:

$$F_{scr} = \frac{{}_sE_f{}^3E_{fa})^{\frac{1}{4}}}{3\lambda_{fba}}\left(-\right)^2$$ (5-4)

where H_s is given in Figures 5-4 and 5-5 as a function of edge stiffener factor, r.

It should be noted that if "ultimate" stress levels are used for computational purposes, safety factors of 4.0 on compressive failures and 2.0 on shear failures are generally applied when developing scantlings for composite materials.

Panels Subject to Uniform, Out-of-Plane Loads

Out-of-plane loads, such as hydrostatic pressure, wind loads and green sea deck loads are of constant concern for marine structures. Hull plating, decks, deckhouse structure and bulkheads all must withstand out-of-plane loads. As with in-plane loads, clamped edge conditions produce maximum stresses at the edges and simply supported edges produce maximum stress at the center of a panel. In extreme loading conditions or with extremely flexible laminates, panels will deform such that it is entirely in a state of tension. This condition is called "membrane" tension, which is covered in Chapter Six. For stiffer panels subject to static loads, classical plate deflection theory requires that combined flexural and tensile stresses provide the following margin of safety:

$$\frac{fb}{fb} + \frac{tb}{tb} \leq \frac{1}{S}$$ (5-5)

where, for simply supported edges:

$$f_{fa} = {}_8\left[{}_f\frac{E_{fba}}{\lambda_{fba}}\left(-\right)^2\left(\frac{\delta}{-}\right)\right]$$ (5-6)

$$f_{ta} = {}_8^2 \, 2.5\,2\left[\frac{E_{tb}}{\lambda_{fba}}\left(-\right)^2\left(\frac{\delta}{-}\right)^2\right]$$ (5-7)

for clamped edges:

$$f_{fa} = {}_8\left[{}_f\frac{E_{fb}}{\lambda_{fba}}\left(-\right)^2\left(\frac{\delta}{-}\right)\right]$$ (5-8)

$$f_{ta} = {}_8^2 \, 2.4\left[\frac{E_{tb}}{\lambda_{fba}}\left(-\right)^2\left(\frac{\delta}{-}\right)^2\right]$$ (5-9)

K_8 is given for panels with $\delta \le 0.5$ in Figure 5-6 as a function of the previously defined edge stiffener factor, r. Multiply δ by K_8 for these panels to get a more accurate deflection, δ. The coefficient C_f is given in Figures 5-7 through 5-9 as a function of m, which, for simply supported edges, is defined as:

$$m = 2. \left(\frac{E_{tb}}{E_{fb}} \right)^{\frac{1}{2}} \left(\frac{\delta}{-} \right) \qquad (5\text{-}10)$$

for clamped edges:

$$m = 2.32 \left(\frac{E_{tb}}{E_{fb}} \right)^{\frac{1}{2}} \left(\frac{\delta}{-} \right) \qquad (5\text{-}11)$$

The ratio of the maximum deflection to the panel thickness, $\dfrac{\delta}{-}$, is found using Figures 5-10 and 5-11. In these Figures, the ratio $\dfrac{\Delta}{-}$ uses the maximum deflection assuming loads resisted by bending. This ratio is calculated as follows, for simply supported edges:

$$\frac{\Delta}{-} = \frac{5 \lambda_{fba}{}^4}{32 E_{fb}{}^4} \qquad (5\text{-}12)$$

for clamped edges:

$$\frac{\Delta}{-} = \frac{\lambda_{fba}{}^4}{32 E_{fb}{}^4} \qquad (5\text{-}13)$$

where:

$$p = \text{load per unit area}$$

Figures 5-7 and 5-8 also require calculation of the coefficient C as follows:

$$C = \frac{E_{tb}}{E_{fb}} \qquad (5\text{-}14)$$

K_8 is given for panels with $\delta \le 0.5$ in Figure 5-6 as a function of the previously defined edge stiffener factor, r. Multiply δ by K_8 for these panels to get a more accurate deflection, δ.

Sandwich Panels

This treatment on sandwich analysis is based on formulas presented in the U.S. Navy's Design Data Sheet DDS-9110-9, ***Strength of Glass Reinforced Plastic Structural Members, Part II - Sandwich Panels*** [19] and MIL-HDBK 23 - ***Structural Sandwich Composites*** [21]. In general, the formulas presented apply to sandwich laminates with bidirectional faces and cores such as balsa or foam. Panels with strongly orthotropic skins (unidirectional reinforcements) or honeycomb cores require detailed analysis developed for aerospace structures. The following notation is used for description of sandwich panel response to in-plane and out-of-plane loads:

A	=	cross sectional area of a sandwich panel; coefficient for sandwich panel formulas
a	=	length of one edge of rectangular panel; subscript for "a" direction
B	=	coefficient for sandwich panel formulas
b	=	length of one edge of rectangular panel; subscript for "b" direction
C	=	subscript for core of a sandwich panel
cr	=	subscript for critical condition of elastic buckling
c	=	subscript for compression; coefficient for edge conditions of sandwich panels
D	=	bending stiffness factor for flat panels
d	=	sandwich panel thickness
E	=	Young's modulus of elasticity
F	=	ultimate strength of a laminate or subscript for face
$F.S.$	=	factor of safety
f	=	induced stress; subscript for bending or flexural strength
G	=	shear modulus
H	=	extensional or in-plane stiffness
h	=	distance between facing centroids of a sandwich panel
I	=	moment of inertia of laminate cross section
K, K_m	=	coefficients for formulas
L	=	unsupported length of panel; core axis for defining sandwich panel core properties
M	=	bending moment
n	=	number of half-waves of a buckled panel
p	=	unit load
Q	=	coefficient for sandwich panel formulas
r	=	radius of gyration; stiffness factor for panels; subscript for reduced
R	=	coefficient for sandwich panel formulas
s	=	subscript for shear
T	=	core axis for defining sandwich core properties
t	=	subscript for tension; thickness of sandwich skins
U	=	shear stiffness factor
V	=	shearing force
W	=	weight; core axis for defining sandwich panel core properties
Z	=	section modulus
$\alpha \ \beta \ \gamma$	=	coefficients for sandwich panel formulas
λ_{fba}	=	$1 - \mu_{fba} \ \mu_{fab}$
μ	=	Poisson's ratio; Poisson's ratio for strain when stress is in the direction of the first subscript, with two subscripts denoting direction
$\delta \ \Delta$	=	deflection of laminate or panel

Out-of-Plane Bending Stiffness

The general formula used to predict the bending stiffness per unit width, *D*, for a sandwich laminate is:

$$D = \frac{1}{\frac{E_{F1\ F1}}{\lambda_{F1}} + \frac{E_{C\ C}}{\lambda_C} + \frac{E_{F2\ F2}}{\lambda_{F2}}} \left[\frac{E_{F1\ F1}}{\lambda_{F1}} \left(\frac{E_{F2\ F2}}{\lambda_{F2}} \right)^2 + \frac{E_{F1\ F1}}{\lambda_{F1}} \left(\frac{E_{C\ C}}{\lambda_C} \right) \left(\frac{F1 + C}{2} \right)^2 + \frac{E_{F2\ F2}}{\lambda_{F2}} \left(\frac{E_{C\ C}}{\lambda_C} \right) \left(\frac{F2 + C}{2} \right)^2 \right]$$

$$+ \frac{1}{12} \left[\frac{E_{F1}{}^3{}_{F1}}{\lambda_{F1}} + \frac{E_C{}^3{}_C}{\lambda_C} + \frac{E_{F2}{}^3{}_{F2}}{\lambda_{F2}} \right] \qquad\qquad (5-15)$$

The above equation applies to sandwich laminates where faces 1 and 2 may have different properties. Values for flexural and compressive stiffness are to be taken in the direction of interest, i.e. a or b direction (0° or 90°). When inner and outer skins are the same, the formula for bending stiffness, D, reduces to:

$$D = \frac{E_F {}_F{}^2}{2\lambda_F} + \frac{1}{12}\left(\frac{2E_F {}_F{}^3}{\lambda_F} + \frac{E_C {}_C{}^3}{\lambda_C}\right)$$ (5-16)

The second term in the above equation represents the individual core and skin stiffness contribution without regard to the location of the skins relative to the neutral axis. This term is often neglected or incorporated using the factor K, derived from figure 5-12. The bending stiffness equation then reduces to:

$$D = \frac{E_F {}_F{}^2}{2\lambda_F}$$ (5-17)

If the sandwich laminate has thin skins relative to the core thickness, the term K will approach unity. If the Poisson's ratio is the same for both the inner and outer skin, then $\lambda_{F1} = \lambda_{F2} = \lambda$ and (5-15) and (5-17), for different inner and outer skins, the expression reduces to:

$$D = \frac{E_{F1} {}_{F1} E_{F2} {}_{F2}{}^2}{\left(E_{F1} {}_{F1} + E_{F2} {}_{F2}\right)\lambda_F}$$ (5-18)

and for similar inner and outer skins:

$$D = \frac{E_F {}_F{}^2}{2\lambda_F}$$ (5-19)

In-Plane Stiffness

The in-plane stiffness per unit width of a sandwich laminate, H, is given by the following equation for laminates with different skins:

$$H = E_{F1} {}_{F1} + E_{F2} {}_{F2} + E_C {}_C$$ (5-20)

and for laminates with similar inner and outer skins:

$$H = 2E_F {}_F + E_C {}_C$$ (5-21)

Shear Stiffness

The transverse shear stiffness of a sandwich laminate with relatively thin skins is dominated by the core and therefore is approximated by the following equation:

$$U = \frac{{}^2}{C} G_C \approx G_C$$ (5-22)

In-Plane Compression

Sandwich panels subject to in-plane compression must first be evaluated to determine the critical compressive load per unit width N_{cr}, given by the theoretical formula based on Euler buckling:

$$N_{cr} = \frac{\pi^2}{2} \qquad (5\text{-}23)$$

By substituting equation (5-18), equation (5-23) can be rewritten to show the critical skin flexural stress, $Fcr_{1,2}$, for different inner and outer skins, as follows:

$$Fcr_{1,2} = \pi^2 \; \frac{E_{F1\,F1}E_{F2\,F2}}{\left(E_{F1\,F1} + E_{F2\,F2}\right)^2}\left(-\right)^2 \frac{E_{F1,2}}{\lambda_F} \qquad (5\text{-}24)$$

and for similar inner and outer skins:

$$Fcr = \frac{\pi^2}{4}\left(-\right)^2 \frac{E_F}{\lambda_F} \qquad (5\text{-}25)$$

In equations (5-24) and (5-25), use $E_F = \sqrt{E_{Fa}E_{Fb}}$ for orthotropic skins and b is the length of the loaded edge of the panel. The coefficient, K, is given by the sum of $K_F + K_M$. K_F is based on skin stiffness and panel aspect ratio and K_M is based on sandwich bending and shear stiffness and panel aspect ratio. K_F is calculated by the following for different inner and outer skins:

$$K_F = \frac{\left(E_{F1\,F1}{}^3 + E_{F2\,F2}{}^3\right)\left(E_{F1\,F1} + E_{F2\,F2}\right)}{12\,E_{F1\,F1}E_{F2\,F2}{}^2}\;MO \qquad (5\text{-}26)$$

and for similar inner and outer skins:

$$K_F = \frac{{}_F{}^2}{3\,{}^2}\;MO \qquad (5\text{-}27)$$

In equations (5-26) and (5-27), K_{MO} is found in Figure 5-13. $K_{MO} = K_M$ when $V = 0$ (ignoring shear force). For $-$ aspect ratios greater than 1.0, assume $K_F = 0$.

Figures 5-14 to 5-25 are provided for determining the coefficient, K_M. These figures are valid for sandwich laminates with isotropic skins where $\alpha = 1.0$; $\beta = 1.0$; and $\gamma = 0.3\,5$; and orthotropic skins where $\alpha = 1.0$; $\beta = 0.$; and $\gamma = 0.2$, with α β n γ defined as follows:

$$\alpha = \sqrt{\frac{E_b}{E_a}} \qquad (5\text{-}28)$$

$$\beta = \alpha\mu_{ab} + 2\gamma \qquad (5\text{-}29)$$

$$\gamma = \frac{G_{ba}}{\sqrt{E_a E_b}} \qquad (5\text{-}30)$$

The figures for K_M require computation of the parameter V, which is expressed as:

$$V = \frac{\pi^2}{2} \qquad (5\text{-}31)$$

Substituting values for bending stiffness, D, and shear stiffness, U and V for different inner and outer skins, can be expressed as:

$$V = \frac{\pi^2 \, {}_C E_{F1 \, F1} E_{F2 \, F2}}{\lambda_F \, {}^2 G_C \left(E_{F1 \, F1} + E_{F2 \, F2} \right)} \qquad (5\text{-}32)$$

and for similar inner and outer skins:

$$V = \frac{\pi^2 \, {}_C E_{F \, F}}{2\lambda_F \, {}^2 G_C} \qquad (5\text{-}33)$$

Figures 5-14 through 5-25 each show cusped curves shown as dashed lines, which represent buckling of the panel with n number of waves. Minimum values of the cusped curves for K_M, which should be used for the design equations, are shown for various values of V.

Face Wrinkling

Face wrinkling of sandwich laminates is extremely difficult to predict, due to uncertainties about the skin to core interface and the initial waviness of the skins. The face wrinkling stress, F_W, required to wrinkle the skins of a sandwich laminate, is given by the following approximate formula:

$$F_W = \left(\frac{E_F E_C G_C}{\lambda_F} \right)^{\frac{1}{3}} \qquad (5\text{-}34)$$

Q is presented in Figure 5-26, when a value for deflection, δ, is known or assumed and K is computed as follows:

$$K = \frac{\delta E_F}{{}_F \quad {}_C} \qquad (5\text{-}35)$$

Face wrinkling is more of a problem with "aerospace" type laminates that have very thin skins. Impact and puncture requirements associated with marine laminates usually results in greater skin thicknesses. Minimum suggested skin thicknesses based on the design shear load per unit length, N_S, is given by the following equation for different inner and outer skins:

$$N_S = {}_{F1 \, F1} + {}_{F2 \, F2} \qquad (5\text{-}36)$$

and for similar inner and outer skins:

$$t_F = \frac{{}_S}{2 \, {}_F} \qquad (5\text{-}37)$$

Equations (5-24) through (5-25) can be used to calculated critical shear buckling, using Figures 5-27 through 5-32 for coefficients K_M and K_{MO}.

Out-of-Plane Loading

Out-of-plane or normal uniform loading is common in marine structures in the form of hydrostatic forces or live deck loads. The following formulas apply to panels with "simply supported" edges. Actual marine panels will have some degree of fixity at the edges, but probably shouldn't be modeled as "fixed." Assumption of end conditions as "simply supported" will be conservative and it is left up to the designer to interpret results.

The following formulas assist the designer in determining required skin and core thicknesses and core shear stiffness to comply with allowable skin stress and panel deflection. Because the "simply supported" condition is presented, maximum skin stresses occur at the center of the panel (x-y plane). Imposing a clamped edge condition would indeed produce a bending moment distribution that may result in maximum skin stresses closer to the panel edge.

The average skin stress, taken at the centriod of the skin, for different inner and outer skins is given by:

$$F_{F1,2} = \frac{2}{2 \quad F1,2} \tag{5-38}$$

and for similar inner and outer skins:

$$F_F = \frac{2}{2 \quad F} \tag{5-39}$$

with K_2 given in Figure 5-34.

The deflection, δ, is given by the following formulas for different inner and outer skins as:

$$\delta = \frac{1}{2}\left(\frac{F1,2}{E_{F1,2}}\right)\left(1 + \frac{E_{F1,2} \; F1,2}{E_{F2,1} \; F2,1}\right)\frac{2}{} \tag{5-40}$$

and for similar inner and outer skins:

$$\delta = 2 \frac{1}{2}\left(\frac{\lambda \; F}{E_f}\right)\left(\frac{2}{}\right) \tag{5-41}$$

K_1 is given in Figure 5-33. The above equations need to be solved in an iterative fashion to ensure that both stress and deflection design constraints are satisfied. Additionally, core shear stress, F_{Cs}, can be computed as follows, with K_3 taken from Figure 5-35:

$$F_{Cs} = \quad 3 \quad - \tag{5-42}$$
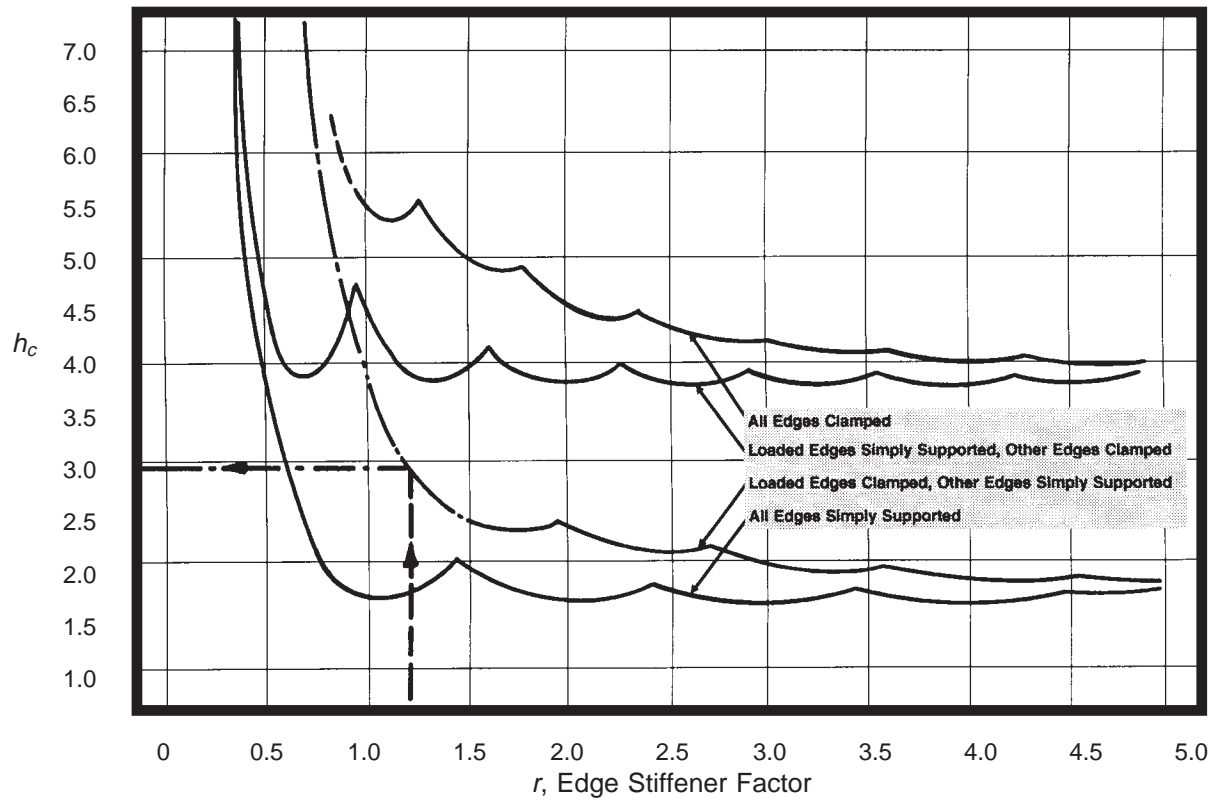
h_c

r, Edge Stiffener Factor

Figure 5-1 h_c as a Function of Edge Stiffener Factor [DDS 9110-9]

h_c

r, Edge Stiffener Factor
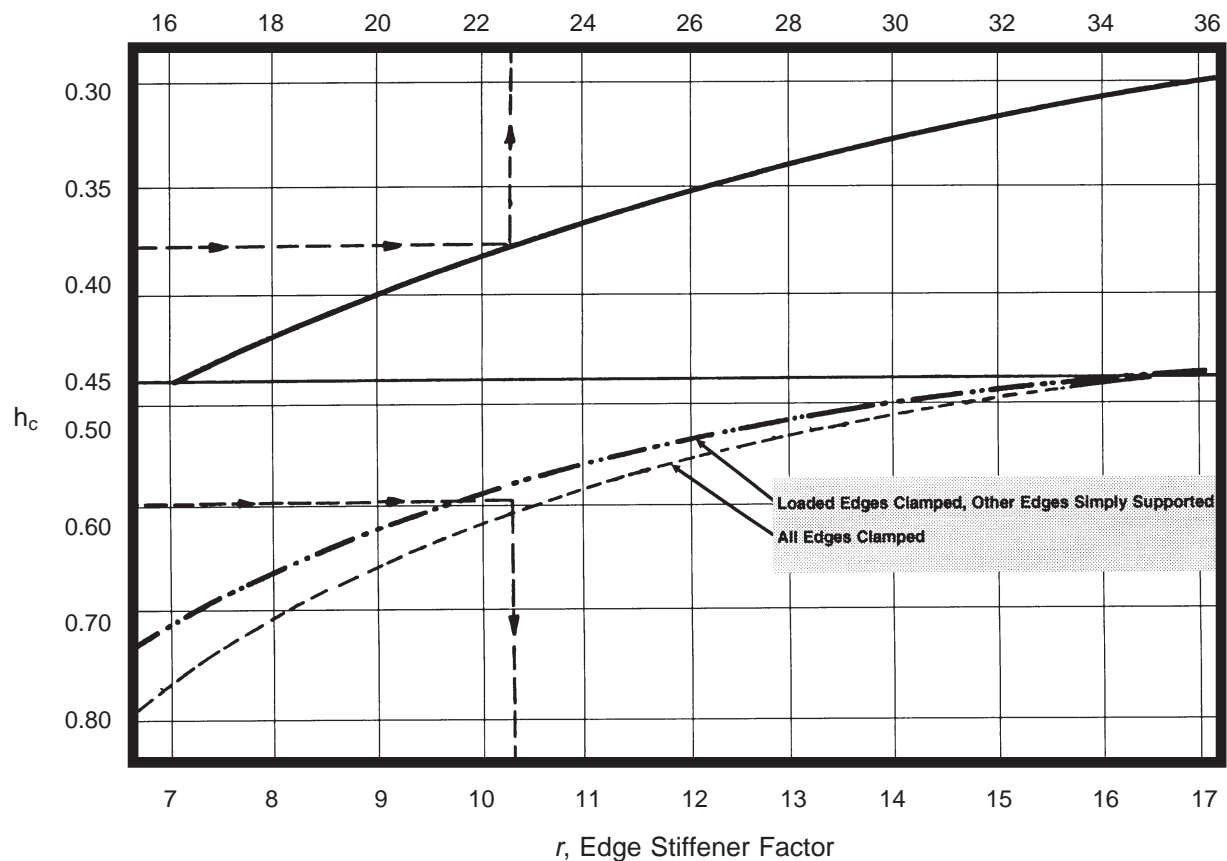
Figure 5-2 h_c as a Function of Edge Stiffener Factor [DDS 9110-9]
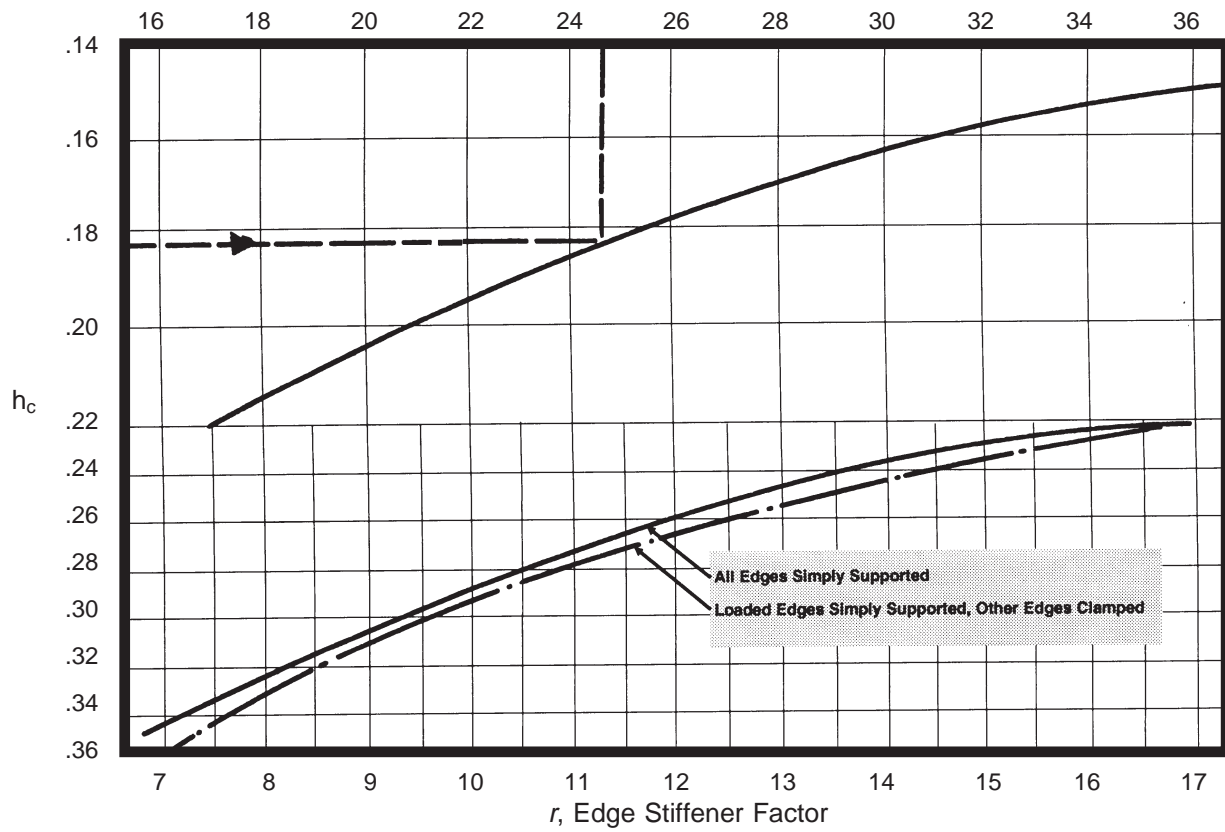
Figure 5-3 h_c as a Function of Edge Stiffener Factor [DDS 9110-9]
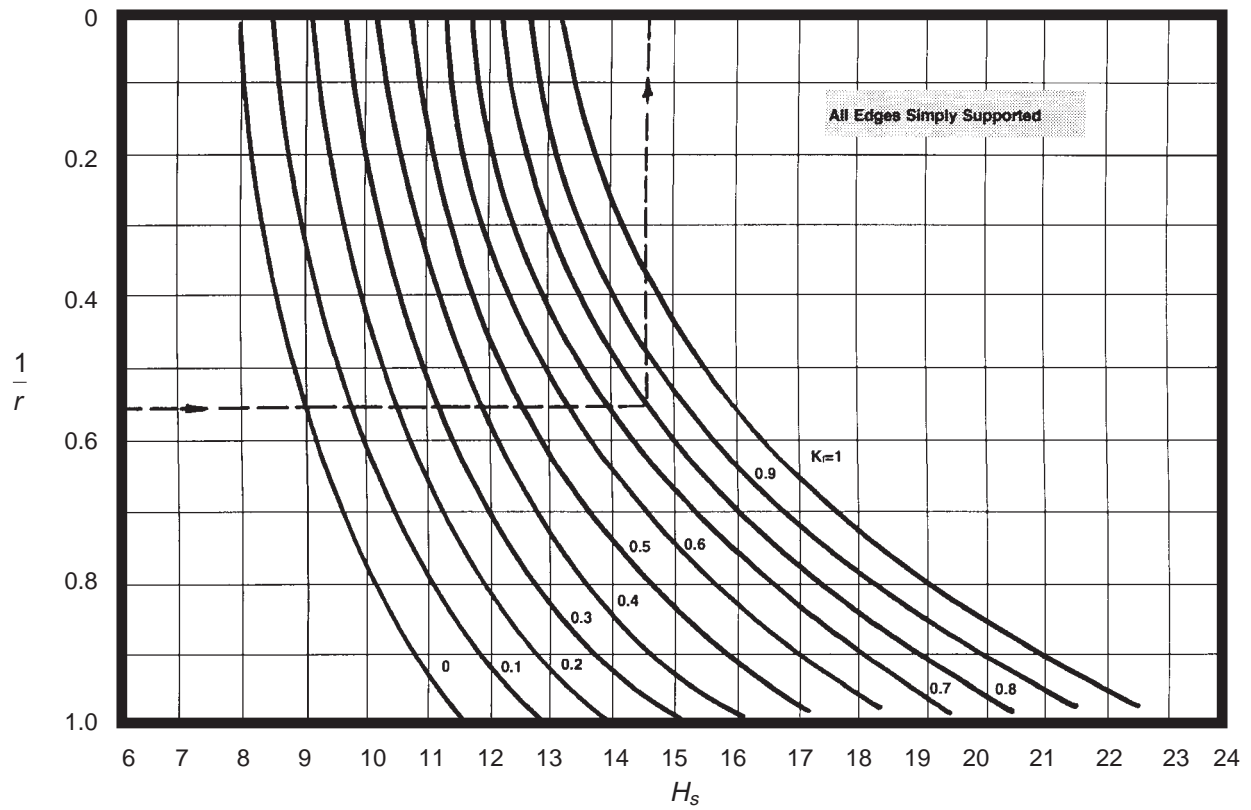
Figure 5-4 H_s as a Function of the Inverse of Edge Stiffener Factor [DDS 9110-9]
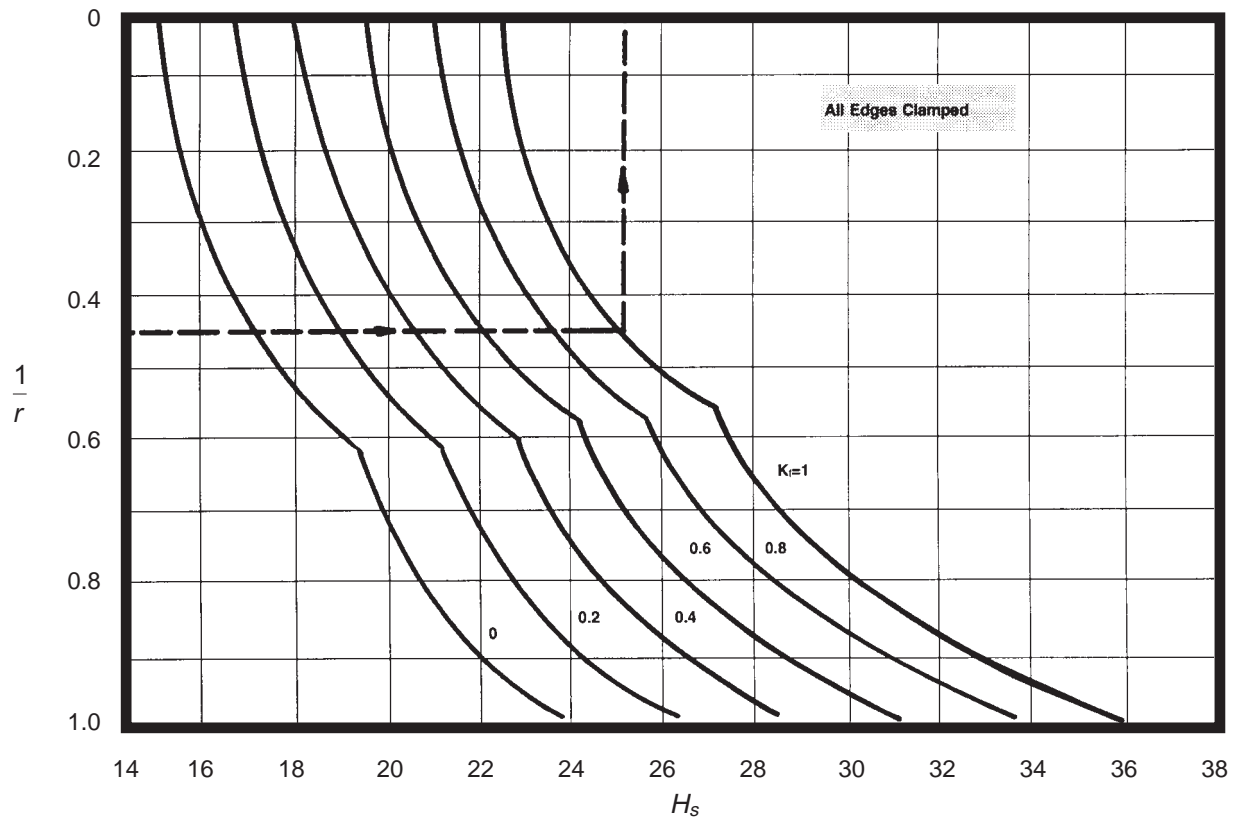
Figure 5-5 H_s as a Function of the Inverse of Edge Stiffener Factor [DDS 9110-9]
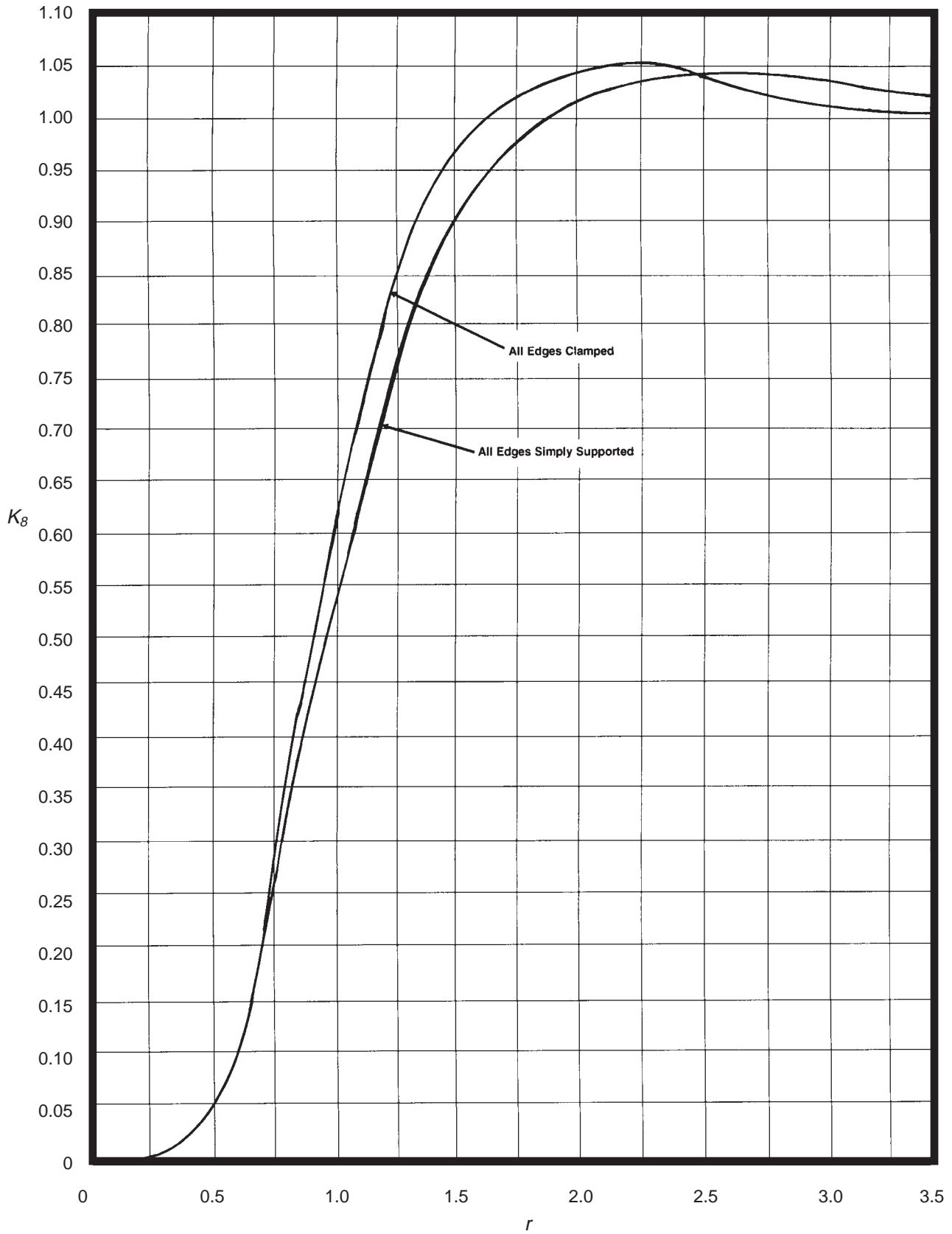
Figure 5-6 K_8 as a Function of Edge Stiffener Factor [DDS 9110-9]

All Edges Simply Supported

Figure 5-7 C_f as a Function of m [DDS 9110-9]

All Edges Clamped
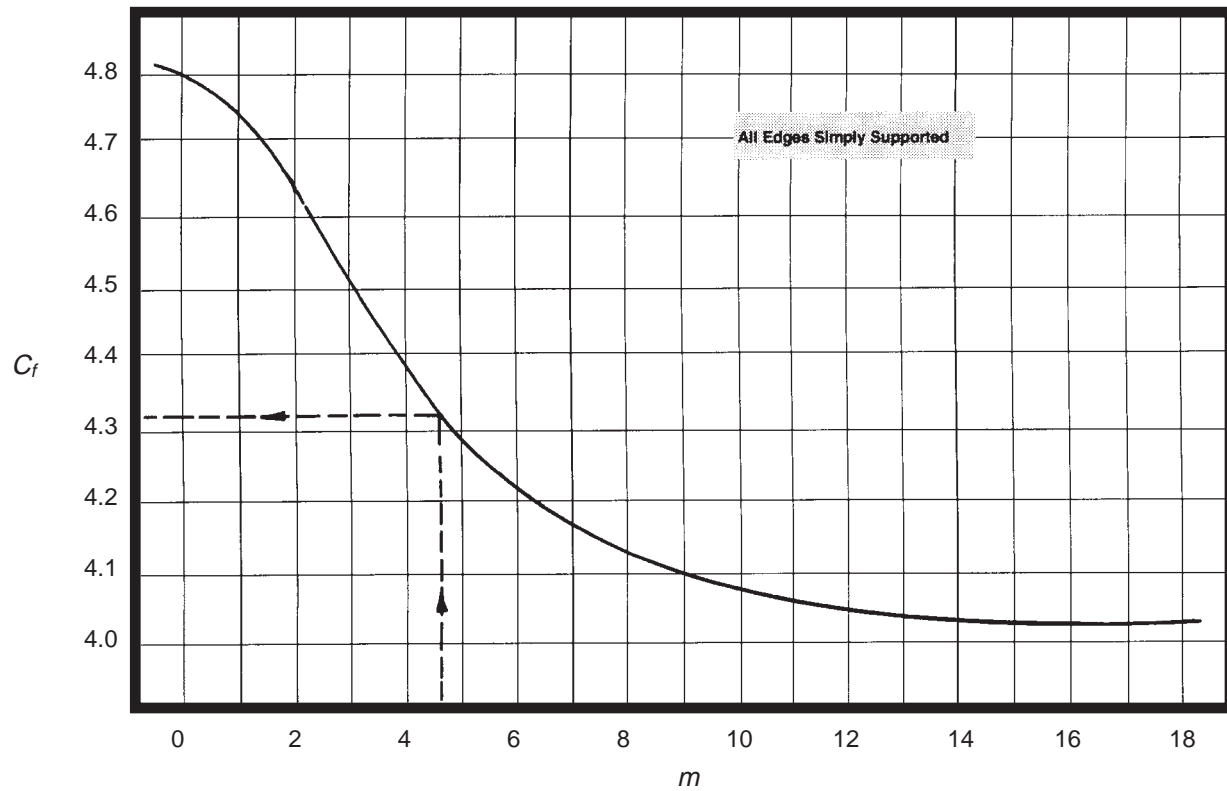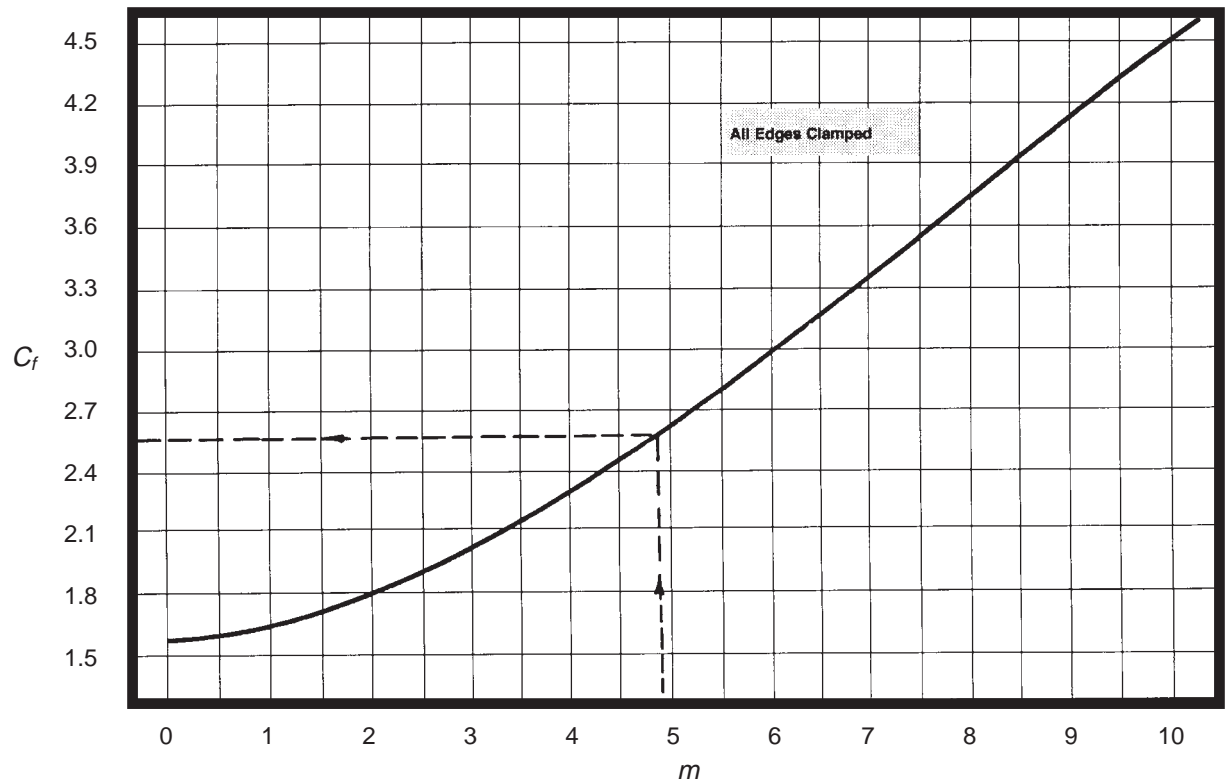
Figure 5-8 C_f as a Function of m [DDS 9110-9]
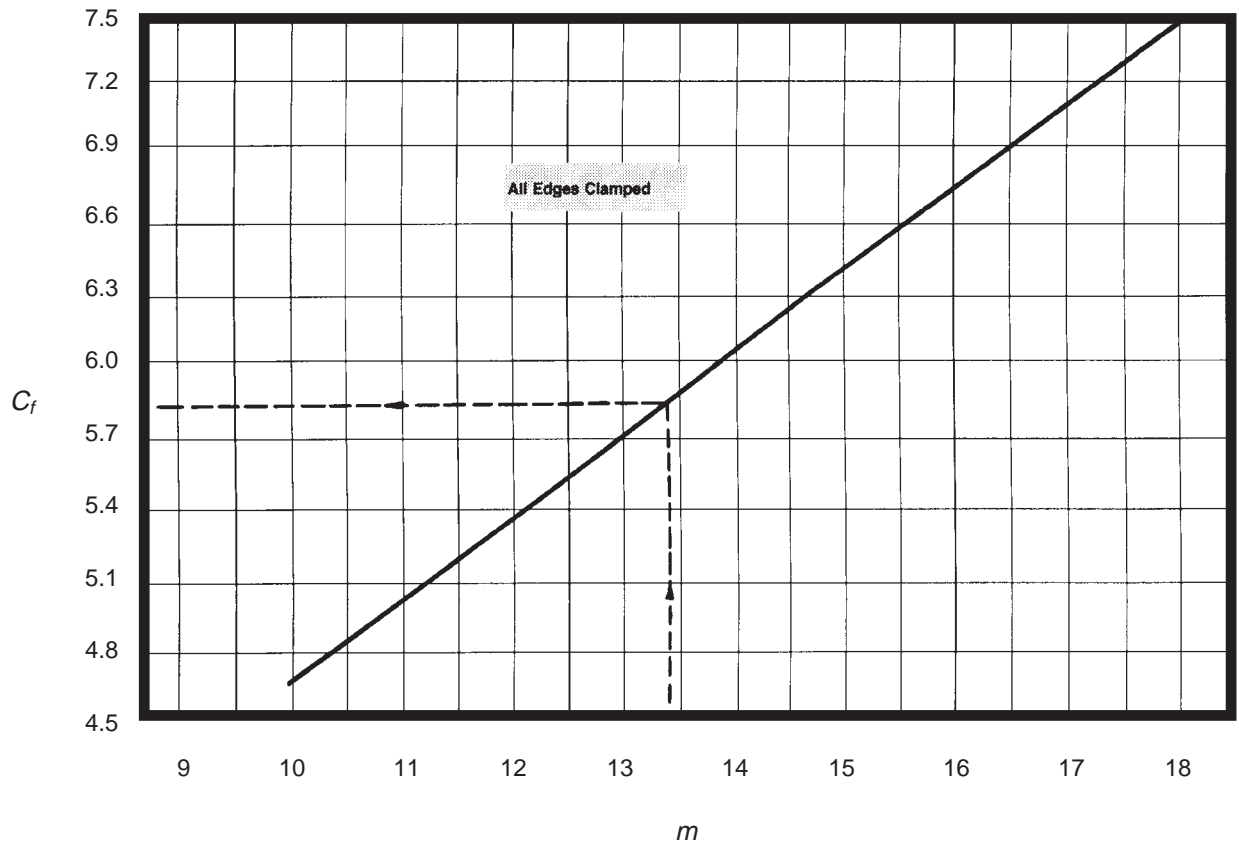
Figure 5-9 C_f as a Function of m [DDS 9110-9]
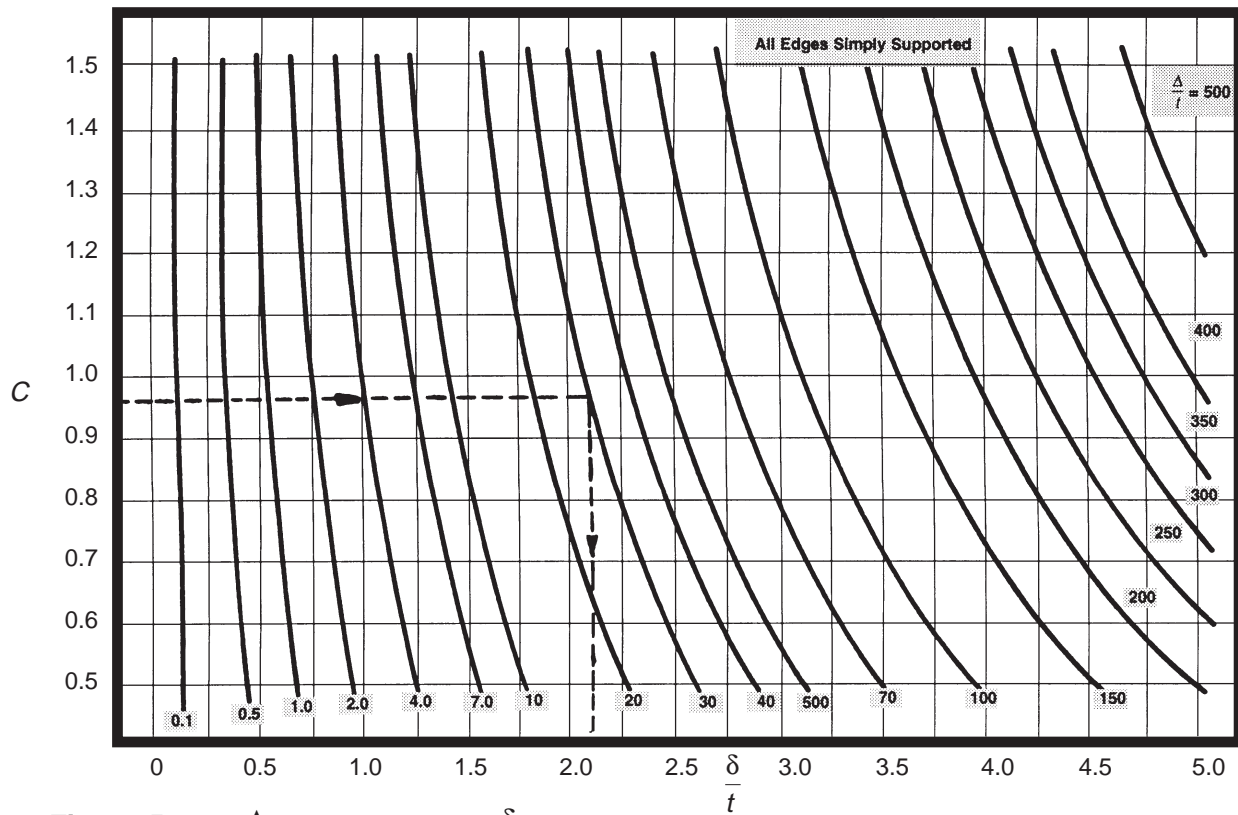
Figure 5-10 $\frac{\Delta}{t}$ as a Function of $\frac{\delta}{t}$ and C [DDS 9110-9]
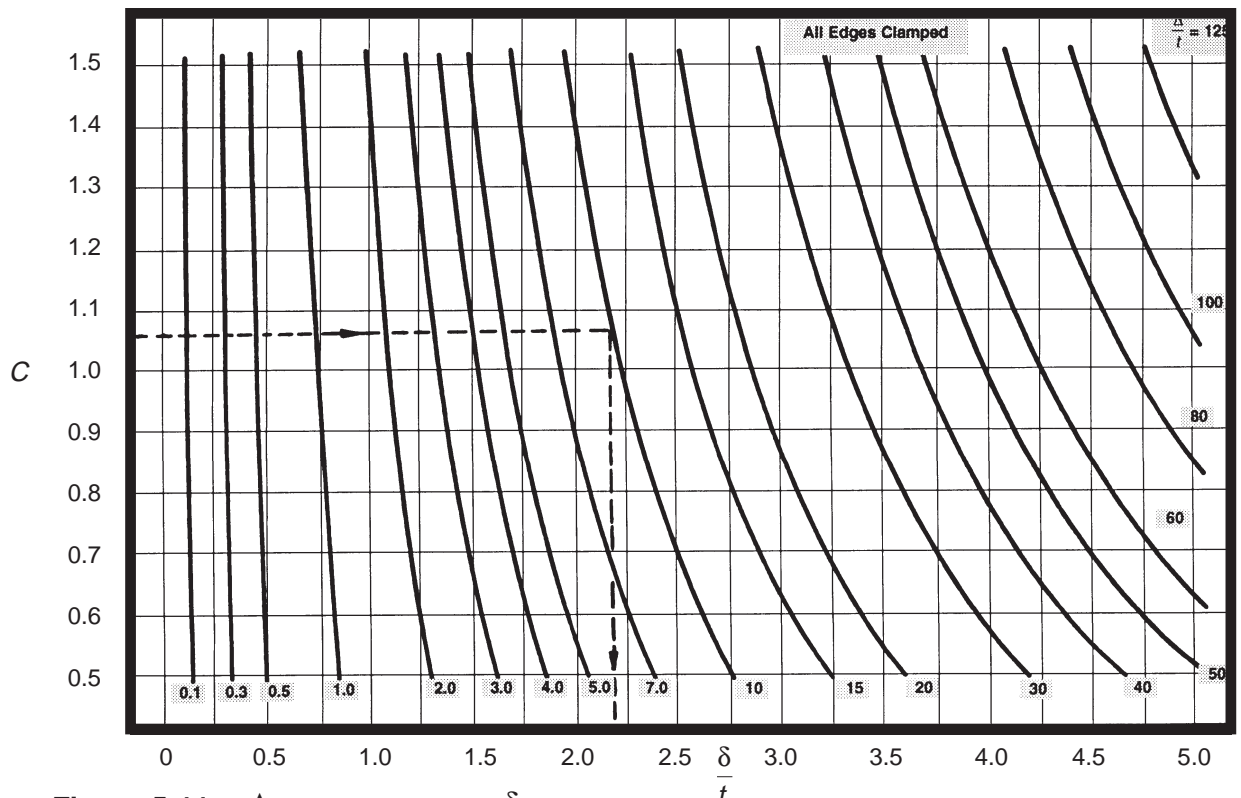
Figure 5-11 $\frac{\Delta}{t}$ as a Function of $\frac{\delta}{t}$ and C [DDS 9110-9]
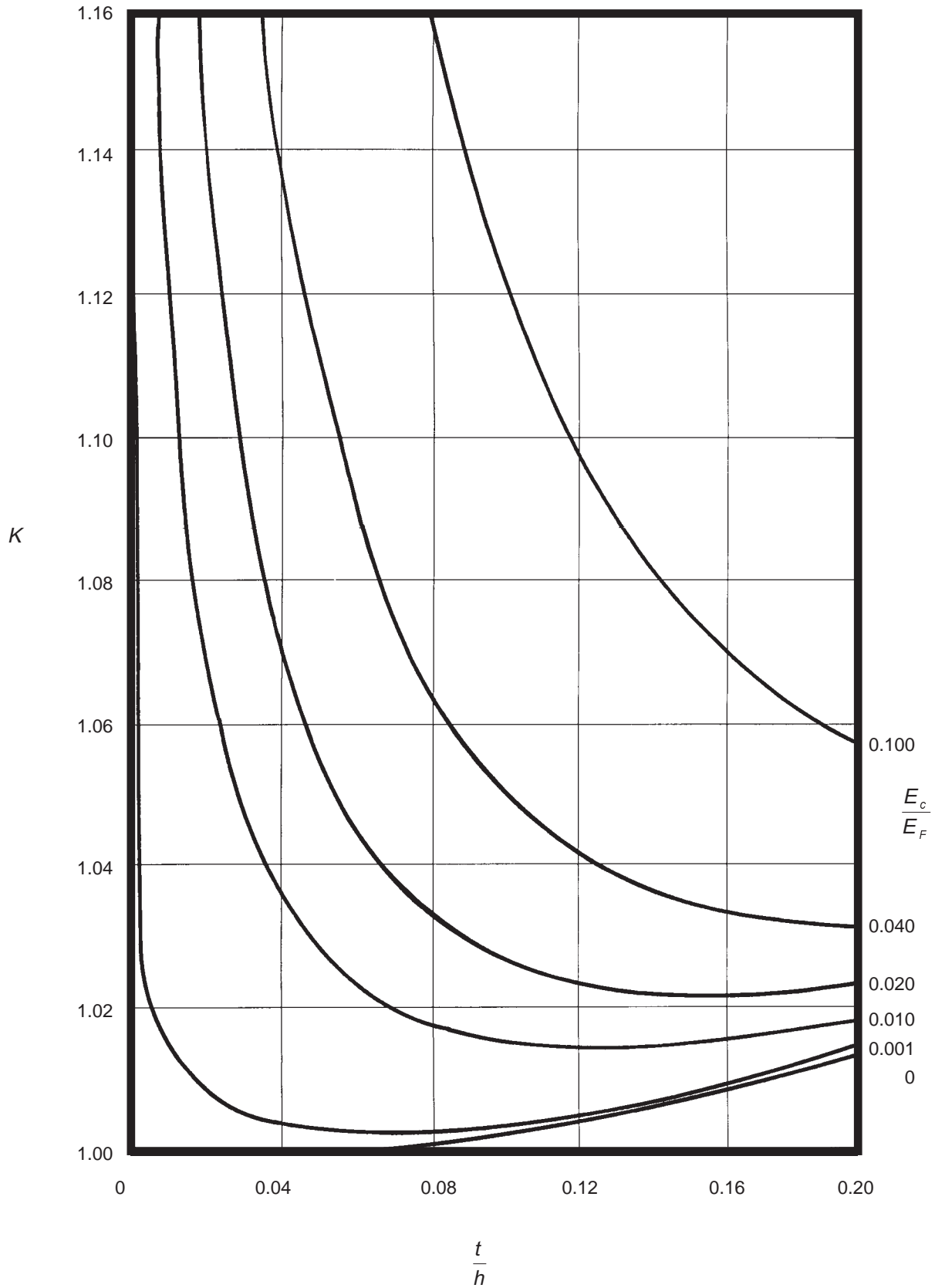
Figure 5-12   Coefficient for Bending Stiffness Factor [DDS 9110-9]
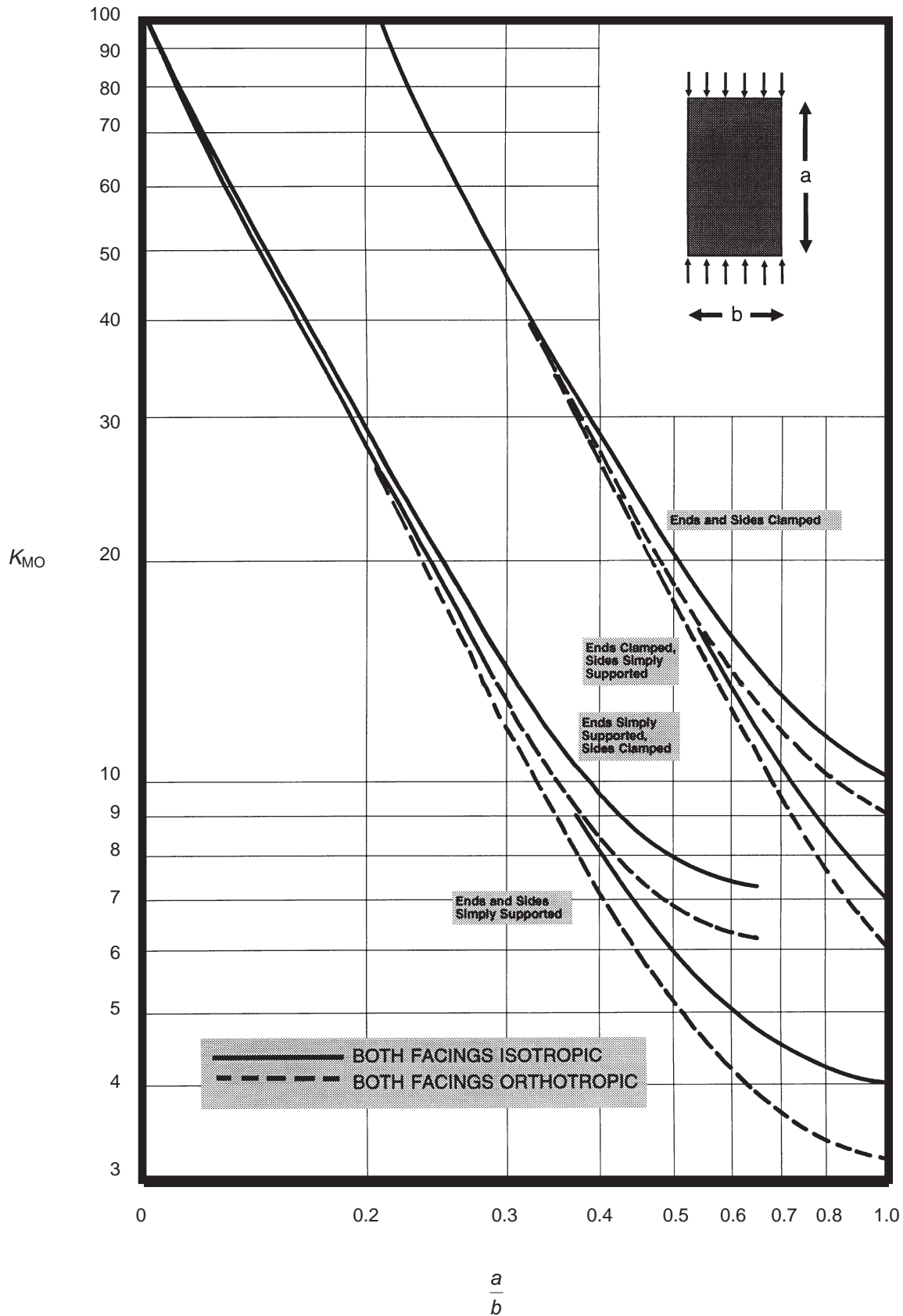
Figure 5-13   Values of K_{MO} for Sandwich Panels in Edgewise Compression [DDS 9110-9]
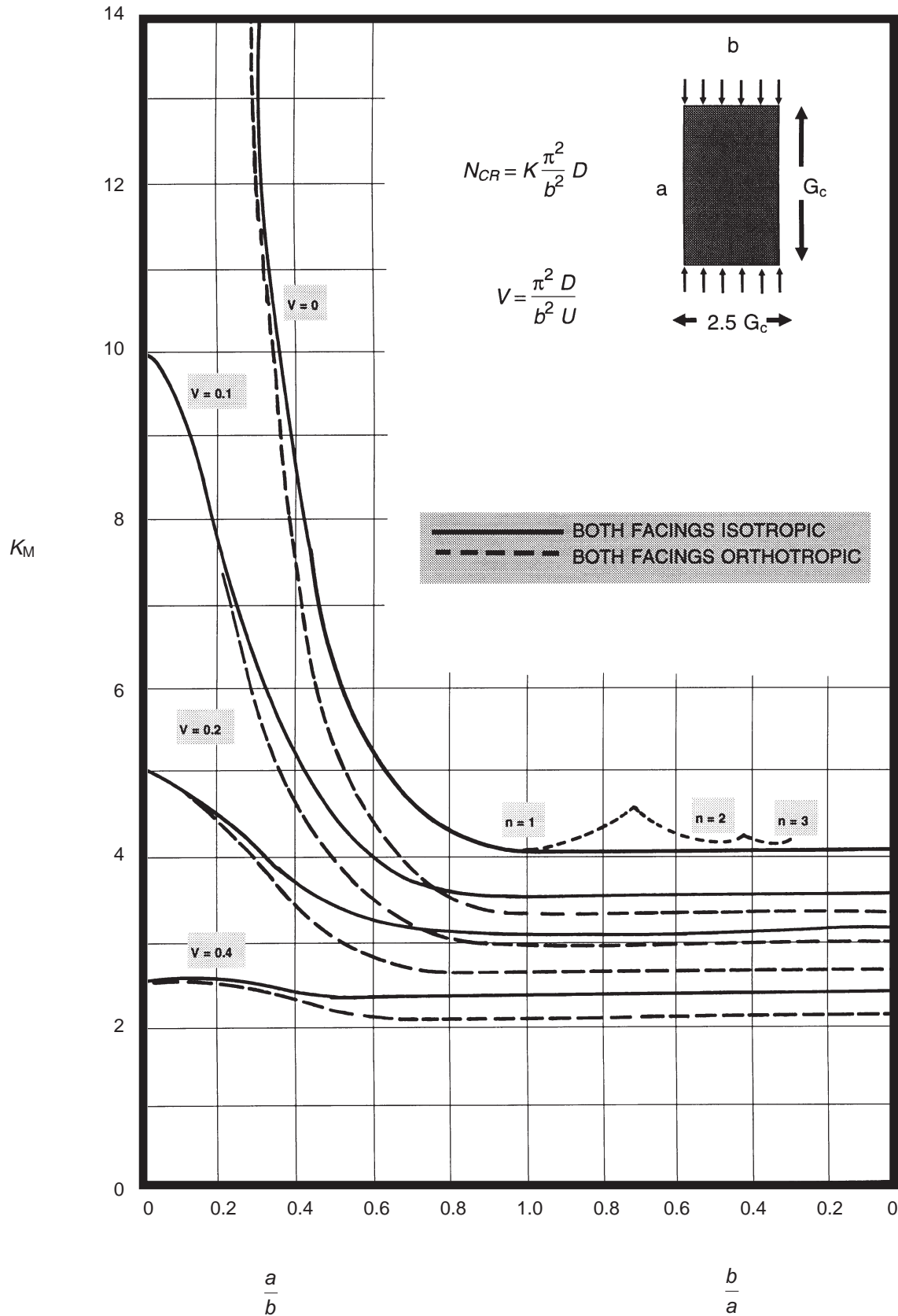
for the Ship Structure Committee   Eric Greene Associates, Inc.

$$N_{CR} = K \frac{\pi^2}{b^2} D$$

$$V = \frac{\pi^2 D}{b^2 U}$$

BOTH FACINGS ISOTROPIC
BOTH FACINGS ORTHOTROPIC

Figure 5-14 K_M for Sandwich Panels with Ends and Sides Simply Supported and Orthotropic Core ($G_{Cb} = 2.5\ G_{Ca}$) [DDS 9110-9]

$$N_{CR} = K \frac{\pi^2}{b^2} D$$

$$V = \frac{\pi^2 D}{b^2 U}$$

BOTH FACINGS ISOTROPIC
BOTH FACINGS ORTHOTROPIC
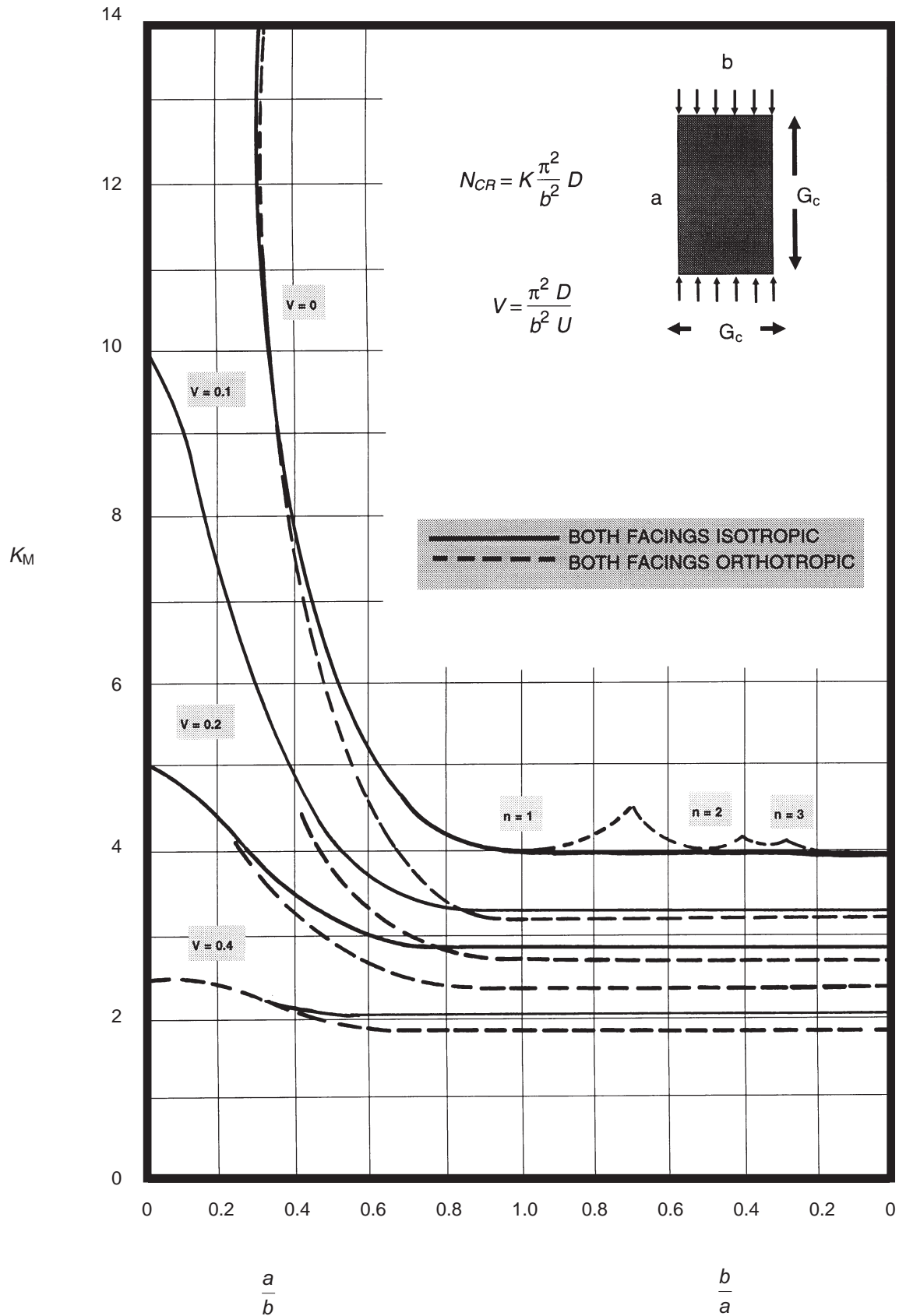
Figure 5-15 K_M for Sandwich Panels with Ends and Sides Simply Supported and Isotropic Core ($G_{Cb} = G_{Ca}$) [DDS 9110-9]

Figure 5-16 K_M for Sandwich Panels with Ends and Sides Simply Supported and Orthotropic Core ($G_{Cb} = 0.4\ G_{Ca}$) [DDS 9110-9]

$$N_{CR} = K \frac{\pi^2}{b^2} D$$

$$V = \frac{\pi^2}{b^2} \frac{D}{U}$$

b

a

G_c

2.5 G_c

V = 0

V = 0.1

V = 0.2

n = 1   n = 2   n = 3

K_M

BOTH FACINGS ISOTROPIC
BOTH FACINGS ORTHOTROPIC

$\frac{a}{b}$

$\frac{b}{a}$

Figure 5-17 K_M for Sandwich Panels with Ends Simply Supported, Sides Clamped
and Orthotropic Core ($G_{Cb} = 2.5\ G_{Ca}$) [DDS 9110-9]

$$N_{CR} = K\frac{\pi^2}{b^2}D$$

$$V = \frac{\pi^2 D}{b^2 U}$$
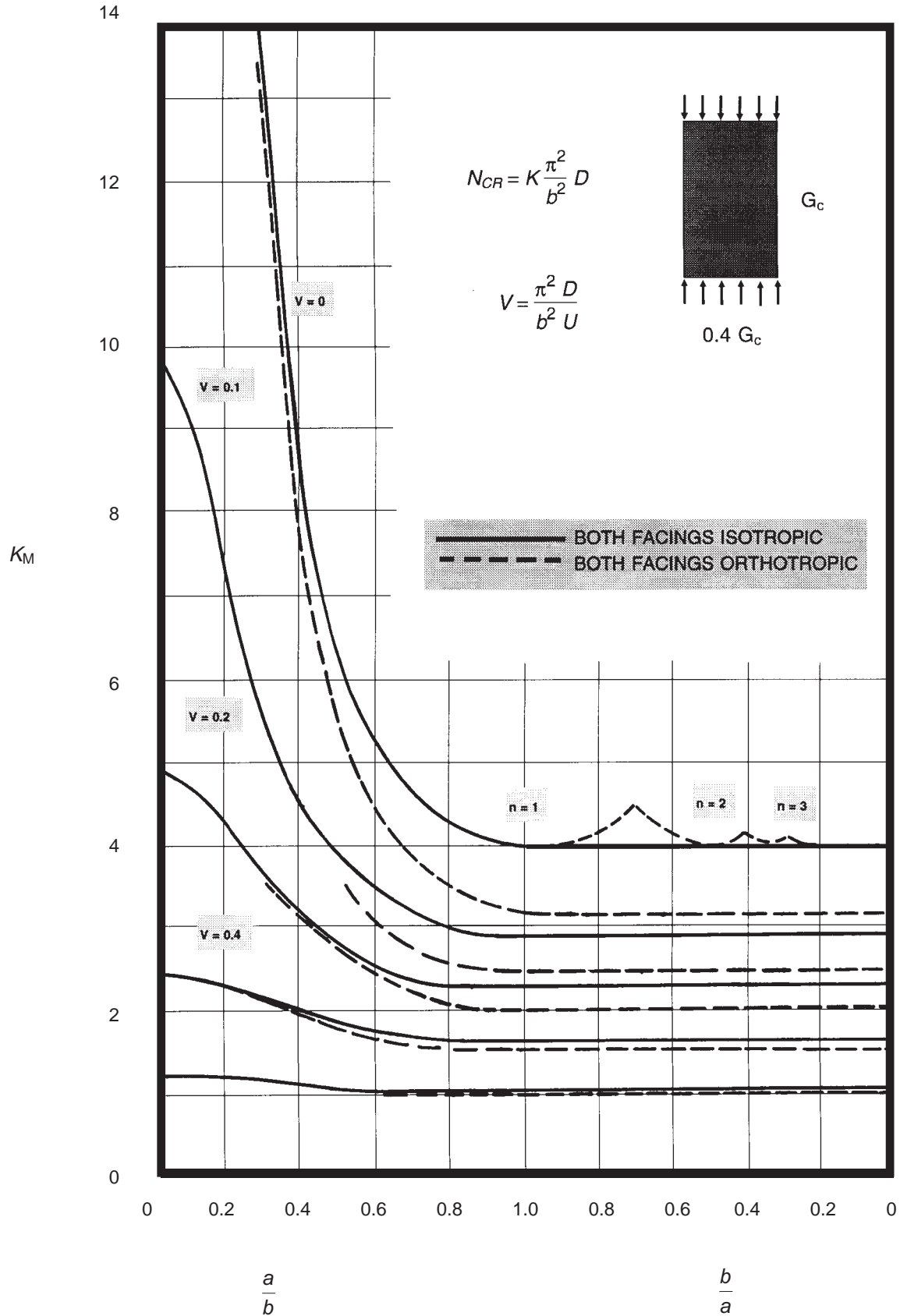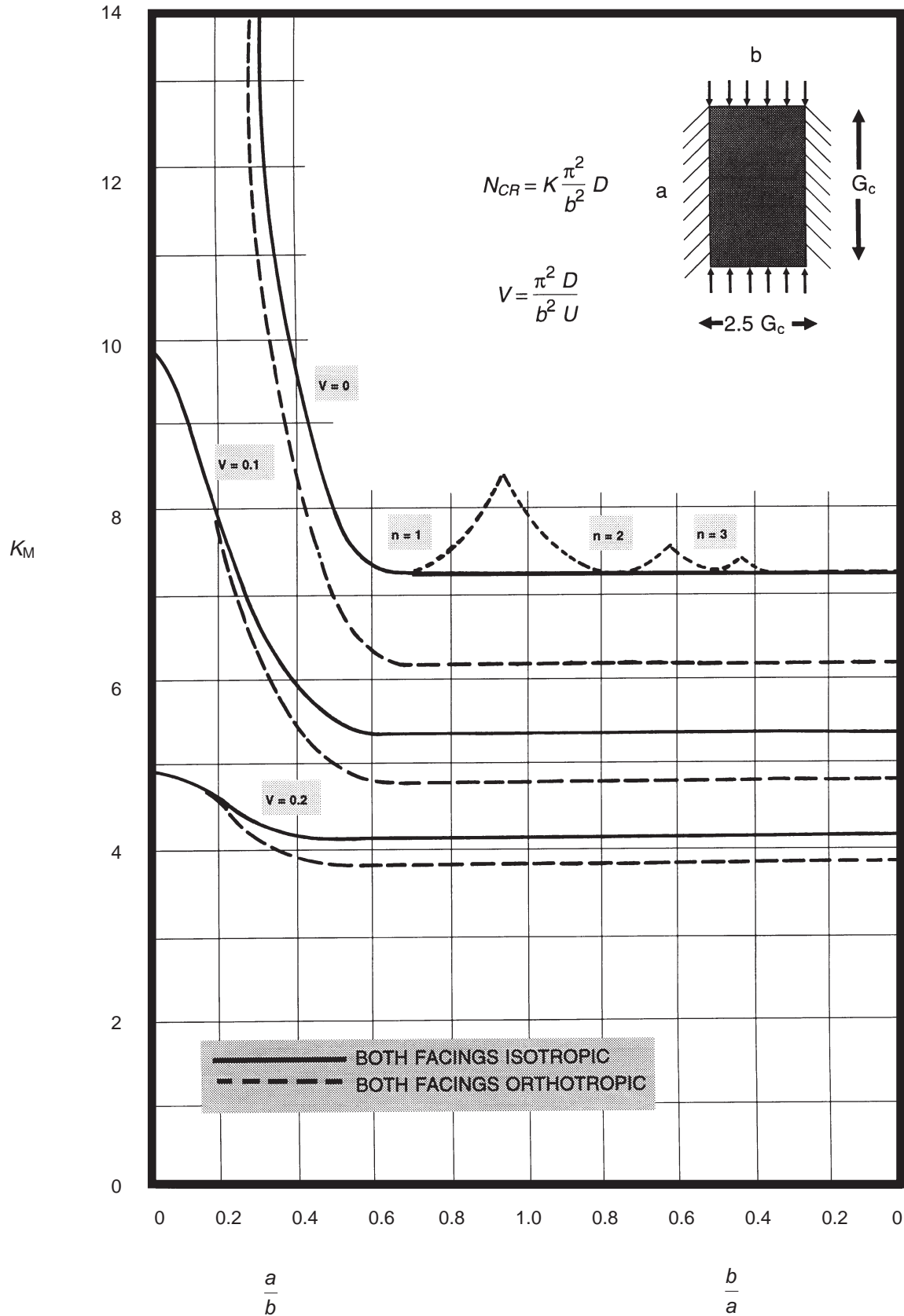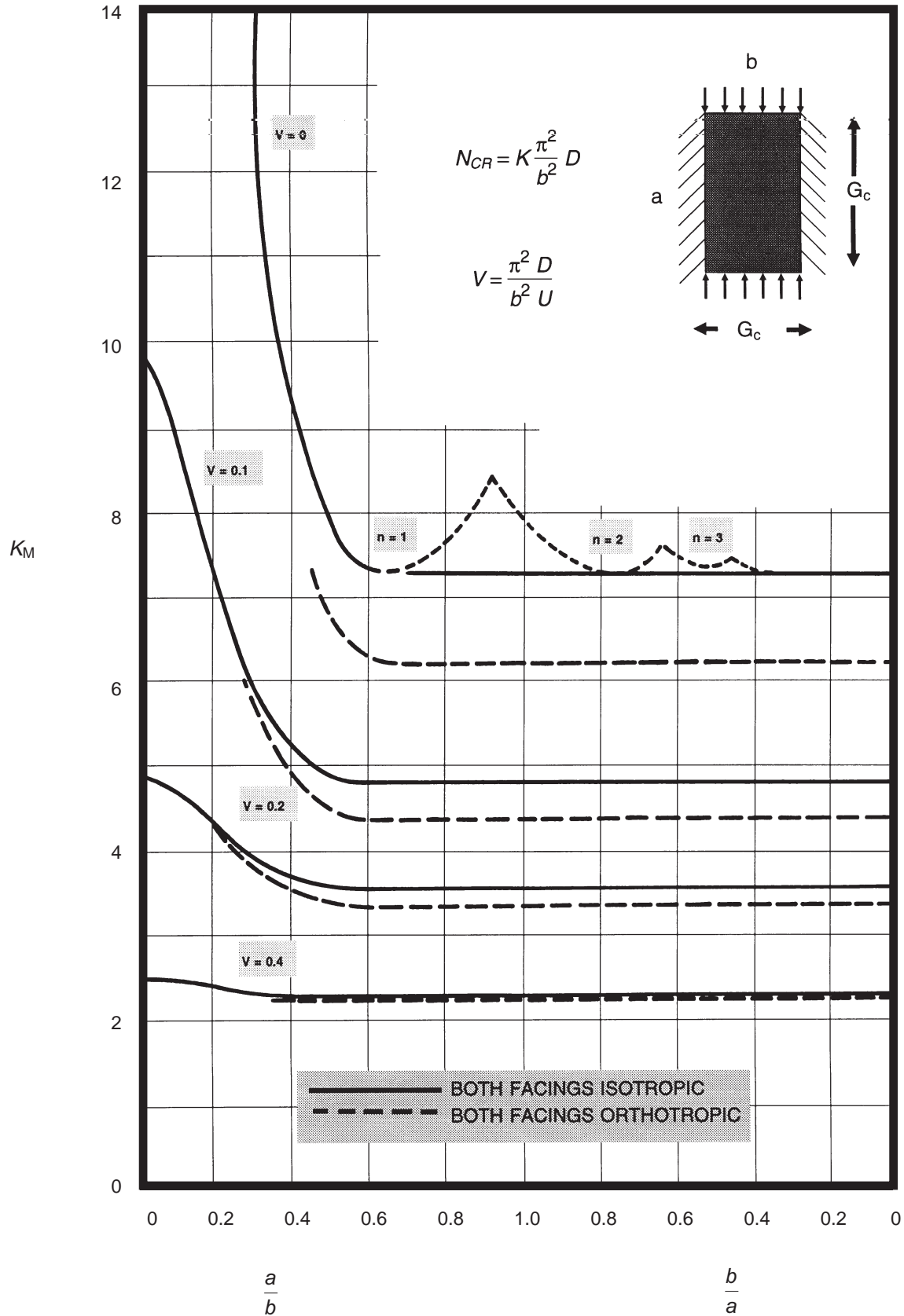
Figure 5-18 K_M for Sandwich Panels with Ends Simply Supported, Sides Clamped
and Isotropic Core ($G_{Cb} = G_{Ca}$) [DDS 9110-9]

Figure 5-19 K_M for Sandwich Panels with Ends Simply Supported, Sides Clamped and Orthotropic Core ($G_{Cb} = 0.4\ G_{Ca}$) [DDS 9110-9]

$$N_{CR} = K \frac{\pi^2}{b^2} D$$

$$V = \frac{\pi^2}{b^2} \frac{D}{U}$$

Figure 5-20 K_M for Sandwich Panels with Ends Clamped, Sides Simply Supported and Orthotropic Core (G_{Cb} = 2.5 G_{Ca}) [DDS 9110-9]

$$N_{CR} = K \frac{\pi^2}{b^2} D$$

$$V = \frac{\pi^2}{b^2} \frac{D}{U}$$

V = 0

V = 0.1

V = 0.2

n = 1

n = 2

BOTH FACINGS ISOTROPIC
BOTH FACINGS ORTHOTROPIC

K_M

$\frac{a}{b}$

$\frac{b}{a}$

Figure 5-21 K_M for Sandwich Panels with Ends Clamped, Sides Simply Supported
and Isotropic Core ($G_{Cb} = G_{Ca}$) [DDS 9110-9]

$$N_{CR} = K \frac{\pi^2}{b^2} D$$

$$V = \frac{\pi^2}{b^2} \frac{D}{U}$$
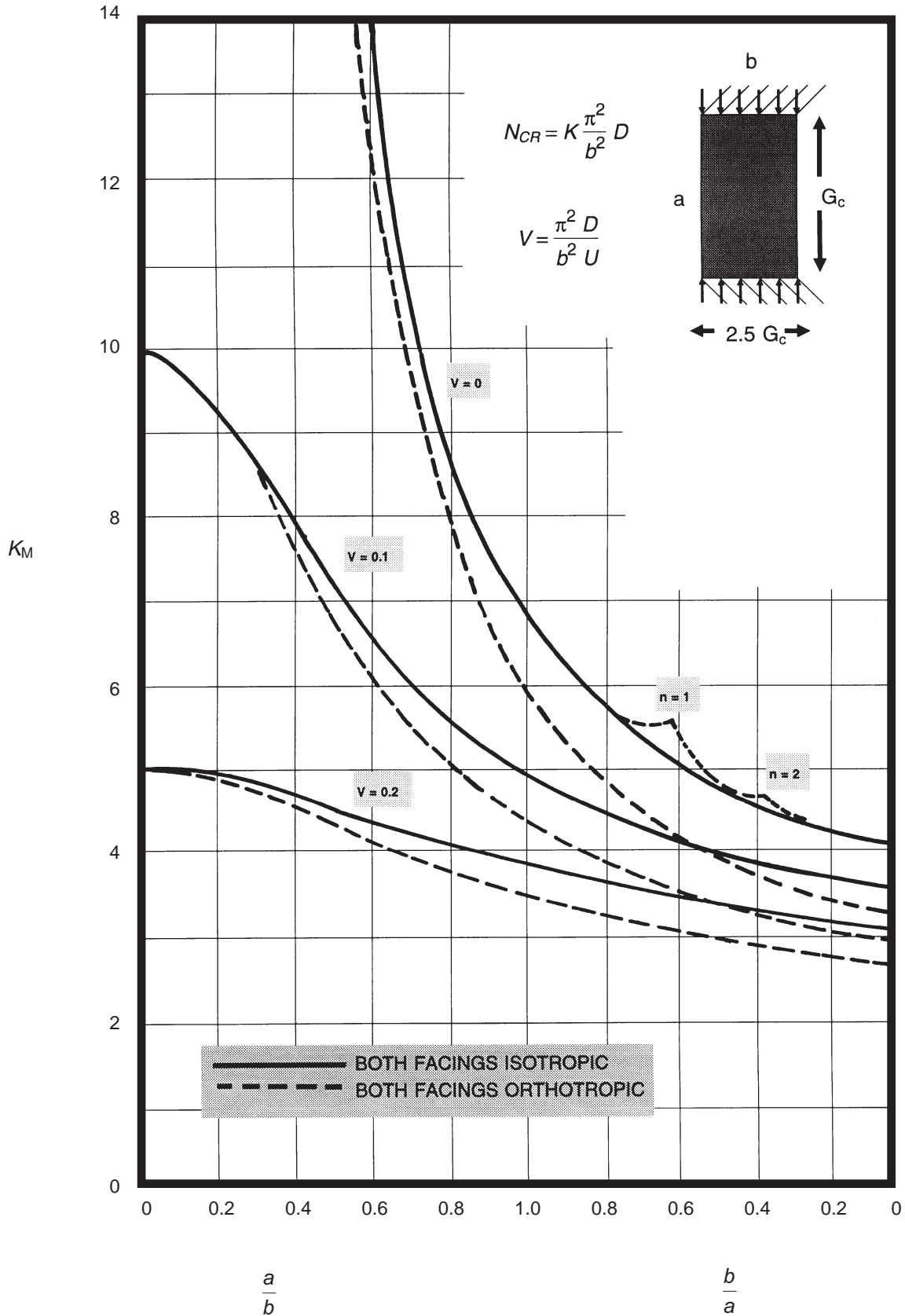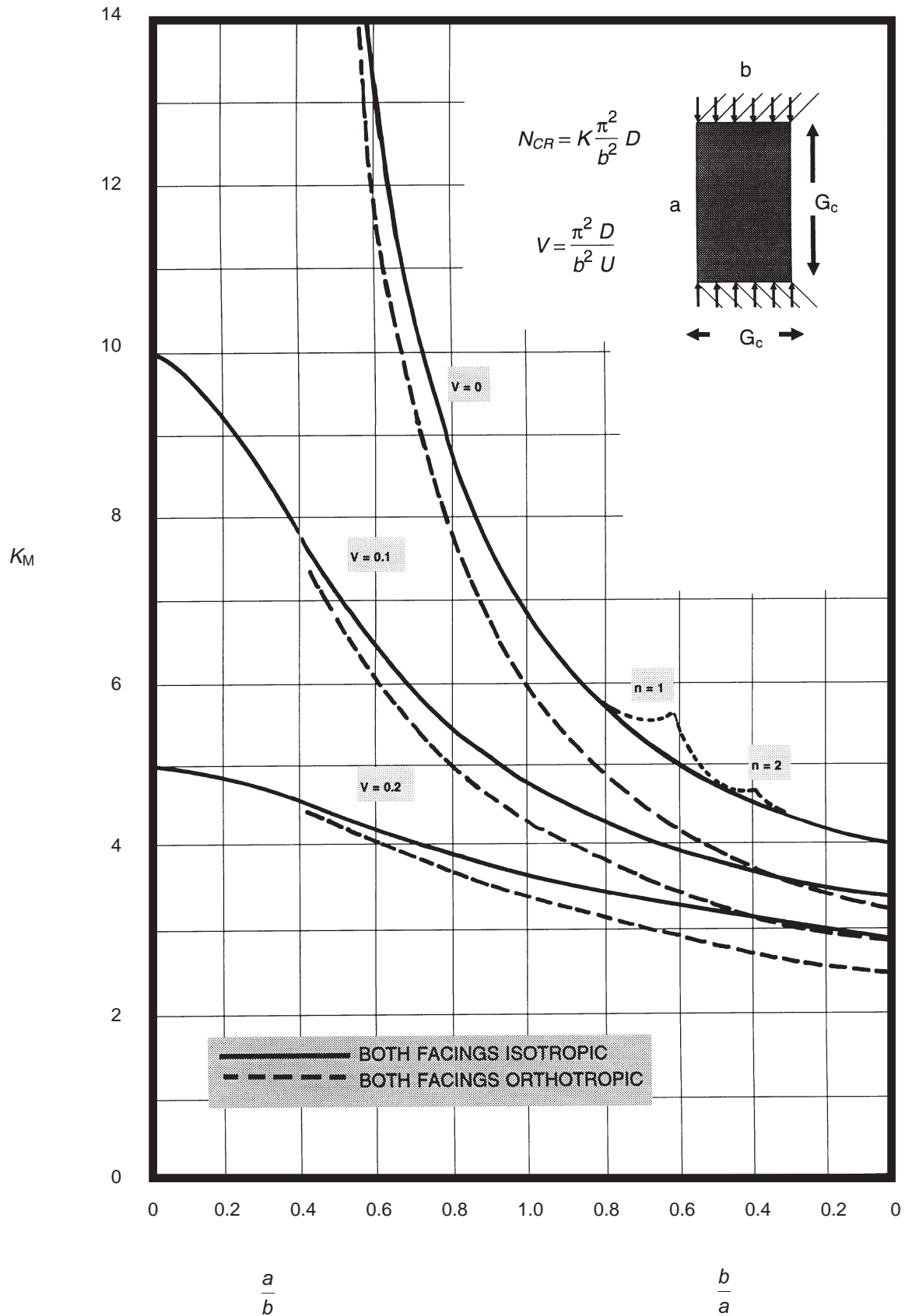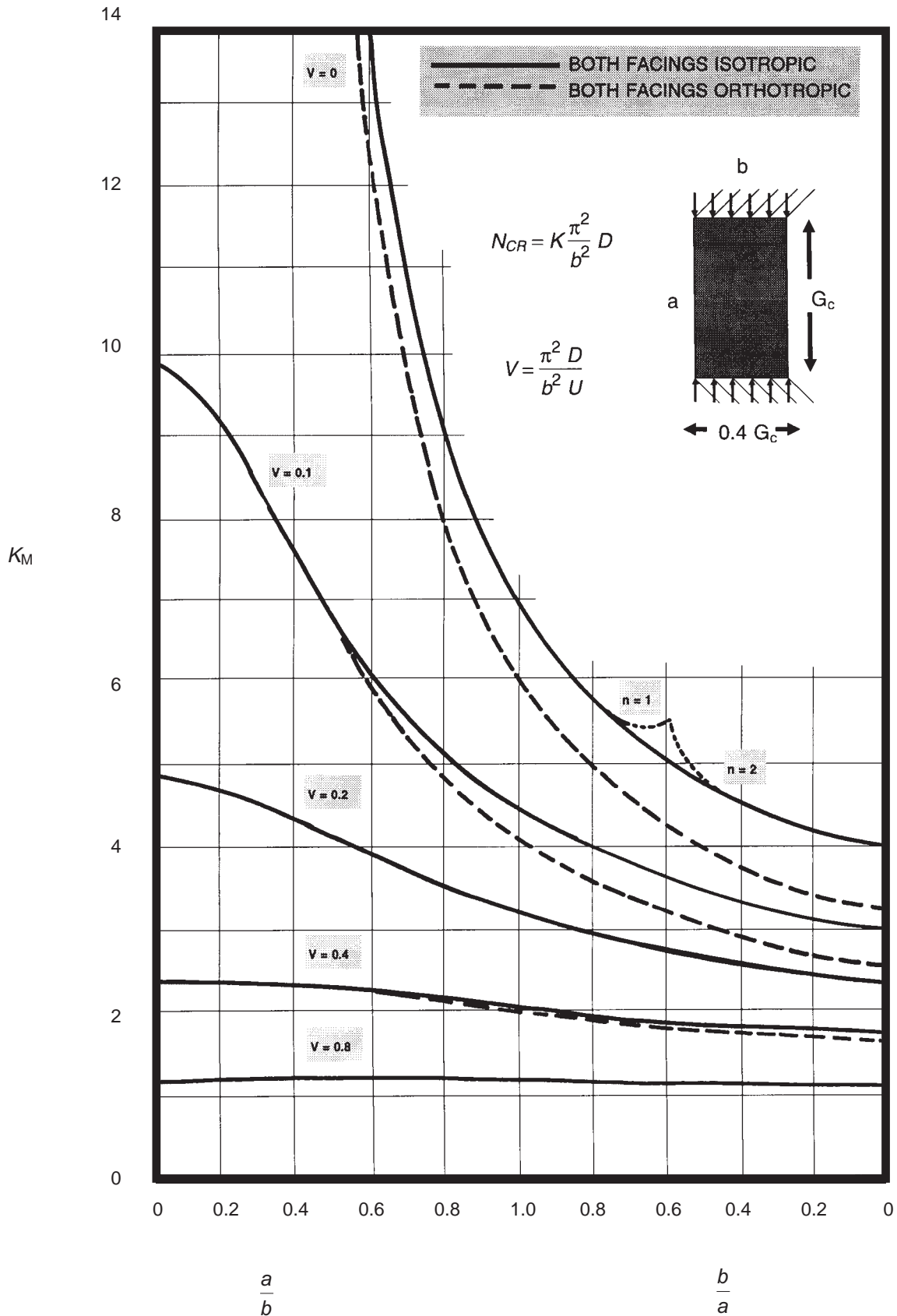
Figure 5-22 K_M for Sandwich Panels with Ends Clamped, Sides Simply Supported and Orthotropic Core ($G_{Cb} = 0.4$ G_{Ca}) [DDS 9110-9]

Figure 5-23 K_M for Sandwich Panels with Ends and Sides Clamped and Orthotropic Core ($G_{Cb} = 2.5\ G_{Ca}$) [DDS 9110-9]

Equations shown in figure:

$$N_{CR} = K \frac{\pi^2}{b^2} D$$

$$V = \frac{\pi^2 D}{b^2 U}$$

Curve labels: $V = 0$, $V = 0.1$, $V = 0.2$, $V = 0.4$, $n = 1$, $n = 2$, $n = 3$

Legend:
— BOTH FACINGS ISOTROPIC
- - - BOTH FACINGS ORTHOTROPIC

Vertical axis: K_M

Horizontal axes: $\frac{a}{b}$ and $\frac{b}{a}$
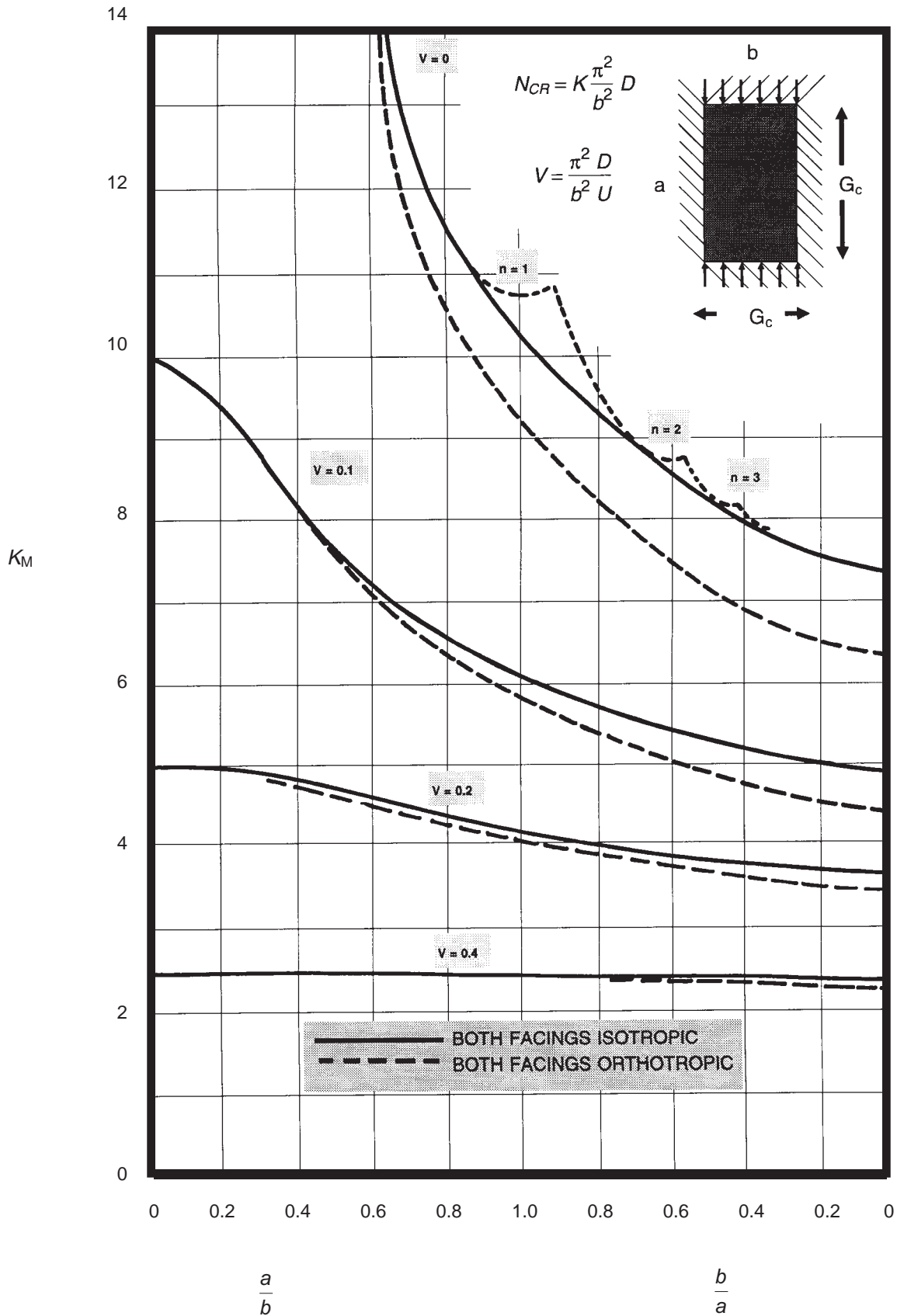
Figure 5-24 K_M for Sandwich Panels with Ends and Sides Clamped and Isotropic Core ($G_{Cb} = G_{Ca}$) [DDS 9110-9]
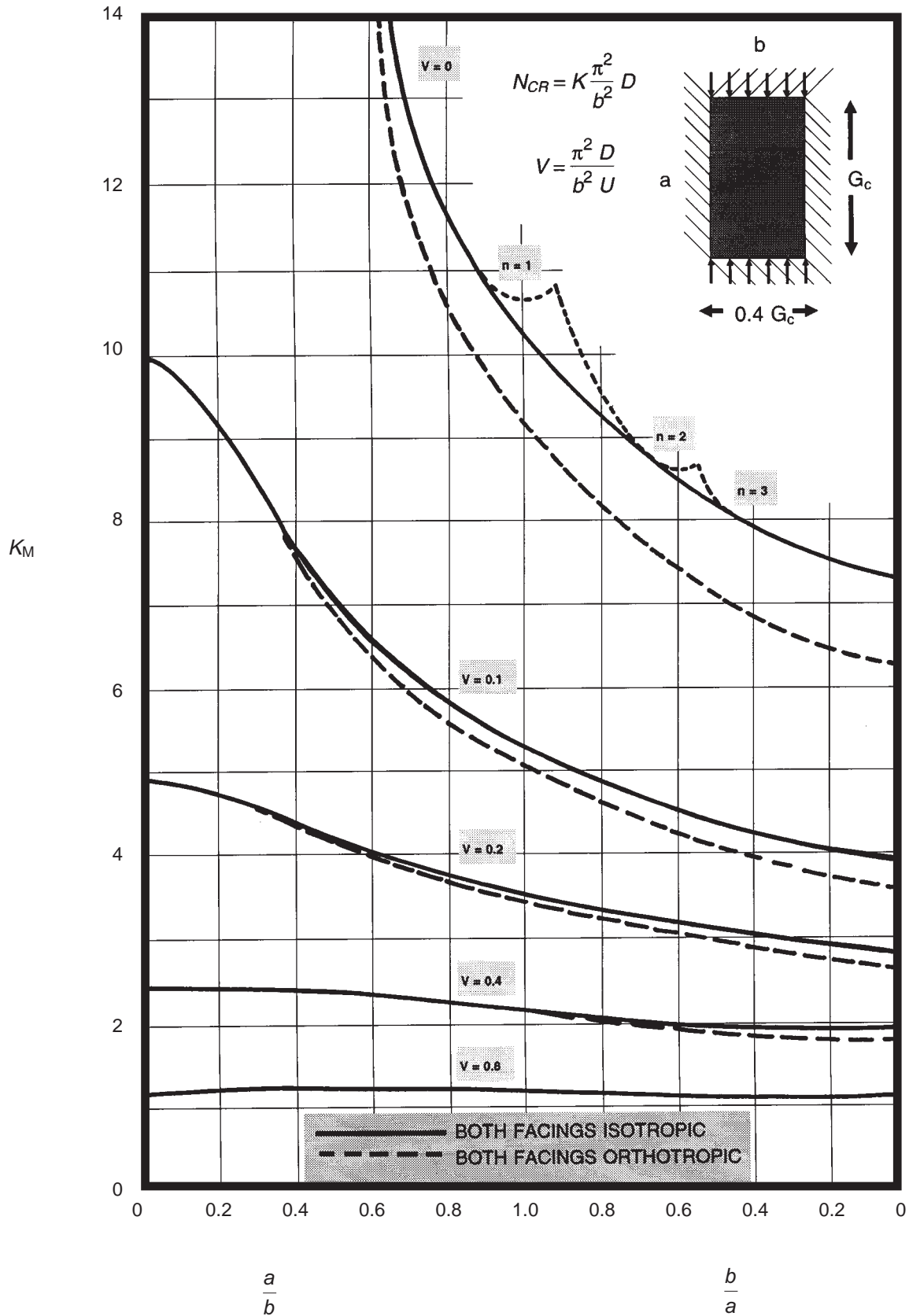
Figure 5-25 K_M for Sandwich Panels with Ends and Sides Clamped and Orthotropic
Core (G_{Cb} = 0.4 G_{Ca}) [DDS 9110-9]
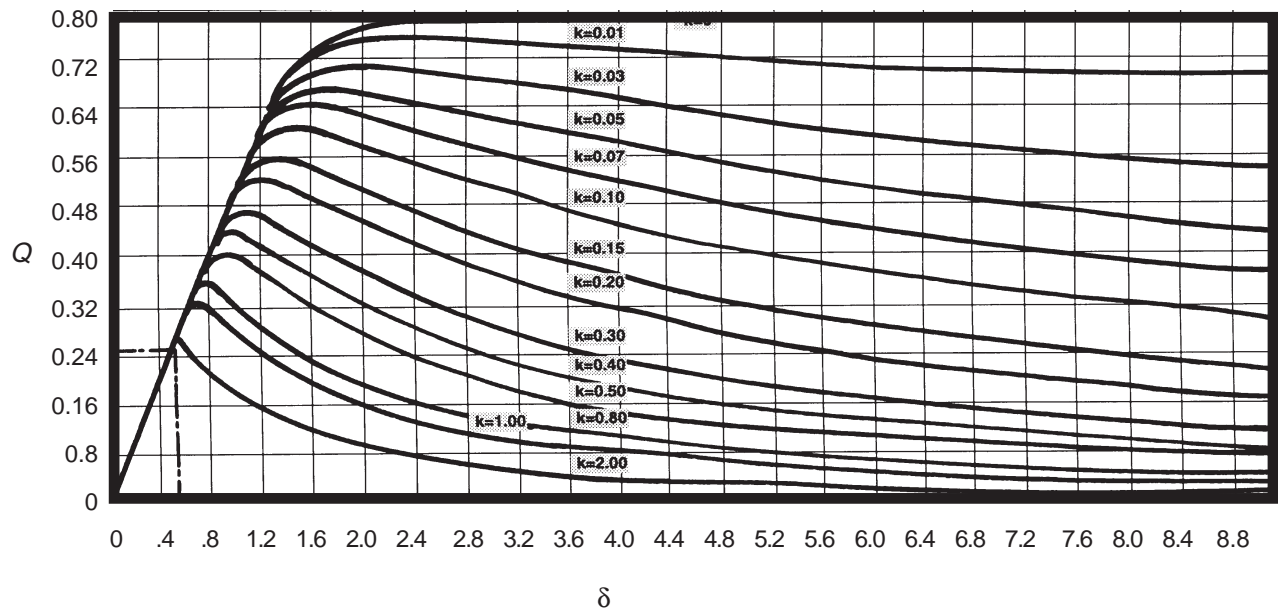
Figure 5-26   Parameters for Face Wrinkling Formulas [DDS 9110-9]
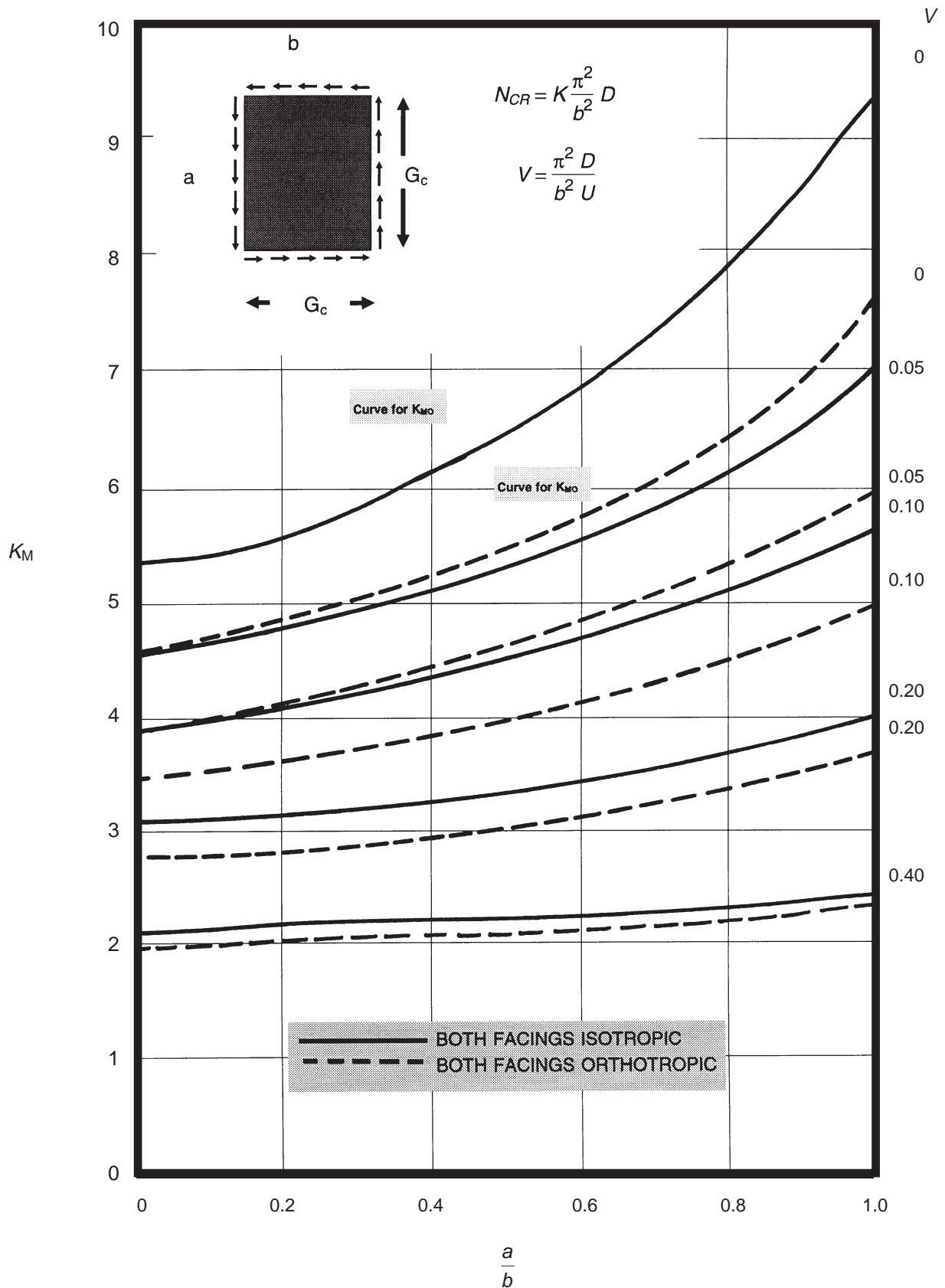
Figure 5-27 *K_M* for Sandwich Panels with All Edges Simply Supported and Isotropic
Core [DDS 9110-9]
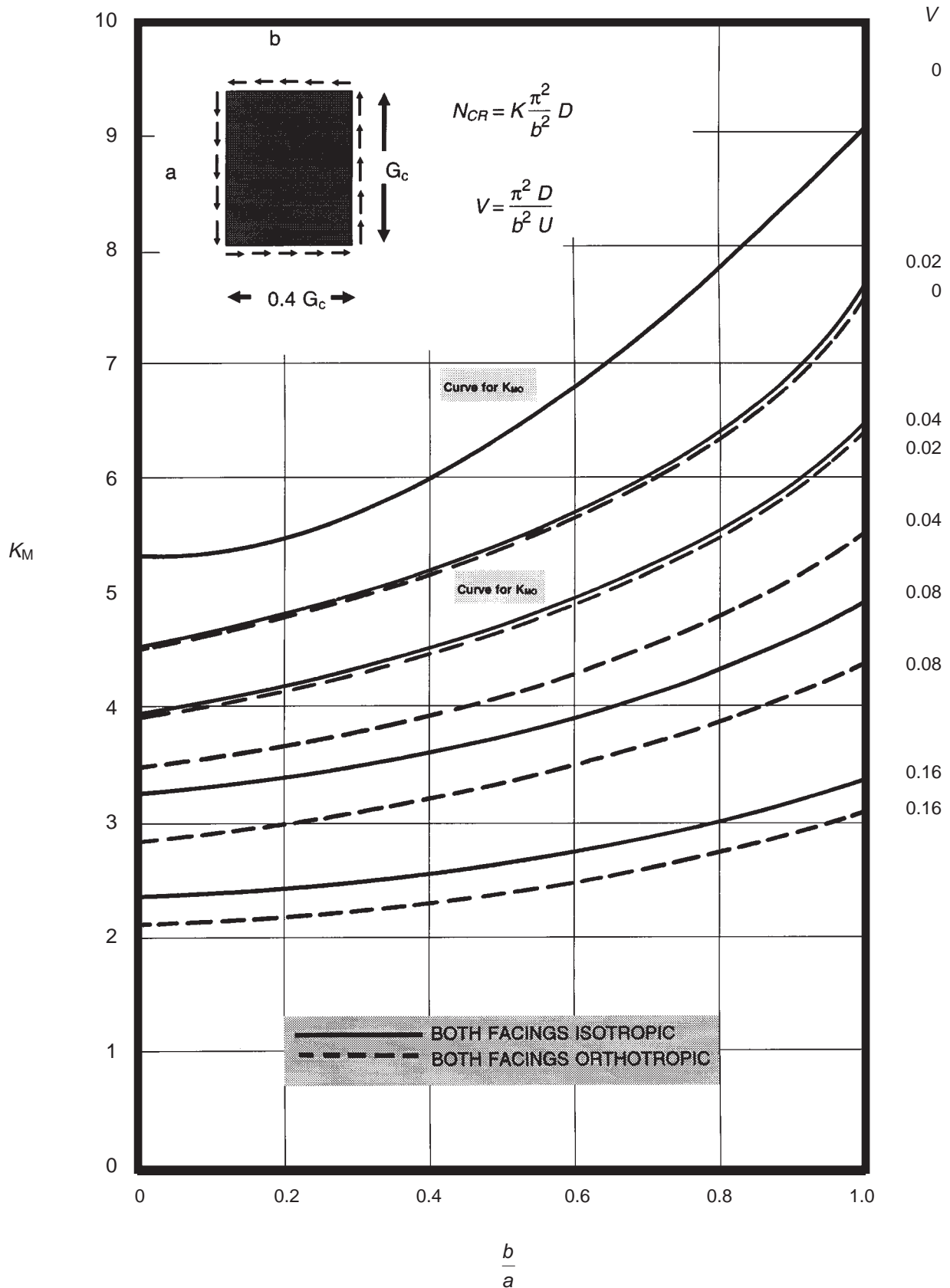
Figure 5-28 K_M for Sandwich Panels with All Edges Simply Supported and Orthotropic Core ($G_{Cb} = 0.4$ G_{Ca}) [DDS 9110-9]
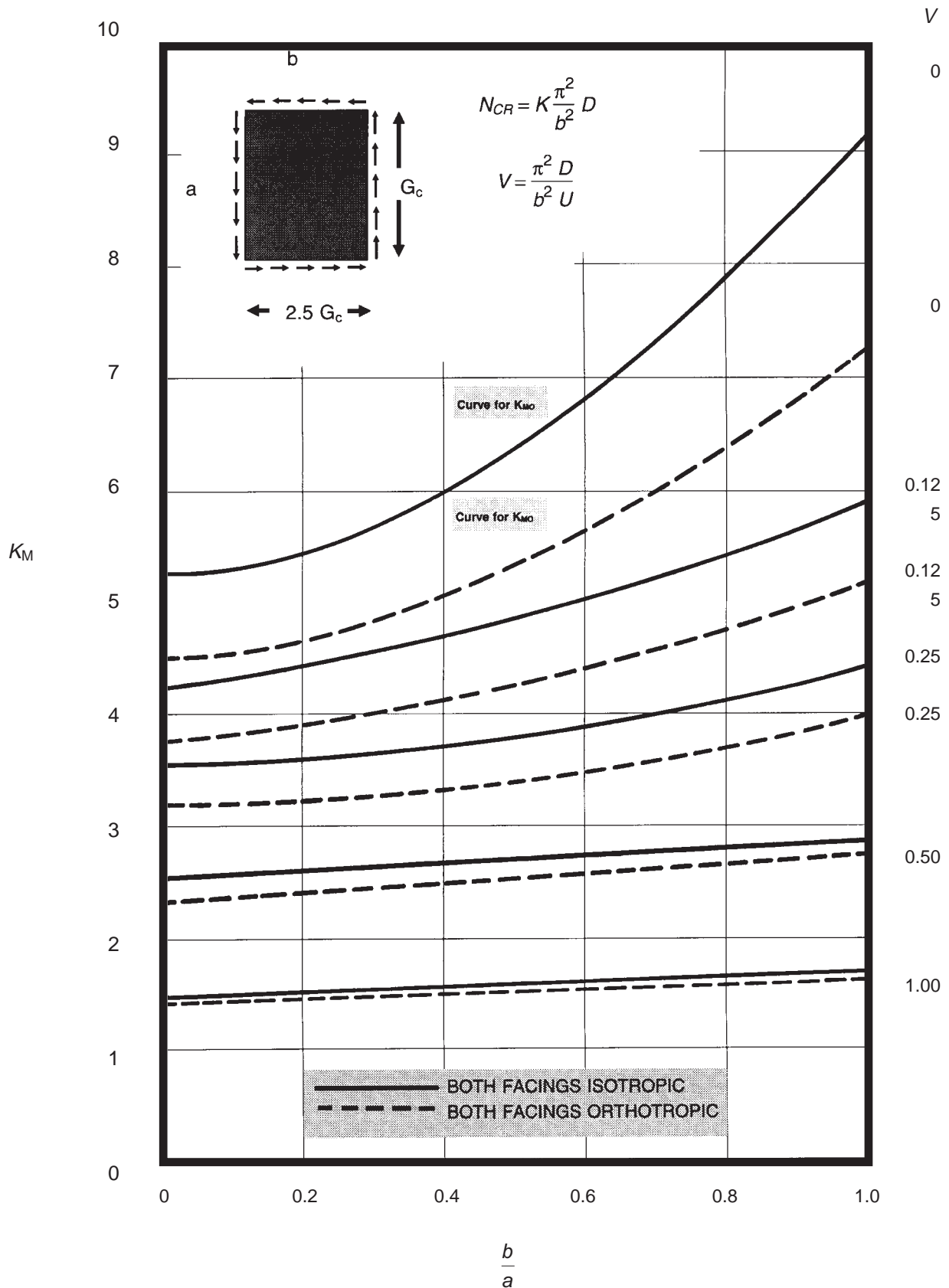
Figure 5-29 K_M for Sandwich Panels with All Edges Simply Supported and Orthotropic Core (G_{Cb} = 2.5 G_{Ca}) [DDS 9110-9]
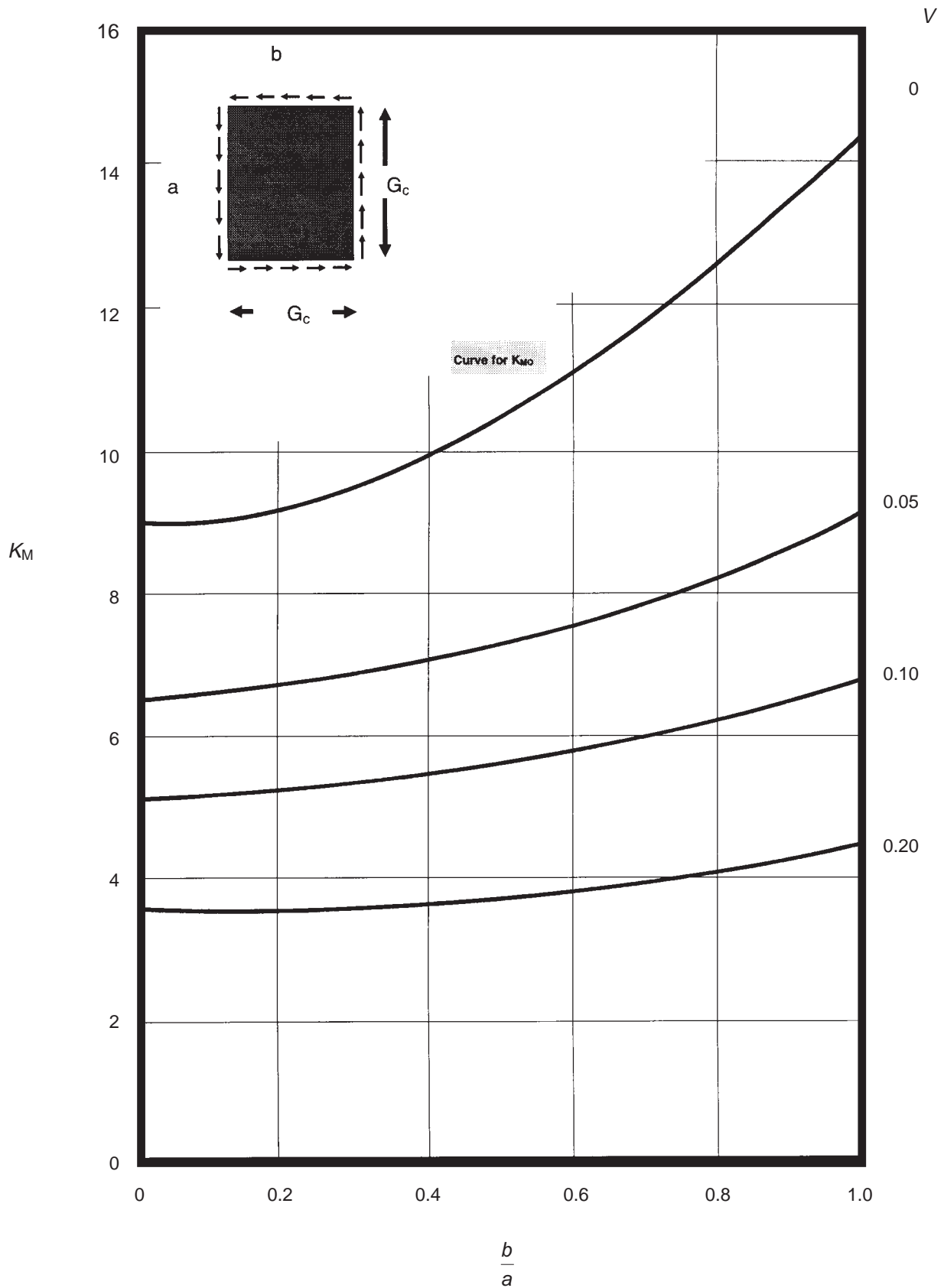
Figure 5-30 K_M for Sandwich Panels with All Edges Clamped, Isotropic Facings and Isotropic Core [DDS 9110-9]

Figure 5-31 K_M for Sandwich Panels with All Edges Clamped, Isotropic Facings and Orthotropic Core ($G_{Cb} = 0.4\ G_{Ca}$) [DDS 9110-9]

Figure 5-32 K_M for Sandwich Panels with All Edges Clamped, Isotropic Facings and Orthotropic Core ($G_{Cb} = 2.5\ G_{Ca}$) [DDS 9110-9]

Figure 5-33 K_1 for Maximum Deflection, δ, of Flat, Rectangular Sandwich Panels with Isotropic Facings and Isotropic or Orthotropic Cores Under Uniform Loads [DDS 9110-9]

for the Ship Structure Committee   Eric Greene Associates, Inc.

Figure 5-34 K_2 for Determining Face Stress, F_F of Flat, Rectangular Sandwich Panels with Isotropic Facings and Isotropic or Orthotropic Cores Under Uniform Loads [DDS 9110-9]

$$F_{C3} = K_3 \, p \, \frac{b}{h}$$

$$V = \frac{\pi^2}{b^2} \frac{D}{U}$$
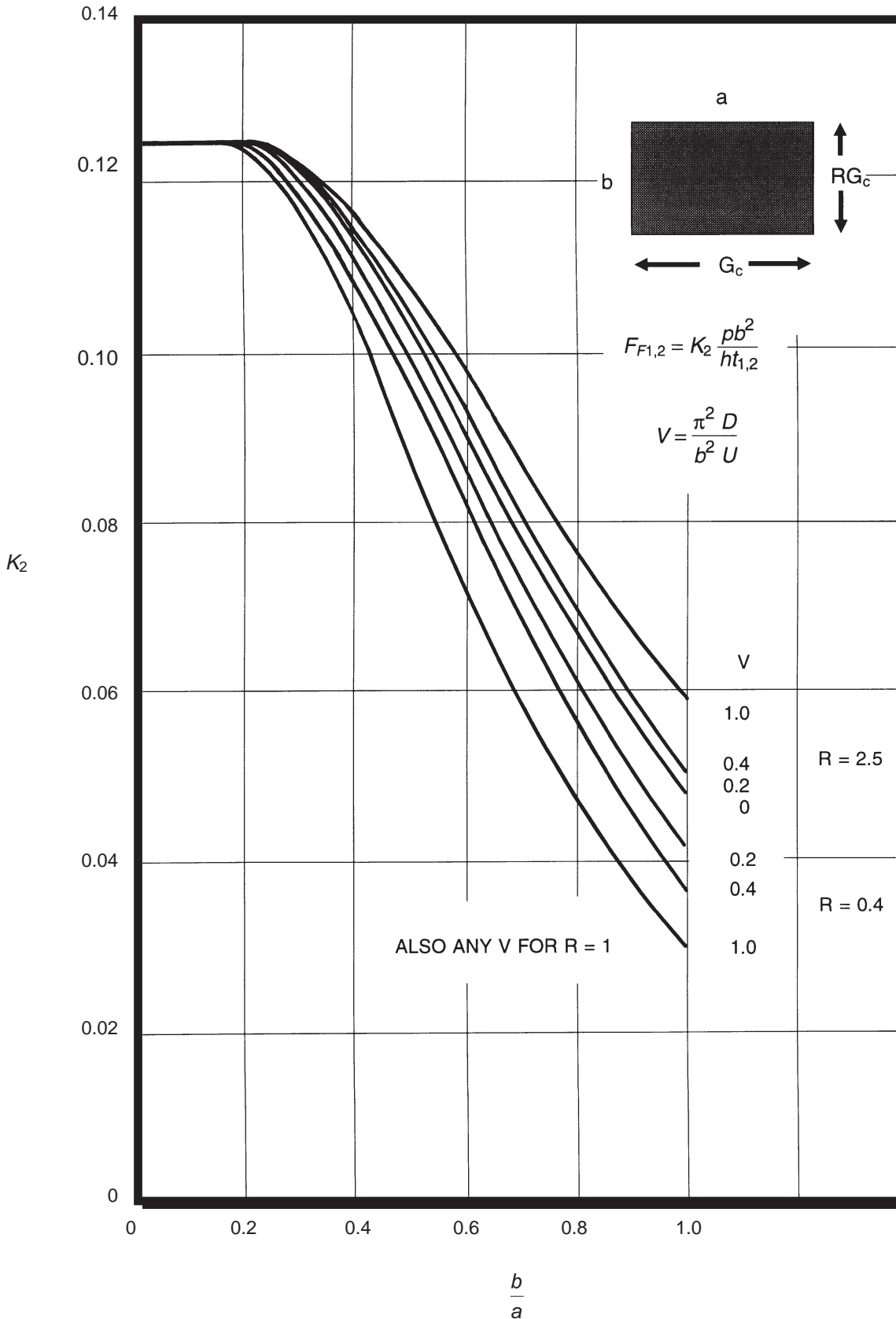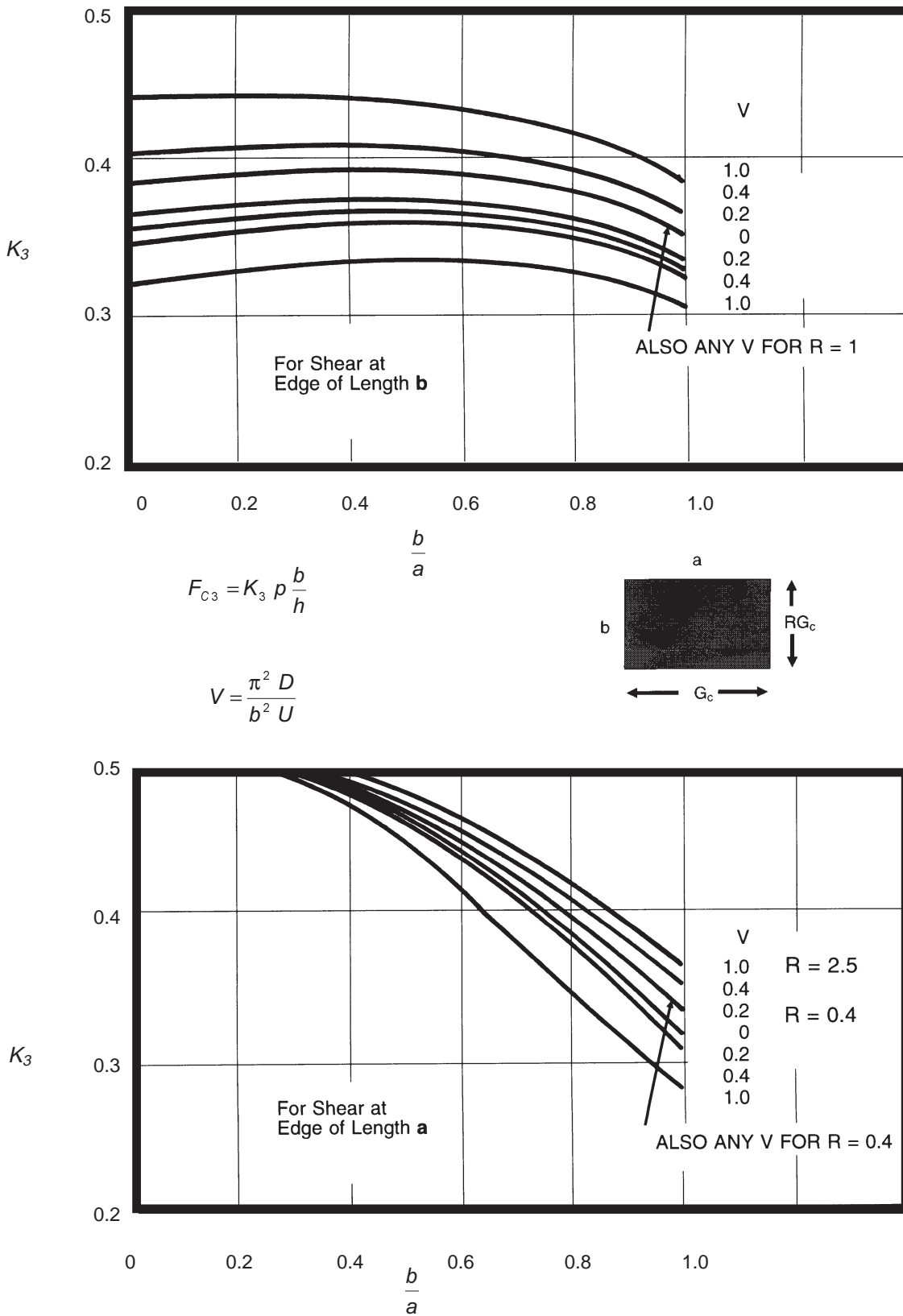
Figure 5-35 K_3 for Determining Maximum Core Shear Stress, F_{Cs}, for Sandwich
Panels with Isotropic Facings and Isotropic or Orthotropic Cores Under Uniform Loads
[DDS 9110-9]

Buckling of Transversely Framed Panels

FRP laminates generally have ultimate tensile and compressive strengths that are comparable with mild steel but stiffness is usually only 5% to 10%. A dominant design consideration then becomes elastic instability under compressive loading. Analysis of the buckling behavior of FRP grillages common in ship structures is complicated by the anisotrophic nature of the materials and the stiffener configurations typically utilized. Smith [22] has developed a series of data curves to make approximate estimates of the destabilizing stress, σ_x, required to produce catastrophic failure in transversely framed structures (see Figure 5-36).
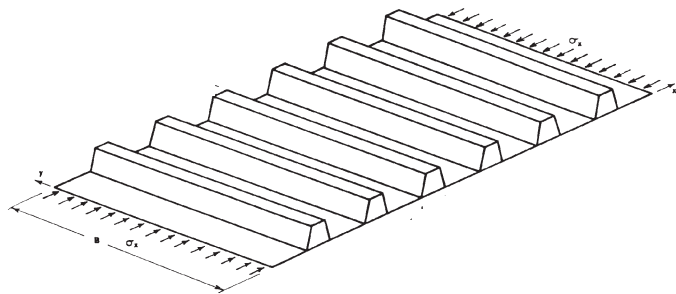
Figure 5-36   Transversely Stiffened Panel [Smith, *Buckling Problems in the Design of Fiberglass Reinforced Plastic Ships*]

The lowest buckling stresses of a transversely framed structure usually correspond to one of the interframe modes illustrated in Figure 5-37.

The first type of buckling (a) involves maximum flexural rotation of the shell/stiffener interface and minimal displacement of the actual stiffener.
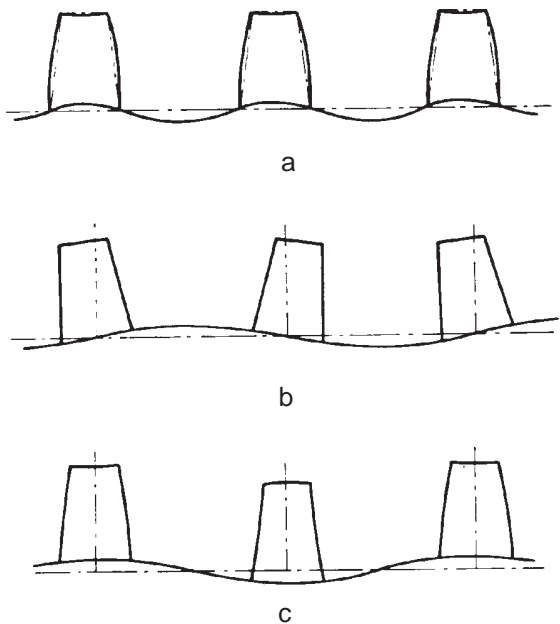
Figure 5-37   Interframe Buckling Modes [Smith, *Buckling Problems in the Design of Fiberglass Plastic Ships*]
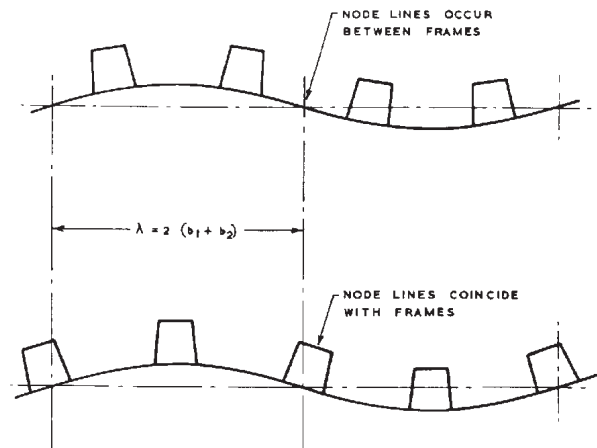
Figure 5-38   Extraframe Buckling Modes [Smith, *Buckling Problems in the Design of Fiberglass Plastic Ships*]

This action is dependent upon the restraining stiffness of the stiffener and is independent of the transverse span.

The buckling phenomena shown in (b) is the result of extreme stiffener rotation, and as such, is a function of transverse span which influences stiffener torsional stiffness.

The third type of interframe buckling depicted (c) is unique to FRP structures, but can often proceed the other failure modes. In this scenario, flexural deformation of the stiffeners produces bending of the shell plating at a half-wavelength coincident with the stiffener spacing. Large, hollow top-hat stiffeners can cause this effect. The restraining influence of the stiffener as well as the transverse span length are factors that control the onset of this type of buckling. All buckling modes are additionally influenced by the stiffener spacing and dimensions and the flexural rigidity of the shell.

Buckling of the structure may also occur at half-wavelengths greater than the spacing of the stiffeners. The next mode encountered is depicted in Figure 5-38 with nodes at or between stiffeners. Formulas for simply supported orthotropic plates show good agreement with more rigorous folded-plate analysis in predicting critical loads for this type of failure. [22] The approximate formula is:

$$N_{xcr} = \frac{\pi^2 D_y}{B^2}\left[\frac{D_1 B^2}{D_y \lambda^2} + \frac{2D_{xy}}{D_y} + \frac{\lambda^2}{B^2}\right] \qquad (5\text{-}43)$$

where:

N_{xcr} = critical load per unit width

D_y = flexural rigidity per unit width

D_1 = flexural rigidity of the shell in the x-direction

D_{xy} = stiffened panel rigidity = $\frac{1}{2}(C_x + C_y)$ with C_y = torsional rigidity per unit width and C_x = twisting rigidity of the shell (first term is dominant)

λ = buckling wavelength

Longitudinally framed vessels are also subject to buckling failure, albeit at generally higher critical loads. If the panel in question spans a longitudinal distance L, a suitable formula for estimating critical buckling stress, σ_{ycr}, based on the assumption of simply supported end conditions is:

$$\sigma_{ycr} = \frac{\dfrac{\pi^2 EI}{AL^2}}{1 + \dfrac{\pi^2 EI}{L^2 GA_s}} \qquad (5\text{-}44)$$

where:

EI = flexural rigidity of a longitudinal with assumed effective shell width

A = total cross-sectional area of the longitudinal including effective shell

GA_s = shear rigidity with A_s = area of the stiffener webs

Buckling failure can occur at reduced primary critical stress levels if the structure is subjected to orthogonal compressive stresses or high shear stresses. Areas where biaxial compression may occur include side shell where lateral hydrodynamic load can be significant or in way of frames that can cause secondary transverse stress. Areas of high shear stress include side shell near the neutral axis, bulkheads and the webs of stiffeners.

Large hatch openings are notorious for creating stress concentrations at their corners, where stress levels can be 3-4 times greater than the edge midspan. Large cut-outs reduce the compressive stability of the grillage structure and must therefore be carefully analyzed. Smith [22] has proposed a method for analyzing this portion of an FRP vessel whereby a plane-stress analysis is followed by a grillage buckling calculation to determine the distribution of destabilizing forces (see Figure 5-39). Figure 5-40 shows the first two global failure modes and associated average stress at the structure's mid-length.
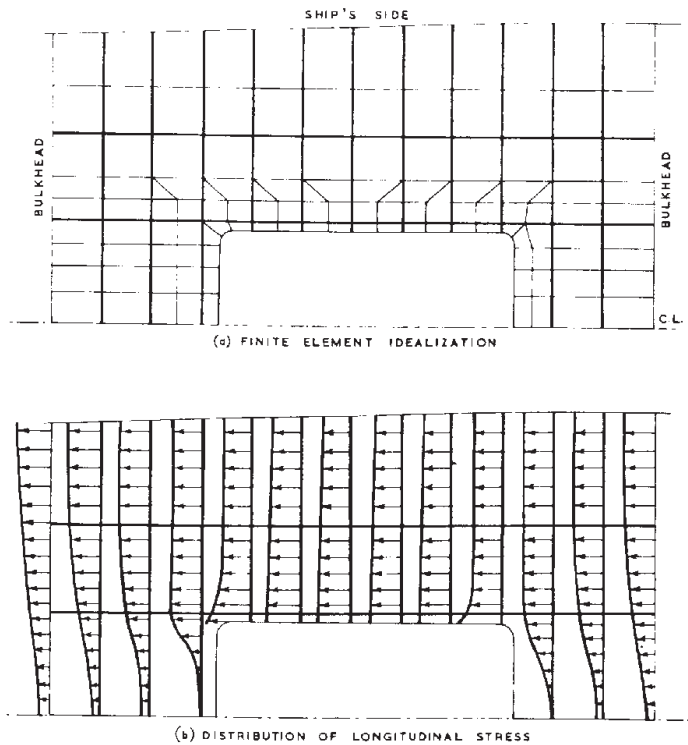
Figure 5-39   Plane Stress Analysis of Hatch Opening [Smith, Buckling Problems in the Design of Fiberglass Plastic Ships]
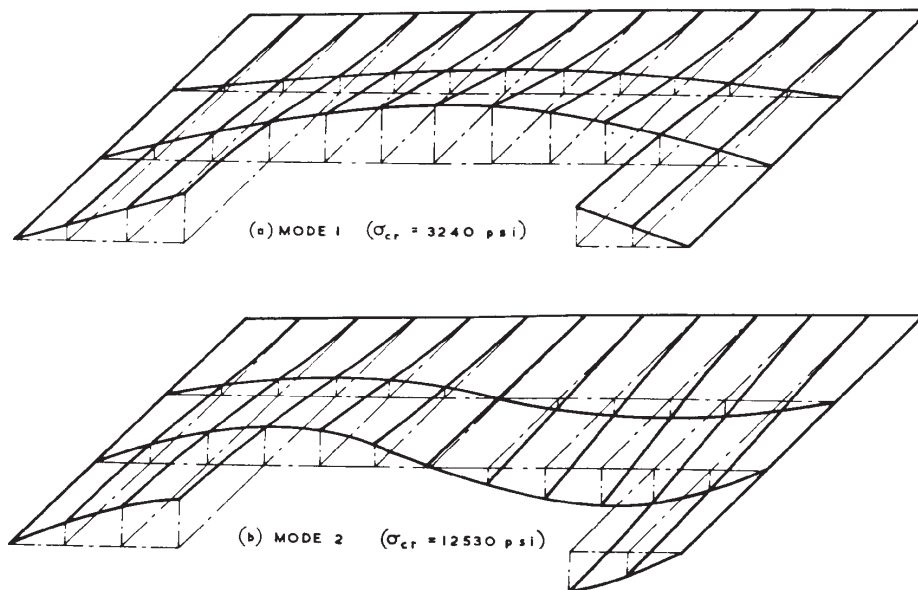
Figure 5-40   Deck Grillage Buckling Modes Near Hatch Opening [Smith, Buckling Problems in the Design of Fiberglass Plastic Ships]

Joints and Details

In reviewing the past four decades of FRP boat construction, very few failures can be attributed to the overall collapse of the structure due to primary hull girder loading. This is in part due to the fact that the overall size of FRP ships has been limited, but also because safety factors have been very conservative. In contrast to this, failures resulting from what is termed "local phenomena" have been observed in the early years of FRP development. As high-strength materials are introduced to improve vessel performance, the safety cushion associated with "bulky" laminates diminishes. As a consequence, the FRP designer must pay careful attention to the structural performance of details.

Details in FRP construction can be any area of the vessel where stress concentrations may be present. These typically include areas of discontinuity and applied load points. As an example, failures in hull panels generally occur along their edge, rather than the center. [23] FRP construction is particularly susceptible to local failure because of the difficulty in achieving laminate quality equal to a flat panel. Additionally, stress concentration areas typically have distinct load paths which must coincide with the directional strengths of the FRP reinforcing material. With the benefit of hindsight knowledge and a variety of reinforcing materials available today, structural detail design can rely less on "brute force" techniques.

Secondary Bonding

FRP structures will always demonstrate superior structural properties if the part is fabricated in one continuous cycle without total curing of intermediate plies. This is because interlaminar properties are enhanced when a chemical as well as mechanical bond is present. Sometimes the part size, thickness or manufacturing sequence preclude a continuous lay-up, thus requiring the application of wet plies over a previously cured laminate, known as secondary bonding. Much of the test data available on secondary bonding performance dates back to the early 1970's when research was active in support of FRP minesweeper programs. Frame and bulkhead connections were targeted as weak points when large hulls were subjected to extreme shock from detonated charges. Reports on secondary bond strength by Owens-Corning Fiberglas [24] and Della Rocca & Scott [25] are summarized below:

- Failures were generally cohesive in nature and not at the bond interface line. A clean laminate surface at the time of bonding is essential and can best be achieved by use of a peeling ply. A peeling ply consists of a dry piece of reinforcement (usually cloth) that is laid down without being wetted out. After cure, this strip is peeled away, leaving a rough bonding surface with raised glass fibers;

- Filleted joints proved to be superior to right-angle joints in fatigue tests. It was postulated that the bond angle material was stressed in more of a pure flexural mode for the radiused geometry;

- Bond strengths between plywood and FRP laminates is less than that of FRP itself. Secondary mechanical fasteners might be considered;

- In a direct comparison between plywood frames and hat-sectioned stiffeners, the stiffeners appear to be superior based on static tests; and

- Chopped strand mat offers a better secondary bond surface than woven roving.

Table 5-2 Secondary Bond Technique Desirability [Della Rocca and Scott, *Materials Test Program for Application of Fiberglass Plastics to U.S.. Navy Minesweepers*]

Preferable Bonding Techniques	Acceptable Bonding Techniques	Undesirable Procedures
Bond resin: either general purpose or fire retardant, resilient	Bond resin: general purpose or fire retardant, rigid air inhibited	No surface treatment
Surface treatment: roughened with a pneumatic saw tooth hammer, peel ply, or continuous cure of rib to panel; one ply of mat in way of bond	Surface treatment: rough sanding	Excessive stiffener faying flange thickness
Stiffener faying flange thickness: minimum consistent with rib strength requirement		
Bolts or mechanical fasteners are recommended in areas of high stress		

Hull to Deck Joints

Since the majority of FRP vessels are built with the deck and hull coming from different molds, the builder must usually decide on a suitable technique for joining the two. Since this connection is at the extreme fiber location for both vertical and transverse hull girder loading, alternating tensile and compressive stresses are expected to be at a maximum. The integrity of this connection is also responsible for much of the torsional rigidity exhibited by the hull. Secondary deck and side shell loading shown in Figure 5-41 is often the design limiting condition. Other design considerations include: maintaining watertight integrity under stress, resisting local impact from docking,
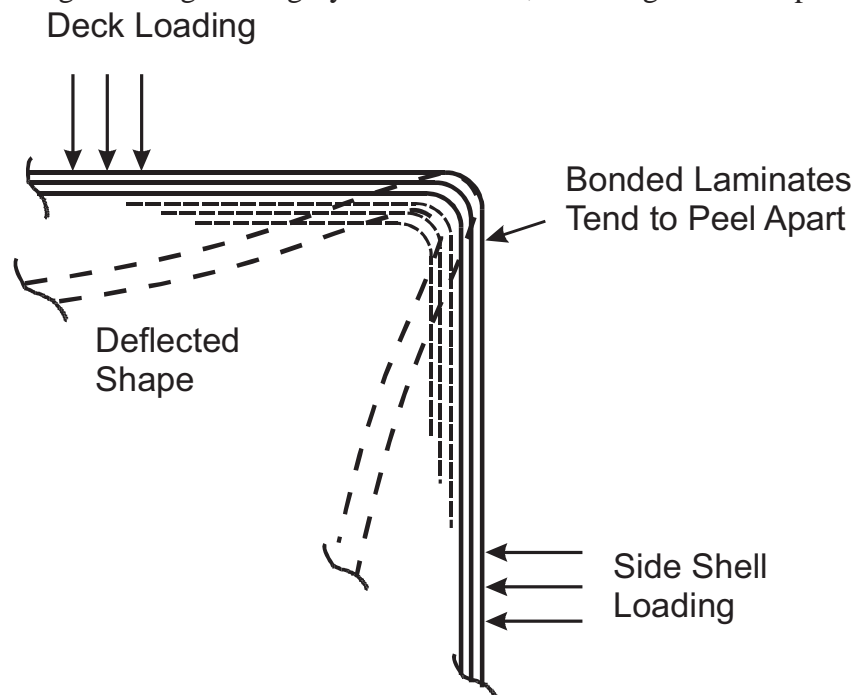
Figure 5-41   Deck Edge Connection - Normal Deck and Shell Loading Produces Tension at the Joint [Gibbs and Cox, *Marine Design Manual for FRP*]

personnel footing assistance, and appearance (fairing of shear). Figure 5-42 shows typical failure modes for traditional sandwich construction with tapered cores. A suggested method for improving hull-to-deck joints is also presented. Transfer of shear loads between inner and outer skins is critical. Note that the lap joint, which used a methacrylate adhesive with a shear strength of 725 psi (50 kg/cm^2) did not fail. This compares with polyester resin, which will typically provide 350 psi (24 kg/cm^2) and epoxy resin, which provides 500 psi (34.5 kg/cm^2) shear strength. [26]

Improved Hull to Deck Joint
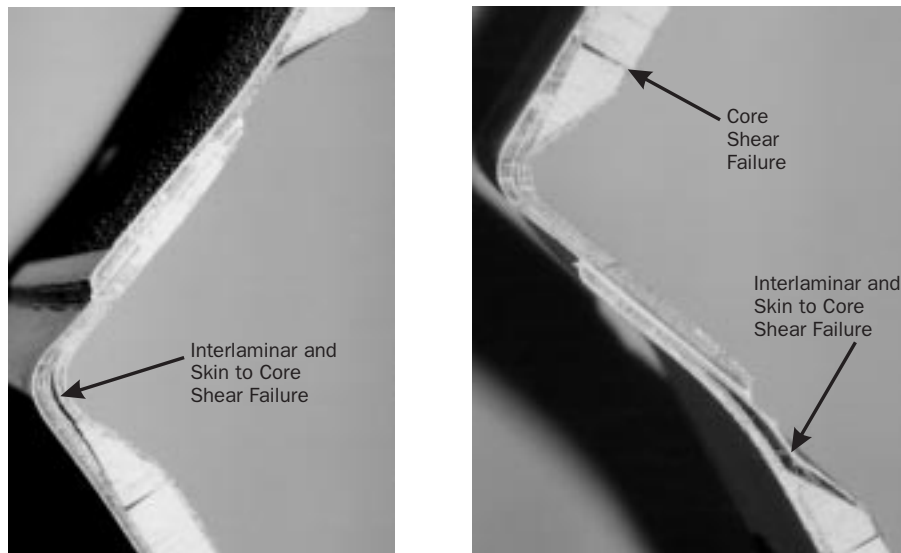
Typical Failures in Tapered Sandwich Joint Configuration

Typical Hull
to Deck Joint
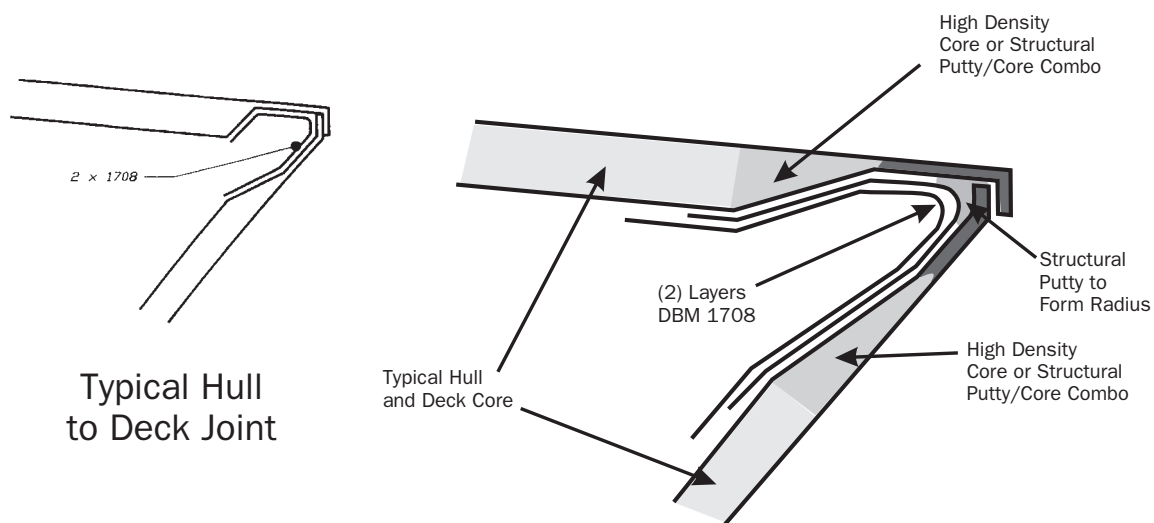
Suggested Improved
Hull to Deck Joint

Figure 5-42   Improved Hull to Deck Joint for Sandwich Core Production Vessels

Bulkhead Attachment

The scantlings for structural bulkheads are usually determined from regulatory body requirements or first principals covering flooding loads and in-plane deck compression loads (see Chapter Three). Design principals developed for hull panels are also relevant for determining required bulkhead strength. Of interest in this section is the connection of bulkheads or other panel stiffeners that are normal to the hull surface. In addition to the joint strength, the strength of the bulkhead and the hull in the immediate area of the joint must be considered. Other design considerations include:

- Some method to avoid creation of a "hard" spot should be used;

- Stiffness of joint should be consistent with local hull panel;

- Avoid laminating of sharp, 90° corners;

- Geometry should be compatible with fabrication capabilities; and

- Cutouts should not leave bulkhead core material exposed.

An acceptable configuration for use with solid FRP hulls is shown in Figure 5-43. As a general rule, tape-in material should be at least 2 inches (50 mm) or $1.4 \times$ *fillet radius* along each leg; have a thickness half of the solid side shell; taper for a length equal to at least three times the tape-in thickness; and include some sort of fillet material. Double bias knitted tapes with or without a mat backing are excellent choices for tape-in material. With primary reinforcement oriented at 45°, all fiberglass adds to the strength of the joint, while at the same time affording more flexibility. Figure 5-44 shows both double-bias tape-in versus conventional woven roving tape-in. When building up layers of reinforcements that have varying widths, it is best to place the narrowest plies on the bottom and work toward increasingly wide reinforcements. This reduces the amount of exposed edges.
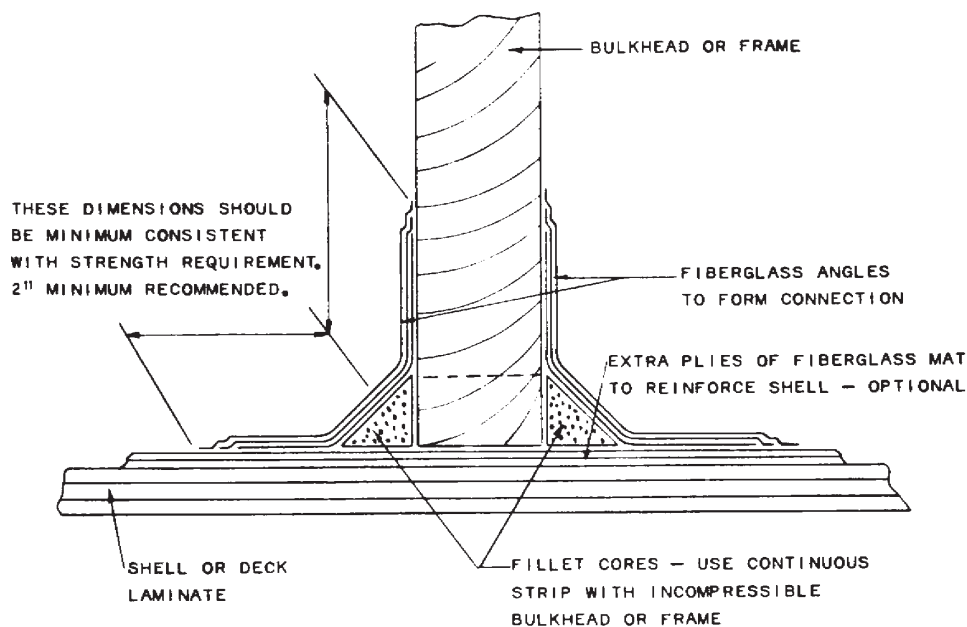
Figure 5-43 Connection of Bulkheads and Framing to Shell or Deck [Gibbs and Cox, *Marine Design Manual for FRP*]
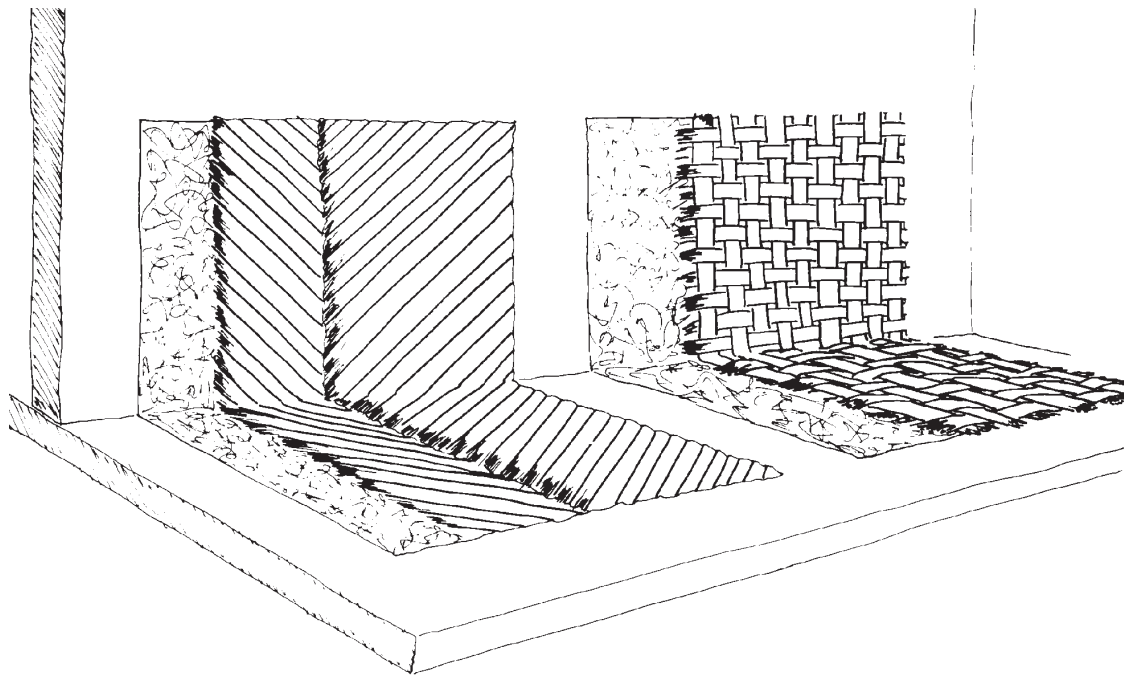
Figure 5-44   Double Bias and Woven Roving Bulkhead Tape-In [Knytex]

Stringers

Stringers in FRP construction can either be longitudinal or transverse and usually have a non-structural core that serves as a form. In general, continuity of longitudinal members should be maintained with appropriate cut-outs in transverse members. These intersections should be completely bonded on both the fore and aft side of the transverse member with a laminate schedule similar to that used for bonding to the hull.

Traditional FRP design philosophy produced stiffeners that were very narrow and deep to take advantage of the increased section modulus and stiffness produced by this geometry. The current trend with high-performance vehicles is toward shallower, wider stiffeners that reduce effective panel width and minimize stress concentrations. Figure 5-45 shows how panel span can be reduced with a low aspect ratio stiffener. Some builders are investigating techniques to integrally mold in stiffeners along with the hull's primary inner skin, thus eliminating secondary bonding problems altogether.

Regulatory agencies, such as ABS, typically specify stiffener scantlings in terms of required section moduli and moments of inertia. [11,12,27] Examples of a single skin FRP stiffener and a high-strength material stiffener with a cored panel are presented along with sample property calculations to illustrate the design process. These examples are taken from USCG NVIC No. 8-87. [27]
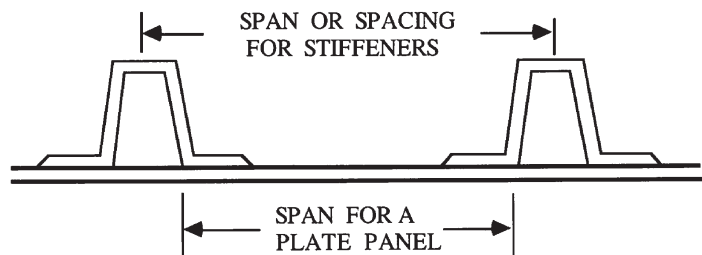
Figure 5-45   Reference Stiffener Span Dimensions [Al Horsmon, USCG NVIC No. 8-87]
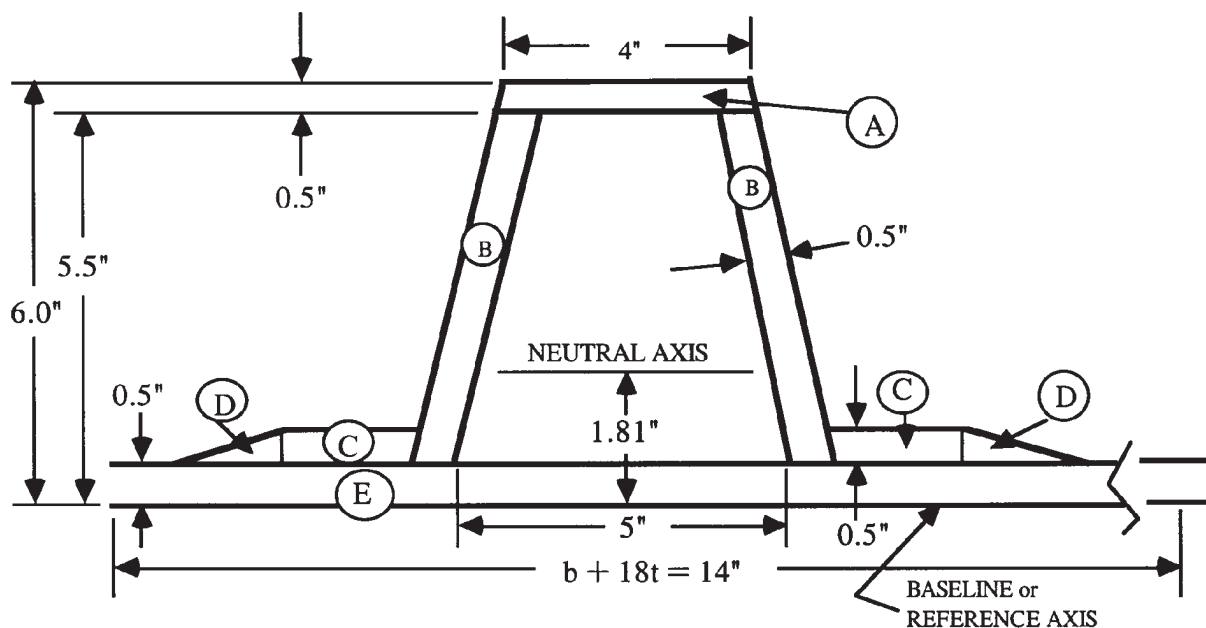
Figure 5-46 Stringer Geometry for Sandwich Construction [Al Horsmon, USCG NVIC No. 8-87]

Table 5-3 Example Calculation for Single Skin Stiffener

Item	b	h	A = b x h	d	Ad	Ad²	i_o
A	4.00	0.50	2.00	5.75	11.50	66.13	0.04
B	0.50	5.10	2.55	3.00	7.65	23.95	5.31
B	0.50	5.10	2.55	3.00	7.65	23.95	5.31
C	2.00	0.50	1.00	0.75	0.75	0.56	0.02
C	2.00	0.50	1.00	0.75	0.75	0.56	0.02
D	3.00	0.50	0.75	0.67	0.50	0.33	0.01
E	14.00	0.50	7.00	0.25	1.75	0.44	0.15
Totals:			16.85		30.55	115.92	10.86

$$d_{NA} = \frac{\sum Ad}{\sum A} = \frac{30.55}{16.85} = 1.81 \text{ inches} \tag{5-55}$$

$$I_{NA} = \sum i_o + \sum Ad^2 - [\,Ad^2\,] = 10.86 + 115.92 - [16.85 \times (1.81)^2] = 71.58 \tag{5-56}$$

$$SM_{top} = \frac{I}{d_{NA\,top}} = \frac{71.58}{4.19} = 17.08 \text{ in}^3 \tag{5-57}$$

$$SM_{bottom} = \frac{I}{d_{NA\,bottom}} = \frac{71.58}{1.81} = 39.55 \text{ in}^3 \tag{5-58}$$
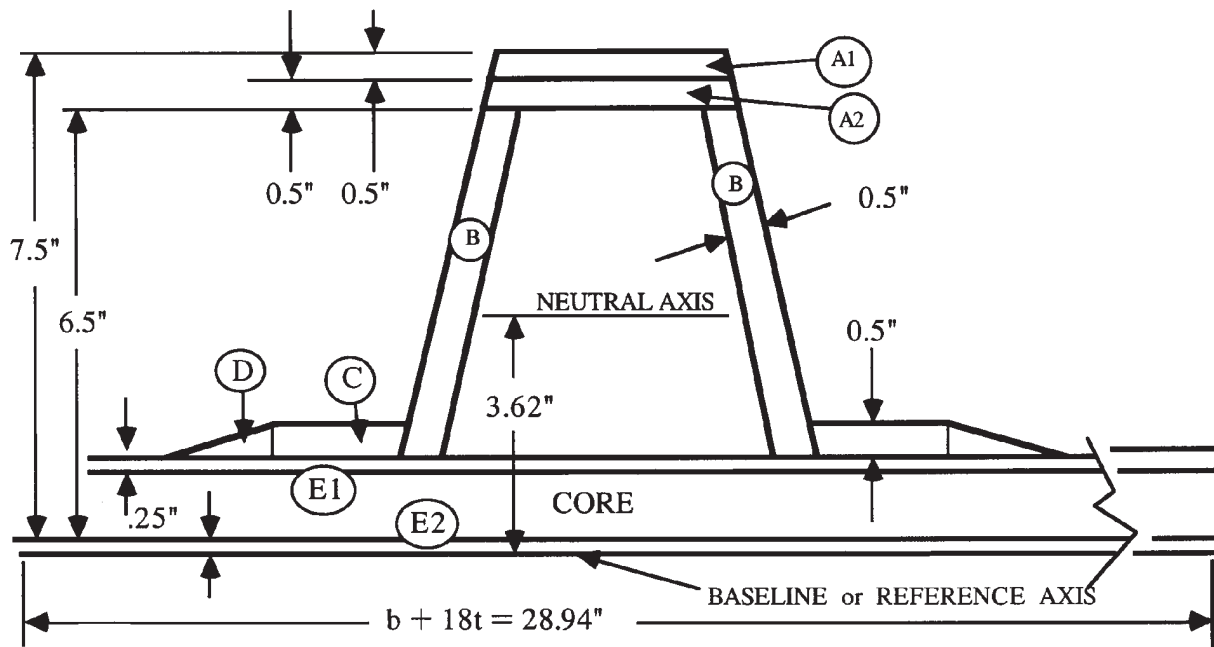
Figure 5-47 Stringer Geometry including High-Strength Reinforcement (3" wide layer of Kevlar® in the top) [Al Horsmon, USCG NVIC No. 8-87]

Table 5-4 High Strength Stiffener with Sandwich Side Shell

Item	b	h	A = b x h	d	Ad	Ad²	i_o
A1	3.70	0.50	3.29*	7.25	23.85	172.93	0.069
A2	3.80	0.50	1.90	6.75	12.83	86.57	0.040
B	0.50	5.00	2.50	4.00	10.00	40.00	5.208
B	0.50	5.00	2.50	4.00	10.00	40.00	5.208
C	2.00	0.50	1.00	1.75	1.75	3.06	0.021
C	2.00	0.50	1.00	1.75	0.75	0.56	0.021
D	3.00	0.50	0.75	0.67	0.50	0.33	0.01
E1	28.94	0.25	7.23	1.37	9.95	13.68	0.038
E2	28.94	0.25	7.23	0.12	0.90	0.11	0.038
Totals:			27.40		70.53	357.24	10.65

$$d_{NA} = \frac{\sum Ad}{\sum A} = \frac{70.53}{27.40} = 2.57 \text{ inches} \qquad (5\text{-}59)$$

$$I_{NA} = \sum i_o + \sum Ad^2 - [\ Ad^2\ ] = 10.65 + 357.24 - [27.40 \times (2.57)^2] = 186.92 \quad (5\text{-}60)$$

$$SM_{top} = \frac{I}{d_{NA\ top}} = \frac{186.92}{4.93} = 37.9 \text{ in}^3 \qquad (5\text{-}61)$$

$$SM_{bottom} = \frac{I}{d_{NA\ bottom}} = \frac{186.92}{2.57} = 72.73 \text{ in}^3$$

(5-62)

SYMBOLS:

b = width or horizontal dimension

h = height or vertical dimension

d = height to center of A from reference axis

NA = neutral axis

i_o = item moment of inertia = $bh^3/12$

d_{NA} = distance from reference axis to real NA

I_{NA} = moment of inertia of stiffener and plate about the real neutral axis

The assumed neutral axis is at the outer shell so all distances are positive.

Note how the stiffened plate is divided into discreet areas and lettered.

Items B and C have the same effect on section properties and are counted twice.

Some simplifications were made for the vertical legs of the stiffener, item B. The item i_o was calculated using the equation for the I of an inclined rectangle. Considering the legs as vertical members would be a further simplification.

Item D is combined from both sides of the required bonding angle taper.

Ratio of elastic moduli $E = \dfrac{E_{Kevlar^{®}}}{E_{E-glass}} = \dfrac{9.8 \text{ msi}}{5.5 \text{ msi}}$

* Effective area of Kevlar$^{®}$ compared to the E-glass = 3.7 x 0.5 x 1.78 = 3.29

The overall required section modulus for this example must also reflect the mixed materials calculated as a modifier to the required section modulus:

$$SM_{Kevlar^{®}} = SM_{E-glass} \times \frac{E_{Kevlar^{®}}}{E_{E-glass}} \times \frac{Ultimate\ Strength_{E-glass}}{Ultimate\ Strength_{Kevlar^{®}}}$$

$$\frac{E_{Kevlar^{®}}}{E_{E-glass}} \times \frac{Ultimate\ Strength_{E-glass}}{Ultimate\ Strength_{Kevlar^{®}}} = \frac{9.8 \text{ msi}}{5.5 \text{ msi}} \times \frac{110 \text{ ksi}}{196 \text{ ksi}} = 1.0$$

Reinforcing fibers of different strengths and different moduli can be limited in the amount of strength that the fibers can develop by the maximum elongation tolerated by the resin and the strain to failure of the surrounding laminate. Therefore, the strength of the overall laminate should be analyzed, and for marginal safety factor designs or arrangements meeting the minimum of a rule, tests of a sample laminate should be conducted to prove the integrity of the design. In this example, the required section modulus was unchanged but the credit for the actual section modulus to meet the rule was significant.

Stress Concentrations

Stress concentrations from out-of-plane point loads occur for a variety of reasons. The largest loads on a boat often occur when the boat is in dry storage, transported over land, removed from the water or placed into the water. The weight of a boat is distributed over the hull while the boat is in the water, but is concentrated at support points of relatively small area when the boat is out of the water. As an example, an 80 foot long 18 foot wide power boat weighing 130,000 pounds would probably experience a hydrostatic pressure of only a few psi. If the boat was supported on land by 12 blocks with a surface area of 200 square inches each, the support areas would see an average load of 54 psi. Equipment mounting, such as rudders, struts, engines, mast and rigging, booms, cranes, etc. can also introduce out-of-plane point loads into the structure through mechanical fasteners.

Hauling and Blocking Stresses

When a vessel is hauled and blocked for storage, the weight of the vessel is not uniformly supported as in the water. The point loading from slings and cradle fixtures is obviously a problem. The overall hull, however, will be subject to bending stresses when a vessel is lifted with slings at two points. Except in extreme situations, in-service design criteria for small craft up to about 100 feet should be more severe than this case. When undergoing long term storage or over-land transit, consideration must be given to what fixtures will be employed over a given period of time. Creep behavior described in Chapter Six will dictate long-term structural response, especially under elevated temperature conditions. Large unsupported weights, such as machinery, keels or tanks, can produce unacceptable overall bending moments in addition to the local stress concentrations. During transportation, acceleration forces transmitted through the trailer's support system can be quite high. The onset of fatigue damage may be quite precipitous, especially with cored construction.

Engine Beds

If properly fabricated, engine beds in FRP vessels can potentially reduce the transmission of machinery vibration to the hull. Any foundation supporting propulsion machinery should be given the same attention afforded the main engine girders.

As a general rule, engine girders should be of sufficient strength, stiffness and stability to ensure proper operation of rotating machinery. Proper bonding to the hull over a large area is essential. Girders should be continuous through transverse frames and terminate with a gradual taper. Laminated timbers have been used as a core material because of excellent damping properties and the ability to hold lag bolt fasteners. Consideration should be given to bedding lag bolts in resin to prevent water egress. Some builders include some metallic stock between the core and the laminate to accept machine screws. If this is done, proper care should be exercised to guarantee that the metal remains bonded to the core. New, high density PVC foam cores offer an attractive alternative that eliminates the concern over future wood decay.

Hardware

Through-bolts are always more desirable than self-tapping fasteners. Hardware installations in single skin laminates is fairly straightforward. Backing plates of aluminum or stainless steel are always preferable over simple washers. If using only oversized washers, the local thickness should be increased by at least 25%. [28] The strength of hardware installations should be consistent with the combined load on a particular piece of hardware. In addition to shear and normal loads, applied moments with tall hardware must be considered. Winches that are mounted on pedestals are examples of hardware that produce large overturning moments.
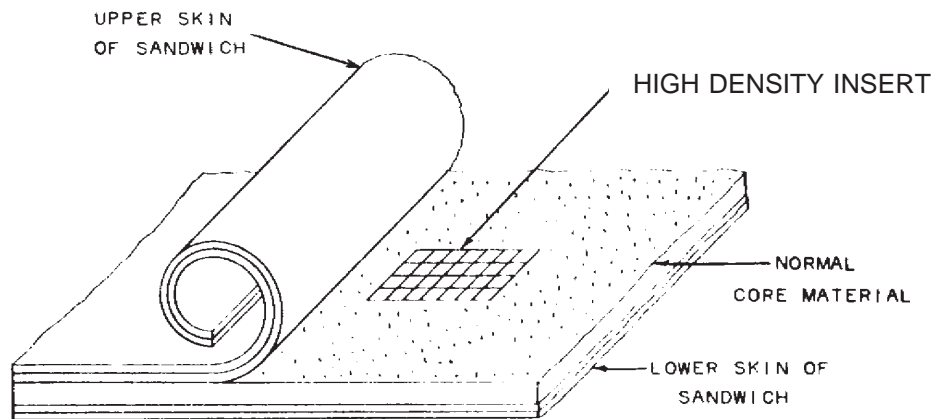
Figure 5-48   High Density Insert for Threaded or Bolted fasteners in Sandwich Construction [Gibbs and Cox, *Marine Design Manual for FRP*]

Hardware installation in cored construction requires a little more planning and effort. Low density cores have very poor holding power with screws and tend to compress under the load of bolts. Some builders simply taper the laminate to a solid thickness in way of planned hardware installations. This technique has the drawback of generally reducing the section modulus of the deck unless a lot of solid glass is used. A more efficient approach involves the insertion of a higher density core in way of planned hardware. In the past, the material of choice was plywood, but high density PVC foam will provide superior adhesion. Figure 5-48 illustrates this technique.

Hardware must often be located and mounted after the primary laminate is complete. To eliminate the possibility of core crushing, a compression tube as illustrated in Figure 5-49 should be inserted.

Nonessential hardware and trim, especially on small boats, is often mounted with screw fasteners. Table 5-5 is reproduced to provide some guidance in determining the potential holding force of these fasteners [29]. This table is suitable for use with mat and woven roving type laminate with tensile strength between 6 and 25 ksi; compressive strength between 10 and 22 ksi; and shear strength between 10 and 13 ksi.
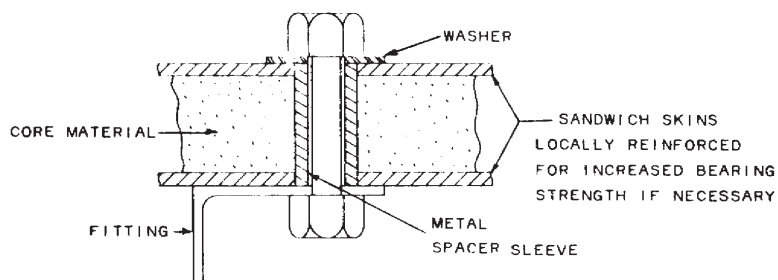
Figure 5-49   Through Bolting in Sandwich Construction [Gibbs and Cox, *Marine Design Manual for FRP*]

Table 5-5 Holding Forces of Fasteners in Mat/Polyester Laminates
[Gibbs and Cox, Marine Design Manual for FRP]

Thread Size	Axial Holding Force				Lateral Holding Force			
	Minimum		Maximum		Minimum		Maximum	
	Depth (ins)	Force (lbs)	Depth (ins)	Force (lbs)	Depth (ins)	Force (lbs)	Depth (ins)	Force (lbs)
Machine Screws								
4 - 40	.1250	40	.3125	450	.0625	150	.1250	290
6 - 32	.1250	60	.3750	600	.0625	180	.1250	380
8 - 32	.1250	100	.4375	1150	.0625	220	.1875	750
10 - 32	.1250	150	.5000	1500	.1250	560	.2500	1350
¼ - 20	.1875	300	.6250	2300	.1875	1300	.3125	1900
⁵⁄₁₆ - 18	.1875	400	.7500	3600	.1875	1600	.4375	2900
⅜ - 16	.2500	530	.8750	5000	.2500	2600	.6250	4000
⁷⁄₁₆ - 14	.2500	580	1.0000	6500	.3125	3800	.7500	5000
½ - 13	.2500	620	1.1250	8300	.3750	5500	.8750	6000
⁹⁄₁₆ - 12	.2500	650	1.2500	10000	.4375	6500	.9375	8000
⅝ - 11	.2500	680	1.3750	12000	.4375	6800	1.0000	11000
¾ - 10	.2500	700	1.5000	13500	.4375	7000	1.0625	17000
Self-Tapping Thread Cutting Screws								
4 - 40	.1250	80	.4375	900	.1250	250	.1875	410
6 - 32	.1250	100	.4375	1100	.1250	300	.2500	700
8 - 32	.2500	350	.7500	2300	.1875	580	.3750	1300
10 - 32	.2500	400	.7500	2500	.1875	720	.4375	1750
¼ - 20	.3750	600	1.0625	4100	.2500	1600	.6250	3200
Self-Tapping Thread Forming Screws								
4 - 24	.1250	50	.3750	500	.1250	220	.1875	500
6 - 20	.1875	110	.6250	850	.1250	250	.2500	600
8 - 18	.2500	180	.8125	1200	.1875	380	.3125	850
10 - 16	.2500	220	.9375	2100	.2500	600	.5000	1500
14 - 14	.3125	360	1.0625	3200	.2500	900	.6875	2800
⁵⁄₁₆ - 18	.3750	570	1.1250	4500	.3125	1800	.8125	4400
⅜ - 12	.3750	700	1.1250	5500	.3750	3600	1.0000	6800

Sandwich Panel Testing

Background
Finite element models can be used to calculate panel deflections for various laminates under worst case loads [30,31], but the accuracy of these predictions is highly dependent on test data for the laminates. Traditional test methods [32] involve testing narrow strips, using ASTM standards outlined in Chapter Four. Use of these tests assumes that hull panels can be accurately modeled as a beam, thus ignoring the membrane effect, which is particularly important in sandwich panels [33]. The traditional tests also cause much higher stresses in the core, thus leading to premature failure [34].

A student project at the Florida Institute of Technology investigated three point bending failure stress levels for sandwich panels of various laminates and span to width ratios. The results were fairly consistent for biaxial (0°, 90°) laminates, but considerable variation in deflection and failure stress for double bias (±45°) laminates was observed as the aspect ratio was changed. Thus while the traditional tests yield consistent results for biaxial laminates, the test properties may be significantly lower than actual properties, and test results for double bias and triaxial laminates are generally inaccurate.

Riley and Isley [35] addressed these problems by using a new test procedure. They pressure loaded sandwich panels, which were clamped to a rigid frame. Different panel aspect ratios were investigated for both biaxial and double bias sandwich laminates. The results showed that the double bias laminates were favored for aspect ratios less than two, while biaxial laminates performed better with aspect ratios greater than three. Finite element models of these tests indicated similar results, however, the magnitude of the deflections and the pressure at failure was quite different. This was probably due to the method of fastening the edge of the panel. The method of clamping of the edges probably caused local stress concentrations and could not be modeled by either pinned- or fixed-end conditions.

Pressure Table Design
The basic concept of pressure loading test panels is sound, however, the edges or boundary conditions need to be examined closely. In an actual hull, a continuous outer skin is supported by longitudinal and transverse framing, which defines the hull panels. The appropriate panel boundary condition is one which reflects the continuous nature of the outer skin, while providing for the added stiffness and strength of the frames. One possible solution to this problem is to include the frame with the panel, and restrain the panel from the frame, rather than the panel edges. Also, extending the panel beyond the frame can approximate the continuous nature of the outer skin.

A test apparatus, consisting of a table, a water bladder for pressurizing the panel, a frame to constrain the sides of the water bladder, and framing to restrain the test panel, was developed and is shown in Figure 5-50. The test panel is loaded on the "outside," while it is restrained by means of the integral frame system. The pressurization system can be operated either manually or under computer control, for pressure loading to failure or for pressure cycling to study fatigue.

Test Results
Sandwich laminates using four different reinforcements and three aspect ratios were constructed for testing. All panels used non-woven E-glass, vinyl ester resin and cross-linked
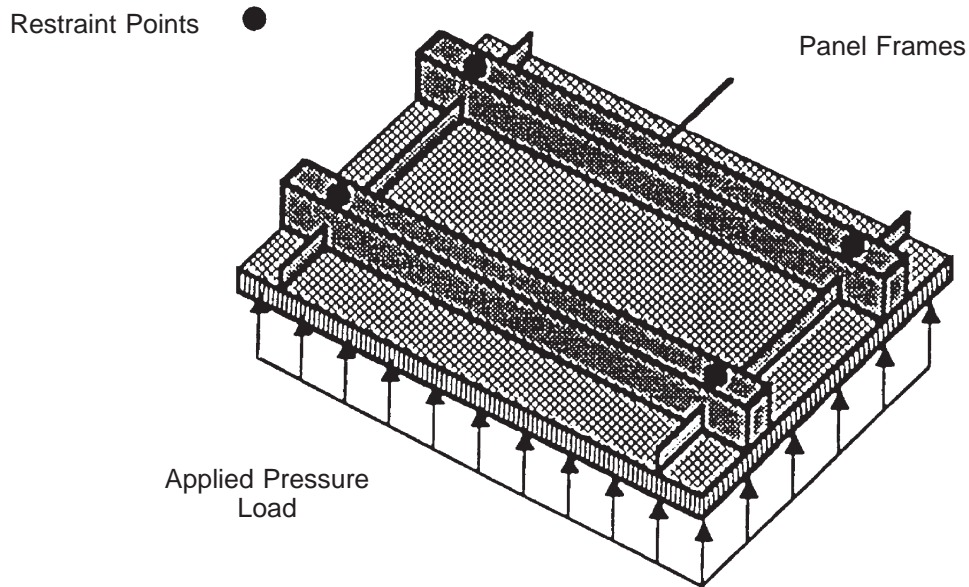
Figure 5-50   Schematic Diagram of Panel Testing Pressure Table [Reichard]

PVC foam cores over fir frames and stringers. The panels were loaded slowly (approximately 1 psi per minute) until failure.

MSC/NASTRAN, a finite element structural analysis program, was used to model the panel tests. The models were run using two different boundary conditions, pinned edges and fixed edges. The predicted deflections for fixed- and pinned-edge conditions along with measured results are shown in Figure 5-51.

The pinned-edge predictions most closely model the test results. Other conclusions that can be made as a result of early pressure table testing include:

- Quasi-isotropic laminates are favored for square panels.

- Triaxial laminates are favored for panels of aspect ratios greater than two.

Deflection increase with aspect ratio until asymptotic values are obtained. Asymptotic values of deflection are reached at aspect ratios between 2.0 and 3.5.

The pressure table test method provides strength and stiffness data for the panel structure but does not provide information about specific material properties. Therefore, the test is best suited for comparing candidate structures.

Testing of Structural Grillage Systems
Figure 5-51 shows a hat-stiffened panel subjected to in-plane and out-of-plane loads tested at the U.S. Naval Academy (see page 190). The structure modeled would be typical of a longitudinally stiffened hull panel. Note the half-sine wave pattern of the collapsed skin even as the panel was subjected to out-of-plane loads from the water bladder with nominal loading. After the panel separated from the stiffeners, the hat sections experienced shear failure.
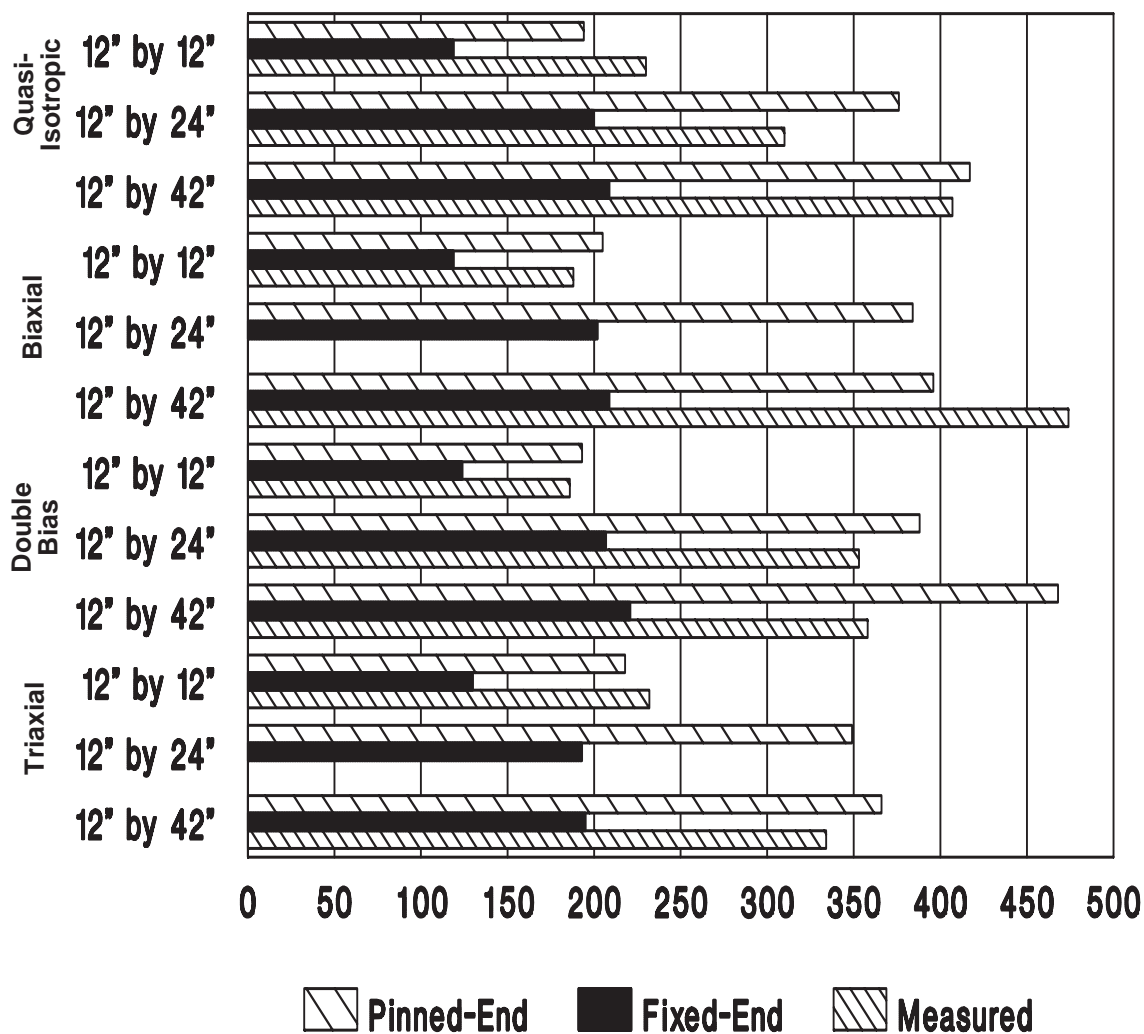
Pinned-End **Fixed-End** **Measured**

Figure 5-51   Computed and Measured Deflections (mils) of PVC Foam Core Panels Subjected to a 10 psi Load [from Reichard, Ronnal P., "Pressure Panel Testing of GRP Sandwich Panels,", MACM' 92 Conference, Melbourne, FL, March 24-26, 1992.
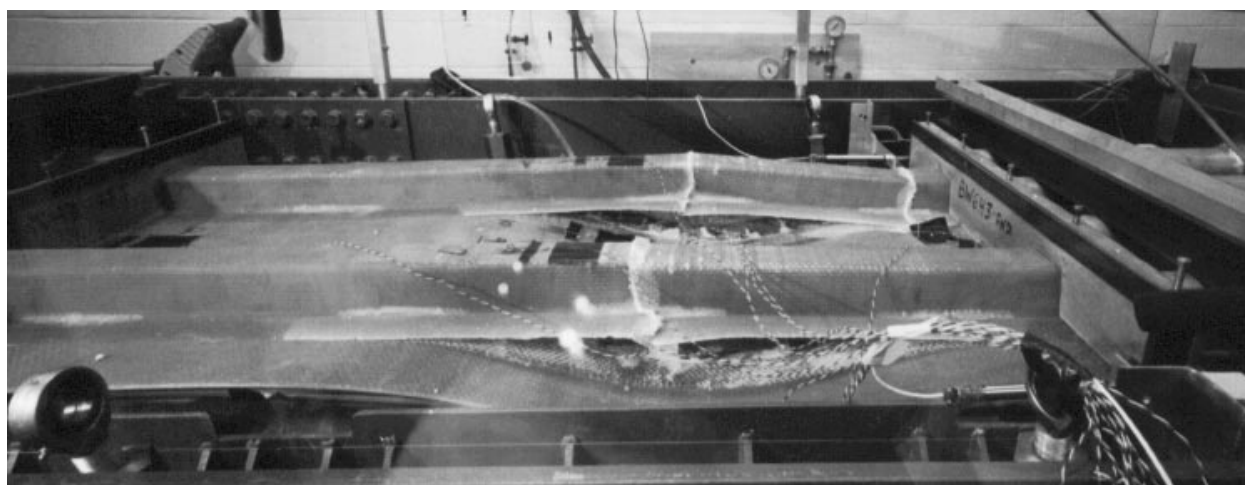
Figure 5-52   Hat-Stiffened Panel Tested to Failure at the U.S. Naval Academy

Hydromat Test System (HTS)

Bill Bertelsen of Gougeon Brothers and Dave Sikarskie of Michigan Technological University have developed a two dimensional panel testing device and governing design equations. The test device, shown in Figure 5-53, subjects panels to out-of-plane loads with simply-supported end conditions. The boundary conditions have been extended to cover sandwich panels with soft cores, thereby enabling characterization of sandwich panels both elastically and at failure. A methodology has been developed for obtaining numerical and experimental values for bending and core shear rigidities, which both contribute to measured deflections.

In the simplest form, the deflection, δ, is given as:

$$\delta = \frac{c_1}{B} + \frac{c_2}{S} \qquad (5\text{-}63)$$

where:

Figure 5-53   Schematic Diagram of the Hydromat Test System [Bertlesen & Sikarskie]

$c_1 \& c_2$ = constants

B = bending stiffness

S = core shear stiffness

Tests were run on panels with varying stiffness to verify the methodology. Table 5-6 summarizes some results, showing the close agreement between experimental and theoretical overall bending and core shear stiffness.

Table 5-6 Summary of Experimental and Theoretical Bending and Shear Stiffness [Bertlesen, Eyre and Sikarskie, *Verification of HTS for Sandwich Panels*]

Panel	Bladder Pressure (kPa)	Total HTS Deflection	$(\varepsilon_x + \varepsilon_y)$ Exp. μ strain	B, exp (10^4 nM)	B, theory (10^4 nM)	S, exp (10^4 nM)	S, theory (10^4 nM)
1	31.0	2.78	463	2.08	2.52	3.48	3.72
2	48.3	2.85	719	2.12	2.55	6.43	5.24
3	75.8	2.49	1062	2.33	2.43	17.68	17.04

Chapter Six - Failure Modes

The use of engineered composite structures requires an insight into the failure modes that are unique to these types of materials. Some people say that composites are "forgiving," while others note that catastrophic failures can be quite sudden. Because laminates are built from distinct plies, it is essential to understand how loads are "shared" among the plies. It is also critical to distinguish between resin dominated failures or fiber dominated failures. Armed with a thorough understanding of the different ways that a structure can fail makes it possible to design a laminate that will "soften" at the point of potential failure and redistribute stress.

Failures in composite structures can be dominated by either "strength" or "stiffness." Strength limited failures occur when unit stress exceeds the load carrying capability of the laminate. Stiffness failures result when displacements exceed the strain limits (elongation to failure) of the laminate.

Tensile failures of composite materials is fairly rare, as filament reinforcements are strongest in tension along their primary axis. Tensile loading in an off-axis direction is a different story. Resin and fiber mechanical properties vary widely in tension, so each must be studied for stress or strain limited failure with off-axis loading scenarios.

Compressive failures in composites are probably the hardest to understand or predict. Failures can occur at a very small-scale, such as the compression or buckling of individual fibers. With sandwich panels, skin faces can wrinkle or the panel itself may become unstable. Indeed, incipient failure may occur at some load well below an ultimate failure.

Out-of-plane loading, such as hydrostatic force, creates flexural forces for panels. Classic beam theory would tell us that the loaded face is in compression, the other face is in tension, and the core will experience some shear stress distribution profile. For three-dimensional panels, predicting through-thickness stresses is somewhat more problematic. Bending failure modes to consider include core shear failure, core-to-skin debonds, and skin failures (tension, compression, and local).

Tensile Failures

The tensile behavior of engineered composite materials is generally characterized by stress-strain curves, such as those shown in Figure 6-1. The ASTM Standard Test Method for Tensile Properties of Plastics, D 638-84, defines several key tensile failure terms as follows:

Tensile Strength = Maximum tensile strength during test

Strain = The change in length per unit

Yield Point = First point on the stress-strain curve where increased strain occurs without increased stress

Elastic limit = The greatest stress that a material can withstand without permanent deformation

Modulus of elasticity = The ratio of stress to strain below the proportional limit

Proportional limit = Greatest stress that a material can withstand with linear behavior

A & E	Tensile strength and elongation at break
B	Tensile strength and elongation at yield
C	Tensile stress and elongation at break
D	Tensile stress and elongation at yield
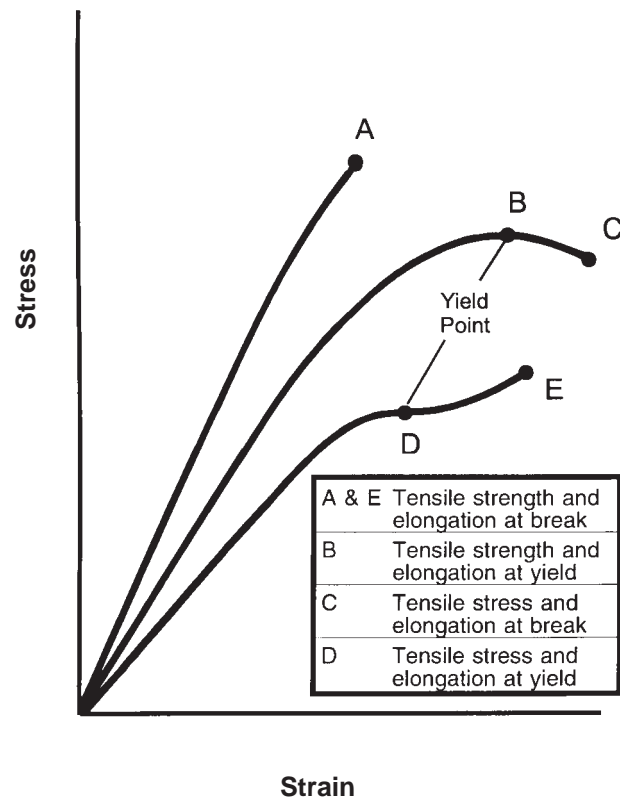
Figure 6-1 Tensile Failure Modes of Engineered Plastics Defined by ASTM [ASTM D 638-84, ASTM, Philadelphia, PA]

Tensile tests are usually performed under standard temperature and humidity conditions and at relatively fast speeds (30 seconds to 5 minutes). Test conditions can vary greatly from in-service conditions and the designer is cautioned when using single-point engineering data generated under laboratory test conditions. Some visible signs of tensile failures in plastics are:

Crazing: Crazes are the first sign of surface tensile failures in thermoplastic materials and gel coat finishes. Crazes appear as clean hairline fractures extending from the surface into the composite. Crazes are not true fractures, but instead are combinations of highly oriented "fibrils" surrounded by voids. Unlike fractures, highly crazed surfaces can transmit stress. Water, oils, solvents and environment can accelerate crazing.

Cracks: Cracking is the result of stress state and environment. Cracks have no fibrills, and thus cannot transmit stress. Cracks are a result of embrittlement, which is promoted by sustained elevated temperature, UV, thermal and chemical environments in the presence of stress or strain. This condition is also termed "stress-cracking."

Stress whitening: This condition is associated with plastic materials that are stretched near their yield point. The surface takes on a whitish appearance in regions of high stress. [36]

Membrane Tension

Large deflections of panels that are constrained laterally at their edges will produce tensile stresses on both faces due to a phenomena called "membrane" tension. Figure 6-2 illustrates this concept and the associated nomenclature. The ASCE *Structural Plastics Design Manual* [36] provides a methodology for approximating large deflections and stresses of isotropic plates when subjected to both bending and membrane stress. For long rectangular plates with fixed ends, the uniform pressure, q, is considered to be the sum of q_b, the pressure resisted by bending and q_m, the pressure resisted by membrane tension. Similarly, the maximum deflection, w_{max}, is defined as the sum of deflection due to plate bending and membrane action. ASCE defines the deflection due to bending as:

$$w_c = 0.156 \frac{(1-v^2)\, q_b\, b^4}{E\, t^3} \tag{6-1}$$

solving (6-1) for "bending pressure":

$$q_b = \frac{6.4\, w_c\, E\, t^3}{(1-v^2)\, b^4} \tag{6-2}$$

where:

E = material stiffness (tensile)

v = Poisson's ratio

t = plate thickness

b = span dimension

The deflection of the plate due only to membrane action is given as:

$$w_c = 0.41 \left[\frac{(1-v^2)\, q_m\, b^4}{E\, t} \right]^{\frac{1}{3}} \tag{6-3}$$

solving (6-3) for "membrane pressure":

$$q_m = \frac{14.5\, w_c^3\, E\, t}{(1-v^2)\, b^4} \tag{6-4}$$

Combining (6-2) and (6-4) results in the following expression for total load:

$$q = \frac{w_c\, E\, t^3}{(1-v^2)\, b^4} \left(6.4 + 14.5 \frac{w_c^2}{t^2} \right) \tag{6-5}$$

The *Manual* [36] suggests that trail thicknesses, t, be tried until acceptable deflections or maximum stresses result. Bending stress for long plates is given as:

$$\sigma_{cby} = 0.75 \, q_b \, b^2 \tag{6-6}$$

Membrane stress is given as:

$$\sigma_{cy} = 0.30 \sqrt[3]{\frac{q_m^2 \, b^2 \, E}{(1-\nu^2) \, t^2}} \tag{6-7}$$

The total stress is the sum of equations (6-6) and (6-7). With thick or sandwich laminates, the skin on the loaded side can be in compression, and thus the combined bending and membrane stress may actually be less than the bending stress alone.
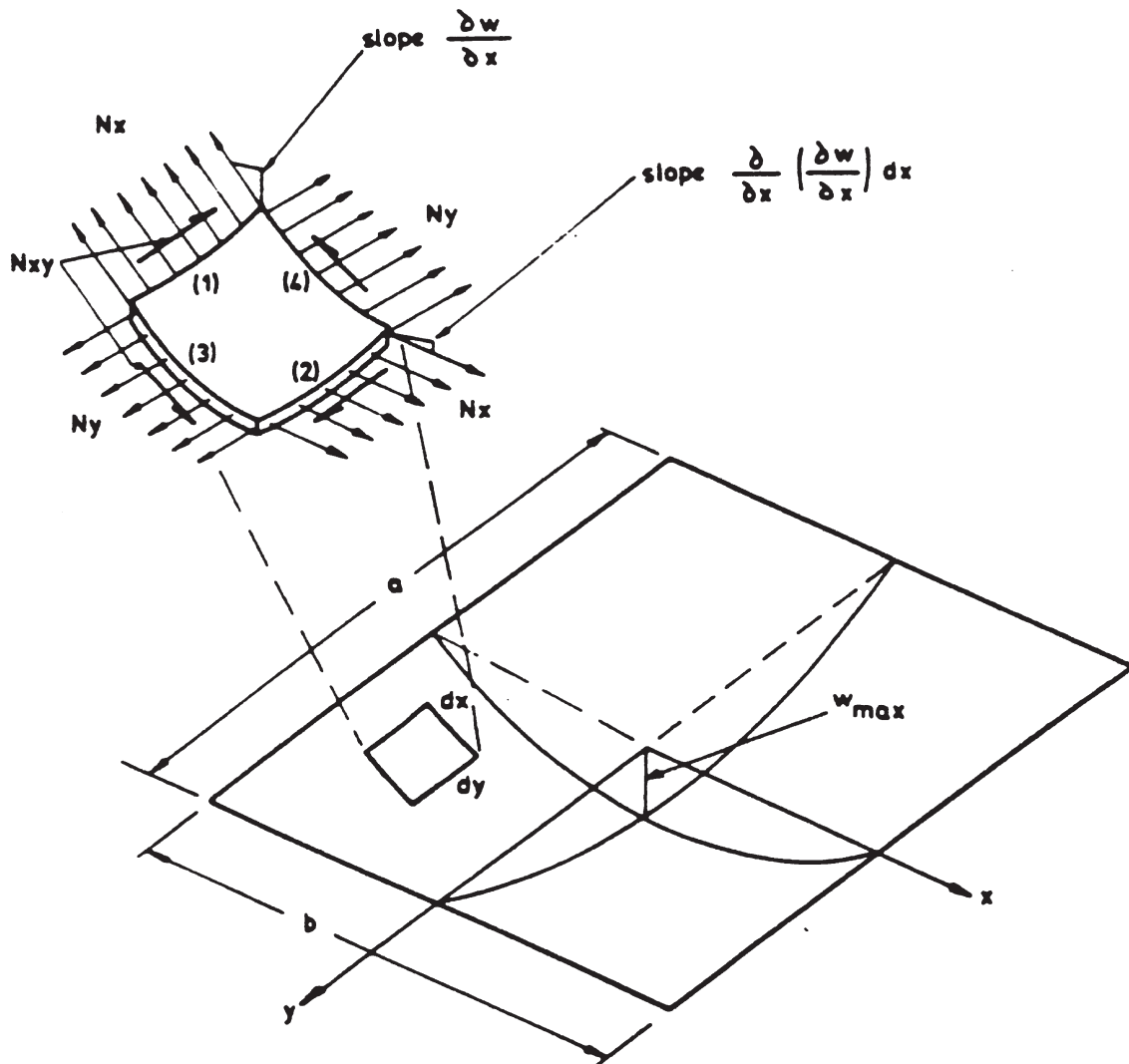
Figure 6-2 Illustration of Membrane Tension in a Deflected Panel

Compressive Failures

Analytical methods for predicting compressive failures in solid and sandwich laminates are presented in Chapter 5. The following discussion describes some of the specific failure modes found in sandwich laminates. Figure 6-3 illustrates the compressive failure modes considered. Note that both general and local failure modes are described.

The type of compressive failure mode that a sandwich laminate will first exhibit is a function of load span, skin to core thickness ratio, the relationship of core to skin stiffness and skin-to-core bond strength.

Large unsupported panel spans will tend to experience general buckling as the primary failure mode. If the core shear

Figure 6-3   Compressive Failure Modes of Sandwich Laminates [Sandwich Structures Handbook, Il Prato]

modulus is very low compared to the stiffness of the skins, then crimping may be the first failure mode observed. Very thin skins and poor skin-to-core bonds can result in some type of skin wrinkling. Honeycomb cores with large cell sizes and thin skins can exhibit dimpling.

General Buckling

Formulas for predicted general or panel buckling are presented in Chapter 5. As hull panels are generally sized to resist hydrodynamic loads, panel buckling usually occurs in decks or bulkheads. Transversely-framed decks may be more than adequate to resist normal loads, while still being susceptible to global, hull girder compressive loads resulting from longitudinal bending moments.

Bulkhead scantling development, especially with multi-deck ships, requires careful attention to anticipated in-plane loading. Superposition methods can be used when analyzing the case of combined in-plane and out-of-plane loads. This scenario would obviously produce buckling sooner than with in-plane loading alone. The general Euler buckling formula for collapse is:

$$\sigma_{critical} \quad = \quad \frac{\pi^2 \, EI}{l^2_{\,cr}} \qquad\qquad\qquad (6\text{-}8)$$

The influence of determining an end condition to use for bulkhead-to-hull or -deck attachment is shown in Figure 6-4. Note that $\sigma_{critical}$ required for collapse is 16 times greater for a panel with both ends fixed, as compared to a panel with one fixed end and one free end.

$l_{cr} = 2l$ $l_{cr} = l$ $l_{cr} = 0.707l$ $l_{cr} = 0.5l$
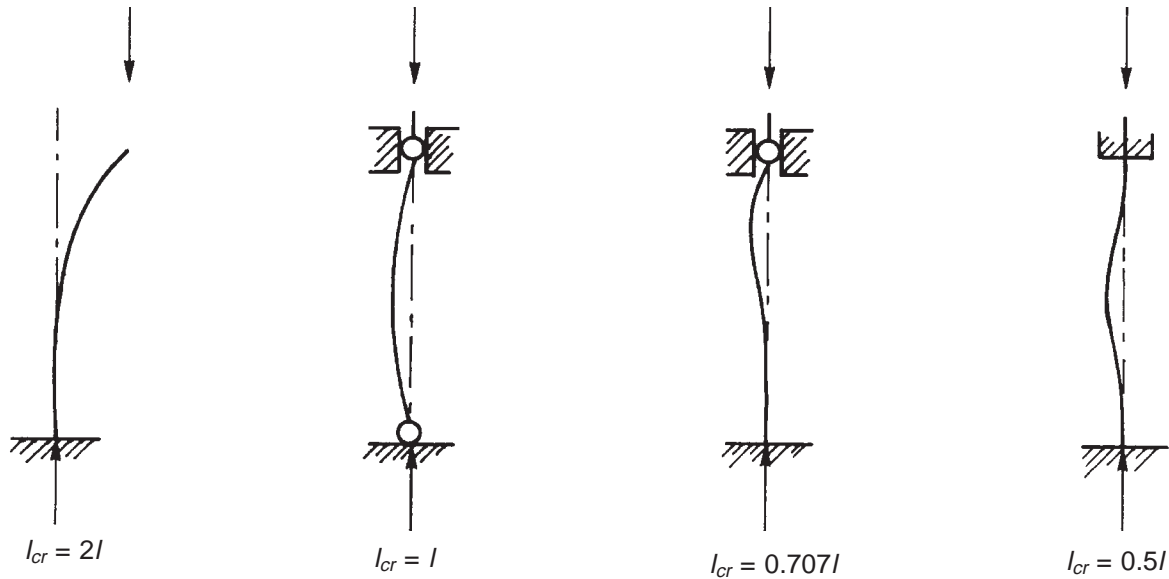
Figure 6-4   Critical Length for Euler Buckling Formula Based on End Condition
[Sandwich Structures Handbook, Il Prato]

Crimping & Skin Wrinkling

Shear crimping of the core will occur when the core shear modulus is too low to transfer load between the skins. When the skins are required to resist the entire compressive load without help from the core, the panel does not have the required overall moment of inertia, and will fail along with the core.

Skin wrinkling is a form of local buckling whereupon the skins separate from the core and buckle on their own. Sandwich skins can wrinkle in a parallel fashion (anti-symmetric), parallel or one side only. The primary structural function of the skin-to-core interface in sandwich laminates is to transfer shear stress between the skins and the core. This bond relies on chemical and mechanical phenomena. A breakdown of this bond and/or buckling instability of the skins themselves (too soft or too thin) can cause skin wrinkling.

Dimpling with Honeycomb Cores

Skin dimpling with honeycomb cores is a function the ratio of skin thickness to core cell size, given by the following relationship:

$$\sigma_{critical} = 2 \frac{E_{skin}}{\left(1 - \mu^2_{skin}\right)} \left(\frac{t_{skin}}{c} \right)$$
(6-9)

where:

t_{skin} = skin thickness

c = core cell size given as an inscribed circle

Bending Failure Modes

The distribution of tensile, compressive and shear stresses in solid laminates subject to bending moments follows elementary theory outlined by Timoshenko [37]. Figure 6-5 shows the nomenclature used to describe bending stress. The general relationship between tensile and compressive stress and applied moment, as a function of location in the beam is:

$$\sigma_x = \frac{M\,y}{I_z} \qquad (6\text{-}10)$$

where:

σ_x = skin tensile or compressive stress

M = applied bending moment

y = distance from the neutral axis

I_z = moment of inertia about the "z" axis
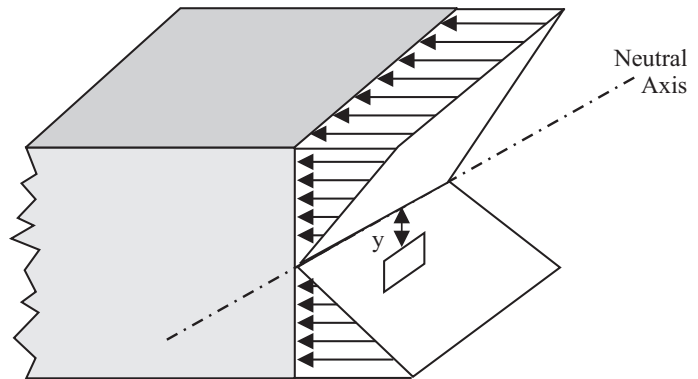
Figure 6-5   Nomenclature for Describing Bending Stress in Solid Beam

As is illustrated in Figure 6-5, the in-plane tensile and compressive stresses are maximum at the extreme fibers of the beam (top and bottom).

Shear stresses resulting from applied bending moments, on the other hand, are zero at the extreme fibers and maximum at the neutral axis. Figure 6-6 shows conceptually the shearing forces that a beam experiences. The beam represented is composed of two equal rectangular bars used to illustrate the shear stress field at the neutral axis.
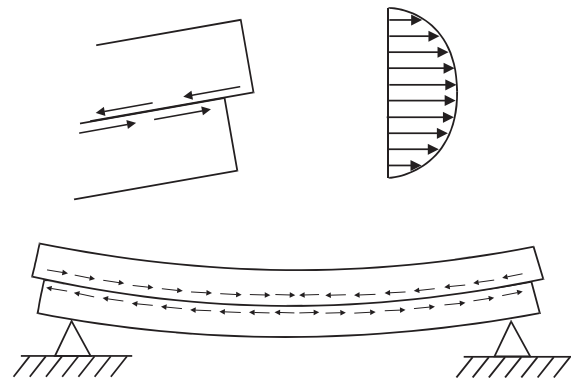
Formulas for general and maximum shear stress as a function of shear load, V, are::

Figure 6-6   Nomenclature for Describing Shear Stress in Solid Beam

$$\tau_{xy} = \frac{V}{2I_z}\left(\frac{h^2}{4} - y^2\right) \qquad (6\text{-}11)$$

$$\tau_{max} = \frac{Vh^2}{8I_z} \qquad (6\text{-}12)$$

Sandwich Failures with Stiff Cores

Sandwich structures with stiff cores efficiently transfer moments and shear forces between the skins, as illustrated in Figure 6-7. Elementary theory for shear-rigid cores assumes that the total deflection of a beam is the sum of shear and moment induced displacement:

$$\delta = \delta_m + \delta_v \qquad\qquad (6\text{-}13)$$

where:

$$\delta_v = \text{shear deflection}$$

$$\delta_m = \text{moment deflection}$$
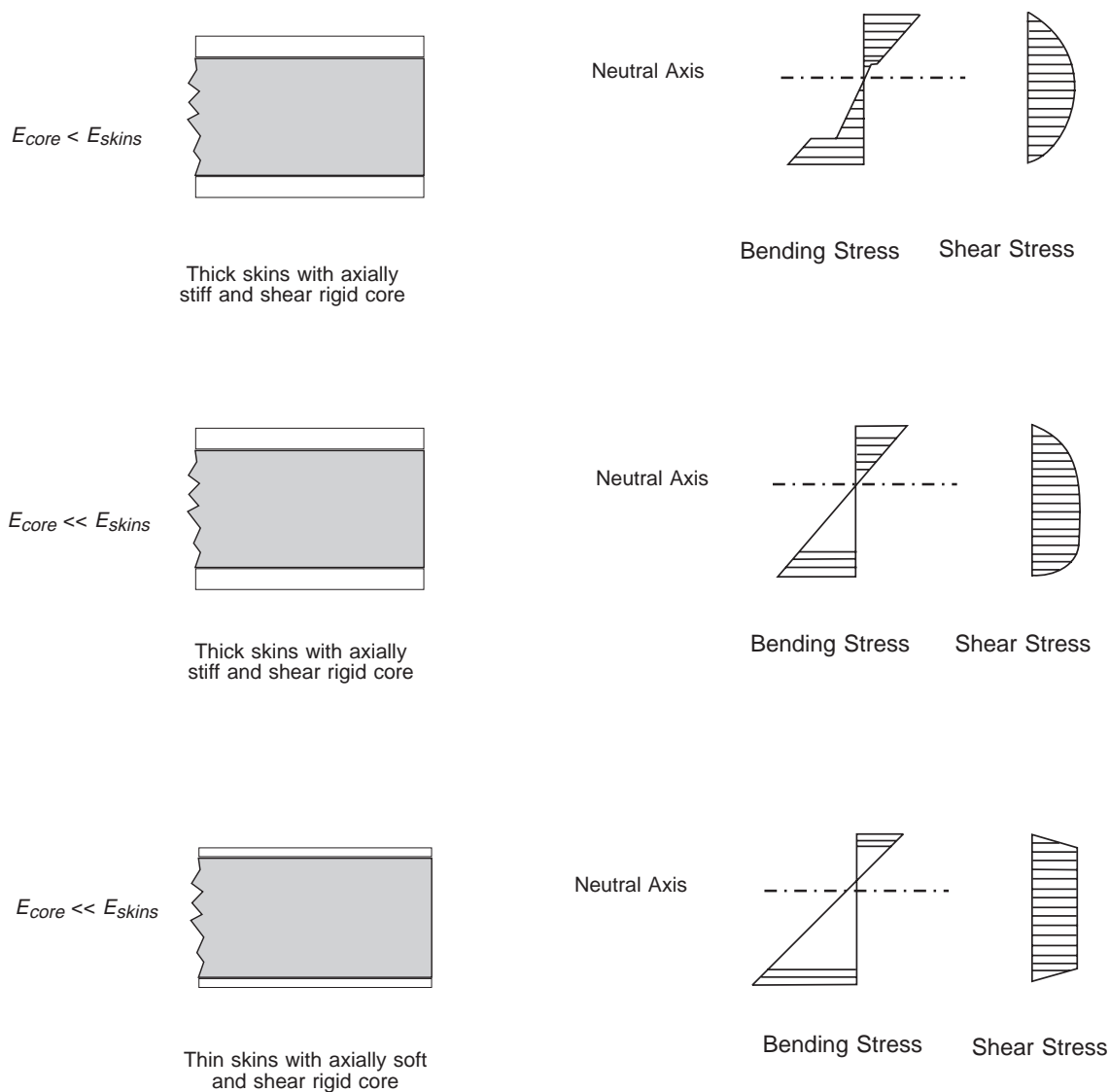
$E_{core} < E_{skins}$

Thick skins with axially
stiff and shear rigid core

Neutral Axis

Bending Stress   Shear Stress

$E_{core} \ll E_{skins}$

Thick skins with axially
stiff and shear rigid core

Neutral Axis

Bending Stress   Shear Stress

$E_{core} \ll E_{skins}$

Thin skins with axially soft
and shear rigid core

Neutral Axis

Bending Stress   Shear Stress

Figure 6-7   Bending and Shear Stress Distribution in Sandwich Beams (2-D) with Relatively Stiff Cores [***Structural Plastics Design Manual*** published by the American Society of Civil Engineers.]

Sandwich Failures with Relatively Soft Cores

Sandwich laminates with soft cores do not behave as beam theory would predict. Because shear loads are not as efficiently transmitted, the skins themselves carry a larger share of the load in bending about their own neutral axis, as shown in Figure 6-8. ASCE [36] defines a term for shear flexibility coefficient as:

$$\theta \approx \frac{L}{2}\left[\frac{D_v}{D_{mf}}\right]^{\frac{1}{2}} \qquad (6\text{-}14)$$

where L is the panel span and D_v and D_{mf} are values for shear and bending stiffness, respectively. Figure 6-9 shows the influence of shear flexibility on shear and bending stress distribution for a simply supported beam.
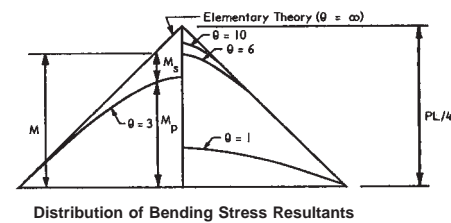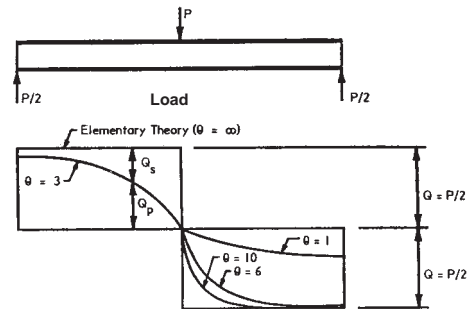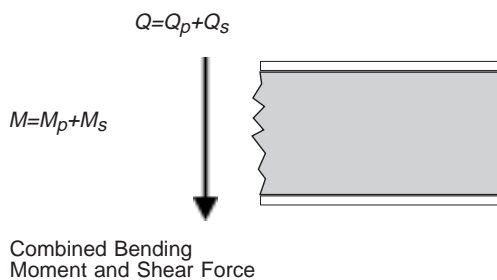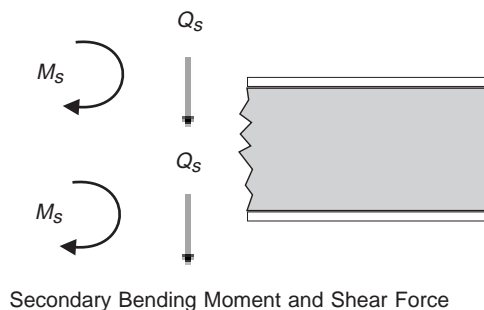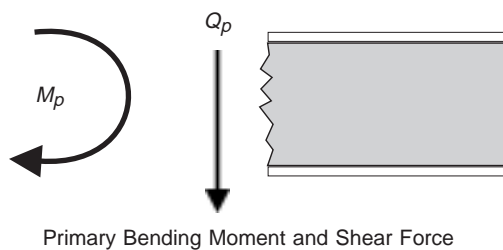
Figure 6-9 Stress Distribution with Flexible Cores [ASCE Manual]
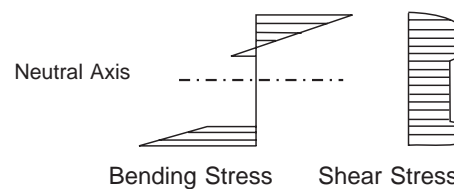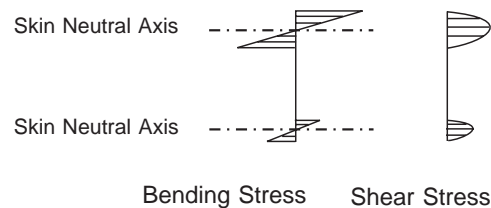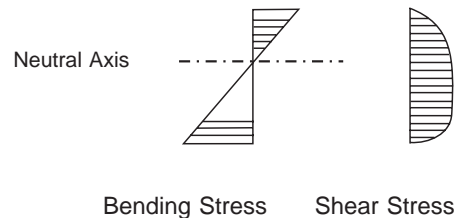
Figure 6-8 Bending and Shear Stress Distribution in Sandwich Beams (2-D) with Relatively Soft Cores [*Structural Plastics Design Manual* published by the American Society of Civil Engineers.]

First Ply Failure

First ply failure is defined by the first ply or ply group that fails in a multidirectional laminate. The load corresponding to this failure can be the design limit load. The total number of plies, the relative stiffnesses of those plies and the overall stress distribution (load sharing) among the plies determines the relationship between first ply failure and last ply (ultimate) failure of the laminate. As an illustration of this concept, consider a structural laminate with a gel coat surface. The surface is typically the highest stressed region of the laminate when subjected to flexural loading, although the gel coat layer will typically have the lowest ultimate elongation within the laminate. Thus, the gel coat layer will fail first, but the load carrying capability of the laminate will remain relatively unchanged.

Strain Limited Failure

The ***ABS Guide for Building and Classing High-Speed Craft*** [38] provides guidance on calculating first ply failure based on strain limits. The critical strain of each ply is given as:

$$\varepsilon_{crit} = \frac{\sigma_{ai}}{E_{ai}\left[\ |\bar{y} - y_i| + \frac{1}{2}\,t_i\ \right]} \tag{6-15}$$

where:

$$\sigma_{ai} = \text{strength of ply under consideration}$$
$$= \sigma_t \text{ for a ply in the outer skin}$$
$$= \sigma_c \text{ for a ply in the inner skin}$$

$$E_{ai} = \text{modulus of ply under consideration}$$
$$= E_t \text{ for a ply in the outer skin}$$
$$= E_c \text{ for a ply in the inner skin}$$

$\bar{y}$ = distance from the bottom of the panel to the neutral axis

y_i = distance from the bottom of the panel to the ply under consideration

t_i = thickness of ply under consideration

σ_t = tensile strength of the ply being considered

σ_c = compressive strength of the ply being considered

E_t = tensile stiffness of the ply being considered

E_c = compressive stiffness of the ply being considered

Stress Limited Failure

The stress or applied moment that produces failure in the weakest ply is a function of the portion of the overall failure moment carried by the ply that fails, FM_i, defined [38] as:

$$FM_i = \varepsilon_{min} \; E_{ai} \; t_i \; \left(|\bar{y} - y_i| \right)^2 \tag{6-16}$$

where:

ε_{min} = the smallest critical strain that is acting on an individual ply

The minimum section moduli for outer and inner skins, respectively, of a sandwich panel based on the failure moment responsible for first ply stress failure is given as:

$$SM_o = \frac{\sum_{i=1}^{n} FM_i}{\sigma_{to}} \tag{6-17}$$

$$SM_i = \frac{\sum_{i=1}^{n} FM_i}{\sigma_{ci}} \tag{6-18}$$

where:

SM_o = section modulus of outer skin

SM_i = section modulus of inner skin

n = total number of plies in the skin laminate

σ_{to} = tensile strength of outer skin determined from mechanical testing or via calculation of tensile strength using a weighted average of individual plies for preliminary estimations

σ_{ci} = compressive strength of inner skin determined from mechanical testing or via calculation of compressive strength using a weighted average of individual plies for preliminary estimations

Creep

Engineered structures are often required to resist loads over a long period of time. Structures subjected to creep, such as bridges and buildings, are prime examples. Deckhouses and machinery foundations are examples of marine structures subject to long-term stress. Just as many marine composite structural problems are deflection-limited engineering problems, long-term creep characteristics of composite laminates has been an area of concern, especially in way of main propulsion shafting, where alignment is critical. The following discussion on creep is taken from the *Structural Plastics Design Manual* published by the American Society of Civil Engineers. [36]

Generalized Creep Behavior

When composite materials are subjected to constant stress, strain in load path areas will increase over time. This is true for both short-term and long term loading, with the later most often associated with the phenomenon known as creep. With long-term creep, the structural response of an engineering material is often characterized as viscoelastic. Viscoelasticity is defined as a combination of elastic (return to original shape after release of load) and viscous (no return to original shape) behavior. When considering plastics as engineering materials, the concept of viscoelasticity is germane. Loads, material composition, environment, temperature all affect the degree of viscoelasticity or expected system creep. Figure 6-10 presents a long-term overview of viscoelastic modulus for two thermoplastic resin systems and a glass/epoxy thermoset system.
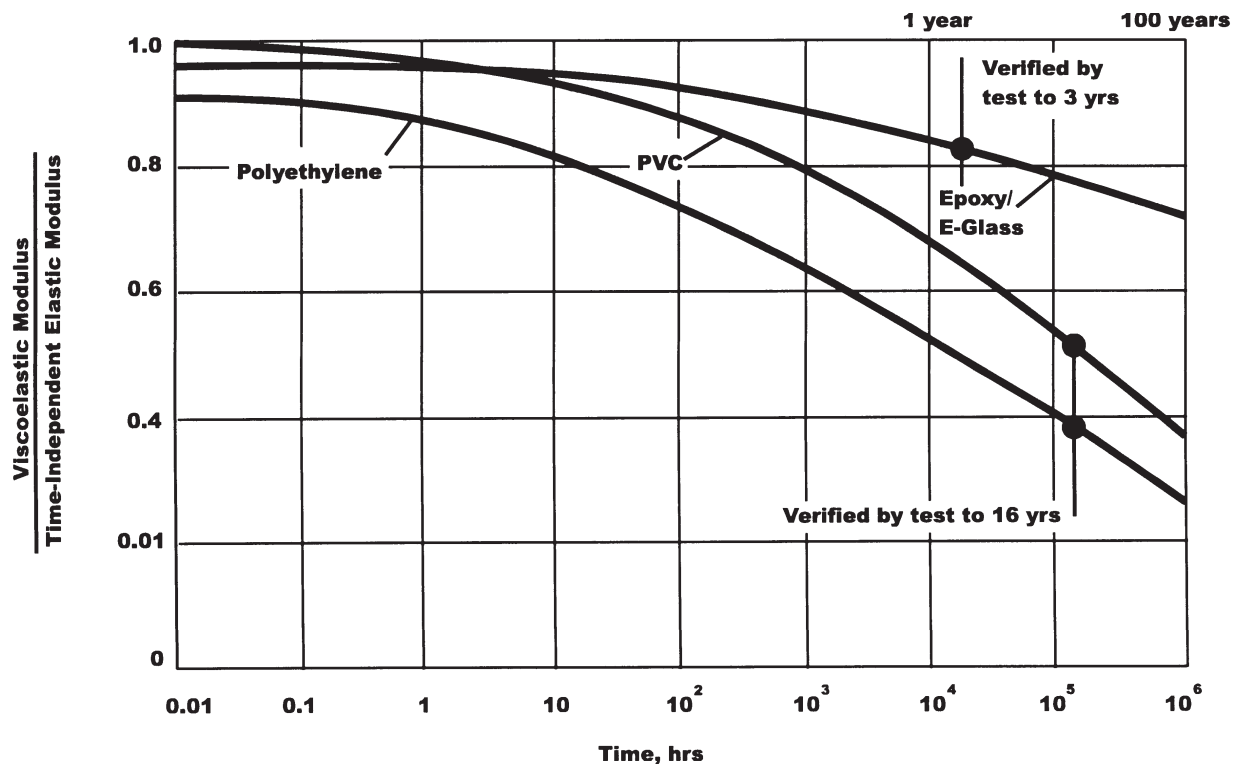
Figure 6-10   Variation in Viscoelastic Modulus with Time [**Structural Plastics Design Manual** published by the American Society of Civil Engineers]

Composite Material Behavior During Sustained Stress

Creep testing is usually performed in tensile or flexure modes. Some data has been developed for cases of multiaxial tensile stress, which is used to describe the case of pressure vessels and pipes under hydrostatic load. Composite material creep behavior can be represented by plotting strain versus time, usually using a log scale for time. Strain typically shows a steep slope initially that gradually levels off to failure at some time, which is material dependent. Ductile materials will show a rapid increase in strain at some point corresponding to material "yield." This time-dependent yield point is accompanied by crazing, microcracking, stress whitening or complete failure. .

Mathematical estimate methods for predicting creep behavior have been developed based on experimentally determined material constants. Findley [36] proposed the following equation to describe strain over time for a given material system:

where:

$$\varepsilon = \varepsilon'_0 + \varepsilon'_t \, t^n \tag{6-19}$$

ε = total elastic plus time-dependent strain (inches/inch or mm/mm)

ε'_0 = stress-dependent, time-independent initial elastic strain (inches/inch or mm/mm)

ε'_t = stress-dependent, time-dependent coefficient of time-dependent strain (inches/inch or mm/mm)

n = material constant, substantially independent of stress magnitude

t = time after loading (hours)

When the continuously applied stress, σ, is less than the constants σ_0 and σ_t given in Table 6-1, equation (6-19) can be rewritten as:

$$\varepsilon = \varepsilon_0 \frac{\sigma}{\sigma_0} + \varepsilon_t \, t^n \, \frac{\sigma}{\sigma_t} \tag{6-20}$$

When E_0, an elastic modulus independent of time is defined as $\dfrac{\sigma_0}{\varepsilon_0}$ and E_t, a modulus that characterizes time-dependent behavior defined as $\dfrac{\sigma_t}{\varepsilon_t}$, equation (6-20) can be given as:

$$\varepsilon = \sigma \left[\frac{1}{E_0} + \frac{t^n}{E_t} \right] \tag{6-21}$$

Constants for the viscoelastic behavior of some engineering polymeric systems are given in Table 6-1. Data in Table 6-1 is obviously limited to a few combinations of reinforcements and resin systems. Indeed, the composition and orientation of reinforcements will influence creep behavior. As composite material systems are increasingly used for infrastructure applications, creep testing of modern material systems should increase.

Table 6-1 Constants for Viscoelastic Equations [*Structural Plastics Design Manual* published by the American Society of Civil Engineers]

Material System	n dimen-sionless	ε_0 ins/in	ε_t ins/in	σ_0 psi	σ_t psi	E_0 10^6 psi	E_t 10^6 psi
Polyester/glass (style 181) - dry	0.090	0.0034	0.00045	15,000	14,000	4.41	31.5
Polyester/glass (style 181) - water immersed	0.210	0.0330	0.00017	80,000	13,000	2.42	76.5
Polyester/glass (style 1000) - dry	0.100	0.0015	0.00022	10,000	8,600	6.67	39.1
Polyester/glass (style 1000) - water immersed	0.190	0.0280	0.00011	80,000	6,500	2.86	60.2
Polyester/glass mat - dry	0.190	0.0067	0.0011	8,500	8,500	1.27	7.73
Polyester/glass woven roving - dry	0.200	0.0180	0.00100	40,000	22,000	2.22	22.0
Epoxy/glass (style 181) - dry	0.160	0.0057	0.00050	25,000	50,000	4.39	100.0
Epoxy/glass (style 181) - water immersed	0.220	0.25	0.00006	80,000	11,000	3.20	200.0
Polyethylene	0.154	0.027	0.0021	585	230	0.0216	0.111
PVC	0.305	0.00833	0.00008	4,640	1,630	0.557	20.5

Fatigue

A fundamental problem associated with engineering uses of fiber reinforced plastics (FRP) is the determination of their resistance to combined states of cyclic stress. [39]   Composite materials exhibit very complex failure mechanisms under static and fatigue loading because of anisotropic characteristics in their strength and stiffness. [40]   Fatigue causes extensive damage throughout the specimen volume, leading to failure from general degradation of the material instead of a predominant single crack. A predominant single crack is the most common failure mechanism in static loading of isotropic, brittle materials such as metals.   There are four basic failure mechanisms in composite materials as a result of fatigue: matrix cracking, delamination, fiber breakage and interfacial debonding.   The different failure modes combined with the inherent anisotropies, complex stress fields, and overall non-linear behavior of composites severely limit our ability to understand the true nature of fatigue. [41]   Figure 6-11 shows a typical comparison of the fatigue damage of composites and metals over time. [42]   As with metal structures, fatigue of composite structures will first occur at structural details where stress concentrations exist.

Many aspects of tension-tension and tension-compression fatigue loading have been investigated, such as the effects of heat, frequency, pre-stressing samples, flawing samples, and moisture [43-49].   Mixed views exist as to the effects of these parameters on composite laminates, due to the variation of materials, fiber orientations, and stacking sequences, which make each composite behave differently.

Fatigue Cycles or Time
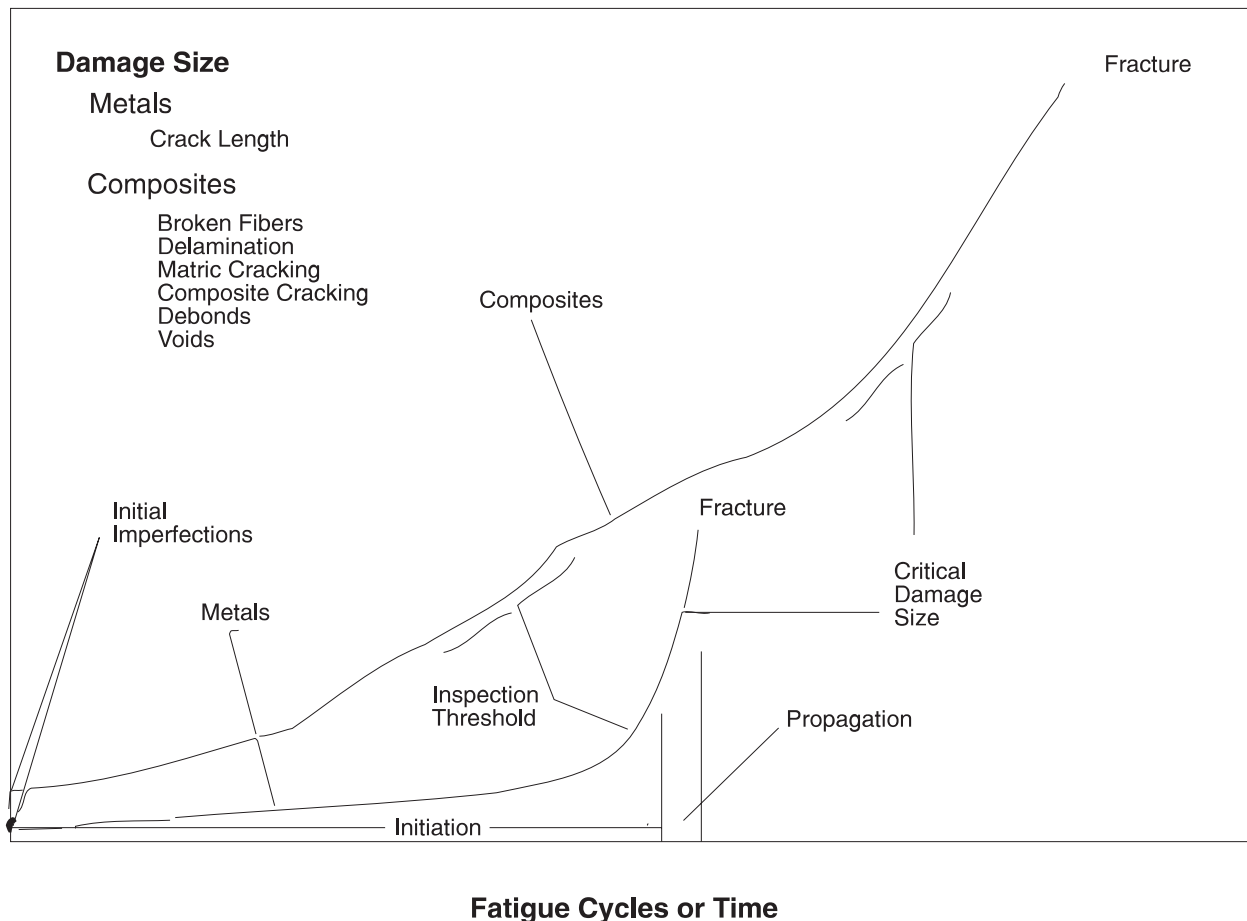
Figure 6-11   Typical Comparison of Metal and Composite Fatigue Damage [from Salkind, *Fatigue of Composites*]

Extensive work has been done to establish failure criteria of composites during fatigue loading [39,43,50,51]. Fatigue failure can be defined either as a loss of adequate stiffness, or as a loss of adequate strength. There are two approaches to determine fatigue life; constant stress cycling until loss of strength, and constant amplitude cycling until loss of stiffness. The approach to utilize depends on the design requirements for the laminate.

In general, stiffness reduction is an acceptable failure criterion for many components which incorporate composite materials. [51] Figure 6-12 shows a typical curve of stiffness reduction for composites and metal. Stiffness change is a precise, easily measured and easily interpreted indicator of damage which can be directly related to microscopic degradation of composite materials. [51]

In a constant amplitude deflection loading situation, the degradation rate is related to the stress within the composite sample. Initially, a larger load is required to deflect the sample. This corresponds to a higher stress level. As fatiguing continues, less load is required to deflect the sample, hence a lower stress level exists in the sample. As the stress within the sample is reduced, the amount of deterioration in the sample decreases. The reduction in load required to deflect the sample corresponds to a reduction in the stiffness of that sample. Therefore, in constant amplitude fatigue, the stiffness reduction is dramatic at first, as substantial matrix degradation occurs, and then quickly tapers off until only small reductions occur.
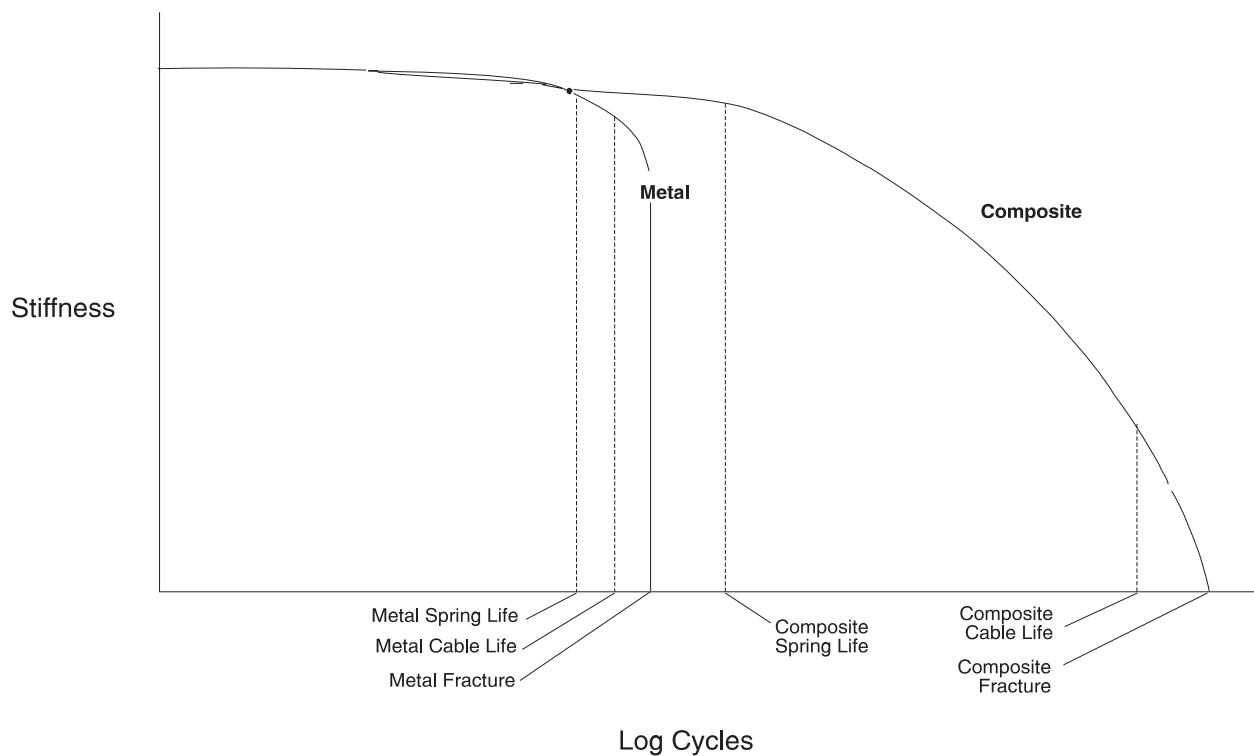
Figure 6-12   Comparison of Metal and Composite Stiffness Reduction [from Salkind, *Fatigue of Composites*]

In a unidirectional fiber composite, cracks may occur along the fiber axis, which usually involves matrix cracking. Cracks may also form transverse to the fiber direction, which usually indicates fiber breakage and matrix failure. The accumulation of cracks transverse to fiber direction leads to a reduction of load carrying capacity of the laminate and with further fatigue cycling may lead to a jagged, irregular failure of the composite material. This failure mode is drastically different from the metal fatigue failure mode, which consists of the initiation and propagation of a single crack. [39] Hahn [52] predicted that cracks in composite materials propagate in four distinct modes. These modes are illustrated in Figure 6-13, where region I corresponds to the fiber and region II corresponds to the matrix.
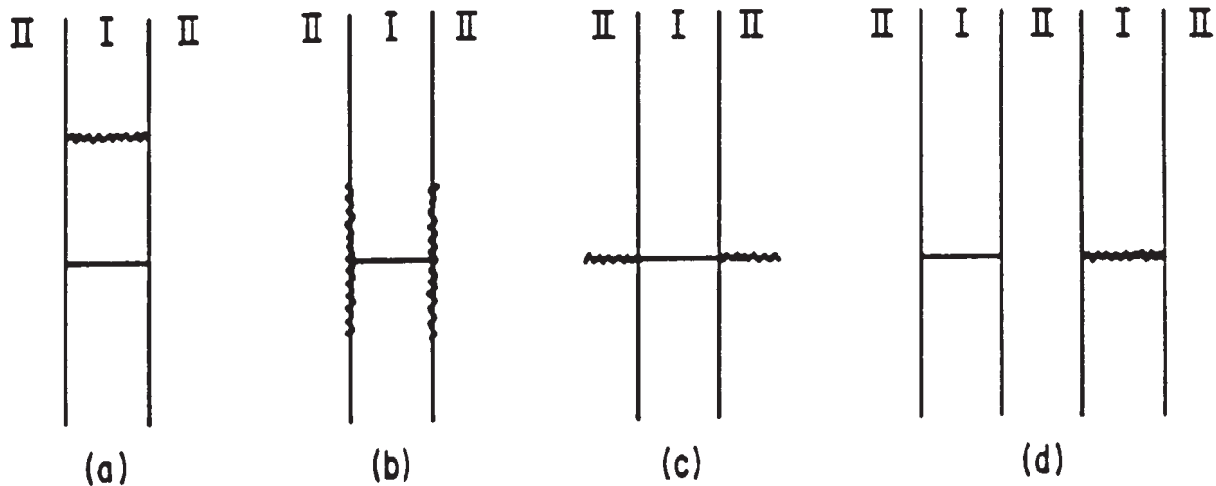
I is the fiber potion of the laminate
II is the resin portion of the laminate

Figure 6-12   Fatigue Failure Modes for Composite Materials - **Mode (a)** represents a tough matrix where the crack is forced to propagate through the fiber. **Mode (b)** occurs when the fiber/matrix interface is weak. This is, in effect, debonding. **Mode (c)** results when the matrix is weak and has relatively little toughness. Finally, **Mode (d)** occurs with a strong fiber/matrix interface and a tough matrix. Here, the stress concentration is large enough to cause a crack to form in a neighboring fiber without cracking of the matrix. **Mode (b)** is not desirable because the laminate acts like a dry fiber bundle and the potential strength of the fibers is not realized. **Mode (c)** is also undesirable because it is similar to crack propagation in brittle materials. The optimum strength is realized in **Mode (a)** as the fiber strengths are fully utilized. [Hahn, *Fatigue of Composites*]

Minor cracks in composite materials may occur suddenly without warning and then propagate at once through the specimen. [39] It should be noted that even when many surface cracks have been formed in the resin, composite materials may still retain respectable strength properties. [53] The retention of these strength properties is due to the fact that each fiber in the laminate is a load-carrying member, and once a fiber fails the load is redistributed to another fiber.

Composite Fatigue Theory

There are many theories used to describe composite material strength and fatigue life. Since no one analytical model can account for all the possible failure processes in a composite material, statistical methods to describe fatigue life have been adopted. Weibull's distribution has proven to be a useful method to describe the material strength and fatigue life. The Weibull distribution is based on three parameters; scale, shape and location. Estimating these parameters is based on one of three methods: the maximum-likelihood estimation method, the moment estimation method, or the standardized variable method. These methods of estimation are discussed in detail in references [54, 55]. It has been shown that the moment estimation method and the maximum-likelihood method lead to large errors in estimating the scale and the shape parameters, if the location parameter is taken to be zero. The standardized variable estimation gives accurate and more efficient estimates of all three parameters for low shape boundaries. [55] Again, the lack of data involving marine composites makes the verification of these theories difficult.

Another method used to describe fatigue behavior is to extend static strength theory to fatigue strength by replacing static strengths with fatigue functions. The power law has been used to represent fatigue data for metals when high numbers of cycles are involved. By adding another term into the equation for the ratio of oscillatory-to-mean stress, the power law can be applied to composite materials. [48]

Algebraic and linear first-order differential equations can also be used to describe the composite fatigue behavior. [50]

There are many different theories used to describe fatigue life of composite materials. However, given the broad range of usage and diverse variety of composites in use in the marine industry, theoretical calculations as to the fatigue life of a given composite should only be used as a first-order indicator. Fatigue testing of laminates in an experimental test program is probably the best method of determining the fatigue properties of a candidate laminate. Further testing and development of these theories must be accomplished to enhance their accuracy. Despite the lack of knowledge, empirical data suggest that composite materials perform better than metals in fatigue situations. Figure 6-14 depicts fatigue strength characteristics for some metal and composite materials. [2]
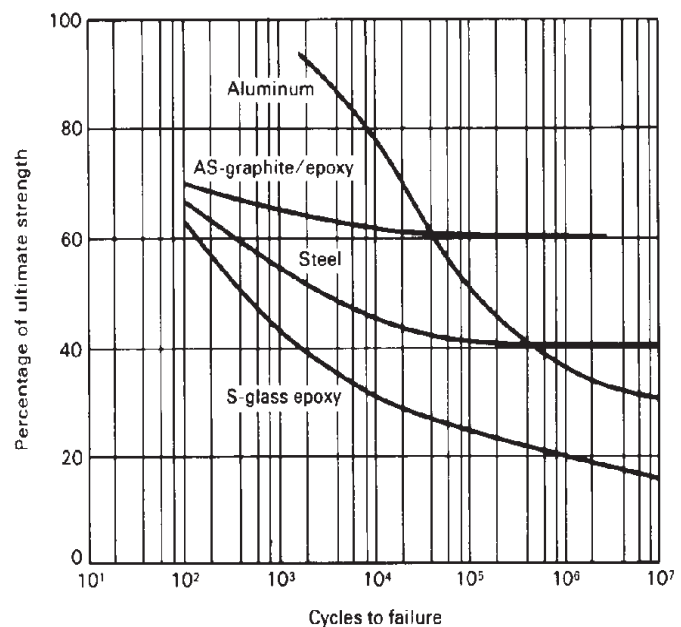
Figure 6-14 Comparison of Fatigue Strengths of Graphite/Epoxy, Steel, Fiberglass/Epoxy and Aluminum [Hercules]

Fatigue Test Data

Although precise predictions of fatigue life expectancies for FRP laminates is currently beyond the state-of-the-art of analytical techniques, some insight into the relative performance of constituent materials can be gained from published test data. The Interplastic Corporation conducted an exhaustive series of fatigue tests on mat/woven roving laminates to compare various polyester and vinyl ester resin formulations. [56] The conclusion of those tests is shown in Figure 6-15 and is summarized as follows:

"Cyclic flexural testing of specific polyester resin types resulted in predictable data that oriented themselves by polymer description, i.e., orthophthalic was exceeded by isophthalic, and both were vastly exceeded by vinyl ester type resins. Little difference was observed between the standard vinyl ester and the new preaccelerated thixotropic vinyl esters."
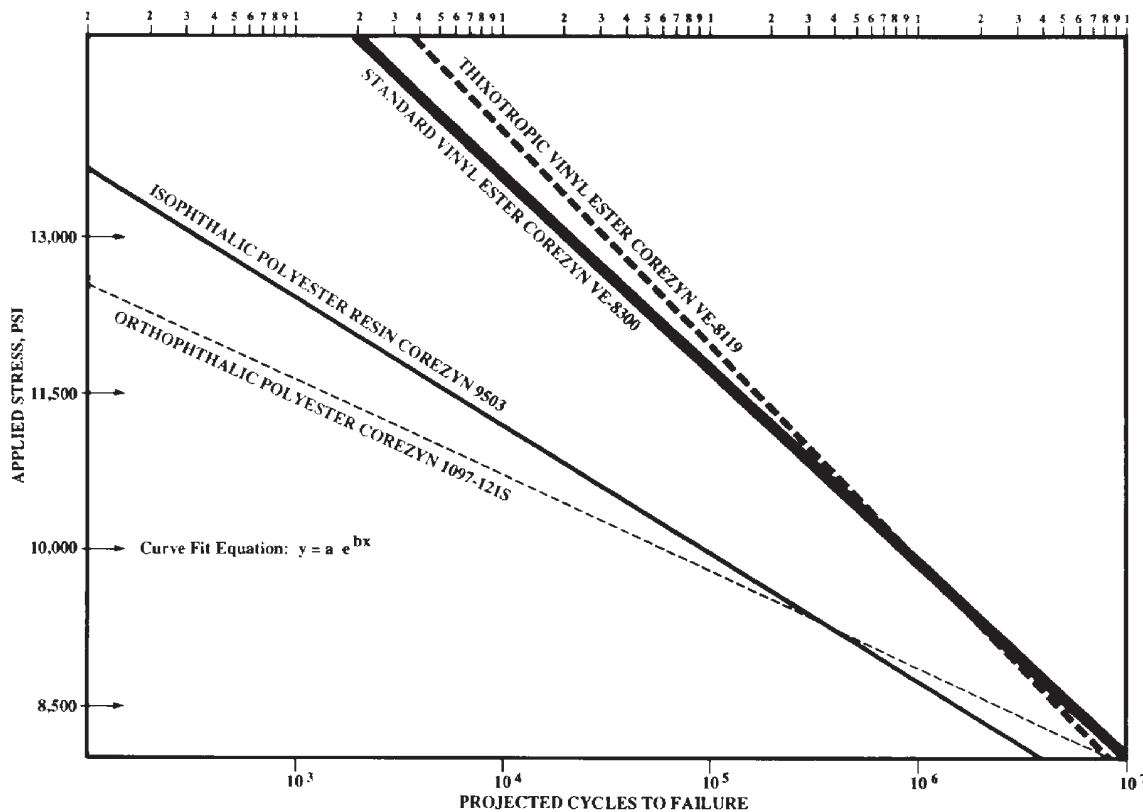
Figure 6-15 Curve Fit of ASTM D671 Data for Various Types of Unsaturated Polyester Resins [Interplastic, *Cycle Test Evaluation of Various Polyester Types and a Mathematical Model for Predicting Flexural Fatigue Endurance*]

With regards to reinforcement materials used in marine laminates, there is not a lot of comparative test data available to illustrate fatigue characteristics. It should be noted that fatigue performance is very dependent on the fiber/resin interface performance. Tests by various investigators [57] suggest that a ranking of materials in order of decreasing

performance would look like:

- High Modulus Carbon Fiber;

- High Strength and Low Modulus Carbon;

- Kevlar/Carbon Hybrid;

- Kevlar;

- Glass/Kevlar Hybrid;

- S-Glass; and

- E-Glass.

The construction and orientation of reinforcement also plays a critical role in determining fatigue performance. It is generally perceived that larger quantities of thinner plies perform better than a few layers of thick plies. Figure 6-16 shows a comparison of various fabric constructions with regard to fatigue performance. As with metal structures, fatigue strength must be compared to static design strength, with the flatter curves in Figure 6-16 more desirable.
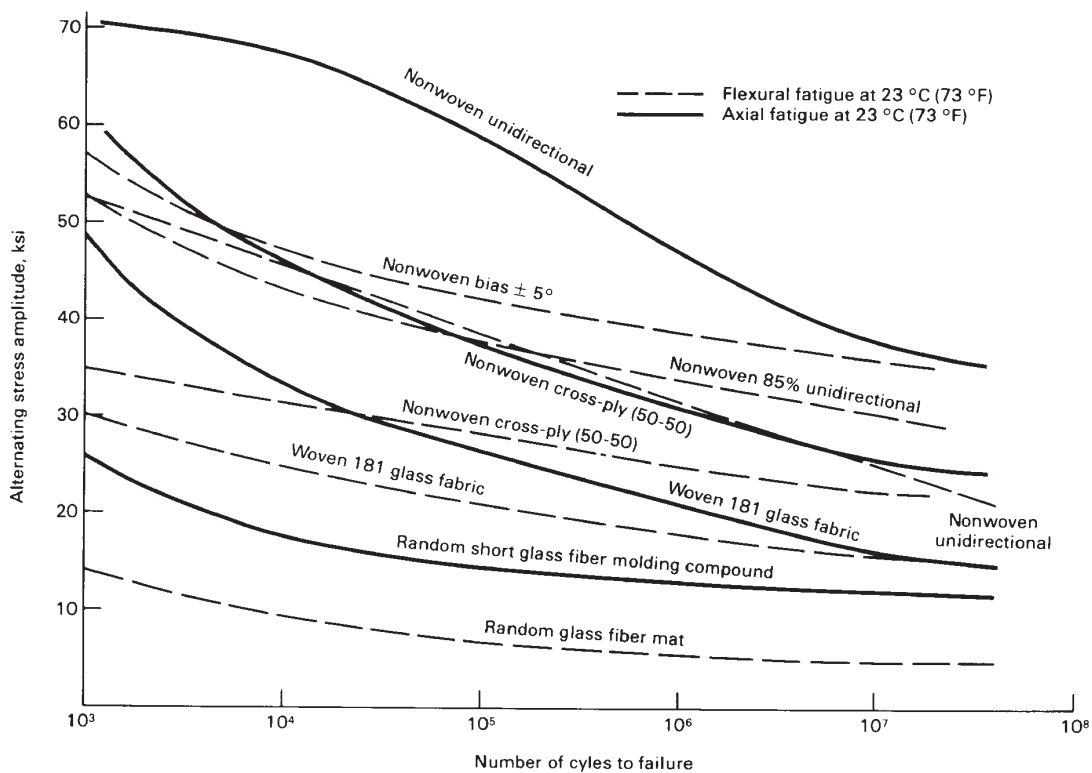
Figure 6-16 Comparitive Fatigue Strengths of Woven and Nonwoven Unidirectional Glass Fiber Reinforced Plasitc Laminates [*ASM Engineers' Guide to Composite Materials*]

Although some guidance has been provided to assist in the preliminary selection of materials to optimize fatigue performance, a thorough test program would be recommended for any large scale production effort that was fatigue performance dependent. This approach has been taken for components such as helicopter and wind turbine rotors, but may be beyond the means of the average marine fabricator.

Impact

The introduction of FRP and FRP sandwich materials into the boating industry has led to lighter, stiffer and faster boats. This requires increased impact performance, since higher speeds cause impact energy to be higher, while stiffer structures usually absorb less impact energy before failure. Thus, the response of a FRP composite marine structure to impact loads is an important consideration. The complexity and variability of boat impacts makes it very difficult to define an impact load for design purposes. There is also a lack of information on the behavior of the FRP composite materials when subjected to the high load rates of an impact, and analytical methods are, at present, relatively crude. Thus, it is difficult to explicitly include impact loads into the structural analysis and design process. Instead, basic knowledge of the principles of impact loading and structural response is used as a guide to design structures for relatively better impact performance.

The response of hull bottom panels to wave impact can be attributed to several mechanisms. Primarily, the entire energy of the impact is absorbed by the structure in elastic deformation, and then released when the structure returns to its original position or shape. Higher energy levels exceed the ability of the structure to absorb the energy elastically. The next level is plastic deformation, in which some of the energy is absorbed by elastic deformation, while the remainder of the energy is absorbed through permanent plastic deformation of the structure. With the exception of thermoplastic materials, composites have limited ability for plastic deformation. Higher energy levels result in energy absorbed through damage to the structure. Finally, the impact energy levels can exceed the capabilities of the structure, leading to catastrophic failure.

The maximum energy which can be absorbed in elastic deformation depends on the stiffness of the materials and the geometry of the structure. Damage to the structural laminate can be in the form of resin cracking, delamination between plies, debonding of the resin fiber interface, and fiber breakage for solid FRP laminates, with the addition of debonding of skins from the core in sandwich laminates. The amount of energy which can be absorbed in laminate and structural damage depends on the resin properties, fiber types, fabric types, fiber orientation, core material, fabrication techniques and rate of impact. Resisting impact with floating objects requires good puncture resistance and stiffer cores often efficiently transfer loads between skins.

Impact Design Considerations

The general principles of impact design are as follows. The kinetic energy of an impact is:

$$K.E. = \frac{m \, v^2}{2} \tag{6-22}$$

where:

v = the collision velocity and m is the mass of the boat or the impactor, whichever is smaller.

The energy that can be absorbed by an isotropic beam point loaded at mid-span is:

$$K.E. = \int_0^L \frac{M^2}{2 \, E \, I} \, ds \tag{6-23}$$

where:

L = the span length

M = the moment

$$E \; = \; \text{Young's Modulus}$$

$$I \; = \; \text{moment of inertia}$$

For the small deformations of a composite panel, the expression can be simplified to:

$$K.E. \; = \; \frac{S^2 \; A \; L \; h^2}{6 \; E \; c^2} \qquad (6\text{-}24)$$

where:

$$S \; = \; \text{the stress}$$

$$A \; = \; \text{cross-sectional area}$$

$$h \; = \; \text{the depth of the beam}$$

$$c \; = \; \text{the depth of the outermost fiber of the beam}$$

From this relationship, the following conclusions can be drawn:

- Increasing the skin laminate modulus E causes the skin stress levels to increase. The weight remains the same and the flexural stiffness is increased.

- Increasing the beam thickness h decreases the skin stress levels, but it also increases flexural stiffness and the weight.

- Increasing the span length L decreases the skin stress levels. The weight remains the same, but flexural stiffness is decreased.

Therefore, increasing the span will decrease skin stress levels and increase impact energy absorption, but the flexural stiffness is reduced, thus increasing static load stress levels.

For a sandwich structure:

$$M \; = \; \frac{S \; I}{d} \qquad (6\text{-}25)$$

$$I \; \approx \; \frac{b \; t \; d^2}{2} \qquad (6\text{-}26)$$

where:

$$S \; = \; \text{skin stress}$$

$$d \; = \; \text{core thickness}$$

$$b \; = \; \text{beam width}$$

$$t \; = \; \text{skin thickness}$$

Thus the energy absorption of a sandwich beam is:

$$K.E. \; = \; \frac{S^2 \; b \; t \; L}{4 \; E} \qquad (6\text{-}27)$$

From this relationship, the following conclusions can be drawn:

- Increasing the skin laminate modulus E causes the skin stress levels to increase. The weight remains the same and the flexural stiffness is increased.

- Increasing the skin thickness t decreases the skin stress levels, but it also increases flexural stiffness and the weight.

- Increasing the span length L decreases the skin stress levels. The weight remains the same, but flexural stiffness is decreased.

- Core thickness has no effect on impact energy absorption.

Therefore, increasing the span will decrease skin stress levels and increase impact energy absorption, while the flexural stiffness can be maintained by increasing the core thickness.

An impact study investigating sandwich panels with different core materials, different fiber types and different resins supports some of the above conclusions. [58] This study found that panels with higher density foam cores performed better than identical panels with lower density foam cores, while rigid cores such as balsa and Nomex® did not fare as well as the foam. This indicates that the softer cores can absorb more energy, which may be desirable for resisting some types of impact. The difference in performance between panels constructed of E-glass, Kevlar®, and carbon fiber fabrics was small, with the carbon fiber panels performing slightly better than the other two types. The reason for these results is not clear, but the investigator felt that the higher flexural stiffness of the carbon fiber skin distributed the impact load over a greater area of the foam core, thus the core material damage was lower for this panel. Epoxy, polyester and vinyl ester resins were also compared. The differences in performance were slight, with the vinyl ester providing the best performance, followed by polyester and epoxy. Impact performance for the different resins followed the strength/stiffness ratio, with the best performance from the resin with the highest strength to stiffness ratio.

General impact design concepts can be summarized as follows:

- Impact Energy Absorption Mechanisms;

- Elastic deformation;

- Matrix cracking;

- Delamination;

- Fiber breakage;

- Interfacial debonding; and

- Core shear.

The failure mechanism is usually that of the limiting material in the composite, however, positive synergism between specific materials can dramatically improve impact performance. General material relationships are as follows:

- Kevlar® and S-glass are better than E-glass and carbon fibers;

- Vinyl ester is better than epoxy and polyester;

- Foam core is better than Nomex® and Balsa;

- Quasi-isotropic laminates are better than Orthotropic laminates; and

- Many thin plies of reinforcing fabric are better than a few thicker plies.

Environmental Degradation

Although composite structures are not subject to corrosion, laminates can sustain long-term damage from water, UV and elevated temperature exposure. Based on the number of pioneering FRP recreational craft that are still in service, properly engineered laminates should survive forty-plus years in service.

Moisture Absorption

Reinforced thermoset composites typically used in a marine environment have been evaluated for water absorption properties, in an attempt to determine the potential effect on mechanical properties when various levels of saturation occur. Also, the initially cosmetic problem of blistering has been extensively studied. Many factors affect the resistance to moisture intrusion of a composite structure.

The rate of moisture absorption into a laminate is known to be a function of time and temperature [59]. Elaborate models have been devised to determine the rate of diffusion of water into the solid. These models are specific to the composition of the laminate, however, as it is established that the raw materials available for marine used vary widely in resistance to water intrusion and degradation.

Moisture Absorption Test Methods

The simplest way to determine water absorption properties of a single-skin laminate is to immerse a rectangular test coupon in water (usually distilled) for a set period of time. After an elapsed period, the coupon is removed from the water, surface water is patted dry with a paper towel, and the coupon is weighed. From the initial and post-immersion weights, the amount of water absorbed (weight %) can be calculated. Examples of this type of method include ASTM D 570 and ISO 62.

These methods are useful for direct comparison of different laminates exposed to the same conditions (for example, 2 week immersion, 23°C, distilled water). It is difficult to determine what the maximum moisture content of a particular laminate could reach in a saturated condition. Indeed, test coupons will reach a point of maximum weight, then the weight will decrease as the polymer matrix degrades and is dissolved or leached into the water [60]. The amount of mass lost may be determined by drying the sample, and comparing the post-immersion dried weight to the original weight.

A more sophisticated method (ASTM D 5229) may be utilized to determine absorption rate and diffusivity of water into the laminate. The equilibrium moisture content may also be found using this technique.

In general the water resistance of various thermoset resins is as shown :

epoxy > vinyl ester > isophthalic > orthophthalic

The effect of reinforcement type cannot be ignored. Kevlar® is recognized to be more hydrophilic than carbon fiber and E-glass, for example [61]. Of course, it is essential to have complete fiber wet-out by resin in any type of laminate to reduce "wicking" of water along the fibers into the laminate.

Effect on Mechanical Properties

Several studies have shown that the mechanical properties of thermoset reinforced laminates deteriorate with increasing moisture content. Unfortunately, most of the data generated has been obtained by immersion in distilled or sea water at elevated temperatures (40°-60°C), in an attempt to accelerate the test procedure. Many environmental exposure tests are accelerated by increasing the severity of exposure conditions, whether by intensification of a light source (weathering), increase of temperature (moisture absorption, blistering), increased concentration of reagent/solvent (corrosion resistance) etc. Little data is available as to mechanical properties after exposure to normal environmental conditions for periods of time corresponding to a predicted service life.

It has been shown that the shear strength (short-beam method) of a single-skin polyester/E-glass laminate may be reduced up to 50% by immersion in distilled water at 60°C for as little as 5 months [62]. Under these conditions the moisture content (weight %) of the laminate was approximately 2.5%. Other tests [63] show an approximate 50% reduction in tensile strength of isophthalic and orthophthalic FRP laminates after 4 months immersion at 65°C followed by 1 year immersion at 25°C.

Epoxy/carbon fiber laminates appear to show little degradation of tensile properties with moisture content of less than 1%. As the moisture content approaches 2% by weight, tensile strength is reduced approximately 20% [64].

The flexural properties of well-saturated (4-5% by weight water) epoxy/Kevlar® laminates are 15% - 20% lower than of dry specimens [61]. It is noted that the "saturation" point of Kevlar®-reinforced laminates is higher than that of carbon or E-glass composites.

Blistering

Hull blistering has generally been regarded as a cosmetic problem, but the effect of water intrusion on mechanical properties can be severe as shown above. The causes of blistering are complex, yet fairly well understood.

Gelcoat and bottom paint, if present, form a semipermeable membrane over the FRP laminate. Water will diffuse through these layers and can degrade the laminate. The rate of diffusion (speed of attack) will depend on the raw materials used to fabricate the laminate. Many of the chemical choices made by resin and gelcoat manufacturers will affect the speed and severity of blister formation.

The problem is complex due to the many factors that have been shown to contribute to the blistering process. A gelcoat formulation may contain up to 20 raw materials, all of which must be chosen to be resistant to hydrolytic degradation. Among these chemicals are:

- Base resin;
- Pigments;
- Fillers; and
- Thixotropic agents.

The laminating resin must also be water resistant. It is a waste of time to use an inferior quality resin in the skin coat, behind a high quality gelcoat. The best solution to prevent blisters (to date) seems to be use of a high quality gelcoat (NPG iso or better) with a vinyl ester skin coat.

It should be noted that the chemicals in the reinforcement also may contribute to the blistering process. For example, different binders (chopped strand) and sizings on E-glass reinforcements will vary with respect to water resistance.

Of course, the fabrication process is also important, in that the gelcoat and resin must be applied and cured properly. Materials must be handled with due regard to preventing contamination from moisture, dirt, oil, etc. Air entrapment, which can lead to excessive voids in the finished laminate, should also be avoided. Preventive maintenance of the hull bottom will delay the onset of blistering.

UV Degradation

The three major categories of resins that are used in boat building, polyester, vinyl ester and epoxy, have different reactions to exposure to sunlight. Sunlight consists of ultraviolet rays and heat.

Epoxies are generally very sensitive to ultraviolet (UV) light and if exposed to UV rays for any significant period of time the resins will degrade to the point where they have little, if any, strength left to them. The vinyl esters, because there are epoxy linkages in them, are also sensitive to UV and will degrade with time, although in general not as rapidly as an epoxy. Polyester, although being somewhat sensitive to UV degradation, is the least sensitive of the three to UV light.

The outer surface of most boats is covered with a gel coat. Gel coats are based on ortho or isopolyester resin systems that are heavily filled and contain pigments. In addition, often there is a UV screen added to help protect the resin, although for most gel coats the pigment itself serves as the UV protector.

In general, the exposure of the gel coats to UV radiation will cause fading of the color which is associated with the pigments themselves and their reaction to sunlight. On white or off-white gel coats, UV exposure can cause yellowing. The yellowing is a degradation of the resin rather than the pigments and will finally lead to the phenomenon known as "chalking." Chalking occurs when the very thin outer coating of resin degrades under the UV light to the point where it exposes the filler and some of the pigment in the gel coat. The high gloss finish that is typical of gel coats is due to that thin layer. Once it degrades and disappears the gloss is gone, and what's left is still a colored surface but it is no longer shiny. Because the pigments are no longer sealed by the thin outer coating of resin, they actually can degrade and lose some of their color eventually loosening up from the finish to giving a kind of a chalky surface effect.

There are some gel coats that are based on vinyl ester resin. These are not generally used in the marine industry, but some boat manufacturers are starting to use them below the water line to prevent blistering, since vinyl ester resins are not typically susceptible to blistering. However, if these resins are used on the top side or the decks of a boat, they will suffer yellowing and chalking very quickly as compared to a good ortho or isopolyester gel coat.

Performance at Elevated Temperatures

In addition to the type of degradation caused by sunlight, the other problem that must be considered is the effects of heat. The sun will actually heat up the gel coat and the laminate beneath it. The amount of damage that can be done depends on a number of factors. First, the thermal expansion coefficient of fiberglass is very different from that of resin. Thus, when a laminate with a high glass content is heated significantly the fiberglass tends to be relatively stable, whereas the resin tries to expand, which it can't because it's held in place by the glass. The result of this is that the pattern of the fiberglass will show through the gel coat in many cases, a phenomenon known as "print through." Of course, if reinforcing fibers are used which have thermal expansion coefficients similar to the resins, it is less likely that print through will occur.

Another consideration in addition to the thermal coefficient of expansion is the temperature at which the resin was cured. Most polyester resins have a heat distortion temperature of around 150-200°F. This means that when the resin becomes heated to that temperature, it has gone above the cure temperature, and the resin will become very soft. When resin becomes soft, the laminate becomes unstable. The resin can actually cure further when it's heated to these temperatures. When it cools down the resin will try to shrink, but since it's been set at the higher temperature and the glass doesn't change dimensions very much, the resin is held in place by the glass, thereby creating very large internal stresses solely due to these thermal effects. This can happen in a new laminate when it's cured and can happen to a laminate that's exposed to the sun and is heated higher than its heat distortion temperature. This can be a problem with all room temperature thermosetting resins: polyester, vinyl ester and epoxies. Heat distortion is less likely to be a problem with vinyl ester and epoxy than with polyester, because the vinyl esters and epoxies usually cure at a higher exotherm temperature.

As mentioned above, the heat distortion temperature of polyester resins can range from about 150°-200°. In Florida or the tropics it's not uncommon to get temperatures in excess of 150° on boats with white gel coats. Temperatures have been measured as high as 180° on the decks of boats with red gel coat, close to 200° on the decks of boats with dark blue gel coat and well over 200° on the decks of boats with black gel coat. This is one of the reasons why there are very few boats with black gel coat. Some sport fishing boats or other boats are equipped with a wind screen which, rather than being clear, is actually fiberglass coated with black gel coat for a stylish appearance. This particular part of these boats suffers very badly from print through problems because the heat distortion temperature or the resin in the gel coat is exceeded. Obviously, during each day and night much temperature cycling occurs. The resin will already be postcured to some extent, however it will still suffer from this cyclic heating and cooling. These temperature cycles tend to produce internal stresses which then cause the laminate to fatigue more rapidly than it normally would.

Another thermal effect in fatigue is caused by shadows moving over the deck of a boat that's sitting in the sun. As the sun travels overhead, the shadow will progress across the deck. At the edge of the shadow there can be a very large temperature differential on the order of 20°-30°. As a result, as that shadow line travels there is a very sharp heating or cooling at the edge, and the differential causes significant stress right at that point. That stress will result in fatigue of the material. Boats that are always tied up in the same position at the dock, so that the same areas of the boat get these shadows traveling across them, can actually suffer fatigue damage with the boat not even being used.

Performance in Fires

Composite materials based on organic matrices are flammable elements that should be evaluated to determine the potential risk associated with their use. In a fire, general purpose resins will burn off, leaving only the reinforcement, which has no inherent structural strength. "T-vessels" inspected by the U.S. Coast Guard must be fabricated using low flame spread resins. These resins usually have additives such as chlorine, bromine or antimony. Physical properties of the resins are usually reduced when these compounds are added to the formulation. There is also some concern about the toxicity of the gases emitted when these resins are burned.

The fire resistance of individual composite components can be improved if they are coated with intumescent paints (foaming agents that will char and protect the component during minor fires). The commercial designer is primarily concerned with the following general restrictions (see appropriate Code of Federal Regulation for detail):

- Subchapter T - Small Passenger Vessels: Use of low flame spread (ASTM E 84 <100) resins

- Subchapter K - Small Passenger Vessels Carrying More Than 150 passengers or with overnight accommodations for 50 - 150 people: must meet SOLAS requirement with hull structure of steel or aluminum conforming to ABS or Lloyd's.

- Subchapter I - Cargo Vessels: Use of incombustible materials - construction is to be of steel or other equivalent material

- Subchapter H - Passenger Vessels: SOLAS requires noncombustible structural materials or materials insulated with approved noncombustible materials so that the average temperature will not rise above a designated temperature

More detail will be given on SOLAS requirements later in this section. The industry is currently in the process of standardizing tests that can quantify the performance of various composite material systems in a fire. The U.S. Navy has taken the lead in an effort to certify materials for use on submarines [65]. Table 6-4 presents some composite material test data compiled for the Navy. The relevant properties and associated test methods are outlined in the following topics. No single test method is adequate to evaluate the fire hazard of a particular composite material system. The behavior of a given material system in a fire is dependent not only on the properties of the fuel, but also on the fire environment to which the material system may be exposed. The proposed standardized test methods [67] for flammability and toxicity characteristics cover the spectrum from small scale to large scale tests. An overview of these tests is provided herein.

Small Scale Tests

Small scale tests are quick, repeatable ways to determine the flammability characteristics of organic materials. Usually, a lot of information can be obtained using relatively small test specimens.
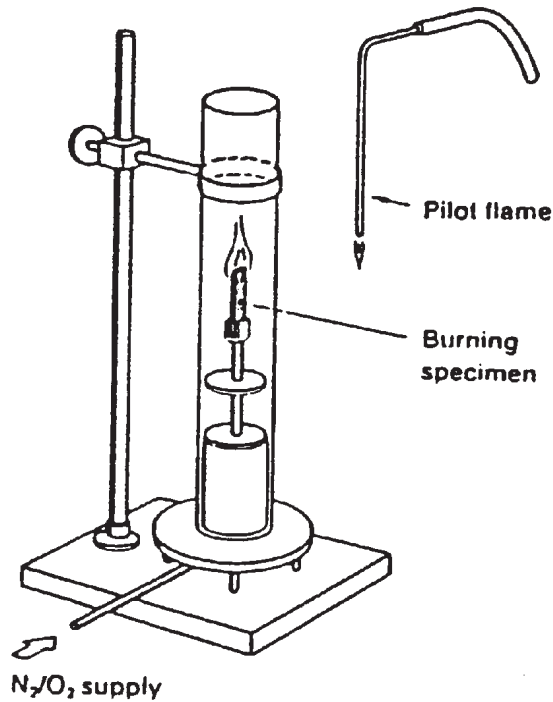
Figure 6-17 Sketch of the Functional Parts of the Limiting Oxygen Index Apparatus [Rollhauser, *Fire Tests of Joiner Bulkhead Panels*]
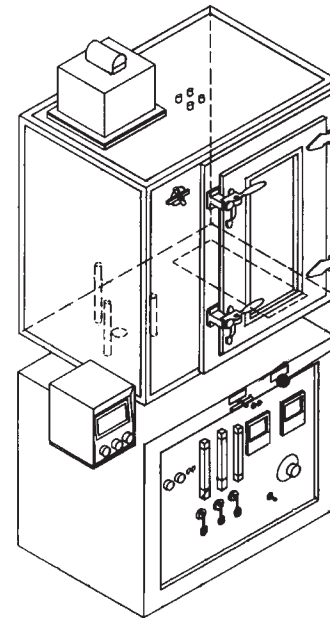
Figure 6-18 Smoke Obscuration Chamber [ASTM E 662]

Oxygen-Temperature Limiting Index (LOI) Test - ASTM D 2863 (Modified)

The Oxygen Temperature Index Profile method determines the minimum oxygen concentration needed to sustain combustion in a material at temperatures from ambient to 570°F. During a fire, the temperature of the materials in a compartment will increase due to radiative and conductive heating. As the temperature of a material increases, the oxygen level required for ignition decreases. This test assesses the relative resistance of the material to ignition over a range of temperatures. The test apparatus is shown in Figure 6-17.

Approximately (40) $\frac{1}{4}$" to $\frac{1}{2}$" x $\frac{1}{8}$" x 6" samples are needed for the test. Test apparatus consists of an Oxygen/Nitrogen mixing system and analysis equipment. The test is good for comparing similar resin systems, but may be misleading when vastly different materials are compared.

N.B.S. Smoke Chamber - ASTM E662

Figure 6-18 shows a typical NBS Smoke Chamber. This test is used to determine the visual obscuration due to fire. The sample is heated by a small furnace in a large chamber and a photocell arrangement is used to determine the visual obscuration due to smoke from the sample.

The test is performed in flaming and non-flaming modes, requiring a total of (6) 3" x 3" x $\frac{1}{8}$" samples. Specific Optical Density, which is a dimensionless number, is recorded. The presence of toxic gases, such as CO, CO_2, HCN and HCl can also be recorded at this time. Table 6-2 shows some typical values recorded using this test.

**Table 6-2 Results of Smoke Chamber Tests (E-662) for Several Materials
[Rollhauser, Fire Tests of Joiner Bulkhead Panels]**

Material	Exposure	Optical Density 20 minutes	Optical Density 5 minutes
Phenolic Composite	Flaming	7	
	Nonflaming	1	
Polyester Composite	Flaming	660	321
	Nonflaming	448	22
Plywood	Flaming	45	
Nylon Carpet	Flaming	270	
Red Oak Flooring	Flaming	300	

Cone Calorimeter - ASTM E 1354

This is an oxygen consumption calorimeter that measures the heat output of a burning sample by determining the amount of oxygen consumed during the burn and calculating the amount of energy involved in the process. The shape of the heating coil resembles a truncated cone. The test apparatus may be configured either vertically or horizontally, as shown in Figure 6-20. The device is used to determine time to ignition, the mass loss of the sample, the sample's heat loss, smoke, and toxic gas generation at a given input heat flux. This is a new test procedure that uses relatively small (4" x 4") test specimens, usually requiring (24) for a full series of tests.

Radiant Panel - ASTM E 162

This test procedure is intended to quantify the surface flammability of a material as a function of flame spread and heat contribution.   The ability of a panel to stop the spread of fire and limit heat generated by the material is measured. A 6" x 18" specimen is exposed to heat from a 12" x 18" radiant heater. The specimen is held at a 45° angle, as shown in Figure 6-19.

The test parameters measured include the time required for a flame front to travel down the sample's surface, and the temperature rise in the stack. The Flame Spread Index, I_s, is calculated from these factors. This number should not be confused with the *FSI* calculated from the ASTM E 84 test, which utilizes a 25-foot long test chamber. Table 6-3 shows some comparative E 162 data.
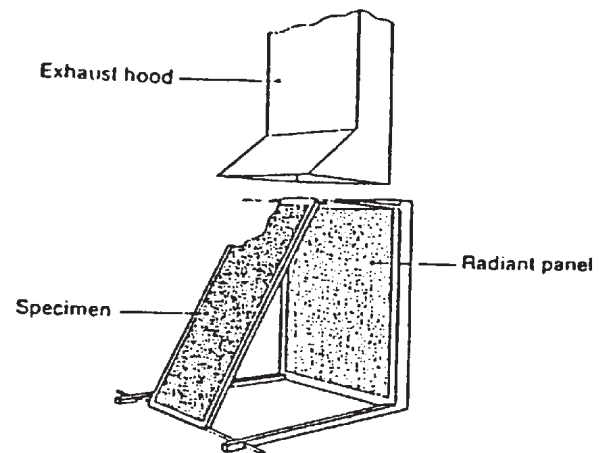
Figure 6-19   Sketch of the Functional Parts of the NBS Radiant Panel Test Configuration [Rollhauser, *Fire Tests of Joiner Bulkhead Panels*]
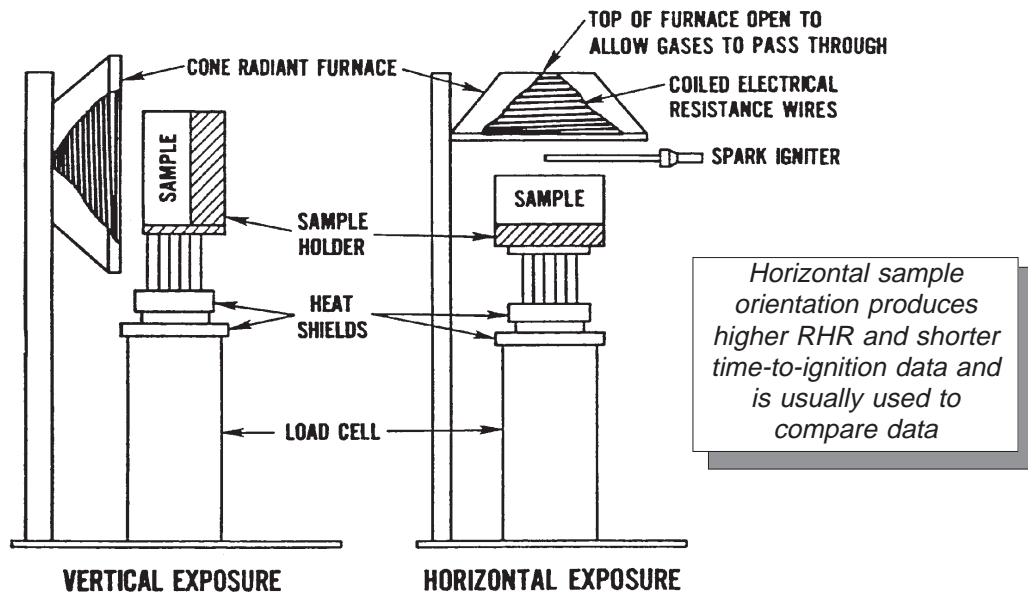
Figure 6-20   Sketch of the Functional Parts of a Cone Calorimeter [Rollhauser, *Fire Tests of Joiner Bulkhead Panels]*

Table 6-3 Flame Spread Index as per MIL-STD 2031(SH) [65] (20 max allowable)

Sorathia (1990)	Graphite/Phenolic	**6**
	Graphite/BMI	**12**
	Graphite/Epoxy	**20**
	Glass/Vinylester with Phenolic Skin	**19**
	Glass/Vinylester with Intumescent Coating	38
	Glass/Vinylester	156
Silvergleit (1977)	Glass/Polyester	31 - 39
	Glass/Fire Retardant Polyester	**5** - 22
	Glass/Epoxy	**1** - 45
	Graphite/Epoxy	32
	Graphite/Fire Retardant Epoxy	**9**
	Graphite/Polyimide	**1** - 59
Rollhauser (1991)	Fire Tests of Joiner Bulkhead Panels	
	Nomex® Honeycomb	**19** - 23
	FMI (GRP/Syntactic core)	**2 - 3**
	Large Scale Composite Module Fire Testing	
	All GRP Module	238
	Phenolic-Clad GRP	36

Table 6-4 Heat Release Rates and Ignition Fire Test Data for Composite Materials [Hughes Associates, *Heat Release Rates and Ignition Fire Test Data for Representative Building and Composite Materials*]

Material/Reference		Applied Heat Flux (kW/m²)	Peak HRR (kW/m²)	Average Heat Release Rate - HRR (kW/m²)			Ignition Time
				1 min	2 min	5 min	
Epoxy/fiberglass	A	25,50,75					32,8,5
Epoxy/fiberglass	B	25,50,75					30,8,6
Epoxy/fiberglass 7mm	C	25,50,75	158,271,304				
Epoxy/fiberglass 7mm	D	25,50,75	168,238,279				
Epoxy/fiberglass 7mm	E	26,39,61	100,150,171				
Epoxy/fiberglass 7mm	F	25,37	117,125				
Epoxy/fiberglass 7mm	G	25,50,75	50,154,117				
Epoxy/fiberglass 7mm	H	25,50,75	42,71,71				
Epoxy/fiberglass 7mm	I	35	92				
Phenolic/fiberglass	A	25,50,75					28,8,4
Phenolic/fiberglass	B	25,50,75					NI,8,6
Phenolic/FRP 7mm	C	25,50,75	4,140,204				
Phenolic/FRP 7mm	D	25,50,75	4,121,171				
Phenolic/FRP 7mm	E	26,39,61	154,146,229				
Phenolic/FRP 7mm	F	25,37	4,125				
Phenolic/FRP 7mm	G	25,50,75	4,63,71				
Phenolic/FRP 7mm	H	25,50,75	4,50,63				
Phenolic/FRP 7mm	I	35	58				
Polyester/fiberglass	J	20	138				
FRP	J	20,34,49	40,66,80				
GRP	J	33.5	81				
Epoxy/Kevlar® 7mm	A	25,50,75					33,9,4
Epoxy/Kevlar® 7mm	B	25,50,75					36,7,6
Epoxy/Kevlar® 7mm	C	25,50,75	108,138,200				
Epoxy/Kevlar® 7mm	D	25,50,75	100,125,175				
Epoxy/Kevlar® 7mm	E	26,39,61	113,150,229				
Epoxy/Kevlar® 7mm	F	20,25,27	142,75,133				
Epoxy/Kevlar® 7mm	G	25,50,75	20,83,83				
Epoxy/Kevlar® 7mm	H	25,50,75	20,54,71				
Epoxy/Kevlar® 7mm	I	35	71				
Phenolic/Kevlar® 7mm	A	25,50,75					NI,12,6

Material/Reference		Applied Heat Flux (kW/m²)	Peak HRR (kW/m²)	Average Heat Release Rate - HRR (kW/m²)			Ignition Time
				1 min	2 min	5 min	
Phenolic/Kevlar® 7mm	B	25,50,75					NI,9,6
Phenolic/Kevlar® 7mm	C	25,50,75	0,242,333				
Phenolic/Kevlar® 7mm	D	25,50,75	0,200,250				
Phenolic/Kevlar® 7mm	E	26,39,64	100,217,300				
Phenolic/Kevlar® 7mm	F	30,37	147,125				
Phenolic/Kevlar® 7mm	G	25,50,75	13,92,117				
Phenolic/Kevlar® 7mm	H	25,50,75	13,75,92				
Phenolic/Kevlar® 7mm	I	35	83				
Phenolic/Graphite 7mm	C	25,50,75	4,183,233				
Phenolic/Graphite 7mm	D	25,50,75	0,196,200				
Phenolic/Graphite 7mm	E	39,61	138,200				
Phenolic/Graphite 7mm	F	20,30,37	63,100,142				
Phenolic/Graphite 7mm	G	25,50,75	13,75,108				
Phenolic/Graphite 7mm	H	25,50,75	13,63,88				
Phenolic/Graphite 7mm	I	35	71				
Phenolic/Graphite 7mm	A	25,50,75					NI,12,6
Phenolic/Graphite 7mm	B	25,50,75					NI,10,6
Epoxy	K	35,50,75		150,185,210	155,170,190	75,85,100	116,76,40
Epoxy/Nextel-Prepreg	K	35,50,75		215,235,255	195,205,240	95,105,140	107,62,31
Bismaleimide (BMI)	K	35,50,75		105,120,140	130,145,170	105,110,125	211,126,54
BMI/Nextel-Prepreg	K	35,50,75		100,120,165	125,135,280	120,125,130	174,102,57
BMI/Nextel-Dry	K	35,50,75		145,140,150	150,150,165	110,120,125	196,115,52
Koppers 6692T	L	25,50,75					263,60,21
Koppers 6692T/FRP	L	25,35,35	59,NR,101	50,55,70	40,65,55	25,65,40	
Koppers 6692T/FRP	L	50,50,75	85,NR,100	60,60,80	50,45,80	40,35,60	
Koppers Iso/FRP	L	50		215	180	150	55
Koppers Iso/Bi Ply	L	50		210	75	145	50
Koppers Iso/FRP	L	50		235	190	160	45
Koppers Iso/mat/WR	L	50		135	115	100	35
Koppers Iso/S2WR	L	50		130	110	0	45
Dow Derakane 3mm	L	35,50,75					
Dow Derakane 25mm	L	35,50,75					
Dow Vinylester/FRP	L	35,50,50		295,225,190	255,195,170	180,145,160	
Dow Vinylester/FRP	L	75,75,75		240,217,240	225,205,225	185,165,185	

Material/Reference		Applied Heat Flux (kW/m²)	Peak HRR (kW/m²)	Average Heat Release Rate - HRR (kW/m²)			Ignition Time
				1 min	2 min	5 min	
Lab Epoxy 3mm	LL	35,50,75					116,76,40
Lab Epoxy/Graphite	L	35,50,75		150,185,210	155,170,190	75,85,100	
Lab BMI 3mm	L	35,50,75					211,126,54
Lab BMI/Graphite	L	35,50,75		105,120,140	130,145,170	105,110,125	
Glass/Vinylester	M	25,75,100	377,498,557	290,240,330		180,220,—	281,22,11
Graphite/Epoxy	M	25,75,100	0,197,241	0,160,160		0,90,—	NI,53,28
Graphite/BMI	M	25,75,100	0,172,168	0,110,130		0,130,130	NI,66,37
Graphite/Phenolic	M	25,75,100	0,159,—	0,80,—		0,80,—	NI,79,—

Designation	Furnace	Reference
A	Cone - H	Babrauskas, V. and Parker, W.J., "Ignitability Measurements with the Cone Calorimeter," Fire and Materials, Vol. 11, 1987, pp. 31-43.
B	Cone - V	
C	Cone - V	Babrauskas, V., "Comparative Rates of Heat Release from Five Different Types of Test Apparatuses," Journal of Fire Sciences, Vol. 4, March/April 1986, pp. 148-159.
D	Cone - H	
E	FMRC - H	
F	Flame Height - V	
G	OSU/02 - V	
H	OSU - V (a)	
I	OSU - V (b)	
J	OSU - V	Smith, E.E., "Transit Vehicle Material Specification Using Release Rate Tests for Flammability and Smoke,"Report No. IH-5-76-1, American Public Transit Association, Washington, DC, Oct. 1976.
K	Cone	Brown, J . E ., "Combustion Characteristics of Fiber Reinforced Resin Panels," Report No. FR3970, U.S.Department of Commerce, N.B.S., April 1987.
L	Cone	Brown, J . E ., Braun, E. and Twilley, W.H., "Cone Calorimeter Evaluation of the Flammability of Composite Materials," US Department of the Navy, NAVSEA 05R25,Washington, DC, Feb. 1988.
M	Cone	Sorathia, U., "Survey of Resin Matrices for Integrated Deckhouse Technology," DTRC SME-88-52, David Taylor Research Center, August 1988.

H = horizontal

V = vertical

NI = not ignited

(a) = initial test procedure

(b) = revised test procedure

Intermediate Scale Tests

Intermediate scale tests help span the gap between the uncertainties associated with small scale tests and the cost of full scale testing. Tests used by the U.S. Navy and the U.S. Coast Guard are described in the following.

DTRC Burn Through Test

This test determines the time required to burn through materials subjected to 2000°F under a controlled laboratory fire condition. This is a temperature that may result from fluid hydrocarbon fueled fires and can simulate the ability of a material to contain such a fire to a compartment. Figure 6-21 shows the arrangement of specimen and flame source for this test. (2) 24" x 24" samples are needed for this test. Burn through times for selected materials is presented in Table 6-5.
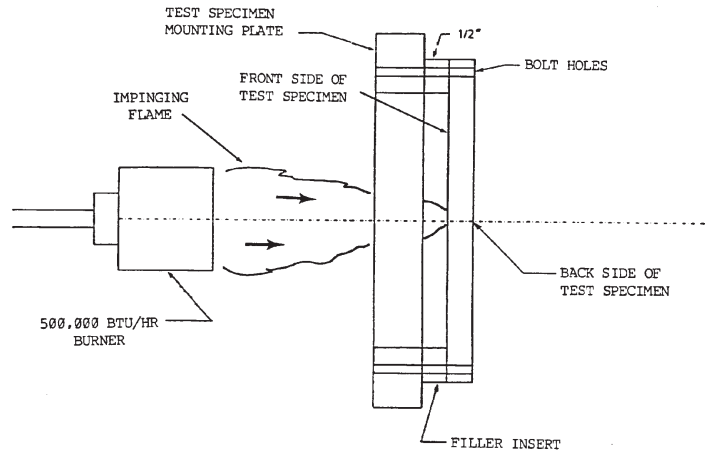
Figure 6-21 Sketch of the DTRC Burn Through Sample and Holder [Rollhauser, *Fire Tests of Joiner Bulkhead Panels*]

**Table 6-5 DTRC Burn-through Times for Selected Materials
[Rollhauser, *Fire Tests of Joiner Bulkhead Panels*]**

Sample	Burn Through Time	Maximum Temperatures, °F, at Locations on Panel, as Indicated at Right			
	Min:Sec	T3	T4	T5	T6
Plywood 1	5:00	300	425	150	125
	4:45	1150	1000	200	1100
Plywood 2	2:40	900	1000	200	200
	2:45	350	100	100	100
Polyester Composite	26:00	not recorded			
	30:00				
Phenolic Composite	>60:00				
Aluminum, ¼"	2:35	450	2000	600	100
	2:05	525	2000	600	200

ASTM E 1317-90, Standard Test Method for Flammability of Marine Finishes

A description and background contained in the test standard provide insight as to why this test may be appropriate for intermediate-scale evaluation of shipboard composite material systems. The test method describes a procedure for measuring fire properties associated with flammable surfaces finishes used on noncombustible substrates aboard ships. The International Safety of Life at Sea (SOLAS) Convention requires the use of marine finishes of limited flame spread characteristics in commercial vessel construction.

Figure 6-22 shows the overall LIFT apparatus geometry, including test specimen and radiant heater. Figure 6-23 shows an E-glass/vinyl ester panel during a test

The increased understanding of the behavior of unwanted fires has made it clear that flame spread alone does not adequately characterize fire behavior. It is also important to have other information, including ease of ignition and measured heat release during a fire exposure. The International Maritime Organization (IMO) has adopted a test method, known as IMO Resolution A.564(14), which is essentially the same as the ASTM test method [66].

The test equipment covered by this test method was initially developed for the IMO to meet the need for defining low flame spread requirements called for by the Safety of Life at Sea (SOLAS) Convention. The need was emphasized when the IMO decided that noncombustible bulkhead construction would be required for all passenger vessels. These bulkheads were usually faced with decorative veneers.
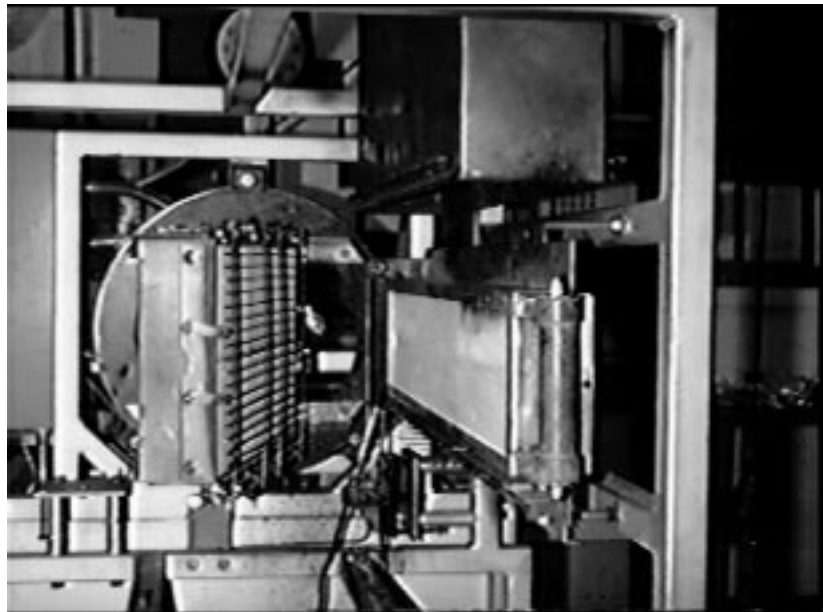
Figure 6-22   LIFT Apparatus Geometry
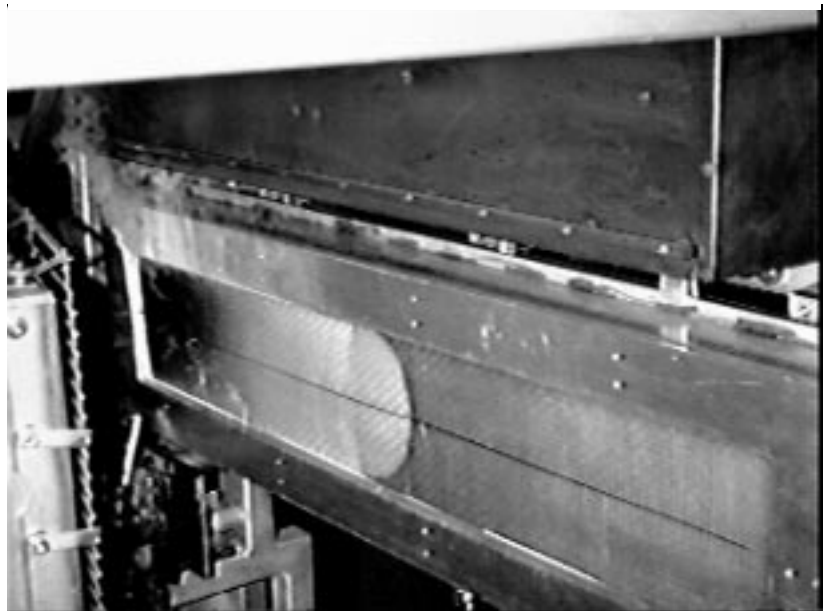
Figure 6-23   LIFT Test Panel at the Time of Ignition

Some of the decorative veneers used on these bulkheads had proved highly flammable during fires. Various national flammability test methods were considered. Development of an International Standards Organization (ISO) test method was considered. Since it became apparent that development of a suitable test by ISO/TC92 would require more time than IMO had envisioned, IMO decided during 1976-1977 to accept an offer from the United States delegation to develop a suitable prototype test. Initial work on the test method was jointly sponsored by the National Institute of Standards and Technology (NIST), then the National Bureau of Standards (NBS), and the United States Coast Guard.

The data presented for several marine "coverings" in Figure 6-24 shows flux at "flame front" as a function "flame arrival time." The dotted lines represent "heat for sustained burning." In general, materials of higher heat of sustained burning and especially those also accompanied with higher critical flux at extinguishment are significantly safer materials with respect to flame spread behavior than the others shown. [66]
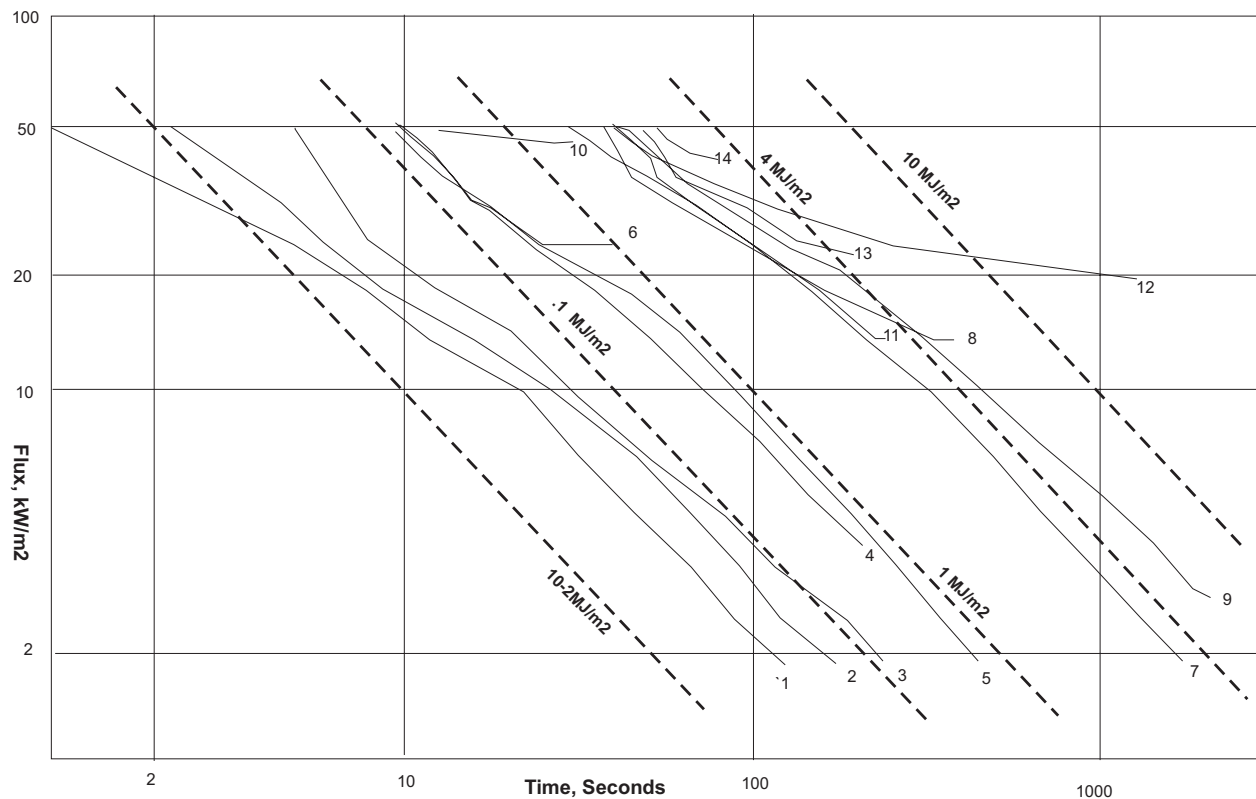
Figure 6-24 ASTM E1317 Flame Front Flux versus Time for:

1	GM 21, PU Foam, PC	2	GM 21, F.R. PU Foam, PCF
3	FAA Foam 0.95 kg/m2	4	Acrylic Carpet 2.7 kg/m2
5	Fiberboard, unfinished 3.3 kg/m2	6	Wool Carpet 2.4 kg/m2
7	Hardboard, unfinished 3.3 kg/m2	8	Fiberboard, F.R. Paint 3.6 kg/m2
9	Fiberboard, unfinished 5.7 kg/ms	10	Marine Veneer, Sweden
11	Gypsum Board, unfinished	12	Hardboard F.R. Paint 8.5 kg/m2
13	Marine Veneer, Sweden	14	Gypsum Board F.R. Paint
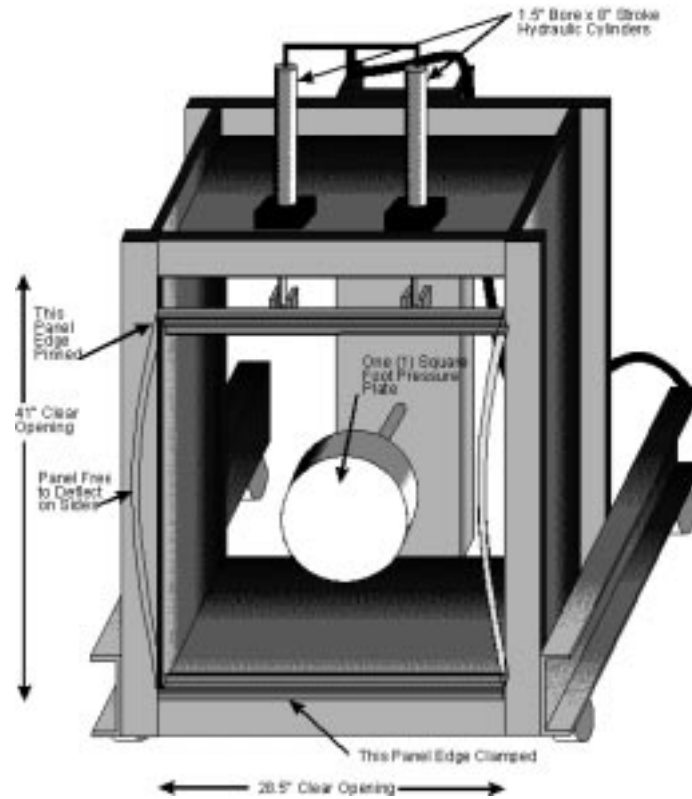
Figure 6-25   Geometry of E 119 Multiplane Load Jig
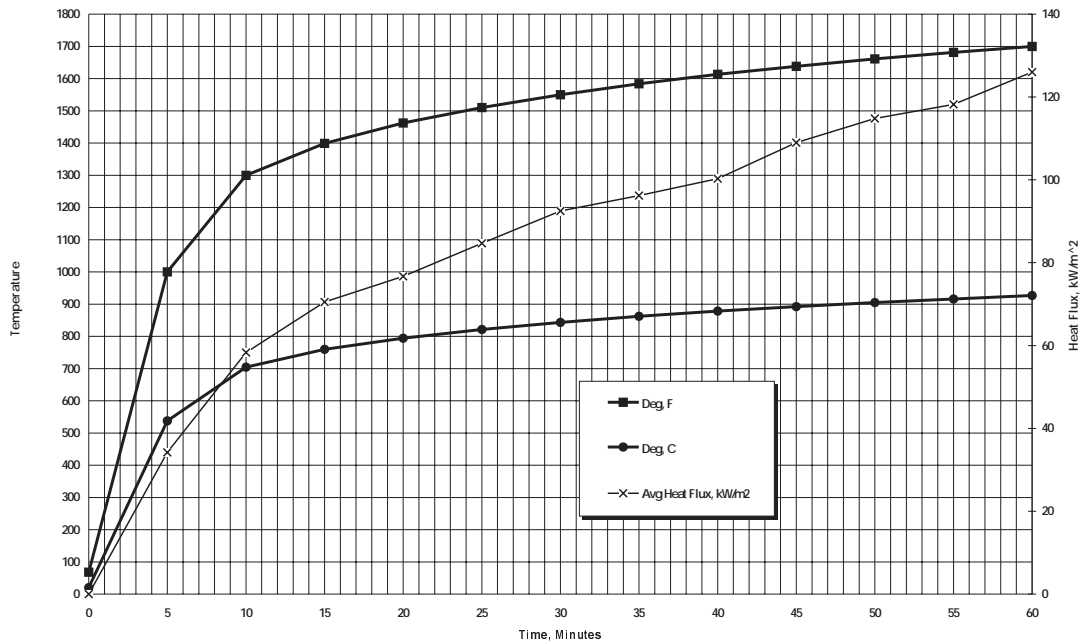
Figure 6-26   Heat Flux from 3-foot Furnace at VTEC using the E 119 (SOLAS) Time/Temperature Curve

The objectives in developing this test method were as follows:

- To provide a test method for selection of materials of limited flammability, and

- To provide a test method capable of measuring a number of material fire properties in as specified a fashion as possible with a single specimen exposure.

It was recognized that there may be several different ways in which these measurements could be utilized. It was suggested that IMO should use the test as a go/no go measuring tool for surface finish materials to limit the severity of their participation in a fire. The fire research community is interested in variable irradiance ignition measurements, coupled with flame spread measurements to derive more basic fire thermal properties of the materials studied. The National Institute of Standards and Technology (NIST) is continuing its research on the correlation of LIFT results with full-scale testing of composite materials under a cooperative research agreement with Structural Composites.

U.S. Navy Quarter Scale Room Fire Test
This test determines the flashover potential of materials in a room when subjected to fire exposure. The test reduces the cost and time associated with full scale testing. A 10' x 10' x 8' room with a 30" x 80" doorway is modeled. (1) 36" x 36" and (3) 36" x 30" samples are required.

3-Foot E 119 Test with Multiplane Load
In the U.S., ASTM E 119 is the generally accepted standard method for evaluating and rating the fire resistance of structural-type building fire barriers. The method involves furnace-fire exposure of a portion of a full-scale fire barrier specimen. The furnace-fire environment follows a monotonically-increasing, temperature-time history, which is specified in the test method document as the standard ASTM E119 fire. The test method specifies explicit acceptance criteria that involve the measured response of the barrier test specimen at the time into the standard fire exposure, referred to as the fire resistance of the barrier design, that corresponds to the desired barrier rating. For example, a barrier design is said to have a three-hour fire-resistance rating if the tested specimen meets specified acceptance criteria during at least three hours of a standard fire exposure. The fire-resistance rating, in turn, qualifies the barrier design for certain uses. Here the term "qualifies" is intended to mean that the barrier design meets or exceeds the fire-resistance requirements of a building code or other regulation.

U.S. Coast Guard regulations for fire protection and the International Conventions for Safety of Life at Sea 1948, 1960 and 1974, require that the basic structure of most vessels be of steel or "material equivalent to steel at the end of the applicable fire exposure." The ASTM E119 fire curve is used as the applicable fire exposure for rating SOLAS decks and bulkheads. These provisions place the burden of proving equivalency on designers who use noncombustible materials other than steel, where structural fire provisions apply. The 1974 SNAME T&R Bulletin 2-21 [67] provides Aluminum Fire Protection Guidelines to achieve these goals for aluminum.

Figure 6-25 shows the geometry of the multiplane load jig developed by Structural Composites used with the E 119 time/temperature curve. A heat flux map of the 3-foot furnace used for E 119 type testing at VTEC is presented in Figure 6-26. Results from an extensive SBIR research project that utilized the multiplane load jig are presented at the end of this Fire Testing section.

Large Scale Tests

These tests are designed to be the most realistic simulation of a shipboard fire scenario. Tests are generally not standardized, instead designed to compare several material systems for a specific application. The goal of these tests is to model materials, geometry and the fire threat associated with a specific compartment.

Corner Tests

Corner tests are used to observe flame spread, structural response and fire extinguishment of the tested materials. The test was developed to test joiner systems. The geometry of the inside corner creates what might be a worst case scenario where the draft from each wall converges. 7-foot high by 4-foot wide panels are joined with whatever connecting system is part of the joinery. Approximately two gallons of hexane fuel is used as the source fire burning in a 1-foot by 1-foot pan [65].

Room Tests

This type of test is obviously the most costly and time consuming procedure. Approximately 98 square feet of material is required to construct an 8-foot by 6-foot room. Parameters measured include: temperature evolution, smoke emission, structural response, flame spread and heat penetration through walls. Instrumentation includes: thermocouples and temperatures recorders, thermal imaging video cameras and regular video cameras [65].

Summary of MIL-STD-2031 (SH) Requirements

The requirements of MIL-STD-2031 (SH), "Fire and Toxicity Test Methods and Qualification Procedure for Composite Material Systems used in Hull, Machinery, and Structural Applications inside Naval Submarines" [65] are summarized here. The foreword of the Standard states:

> "The purpose of this standard is to establish the fire and toxicity test methods, requirements and the qualification procedure for composite material systems to allow their use in hull, machinery, and structural applications inside naval submarines. This standard is needed to evaluate composite material systems not previously used for these applications."

Table 6-6 summarizes the requirements outlined in the new military standard. It should be noted that to date, no polymer-based systems have been shown to meet all the criteria of MIL-STD-2031 (SH).

Table 6-6 General Requirements of MIL-STD-2031 (SH), *Fire and Toxicity Test Methods and Qualification Procedure for Composite Material Systems Used in Hull, Machinery and Structural Applications Inside Naval Submarines*

Fire Test/Characteristic		Requirement		Test Method
Oxygen-Temperature Index (%)	The minimum concentration of oxygen in a flowing oxygen nitrogen mixture capable of supporting flaming combustion of a material.	**Minimum** % oxygen @ 25°C % oxygen @ 75°C % oxygen @ 300°C	35 30 21	ASTM D 2863 (modified)
Flame Spread Index	A number or classification indicating a comparative measure derived from observations made during the progress of the boundary of a zone of flame under defined test conditions.	**Maximum** 20		ASTM E 162
Ignitability (seconds)	The ease of ignition, as measured by the time to ignite in seconds, at a specified heat flux with a pilot flame.	**Minimum** 100 kW/m^2 Flux 75 kW/m^2 Flux 50 kW/m^2 Flux 25 kW/m^2 Flux	60 90 150 300	ASTM E 1354
Heat Release Rate (kW/m2)	Heat produced by a material, expressed per unit of exposed area, per unit of time.	**Maximum** **100 kW/m^2 Flux** Peak Average 300 secs **75 kW/m^2 Flux** Peak Average 300 secs **50 kW/m^2 Flux** Peak Average 300 secs **25 kW/m^2 Flux** Peak Average 300 secs	 150 120 100 100 65 50 50 50	ASTM E 1354
Smoke Obscuration	Reduction of light transmission by smoke as measured by light attenuation.	**Maximum** D_s during 300 secs D_{max} occurrence	100 240 secs	ASTM E 662

Fire Test/Characteristic		Requirement	Test Method
Combustion Gas Generation	Rate of production of combustion gases (e.g. CO, CO_2, HCl, HCN, NO_x, SO_x, halogen, acid gases and total hydrocarbons.	25 kW/m^2 Flux **Maximum** CO 200 ppm CO_2 4% (vol) HCN 30 ppm HCL 100 ppm	ASTM E 1354
Burn Through Fire Test	Test method to determine the time for a flame to burn through a composite material system under controlled fire exposure conditions.	No burn through in 30 minutes	DTRC Burn Through Fire Test
Quarter Scale Fire Test	Test method to determine the flashover potential of materials in a room when subjected to a fire exposure.	No flashover in 10 minutes	Navy Procedure
Large Scale Open Environment Test	Method to test materials at full size of their intended application under controlled fire exposure to determine fire tolerance of ease of extinguishment.	Pass	Navy Procedure
Large Scale Pressurable Fire Test	Method to test materials using an enclosed compartment in a simulated environment under a controlled fire exposure.	Pass	Navy Procedure
N-Gas Model Toxicity Screening	Test method to determine the potential toxic effects of combustion products (smoke and fire gases) using laboratory rats.	Pass	Navy Procedure

Review of SOLAS Requirements for Structural Materials in Fires

SOLAS is the standard that all passenger ships built or converted after 1984 must meet. Chapter II-2 *Fire Protection, Fire Detection and Fire Extinction* defines minimum fire standards for the industry. SOLAS divides ships into three class divisions and requires different levels of fire protection, detection and extinction. Each class division is measured against a standard fire test. This test is one in which specimens of the relevant bulkheads or decks are exposed in a fire test furnace to temperatures corresponding approximately to the *Standard Time-Temperature Curve* of ASTM E119, which is shown in Figure 6-27 along with other standards. The standard time-temperature curve for SOLAS is developed by a smooth curve drawn through the following temperature points measured above the initial furnace temperature:

- at the end of the first 5 minutes 556°C (1032°F)
- at the end of the first 10 minutes 659°C (1218°F)
- at the end of the first 15 minutes 718°C (1324°F)
- at the end of the first 30 minutes 821°C (1509°F)
- at the end of the first 60 minutes 925°C (1697°F)
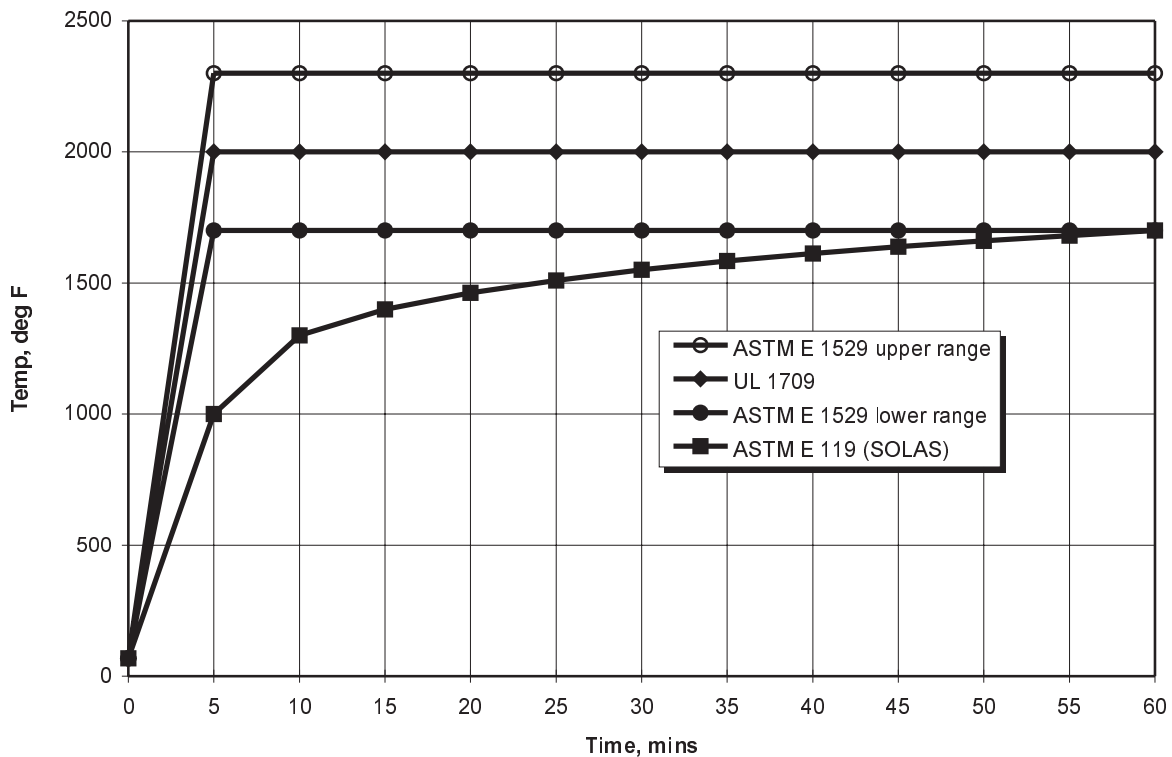
Figure 6-27 Comparison of Three Fire Tests [Rollhauser, *Integrated Technology Deckhouse*]

Noncombustible materials are identified for use in construction and insulation of all SOLAS class divisions. Noncombustible material is a material which neither burns nor gives off flammable vapors in sufficient quantity for self-ignition when heated to approximately 750°C (1382°F), this being determined to the satisfaction of the administration (IMO or USCG) by an established test procedure. Any other material is a combustible material.

Class divisions are A, B, and C. "A" class divisions are bulkheads and decks which:

> a. shall be constructed of steel or other equivalent material;
>
> b. shall be suitably stiffened;
>
> c. shall be so constructed as to be capable of preventing the passage of smoke and flame to the end of the one-hour standard fire test;
>
> d. shall be insulated with approved noncombustible materials such that the average temperature of the unexposed side will not rise more than 139°C (282°F) above the original temperature, nor will the temperature, at any one point, including any joint, rise more than 180°C (356°F) above the original temperature, within the time listed below:
>
> - Class "A-60" 60 minutes
> - Class "A-30" 30 minutes
> - Class "A-15" 15 minutes
> - Class "A-0" 0 minutes

"B" class divisions are those divisions formed by bulkheads, decks, ceilings or linings and:

> a. shall be constructed as to be capable of preventing the passage of smoke and flame to the end of the first half hour standard fire tests;
>
> b. shall have an insulation value such that the average temperature of the unexposed side will not rise more than 130°C (282°F) above the original temperature, nor will the temperature at any point, including any joint, rise more than 225°C (437°F) above the original temperature, within the time listed below:
>
> - Class "B-15" 15 minutes
> - Class "B-0" 0 minutes
>
> c. they shall be constructed of approved noncombustible materials and all materials entering into the construction and erection of "B" class divisions shall be noncombustible, with the exception that combustible veneers may be permitted provided they meet flammability requirements (ASTM E-1317).

"C" divisions shall be constructed of noncombustible material

Naval Surface Ship Fire Threat Scenarios

The fire threat on surface ships may be self inflicted during peacetime operations or can be the result of enemy action. The later case is generally much more severe, although the database on recent Navy experience deals almost exclusively with events in the former category. Some fire source data suitable for comparing surface ships to submarines is presented in Table 6-7. For both types of combatants, about two-thirds of all fires occur in port or at a shipyard during overhaul.

Table 6-7 Fire Source Data for Naval Combatants

FIRE SOURCE	Surface Ships[1] 1983 - 1987		Submarines[2] 1980 - 1985	
	Number	**Percent**	**Number**	**Percent**
Electrical	285	39%	100	61%
Open Flame/Welding	141	19%	23	14%
Flammable Liquid/Gas	0	0%	13	8%
Radiant Heat	102	14%	8	5%
Matches/Smoking	40	5%	1	1%
Explosion	7	1%	1	1%
Other	89	12%	0	0%
Unknown	68	9%	18	11%
TOTAL:	732	100%	164	100%

[1] Navy Safety Center Database, Report 5102.2
[2] NAVSEA Contract N00024-25-C-2128, "Fire Protection Study," Newport News Shipbuilding

Fires onboard surface ships are usually classified by the severity of a time/temperature profile. Fire scientists like to quantify the size of a fire in terms of flux rate (kW/m^2). The following is a rough relationship between fire type and size:

- Small smoldering fire: 2 - 10 kW/m^2
- Trash can fire: 10 - 50 kW/m^2
- Room fire: 50 - 100 kW/m^2
- Post-flashover fire: > 100 kW/m^2

A post-flashover fire would represent an event such as the incident on the *USS STARK*, where Exocet missile fuel ignited in the space.

From the non-combat data presented in Table 6-7, it should be noted that 90% of the reported fires were contained to the general area in which they were started. 75% of the fires were extinguished in under 30 minutes. Most fires occurred in engineering spaces.

Table 6-8 Relative Merit of Candidate Resin Systems for Elevated Temperatures

Resin System		Properties	Price Range $/lb	Room Temp Strength	High Temp Strength	Rate of Heat Release	Smoke & Toxicity
Thermosets	Polyester	Polyester resins are the most common resins used in the marine industry because of their low cost and ease of manufacture. Isophthalic polyesters have better mechanical properties and show better chemical and moisture resistance than ortho polyester	.66 - .95	1	1	1	2
	Epoxy	Excellent mechanical properties, dimensional stability and chemical resistance (especially to alkalis): low water absorption; self-extinguishing (when halogenated); low shrinkage; good abrasion resistance; very good adhesion properties	2.00 - 10.00	3	1	1	1
	Vinyl Ester	Good mechanical, electrical and chemical resistance properties; excellent moisture resistance; intermediate shrinkage	1.30 - 1.75	2	1	1	1
	Phenolic	Good acid resistance; good electrical properties (except arc resistance); high heat resistance	.60 - 5.00	1	3	2	2
	Bismaleimides	Intermediate in temperature capability between epoxy and polyimide; possible void-free parts (no reaction by-product); brittle	10.00 - 25.00	1	3	2	2
	Polyimides	Resistant to elevated temperatures; brittle; high glass transition temperature; difficult to process	22.00	3	3	2	2
Thermoplastics	Polyether Ether Ketone (PEEK)	Good hot/wet resistance, impact resistant; rapid, automated processing possible	21.50 - 28.00	2	2	2	2
	Poly Phenylene Sulfide (PPS)	Good flame resistance and dimensional stability; rapid, automated processing possible	2.00 - 6.00	1	2	3	3
	Poly Ether Sulfone (PES)	Easy processability; good chemical resistance; good hydrolytic properties	4.40 - 7.00	2	1	3	3
	Poly Aryl Sulfone (PAS)	High mechanical properties; good heat resistance; long term thermal stability; good ductility and toughness	3.55 - 4.25	2	2	3	2

Legend

1   poor

2   moderate

3   good

International Maritime Organization (IMO) Tests

IMO Resolution MSC 40(64) outlines the standard for qualifying marine materials for high speed craft as fire-restricting. This applies to all hull, superstructure, structural bulkheads, decks, deckhouses and pillars. Areas of major and moderate fire hazard must also comply with a SOLAS-type furnace test (MSC.45(65)) with loads.

IMO Resolution MSC 40(64) on ISO 9705 Test

Tests should be performed according to the standard ISO 9705, the Room/Corner Test. This standard gives alternatives for choice of ignition source and sampling mounting technique. For the purpose of testing products to be qualified as "fire restricting materials" under the IMO High-Speed Craft Code, the following should apply:

- Ignition source: Standard ignition source according to Annex A in ISO 9705, i.e. 100 kW heat output for 10 minutes and thereafter 300 kW heat output for another 10 min. Total testing time is 20 minutes; and

- Specimen mounting: Standard specimen mounting, i.e. the product is mounted both on walls and ceiling of the test room. The product should be tested complying to end use conditions.

Calculation of the Parameters Called for in the Criteria

The maximum value of smoke production rate at the start and end of the test should be calculated as follows: For the first 30 seconds of testing, use values prior to ignition of the ignition source, i.e., zero rate of smoke production, when calculating average. For the last 30 seconds of testing use the measured value at 20 minutes, assign that to another 30 seconds up to 20 minutes and 30 seconds and calculate the average. The maximum heat release rate (HRR) should be calculated at the start and the end of the test using the same principle as for averaging the smoke production rate. The time averages of smoke production rate and HRR should be calculated using actual measured values that are not already averaged, as described above.

Criteria for Qualifying Products as "Fire Restricting Materials"

- The time average of HRR excluding the ignition source does not exceed 100 kW;

- The maximum HRR excluding the HRR from the ignition source does not exceed 500 kW averaged over any 30 second period of the test;

- The time average of the smoke production rate does not exceed 1.4 m^2/s;

- The maximum value of smoke production rate does not exceed 8.3m^2/s averaged over any period of 60 seconds during the test;

- Flame spread must not reach any further down the walls of the test room than 0.5 m from the floor excluding the area which is within 1.2 meter from the corner where the ignition source is located; and

- No flaming drops or debris of the test sample may reach the floor of the test room outside the area which is within 1.2 meter from the corner where the ignition source is located

Front View

Top View
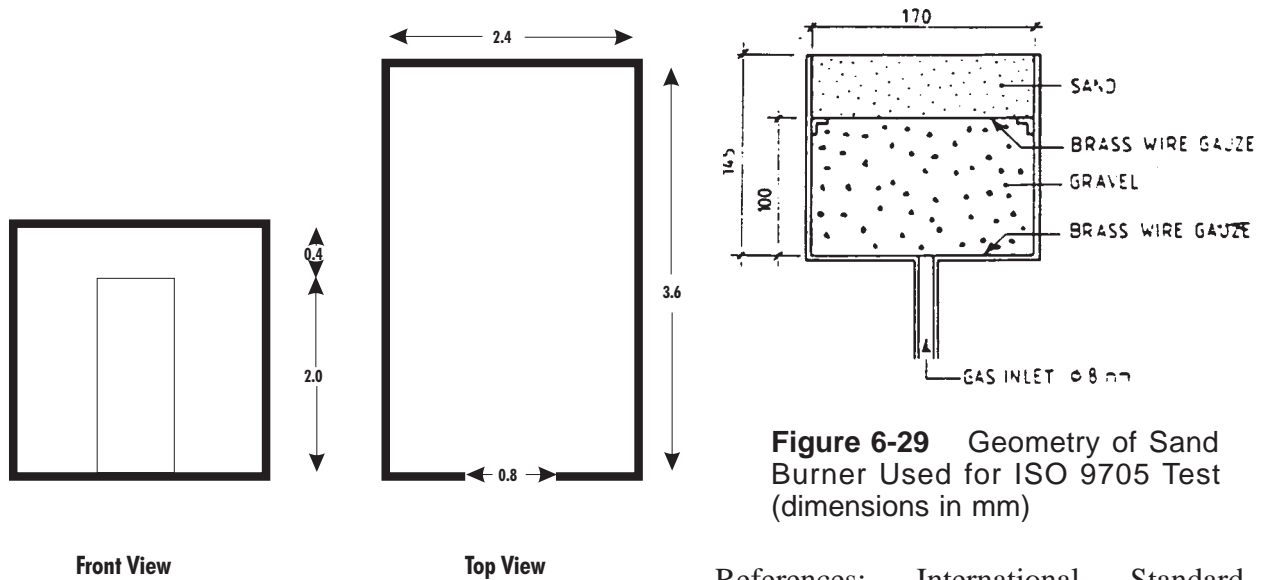
Figure 6-28   Fire Test Room Dimensions (in Meters) for ISO 9705 Test
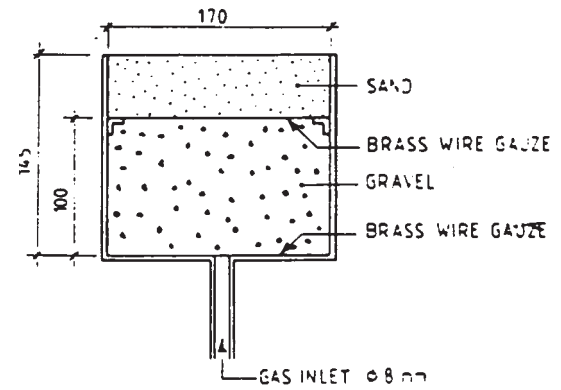
Figure 6-29   Geometry of Sand Burner Used for ISO 9705 Test (dimensions in mm)

References: International Standard ISO/DIS 9705, *Fire Tests - Full Scale Room Test for Surface Products*, available from ANSI, 11 West 42nd Street, New York, NY 10036.

Required Test Panels:

(1) 4' x 4'
(2) 2' x 8'
(4) 1' x 4'

170mm x 170mm sand burner run @ 100kW & 300kW
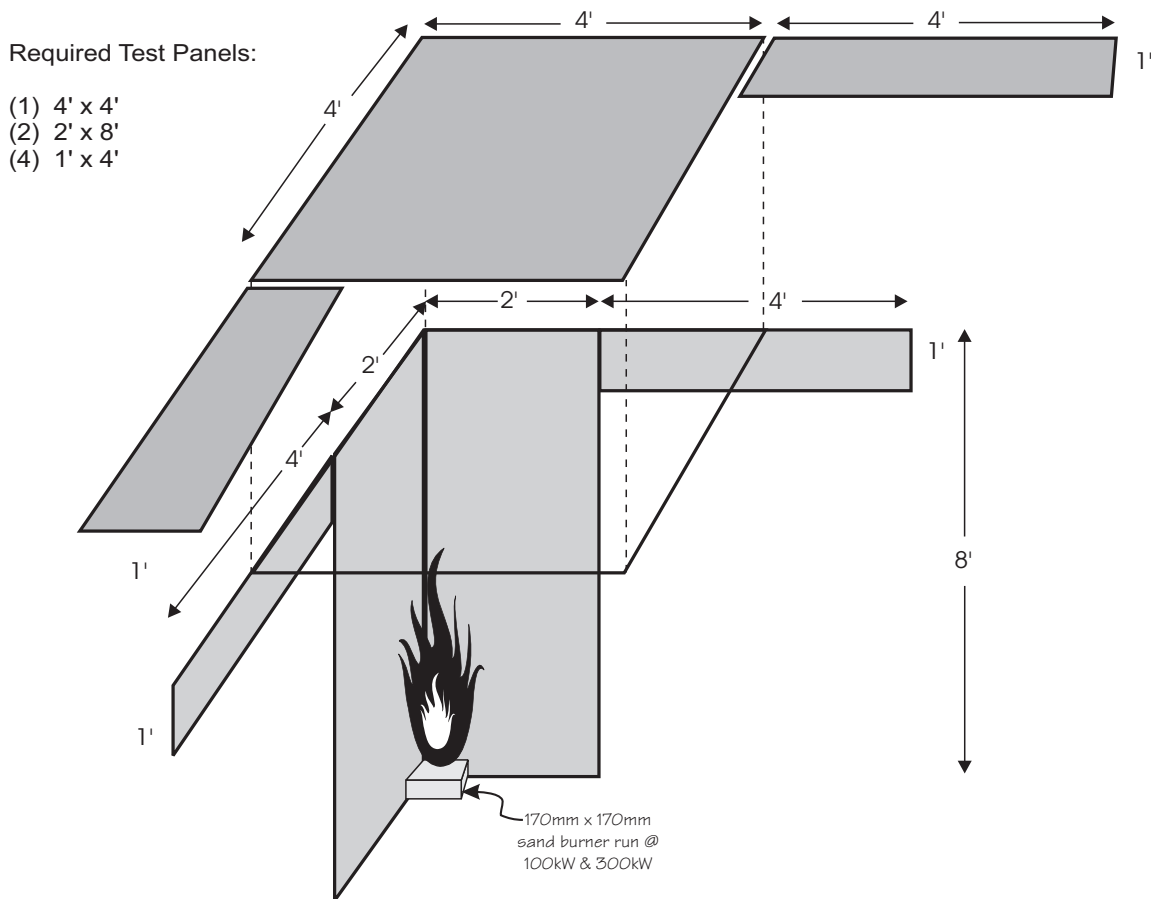
Figure 6-30   Coverage for Modified ISO 9705 Test Using (2) 4' x 8' Sheets of Material

Figure 6-31 ISO 9705-Type Test with Reduced Material Quantities at VTEC Laboratories

Thermo-Mechanical Performance of Marine Composite Materials

The main testing undertaken under a Navy-sponsored SBIR Program [68] involved the thermo-mechanical characterization of panels made from typical composite materials used in advanced marine construction. The following describes how the test procedure evolved and what types of panels were tested to verify the methodology.

Fire Insult

The time/temperature curve prescribed by ASTM E119 was adopted for the test. This fire insult is used widely throughout the building industry, and therefore much data on building material performance exists. This fire curve is also recognized by the SOLAS Convention and the U.S. Coast Guard (Title 46, Subpart 164.009) and is representative of most Class A fire scenarios. Under consideration by the Navy for Class B fires is the proposed UL 1709 and ASTM P 191 fire curves, which reach a higher temperature faster. This would be more representative of a severe hydrocarbon pool-fed fire. Data for one hour of all three of these fire curves are presented in Figure 6-26.

Mechanical Loading

The objective of the thermo-mechanical test program was to evaluate a generic marine structure with realistic live loads during a shipboard fire scenario. A panel structure was chosen, as this could represent decking, bulkheads or hull plating. Loads on marine structures are unique in that there are usually considerable out-of-plane forces that must be evaluated. These forces may be the result of hydrostatic loads or live deck loads, from equipment or crew. In-plane failure modes are almost always from compressive forces, rather than tensile.

Given the above discussion, a multi-plane load jig, shown in Figure 6-25, was conceived. This test jig permits simultaneous application of compressive and flexural forces on the test panel during exposure to fire. The normal load is applied with a circular impactor, measuring one square foot. This arrangement is a compromise between a point load and a uniform pressure load. A constant load is maintained on the panel throughout the test, which produces a situation analogous to live loads on a ship during a fire. Failure is determined to be when the panel can no longer resist the load applied to it.

The load applied during the tests was determined by a combination of calculations and trial-and-error in the test jig. Panels 1 through 7 (except 3) were used to experimentally determine appropriate applied pressures in-plane and out-of-plane. The goal of the test program was to bring the laminate to a point near first ply failure under static conditions. This required loads that were approximately four times a value accepted as a design limit for this type of structure in marine use.

Early screening test showed that the normal deflection of a panel under combined load followed somewhat predictions of a simple two-dimensional beam. For a beam with fixed ends, deflection is:

$$y = \frac{P\,l^3}{192\,E\,I} \qquad\qquad (6\text{-}28)$$

For a beam with pinned ends, deflection is:

$$y = \frac{P\,l^3}{48\,E\,I}$$

(6-29)

where:

y = displacement, inches
P = load, pounds
l = panel span (36 inches)
E = Stiffness, pounds/in^2
I = moment of inertia, in^4

For the test jig with the bottom fixed and the top pinned, the following expression approximates the response of the sandwich panels tested:

$$y = \frac{P\,l^3}{62\,E\,I}$$

(6-30)

The above expression is used to back out a value for stiffness, *EI*, of the panels during the test that is based on the displacement of the panel at the location that the normal load is applied.

By having one end of the panel pinned in the test fixture, the test laminate effectively models a marine panel structure with a 72" span and fixed ends. If this panel were to be used for the side structure of a deckhouse, the allowable design head under the American Bureau of Shipping Rules for FRP Vessels is about 5 feet.

Finally, the applied compressive load of 6000 pounds works out to be just over 2500 pounds per linear foot. The normal load of 1000 pounds equates to just under 150 pounds per square foot. The full-scale E 119 tests done for the Navy at Southwest Research Institute in September, 1991 [68] in support of the Integrated Technology Deckhouse program used compressive loads of 3500 pounds per linear foot and a normal force of 175 pounds per square foot. IMO Resolution MSC.45(65), which establishes test procedures for "fire-resisting" division of high speed craft, calls for 480 pounds per linear foot compressive load on bulkheads and 73 lbs/ft^3 normal load on decks.

Test Panel Selection Criteria

The key parameter that was varied for the test program was panel geometry, rather than resin or insulation. The objective for doing this was to validate the test method for as many different types of composite panel structures.

Most of the test panels were of sandwich construction, as this represents the most efficient way to build composite marine vehicles and will be more common than solid laminates for future newbuildings. Each geometry variation was tested in pairs using both a PVC and balsa core material. These materials behave very differently under static, dynamic and high temperature conditions, and therefore deserve study. The following panels were tested:

- Panels 1 and 2 were tested with no load to obtain initial thermocouple data.

- Panel 3 was a bare steel plate that was tested in the middle of the program to serve as a baseline for comparison.

- Panels 4 and 5 were tested with only out-of-plane loads to determine test panel response. Similarly, panels 6 and 7 were used to test in-plane loads only.

- Panels 8 and 9 represented the first test of combined loading at the established test levels.

- Panels 10 and 11 utilized a double core concept to create a "club sandwich" structure. This fire hardened concept, also proposed by Ron Purcell of NSWC, Carderock and Ingalls Shipbuilding, assumes that the inner skin will survive the fire insult to create a sandwich structure with a reduced, but adequate, I (the test jig was modified to accommodate panels using this concept that are up to 4" thick and require higher normal loads for testing).

- Panels 12 and 13 used woven reinforcements instead of knits.

- Panel 14 had a staggered stiffener geometry, which has been shown to reduce the transmission of mechanical vibrations. This concept was test to determine if the heat transfer path would also be retarded. This panel was also the only one tested with an air gap as an insulator.

- Panel 15 was made with a very dry last layer of E-glass and a single layer of insulation.

- Panels 16 and 17 were made from 1/2" cores with hat-stiffeners applied. These tests were performed to determine if secondary bonds would be particularly susceptible to elevated temperature exposure.

- Panels 18 and 19 had carbon fiber reinforcement in their skins.

- Panels 20 and 21 were made with flame retardant modifiers in the resin system, 5% Nyacol and 25% ATH, respectively. These tests were performed to determine the effect these additives had on elevated temperature mechanical performance.

- Panel 22 used a higher density PVC core.

- Panel 23 used the "ball" shaped loading device.

- Panel 24 was a PVC-cored sandwich panel with aluminum skins, with insulation. Panel 25 was the same as 24, without any insulation.

- Panels 26 and 27 were solid laminates, using vinyl ester and iso polyester resins, respectively.

- Panels 28 and 29 were tested with the "line" loading device.

- Panel 30 was a balsa-cored sandwich panel with aluminum skins.

Test Results

The general arrangement for panels tested with insulation is shown in Figure 6-32. The thermo-mechanical test data for panels evaluated under this program is presented in plots similar to Figure 6-33.
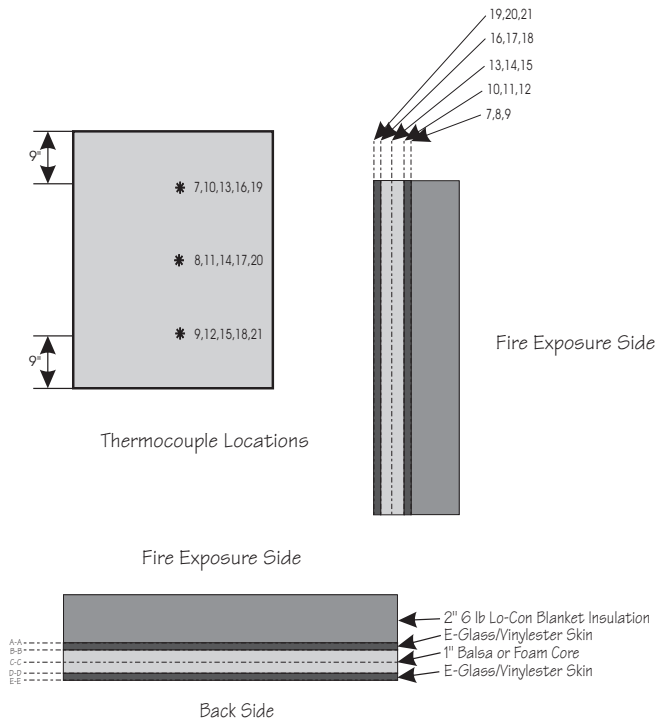
Thermocouple Locations

Fire Exposure Side

Back Side

Figure 6-32 General Arrangement for 3-foot Panels Tested under E-119 Insult with Insulation

Balsa versus PVC Core

As a general rule, the sandwich laminates with balsa cores would endure the full 60 minutes of the E 119 test. Stiffness reduction was only to about 50% of the original stiffness. As the panels were loaded to first ply failure before the furnace was started, a residual safety factor of about two was realized with these structures. By contrast, the PVC cores behaved as a thermoplastic material is expected to and gradually lost stiffness after a period of time. This usually occurred after about 40 minutes. Stiffness reduction was normally to 25%, which still left a safety factor of one just before failure.
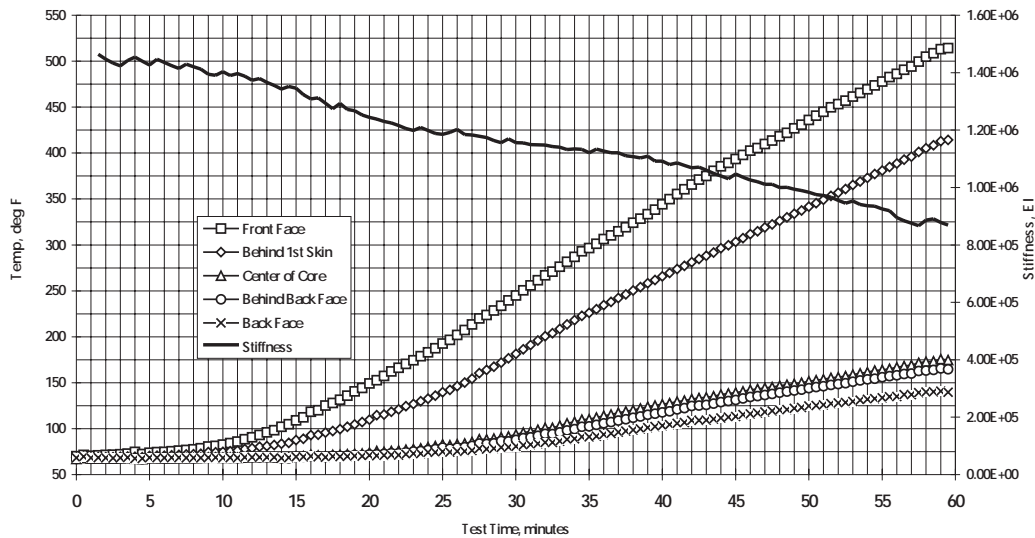
Figure 6-33 Stiffness and Temperature Data for Balsa-Cored E-Glass/Vinyl Ester Panel with 2″ Lo-Con Ceramic Insulation Tested with Multiplane Load Jig and E-119 Fire

The consistency shown in test duration and stiffness reduction characteristics for a variety of geometries suggests that the test procedure is a valid method for evaluating how composite material structures would behave during a fire. Although the PVC-cored laminates failed through stiffness reduction sooner than balsa cores, the panels usually did not show signs of skin to core debonding because to cores got soft and compliant. If loads were removed from the PVC panels after the test, the panel would return to its near normal shape. Conversely, if load was maintained after the test, permanent deformation would remain. Data for a balsa-cored panel, which was one of the better performers, is presented in Figure 6-33.

Steel Plate, Unprotected

Steel plates of 1/4" nominal thickness were tested in the load jig without insulation to characterize how this typical shipboard structure would behave during a fire. The initial plate was loaded to 2000 pounds in-plane, which turned out to cause Euler buckling as the stiffness of the steel reduced. The test was repeated with minimal loads of 500 pounds, but the plate still failed after about 18 minutes. It should be noted that the back face temperature exceeded 1000 °F.

Double 1/2" Cores - "Club Sandwich"

Both the PVC and the balsa double core configurations endured the full 60 minute test. The PVC-cored panel saw a stiffness reduction to about 25%, while the balsa only went to 50%. Both panels lost stiffness in a near linear fashion, which suggests that this is a suitable fire-hardening concept.

Woven Roving Reinforcement

The panels made with woven roving E-Glass reinforcement behaved similarly to those made with knit reinforcements. On a per weight basis, the knit reinforcements generally have better mechanical properties.

Staggered Stiffener

The staggered stiffener panel proved to perform very well during the fire tests, albeit at a significant weight penalty. It is interesting to note that temperatures behind the insulation never exceeded 350°F, a full 200° cooler than the other panels. The air gap insulation technique deserves further study.

Dry E-Glass Finish

Thermocouple data has shown that the thermoconductivity of and FRP ply reduces an order of magnitude as the resin becomes pyrolyzed. Going on this theory, a panel was constructed with a heavy last E-Glass ply that was not thoroughly wetted out. This produced a panel with a dry fiberglass finish. Although this did not perform as well, as 1" of ceramic blanket, it did insulate the equivalent of 0.25". This finish also provides a surface that could provide a good mechanical bond for application of a fire protection treatment.

Stiffened Panels

The hat-stiffened panels performed somewhat better than expected, with no delamination visible along the stringer secondary bond. Although temperatures at the top of the hat section got to 650°F, the side wall remained intact, thus providing sufficient stiffness to endure 50 - 55

minutes of testing. The performance difference between the balsa and PVC panels was not so apparent with this configuration.

Carbon Fiber Reinforcement

The addition of carbon fiber reinforcement to the skins did not significantly change the fire performance of the laminate. Overall, the stiffness of the panels increased greatly with the modest addition of carbon fiber. The modulus of the skins was best matched to the structural performance of the balsa core.

Flame Retardants

Flame retardants are generally added to resin systems to delay ignition and/or reduce flame spread rate. Both the formulations tested did not significantly degrade the elevated temperature mechanical performance of the laminates. The ATH performed slightly better than the Nyacol.

High Density PVC Core

Because a consistent thermal degradation of the PVC cores was noted after about 40 minutes, a high density H-130 was tested. This panel unfortunately failed after about the same amount of time due to a skin-to-core debond. This failure mode is often common when the mechanical properties of the core material are high.

Load with Ball Impactor

A spherical ball loading device was used on a PVC-cored panel to see if the test results would be altered with this type of load. The results were essentially the same as with the flat load application device.

Aluminum Skins

PVC-cored panels with aluminum failed slightly sooner than their composite counterparts. The insulated, balsa-cored panel with aluminum skins endured the entire test, with only modest stiffness reduction. The temperature behind the insulation never got above 450°F, which suggests that significant lateral heat transfer along the aluminum face may have been occurring.

Solid Laminates

The solid laminates were able to maintain relatively low front face temperatures due to overall improved through-thickness thermal conduction, as compared to sandwich laminates. The vinyl ester laminate performed better than the ortho polyester.

Line Load Device

A line loading device was used on PVC-cored and balsa-cored panels to see if the test results would be altered with this type of load. The results were essentially the same as with the flat load application device.

Conclusions and Recommendations

Conclusions

Throughout the Guide, an attempt was made to present state-of-the-art data and analysis methods for designing marine composite structures. Some areas of the Guide are based on very recent data, while others rely on research and materials that were developed some time ago. In this section, an assessment of what our current knowledge base is and what research gaps remain will be presented.

The use of composite materials in marine structures requires a thorough understanding of loads, materials and structural mechanics. Composite materials are often referred to as "engineered" materials because the designer has so much control over the mechanical properties of a structure. Material selection, orientation and fabrication process are all crucial in determining laminate performance.

Composite materials were first used in the marine industry because of the potential for reduced maintenance costs and the ability to mold many copies of a complex shape. As materials, processes and sandwich laminates evolved, it was understood that high speed craft could be made lighter and faster through the exploitation of composite materials. Slamming loads have emerged as the dominate design force for many applications. The reader is advised to consult with the appropriate classification society for the latest design methodology on high speed craft. The following is a partial list of classification society publications:

Publication	Version	Organization	Address
Guide for Building and Classing High-Speed Craft	October 1990 October 1996 DRAFT	American Bureau of Shipping	Two World Trade Center, 106th Flr, New York, NY 10048
Rules for Classification of High Speed and Light Craft	Part 2 Chp 4 FRP Jan 91 Part 3 Chp 1 Load Jul 96	Det Norske Veritas	70 Grand Ave., River Edge, NJ 07661
Rules and Regulations for the Classification of Special Service Craft	January 1996	Lloyd's Register of Shipping	71 Fenchurch Street, London EC3M 4BS, UK

The design methodology associated with composite materials requires prioritization of design goals; namely strength, stiffness, cosmetics, and cost. Because composite panels can have a wide range of moments of inertia, stiffener spacing can also vary a lot. This gives the designer quite a bit of latitude to accommodate outfitting requirements.

Composite materials for marine applications have advanced over the years; especially core materials and resins. Reinforcements are available in new styles and fibers that were once considered exotic are now used more commonly in critical areas. The lure of composites has always been very high tensile properties of individual fibers, which material manufacturers love to publish. The presentation on micromechanics in Chapter Four was designed to impress upon the reader the importance of fiber/resin interaction and the critical nature of off-axis loads.

Although marine composite materials have changed over the years, the analysis methods presented for solid and sandwich panels remains valid. Indeed, Military Handbooks 17 and 23 were derived for the aerospace community, which has used high-strength/stiffness materials for years. These formulas are good for static analysis with end conditions as noted. Caution must always be exercised when any of the following conditions exist:

- Uncertain material properties
- Dynamic loads
- Unknown end conditions
- "Soft" cores with nonlinear behavior

The panel test methods presented are useful for comparing candidate laminate systems for a particular application. Laminates should always be built in a fashion similar to the end product and tested for mechanical properties before proceeding with any project that deviates from empirical knowledge. This would include trying new materials, structural design concepts or increasing design loads (bigger and/or faster). Care should always be exercised when panels are under compressive collapse loads or with structural details that create stress concentrations.

Composite laminates fail in a variety of ways, with the most common being delamination. With the exception of highly loaded advanced laminates (carbon fiber, low resin content, etc.), failures are generally not catastrophic. Indeed, with sandwich laminates, it is difficult to compromise hull integrity. Composite laminates will generally deform until a ply within the laminate reaches its elastic limit. After this ply fails, successive plies will then fail. Strain limits of both the reinforcement and resin system control failure. With the exception of thermoplastics, composites do not have the same ability as metals to plastically deform. Instead, this energy is dissipated through increased panel deflection and then delamination.

Resin systems are organic, and therefore must be protected in medium to large fires to prevent them from acting as a fuel source. Certain resins act better than other but in general, unprotected composite structure will not burn without a substantial initiation source. Composites do act as excellent insulators, which serves to protect areas outside the space on fire. Testing of "systems" on the appropriate scale for fire performance characteristics is highly recommended.

Recommendations

The data presented in Appendix A represents an initial attempt by the industry to compile a comprehensive set of test data on typical marine composite laminates in use today. Although this is a major advance over what has previously been published, there are many "gaps" in the database where test data does not exist or has not been reported. This is especially true for shear data and Poisson's ratio. An expanded database of test data represents a very high priority for the advancement of analytical techniques. The requirements for additional test data go beyond filling the "gaps" in Appendix A which covers static properties of uniaxial test specimens. Specific research projects are required to address the following testing issues:

- Establish "most realistic" test method for determining in-plane shear properties, including specimen size and fixturing;

- Standardize and expand testing with two-dimensional test procedure, such as the Hydromat system, to include a wide variety of sandwich laminates and demonstrate the ability to "back out" engineering data;

- Update information on the performance of fasteners based on current typical laminates. The work presented at the 1996 MACM Conference (McDevitt, D.T, Gregory, W.E, and Kurzweil, A.D., "Development of a Preliminary Design Procedure for Self-Tapping Screws for Application to Surface Ship Hull Structures Fabricated from Glass Reinforced Plastic (GRP)" is an excellent basis for additional research;

- Test data on creep performance is also very dated and based on specific laminates that are not commonly used today for structural applications. Higher fiber content laminates and today's resin systems may prove to have improved creep properties. Constants for viscoelastic equations for these laminates need to be developed; and

- Fatigue data is always difficult to acquire because of the time required to get meaningful results. Nevertheless, this area of research represents a large "gap" in our knowledge base of composite material systems. Materials and design details need to evaluated for fatigue performance as the industry pushes for longer service life.

A second priority for the industry is the development of a universally accepted laminate analysis program based on test data and the "panel" formulas from MIL HDBKs 17 and 23 presented graphically in Chapter Five. The data and analysis program should be in a spreadsheet format, such as Microsoft® Excel. This would let the user enter and change data values and adjust formula coefficients to suit boundary conditions.

Another requirement of the advanced marine composites industry is for a finite element analysis package tailored to the structures, loads and materials associated with marine systems. A research project could undertake parametric studies to evaluate the influence of boundary conditions; element types; mesh density; modeling of sandwich laminates; dynamic analysis; and application of material property data. A cost effective method to accomplish these objectives would be to start with an established FEA package and develop appropriate "shells" specific to composite marine systems.

The marine composites industry also needs assistance in the development of "systems" that are fire tolerant and can meet domestic and international regulations. There has been some ongoing research in this area involving intermediate-scale testing of fire protection systems and standard laminates to understand thermo-mechanical performance. The remaining research should focus on the following two areas:

- Conduct small-scale mechanical tests (flexural) of test laminates at elevated temperatures to determine property degradation for polyester, vinylester, epoxy and phenolic resin systems. Specimens should be isothermally heated. Additional types of tests (shear) may prove necessary, as may an investigation into creep properties at elevated temperatures; and

- Assemble research data on fire protection systems and thermal profiles of composite material laminates subjected to heat fluxes to develop a guide similar to SNAME Technical & Research Bulletin 2-21, "Aluminum Fire Protection Guidelines," July 1974.

ASTM 25.01 has undertaken an initiative to develop a standard guide for structural details for steel ships. Shipyards will be surveyed and a "catalog" of details reproduced in CAD format will evolve. This will assist the industry in developing standard specifications for bidding purposes and to track the performance of a particular detail over time. The marine composites industry could also follow this example and produce a catalog of standard details and method for calling out laminate schedules.

Standardization can also help the industry if a methodology for integrating composite construction with standard shipyard practice was developed. The largest shipyards in the country have shown a willingness to subcontract composite construction rather than develop an in-house expertise. Because the manufacturing "cultures" of composite fabricators and large shipyards is very divergent, difficulties in the integration of business practices and modular components can be anticipated. The development of standard "process descriptions" would go a long way to alleviating some of these problems. ABS has endorsed this proposal recommendation and would be an invaluable resource for such a project.

The recommendations presented here, not necessarily in the order of priority, are the opinions of the author based on research associated with this and other recent research projects in the area of marine composites. The value of any research is only as good as the number of people it reaches. The field of marine composites is very diverse, with no single professional society representing all interested parties. Therefore, it is recommended that various outlets be utilized to announce published reports. Specialized databases with direct mailings are always the most effective. The contractor maintains a database of builders that assisted with questionnaires during the writing and updating of SSC-360. ***Professional Boatbuilder***, SNAME, ASNE, CFA and SAMPE professional journals should also contain notices of available research reports.

The opportunities for composite materials in the marine environment continue to grow as the demand to balance cost and performance becomes more acute. As a highly "engineerable" material, composite laminates require care in the selection of analytical tools. Guidance on methodology and some fundamental formulas have been presented in the Guide. The marine composite designer will invariably develop his or her own set of design tools. If the industry can develop an accepted set of test standards; produce a good database on currently used laminates; develop an editable laminate analysis program and customize an FEA program, then we will be in a position to wean ourselves off of empirical methods.

Design Equations for FRP Ship Hulls
Johns Hopkins University Applied Physics Lab (JHU/APL)
Carderock Division, Naval Warfare Center (CDNSWC)

APL contact: Jack Roberts 410-792-6000, ext 3788, Paul Wienhold 410-792-6000 ext 3165

APL is undertaking an effort to verify appropriate design equations suitable for use in predicting the performance of "marine" composite panels under combined compression (in-plane) and flexural (out-of-plane) loading. A number of panels will be tested on the US Naval Academy's panel tester. Figure 1 is a schematic drawing of the test fixture.

USNA Ship Structures Laboratory
Grillage Test Fixture
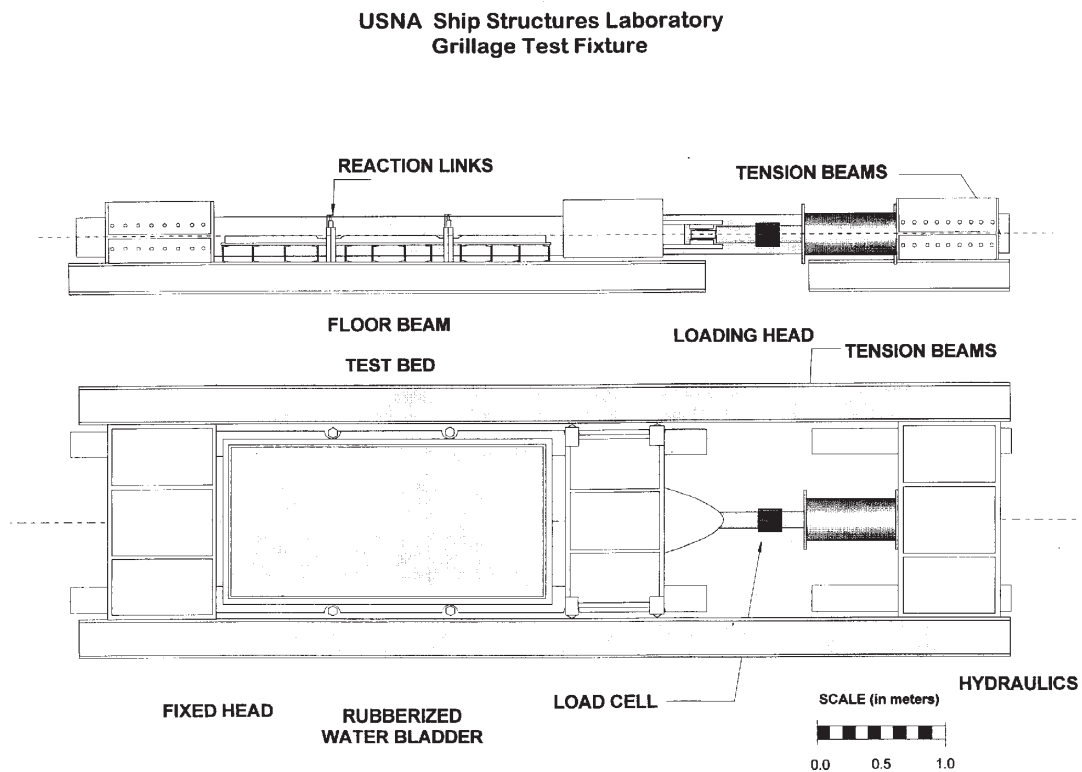
Figure 1 Panel Tester at the US Naval Academy (3-foot wide panels; 330,000 pound compression loading capability; 40 psi bladder loading capability)

The following table summarizes the panels that will be tested to verify design equations:

Panel Description	Size	In-Plane Compression Tested to Failure	Out-of-Plane Normal Load Tested to d=w/200	Retest Previous Panels with Combined Loading to Failure
Unstiffened	3' x 6'	3 (TPI)	3 (TPI)	3 (TPI)
Hat-stiffened	3' x 4'	3 (Seemann or Sunres)	3 (Seemann or Sunres)	3 (Seemann or Sunres)
Sandwich	3' x 4'	3 (TPI)	3 (TPI)	3 (TPI)

All tests will be instrumented with strain gages, load cells and displacement transducers. A total of 27 tests will be run at a cost of approximately $1k each.

Development of Analysis Tools for Thick, Marine Composites
Carderock Division, Naval Warfare Center (CDNSWC)

University of Delaware contact: Jack Gillispie 302-831-8702
UCLA, Santa Barbara contact: Keith Kenwood 805-893-3381
NSWC TPOC: Karin Gipple 410-293-5218

Background
Common structural details such as angle brackets, stiffeners, bonded/bolted joints, and curved frames, constructed of fiber reinforced composite materials, are subject to out-of-plane stresses either directly from loading or indirectly by geometry. These out-of-plane stresses, combined with minimum inherent out-of-plane material properties make the design of components with such stress states very difficult In addition there is a lack of data and experience to assist an engineer in assessing the effect of out-of-plane stresses m composites.

In response to the existence of these issues in Navy structures, Code 60 is conducting a 6.2 program to theoretically and experimentally investigate methods for developing static and fatigue through thickness properties for composites, to be used in the design and analysis of thick, structural details. To compliment this in-house effort, Code 60 is soliciting contractual help in the development of design procedures to screen and asses the effect of combined stress states (enplane and through-thickness) in joints or structural details in composite structures. The procedures developed shall be based on engineering experience in design and failure analysis, in order to insure the procedures developed are as meaningful and useful to the Navy as possible.

Statement of Work
Phase I Development and Evaluation of Preliminary Design Tools
Task 1 - Develop and document meaningful procedures to screen and assess the effect of through-thickness dominated stress states in joints or details in composite structures. The procedure should address combined stress states such as in-plane and through-thickness stresses, and through-thickness tension and shear. The procedure should also be applicable to a wide range of composite material systems and detail geometries. For instance current Navy programs use materials ranging from autoclave cured carbon reinforced prepreg to hand layed glass woven roving polyester.

Task 2 - Conduct parametric studies on common structural features, using the developed procedure and the experience of the contractor, to establish rules-of-thumb for design and selection of typical structural details with combined stress states.

Phase II Develop a Fatigue Life Prediction Methodology
Task 1 - Develop a fatigue life methodology for composite materials subjected to combined through-thickness and inplane stress states. This philosophy must account for the relationship between coupon level specimens and full-scale structures to assist in using existing data developed for coupon level specimens, and to guide development of new coupon level test specimens to assist structural design.

Verification of the HYDROMAT Test System as a Viable Means of Testing Two-Dimensional Sandwich Panels
SNAME HS-9 and ASTM D30.05

Gougeon Brothers Inc. contact: William D. Bertelsen 517-684-7286
Michigan Technological University contact: David L. Sikarskie

Introduction
The Hydromat Test System was originally developed by Gougeon Brothers, Inc. for static and fatigue testing of marine composite sandwich panels. In its original form, the fixture had a number of deficiencies, including poorly defined boundary conditions and poorly defined pressure loading of the panels. After some modification of the apparatus, these issues were studied extensively, clarified, and presented in a recent conference paper. While the study established the fixture as a viable device for testing isotropic, homogeneous, monolithic plates, a number of questions remain to be answered for composite sandwich plates. Sandwich plates which have low density, low shear stiffness/shear strength cores behave quite differently than isotropic plates. Several ratios of sandwich elastic properties and geometries need to be tested to ensure that the fixture is not introducing anomalies into the test results.

Work Statement Summary
Part 1: Boundary Condition Study
For the boundary condition study, an isotropic, homogeneous face sheet (aluminum) and an isotropic, homogeneous core (structural foam) will be tested. However, at least two different core materials (low-modulus, high-modulus) with a combination of face-sheet thicknesses will be tested to see if simply-supported boundary conditions can be maintained over a range of core materials and panel geometries. An analytical solution will be developed to determine whether simply-supported boundary conditions are attained.

Part 2: Composite Sandwich Panel Study
For this study, the primary focus will be on panels for which the material properties and panel geometry will be such that failure occurs in the small-deflection range. Two types of composite face sheets will be considered, random mat and orthotropic. In order to represent a practical range of marine sandwich panels, at least two different typos of core materials will be used: structural foam and balsa wood. Results will focus on two general areas, elastic behavior and failure. One of the main purposes of the elastic behavior study is to be able to determine experimentally the flexural and shear rigidities of the panel. Once the generic analytical solution for a given sandwich plate is known, a combined analytical/experimental technique can be employed for obtaining these properties, i.e., by using measured deflection data at several points, the flexural and shear rigidities can be back-calculated from the analytical solution.

Research on Advanced Composites in Construction
National Science Foundation, Div of Civil and Mechanical Systems

National Science Foundation contact: Dr. John Scalzi 703-306-1361
Penn State University contact: Dr. Toni Nanni 814-865-6394

Fundamental and applied research needed to support the successful implementation of FRP composites in construction is deficient. Research funding is also very limited and no continuity of funding or sustained research support is assured. A coordinated program is a better guarantee that federal funds are used efficiently because it sets a defined research agenda, provides recommendations for sustained budget support and will increase the accountability and visibility of the research teams. Finally, the coordinated program can shorten the time needed for technology transfer because of the continuity in effort.

The Civil Engineering Research Foundation (CERF) of the American Society of Civil Engineers (ASCE) is developing policy documents for the High-Performance Construction Materials Program (CONMat) which will include advanced composites. In addition, the coordinated research effort in FRP composites follows the guidelines established by the NSF Civil Infrastructure Systems (CIS) Task Group (6) in that it focuses on identifying and creating new technologies for application in the civil infrastructure. The following table summarizes proposed areas of research related to design and budget recommendations:

Topic Area	Total $M (1-3yrs)	Total $M (4-5yrs)	Analysis & Design $M
Reinforced Concrete	$5.5	$5.0	$2.5
Prestressed Concrete and Cables	3.8	2.7	0.4
Structural Shapes	6.4	4.2	2.0
Structural Systems	11.4	2.1	1.5
Repair and Rehabilitation Systems	11.9	11.4	nsp
Total:	$39.0	$25.4	$6.4

Several general points have emerged independently from the specifics of the strategic research plan during the deliberations of the Planning Committee. These points, important for the implementation of new technology for the revitalization of the U.S. civil infrastructure system, are:

- need for integration from the start involving end-users, academic community, industry (i.e., manufacturers, designers, and contractors), and government agencies

- need for indivisible systems including new product/technology, acceptance criteria (standards), design guidelines, and code recognition

- need to develop cost data and realistic cost estimation methods

- need for establishing a new professional society dedicated to advanced composites for construction

Classification Society Rules

ABS contact: William Lind 504-523-5973
ABS High-Speed Craft Guide, October 1990
Materials
Basic mat/WR glass/polyester resin laminate used with allowance for use of other
reinforcements and resins.
Fabrication and Quality Control
QC to include material receipt QA, gel time and lamination monitoring, barcol hardness testing
and laminate testing to ASTM 790(M) , ASTM D 638(M) or D 3039, ASTM D 695 (M) or
3410, FTMS 406 1041, ASTM D 3846, ASTM C 273 and ASTM C 393.
Details and Fasteners
Guidance is provided for structural continuity, avoidance of stress concentrations, stiffener
details and fastener arrangements.
Design Pressures
Bottom structure design pressure given as a function of displacement, waterline length, beam,
trim, deadrise angle, design speed, design area factor (actual panel area related to a reference
area) and vertical acceleration distribution factor (as a function of longitudinal position).
Plating
Skin thickness defined for isotropic and orthotropic single-skin laminate as a function of
geometry, design stress and design pressure. For isotropic and orthotropic sandwich laminates,
strength (SM) and stiffness (I) is prescribed as a function of geometry, design stress, design
pressure, and skin compressive and tensile modulii. Shear strength, skin stability and minimum
skin thickness is also considered for sandwich laminates.

DnV contact: Joar Bengaard 201-488-0112
DnV Rules for Classification of High Speed Light Craft, 1985
Structural Principles
Definition of geometry for bottom, side, deck, bulkhead and deckhouse structures is provided
based on vessel with continuous longitudinals and web frames.
Manufacturing
QC procedures prescribed for raw material storage, manufacturing conditions, primary and
secondary bond fabrication procedures, and general QC items.
Materials
Raw materials to have DnV material certificate. Testing is to be done to ISO 3268-1978 and
ISO 1922 or ASTM C 273-61.
Sandwich Panels
Skin thickness and core shear and compression properties are prescribed as a function of
structural member. For panels subject to bending loads, allowables are prescribed for normal
stresses in skin laminates and core shear stresses, local skin buckling, and deflections.
Single Skin Panels and Stiffeners
Single skin constructions are of defined thickness according to structural member. For members
with out-of-plane loads, consideration is given to combined bending and membrane stresses and
allowable stresses and deflections. Stiffener SM is defined as a function of structural member.
Web Frames and Girder Systems
Specifications cover continuity of members, effective dimensions and bond area, strength
requirements and a treatment of complex girder systems.

Update of MARINE COMPOSITES (SSC-360) for Navy Use

NSWC, Carderock contact: Loc Nguyen 301-227-4125

Statement of Work

1   APPLICATIONS

Since the original SSC effort was started over five years ago, the marine composites industry has changed dramatically, both in the high-tech arena, with the construction of the new class of America's Cup yachts, and in large cruising boat market, with vessels in excess of 150 feet under construction. Although stifled by U.S. Coast Guard regulations, numerous concepts for large, high-performance passenger ferries have been explored by U.S. manufacturers. The Navy's minehunter program has also brought two large shipyards into the composites market. Numerous other traditional metal yards have undertaken projects with composites.

Cross-fertilization of the pleasure/commercial and military industries has also flourished with some high quality recreational boat builders diversifying into military products.

The aerospace industry has focused their efforts on the lower technology components using cost effective manufacturing technology. This is a change in thrust from previous emphasis on high performance material systems that were unlikely to find their way on to ships. Fire is an issue with aircraft interior components and with cargo containers under development.

Industrial applications of composite materials has also changed in the last five years. Projects such as truck components, bridge structures, pier structures, replacement underground fuel tanks and structural elements in corrosive environments all have elements in common with marine applications. Transportation and housing applications have generated much test data on fire performance and producibility

2   MATERIALS

Reinforcement products are becoming more available in hybrid form, which can have the effect of maximizing the cost effectiveness of a high performance material. Lower cost, thermoplastic products are also being developed for the marine industry. Thicker grades of products are becoming available as boat builders develop the techniques to process these materials. Multi-axial, 3-D and preform products are becoming more available as process machinery comes on line.

New, specialty resins have been developed to meet specific markets. The technique of blending two resin systems to achieve the desirable properties of each is becoming more common. Properties being optimized include:

    Toughness - impact resistance
    Blister resistance
    Elevated temperature performance and fire resistance
    Superior handling and curing characteristics
    Compliance with air quality standards

Core materials also have evolved over the past five years. Manufacturers have improved the bonding characteristics of surface finishes, especially with marine grade products. New foams have been developed to withstand higher processing temperatures associated with autoclave cure of parts.

3   DESIGN

With over 25 years of composites technology development (much sponsored by the government), data resources exist to permit the development of a composites design guide for the marine industry. Although the design chapter will build on accepted composite material methods, it will also reflect practices and requirements unique to the marine and offshore environment.

The design section of the guide will be expanded to cover sandwich construction and panel structures more thoroughly. Sandwich laminates have recently been used successfully on the largest private and naval vessels. Naval architects and regulatory agencies have revisited the question of design pressures for high performance vehicles. This research has become an integral part of leading edge design of composites for marine vehicles.

A comprehensive review of composite design procedures and computer software packages will be also undertaken. This section will direct the reader to analysis methods that are best suited for a particular structure subject to anticipated loads, i.e.. thick section pressure hull, shock loaded structure, out-of-plane loaded panels, impact resistant laminate, etc.

In the book update, particular attention will be given to state-of-the-art joining technologies. This overview will include transition techniques used with composites, new adhesives, technology using mechanical fasteners and joining to metallic structures. Emphasis will be placed on detail design cases that have confronted the Navy during recent and anticipated prototype programs.

4   PERFORMANCE

As material systems are pushed to their limits, more information about ultimate failure loads and mechanisms is obtained. Composite marine structures have traditionally been overbuilt to accommodate uncertainties in material performance and construction variables. Several diverse "design competitions" around the world in recent years has driven marine composite design and construction closer to the advanced material leading edge. The highest profile of these was the America's Cup competition that featured a new, lightweight boat. On the military side, several navies around the world have constructed mine counter-measure vessels using various composite construction techniques. Offshore powerboat racing and high performance motor yachts have also contributed to improved performance of composite hull structures.

New applications for composite materials have been the driving force behind some long-term investigations on the performance of laminated structures. New material systems and sandwich constructions have been tested for fatigue, impact, long-term creep and moisture resistance. This information is quite useful to designers of marine composite systems. Overviews of recent and ongoing studies will be added to the Performance chapter in the book. Additionally, in-service experience of military craft, such as the RIB concept will be highlighted.

The Navy must consider the supportability of any major ship structure that it intends to place in service. Composite materials have demonstrated the ability to be easily repaired in the field, especially when complex shapes are involved. However, the issue of repair procedures remains a question among Navy personnel, primarily because no documentation exists that illustrates the advantages of composite materials for repair work. A major overhaul to expand the repair section and include Navy procedures will be undertaken as part of the proposed effort.

5   FABRICATION

Composite marine structures have proven themselves with over 30 years of punishing at-sea service. The cost competitiveness issue has also been demonstrated for smaller, production craft. The challenge of the 90's remains the issue of fabricating large, limited production marine systems on a cost-competitive basis with aluminum and steel. Moreover, shipyards traditionally trained to work with steel must also be able to adapt to the unique requirements of composite construction. The U.S. minehunter program has spawned two approaches to establishing a facility to construct large composite hulls. A review of shipyard requirements and state-of-the-art equipment will be included in the update to give the reader an appreciation for the "total" composite ship manufacturing process. A particular emphasis will be placed on large-scale marine and industrial fabrication operations to provide insight on how the marine composites infrastructure can be bolstered in this country. Both production Navy applications for components, such as doors, piping, etc. and custom one-off assemblies will be examined.

In an era where cost rather than performance has become the primary design driver, composite materials offer an excellent life-cycle alternative to metals. However, fabrication techniques cannot be based on examples found in the aerospace industry. High-tech yacht builders are using construction techniques that are cost-effective, yet produce high quality products. The move to closed-mold and partial closed-mold processes to meet air quality standards will also be addressed in the update.

6   TESTING

Standardized testing of composite structures for marine use is a difficult problem. Geometries and load scenarios are usually quite complex, as is the myriad combinations of materials available to the designer. Combine this with the generally limited resources of the industry and we get a scattering of test data not suitable for comparison. Test programs usually take the form of parametric studies targeted to a specific design. For the Navy, this has resulted in a very limited combination of materials that have been considered for use because the demanding performance requirements traditionally lead to extensive test programs.

The Society of Naval Architects and Marine Engineer's (SNAME) Materials Panel (HS-9) recently met to discuss the problem of assembling a database of test data for use as a primary design tool. The format used by the offerer in the original SSC publication was cited as the most comprehensive effort to date. As a member of that SNAME panel, the offerer will work with SNAME and the Navy to expand the database of test results in a format most useful to the industry. It is anticipated that the update will include test results from Navy and other test programs covering candidate laminate systems. To date, this type of information has only been available to the limited number of people directly involved with a particular project.

An expanded section of fire performance of composite materials will also be included, based on the $500K, two-year research effort near completion by the offerer. Test data on protected and unprotected composite systems will be presented in such a way as to allow the marine designer to make preliminary material selection based on anticipated fire threats.

7   REFERENCE

The reference chapter will be updated to include the latest design and regulatory procedures of the U.S. Navy, the U.S. Coast Guard and the American Bureau of Shipping. The offerer will also include a source list containing information on material suppliers, fabricators, design services and key government departments active in the marine composites community.

Composite Ship Superstructure System
project funded under MARITECH under sol BAA 94-44

Structural Composites, Inc, contact: Dr. Ron Reichard,   407-951-9464

FRP manufacturing technology presently utilized in the marine small craft industry is not suitable for production of large ship superstructures due to tooling costs and high labor costs. The key to developing a cost effective FRP superstructure is to minimize the labor and tooling costs. The approach presented here is to mass produce simple elements, using existing cost competitive technologies, which can be quickly and easily joined to produce a variety of structural configurations. The system proposed consists of flat FRP sandwich panels, FRP angles and FRP bonding plates. It is based on the systems involving FRP sandwich panels and steel framing tested by the U.S. Navy, except that this proposed system utilizes FRP framing, eliminating potential problems with different thermal expansion coefficients, thermal conductivity, fastening of the panels to the frames and corrosion.

Flat sandwich panels are presently manufactured by a number of commercial companies for a variety of applications. The cost and quality of the various panels vary widely, depending on the application and manufacturing process. There are two processes presently in use for mass producing inexpensive commercial GRP sandwich panels: vacuum bagging and vacuum compression molding (VCM.) Foam core panels for refrigerator trucks and portable housing are constructed using this process. The process involves placing layers of E-glass fabric on a flat mold surface, distributing resin over the fabric, placing the core material, placing additional layers of E-glass fabric, distributing additional resin, covering the laminate with a vacuum bag, drawing a vacuum and placing the panel in a large oven to accelerate cure. VCM is similar, except that a semi-rigid top mold is used in place of a vacuum bag. This process is used by FRP Technologies Inc. to produce GRP foam sandwich roof panels for industrial and residential use. Both processes reduce labor to a small fraction of the total panel cost, which is primarily a function of the raw material costs.

The angles and bonding plates will be produced by pultrusion, one of the most cost effective FRP manufacturing processes. The cross-sections are standard structural shapes for which many pultruders presently have tooling. However, most pultruded structural members are produced with a mat and unidirectional roving laminate. These members have poor stiffness and strength in the transverse and shear directions, thus are not suitable for this superstructure system. Recent developments in pultrusion involve pulling knitted or stitched fabrics, allowing off-axis plies in the laminate. These structural members have excellent mechanical properties in the transverse and shear directions, thus making them suitable for this superstructure system.

Current regulations are designed for steel construction, but FRP materials and structures do not behave like steel. It is likely to take considerable time and effort before these regulations are changed. The approach presented here is to develop and certify a specific superstructure system. Many of the issues involved in developing generalized regulations can be avoided by seeking regulatory approval of a specific system. Also, there is a considerable body of information on design and testing of specific composite superstructure components generated by the U.S. Navy's composite deck house program which can be utilized in this program.

Advanced Materials Technology as Applied to Ship Design and Construction project funded under MARITECH under sol BAA 94-44

University of California, San Diego contact: Dr. Robert Asaro 619-534-6888

Structural Design
The use of composite materials requires that sophisticated finite element (FEM) computational analysis tools be developed and used to accurately predict overall static and dynamic behavior as well as detailed local three-dimensional stress information for failure predictions.

In the course of the structural design, the aforementioned FEM will be used to assist in the structural design, analysis, and optimization of global structure and local structural elements. This will entail the development of complete 3-dimensional linear and nonlinear FEM models of advanced composite hull structure. These models will be used for determining the global static and dynamic response (time-dependent displacements and stresses) of the proposed advanced composite vessel to the critical ship structural loads. In addition, they will provide valuable insight of the critical internal load-path distribution and the relative magnitudes of the internal shear and moment distributions. In addition, highly focused two- and three-dimensional FEM models will be constructed to study the most highly stressed regions as well as the most critical components including the composite bolted/bonded joints and the composite-to-metal interfaces.

Margins of safety and fatigue life predictions will be calculated by applying failure criteria that describe buckling and fracture. These failure criteria are built into specialized nonlinear finite element codes. As an example of the use of complete (global) and localized FEM models, fatigue-life predictions of highly stressed members and joints are often performed in a three phase process, where the first phase involves determining the internal load distribution of a global finite element model subjected to approximately 150-200 different hydrodynamic load cases (varying wave length and wave angle), second, an intermediate model of highly loaded regions of the vessel is analyzed to locate highly stressed regions, and third, detailed FEM models of the highly stressed composite joints and composite-to-metal interfaces are analyzed.

In conjunction with the above studies, static and dynamic validation tests will be performed at the UCSD Powell Structural Systems Testing Laboratory on a wide range of fabricated composite ship components including (1) large stiffened sandwich laminate panels that can be used for deck and hull components where different skin (fiber, resin) and core materials, as well as stiffener location, geometry, and attachment (integral fabrication versus secondary bond) will be investigated, (2) bonded and/or bolted joint configurations where different geometries, materials (graphite, glass) and ply material definitions (use of unidirectional tape versus woven fabric and three-dimensional knits in higwy stressed joints) will be studied, and (3) full-scale static/dynamic testing of critical hull sections up to 65 foot length.

In the design process, specialized software will be used for estimating the structural loads (e.g. SMP for wave-induced bending moments and wave slamming) and for structural analysis (e.g. ABAQUS, MSC/NASTRAN, specialized nonlinear composite FEM codes, and MAESTRO for 3-D structural analysis and optiniization using probabilistic techniques).

Composite Materials Handbook (MIL-HDBK-17)
U.S. Army Research Laboratory

U.S. Army contact (Co-Chairman, MIL-HDBK-17): Dr. Gary Hagnaauer 617-923-5121

Introduction

The standardization of a statistically-based mechanical property data base, procedures used, and overall material guidelines for characterization of composite material systems is recognized as being beneficial to both manufacturers and governmental agencies. A complete characterization of the capabilities of any engineering material system is primarily dependent on the inherent material physical and chemical composition. Therefore, at the material system characterization level, the data and guidelines contained in this handbook are applicable to military and commercial products and provide the technical basis for establishing statistically valid design values acceptable to certificating or procuring agencies.

This handbook specifically provides statistically-based mechanical property data on current and emerging polymer matrix composite materials, provides guidelines for the analysis and presentation of data, and provides fabrication and characterization documentation to ensure repeatability of results or reliable detection of differences. The primary focus of MIL-HDBK-17 in the overall characterization/design procedure as commonly applied to composites is shown in the figure below.

Scope

MIL-HDBK-17 will ultimately be published in three volumes:

Volume I

Provides guidelines for the characterization of composite material systems to be used in aerospace vehicles and structures. Composite material systems must normally be evaluated in accordance with these, or equivalent guidelines, in order to be considered acceptable by government certification and procuring agencies.

Volume II

Will provide a compilation of statistically-based mechanical property data for current and emerging composite material systems used in the aerospace industry. B-basis strength and strain-to-failure values will be presented along with related data.

Volume III

Will provide information regarding materials and fabrication procedures, quality control, and design and analysis.

Text References

1   Scott, Robert J., <u>Fiberglass Boat Design and Construction</u>, Second Edition, The Society of Naval Architects and Marine Engineers, 1996.

2   <u>Engineers' Guide to Composite Materials</u>, Metals Park, OH; American Society for Metals, 1987 ed.

3   Cook Polycor Polyester Gel Coats and Resins, Applications Manual, 6th Edition, Cook Paint and Varnish Company, Kansas City, MO, 1986.

4   Feichtinger, K.A. "Methods of Evaluation and Performance of Structural Core Materials Used in Sandwich Construction," Proc. of the 42nd Annual Conference SPI Reinforced Plastics/Composites Institute. 2-6 Feb., 1987.

5   Johannsen, Thomas J., <u>One-Off Airex Fiberglass Sandwich Construction</u>, Buffalo, NY: Chemacryl, Inc., 1973.

6   Hexcel, "HRH-78 Nomex$^{®}$ Commercial Grade Honeycomb Data Sheet 4400." Dublin, CA., 1989.

7   <u>Principles of Naval Architecture</u>, by the Society of Naval Architects and Marine Engineers. New York, 1967.

8   Evans, J. Harvey, <u>Ship Structural Design Concepts</u>, Cambridge, MD; Cornell Maritime Press, 1975.

9   Noonan, Edward F., <u>Ship Vibration Guide</u>, Washington, DC; Ship Structure Committee, 1989.

10   Schlick, O., "Further Investigations of Vibration of Steamers," R.I.N.A., 1894.

11   <u>Guide for Building and Classing Offshore Racing Yachts</u>, by the American Bureau of Shipping, Paramus, NJ, 1986.

12   <u>Guide for Building and Classing High-Speed and Displacement Motor Yachts</u>, by the American Bureau of Shipping, Paramus, NJ, 1990.

13   Heller, S.R. and Jasper, N.H., "On the Structural Design of Planing Craft," <u>Transactions</u>, Royal Institution of Naval Architects, (1960) p 49-65.

14   DnV *Rules for Classification of High Speed Light Craft*, Det Norske Veritas, Hovik, Norway, 1985

15   NAVSEA *High Performance MarineCraft Design Manual Hull Structures*, NAVSEACOMBATSYSENGSTA Report 60-204, July 1988. Distribution limited.

16   Schwartz, Mel M., <u>Composite Materials Handbook</u>, McGraw Hill, New York, 1984.

17   Tsai, Stephen W., <u>Composites Design</u>, Third edition, Tokyo, Think Composites, 1987.

18   X.S. Lu & X.D. Jin, "*Structural Design and Tests of a Trial GRP Hull*," <u>Marine Structures</u>, Elsever, 1990

19   Department of the Navy, DDS-9110-9, <u>Strength of Glass Reinforced Plastic Structural Members</u>, August, 1969, document subject to export control.

20   Department of the Army, <u>Composite Material Handbook, MIL-HDBK-17</u>, U.S. Army
      Research Lab, Watertown, MA.

21   Department of the Army, <u>Composite Material Handbook, MIL-HDBK-23</u>, U.S. Army
      Research Lab, Watertown, MA

22   Smith, C.S., "Buckling Problems in the Design of Fiberglass-Reinforced Plastic Ships,"
      <u>Journal of Ship Research</u>, (Sept., 1972) p. 174-190.

23   Reichard, Ronnal P., "FRP Sailboat Structural Design: Details Make the Difference,"
      Proc. of the 17th AIAA/SNAME Symposium on the Aero/Hydrodynamics of Sailing:
      The Ancient Interface. Vol. 34 31 Oct. - 1 Nov. 1987.

24   Owens-Corning Fiberglas Corp., "Joint Configuration and Surface Preparation Effect on
      Bond Joint Fatigue in Marine Application," Toledo, OH, 1973.

25   Della Rocca, R.J. and Scott, R.J., "Materials Test Program for Application of Fiberglass
      Reinforced Plastics to U.S. Navy Minesweepers," 22nd Annual Technical Conference,
      The Society of the Plastics Industry, Inc.

26   Naval Material Laboratory, New York Naval Shipyard, <u>Design Manual for Joining of
      Glass Reinforced Structural Plastics</u>, NAVSHIPS 250-634-1, August 1961.

27   Horsmon, Al, "Notes on Design, Construction, Inspection and Repair of Fiber Reinforced
      Plastic (FRP) Vessels," USCG NVIC No. 8-87, 6 Nov. 1987.

28   <u>Rules for Building and Classing Reinforced Plastic Vessels</u>, by the American Bureau of
      Shipping, Paramus, NJ, 1978.

29   Gibbs & Cox, Inc., <u>Marine Design Manual for Fiberglass Reinforced Plastics</u>, sponsored
      by Owens-Corning Fiberglas Corporation, McGraw-Hill, New York, 1960.

30   Reichard, Ronnal P., and Gasparrina, T., "Structural Analysis of a Power Planing Boat,"
      SNAME Powerboat Symposium, Miami Beach, FL, Feb 1984.

31   Reichard, Ronnal P., "Structural Design of Multihull Sailboats," First International
      Conference on Marine Applications of Composite mateials, Melbourne, FL, Florida
      Institute of Technology, March, 1986.

32   1988 Annual Book of ASTM Standards, Vols 8.01, 8.02, 8.03, 15.03, ASTM, 1916 Race
      Street, Philadelphia, PA.

33   Weissmann-Berman, D., "A Preliminary Design Method for Sandwich-Cored Panels,"
      Proceedings of the 10th Ship Technology and Research (STAR) Symposium, SNAME
      SY-19, Norfolk, VA, May 1985.

34   Sponberg, Eric W., "Carbon Fiber Sailboat Hulls: How to Optimize the Use of an
      Expensive Material," <u>Journal of Marine Technology</u>, 23 (2) aPRIL, 1986.

35   Riley, C. and Isley, F., "Application of Bias Fabric Reinforced Hull Panels," First
      International Conference on Marine Applications of Composite mateials, Melbourne, FL,
      Florida Institute of Technology, March, 1986.

36   <u>Structural Plastics Design Manual</u> published by the American Society of Civil Engineers,
      ASCE Manuals and Reports on Enginering Practice No. 63, New York, 1984.

37   Timoshenko, S., <u>Strength of Materials, Part I, Elementary Theory and Problems</u>, Robert
      E. Krieger Publishing, Huntington, NY 1976.

38   <u>Guide for Building and Classing High-Speed Craft</u>, Preliminary Draft, October 1996,
      American Bureau of Shipping, Houston, TX.

39   Hashin, Z. "Fatigue Failure Criteria for Unidirectional Fiber Composites," <u>Journal of
      Applied Mechanics</u>, Vol. 38, Dec 1981, p 846-852.

40   Kim, R.Y., "Fatigue Behavior," <u>Composite Design 1986</u>, Section 19, S.W. Tsia, Editor,
      Think Composites, Dayton OH 1986.

41   Goetchius, G.M., "Fatigue of Composite Materials," <u>Advanced Composites II, Expanding
      the Technology</u>, Third Annual Conference on Advanced Composites, Detriot, MI, 15-17
      Sep. 1987, p. 289-298.

42   Salkind, M.J., "Fatigue of Composites," Composite Materials: Testing and Design
      (Second Conference), ASTM STP 497, 1972, p. 143-169.

43   Chang, F.H, Gordon, D.E. and Gardner, A.H., "A Study of Fatigue Damage in
      Composites by Nondestructive Testing Techniques," <u>Fatigue of Filamentary Composite
      Materials</u>, ASTM STP 636, Reifsnider, K.L. and Lauraitis, K.N., Editors, ASTM, 1977, p
      57-72.

44   Kasen, M.B. Schramm, R.E. and Read, D.T., "Fatigue of Composites at Cyrogenic
      Temperatures," <u>Fatigue of Filamentary Composite Materials</u>, ASTM STP 636, Reifsnider,
      K.L. and Lauraitis, K.N., Editors, ASTM, 1977, p 141-151.

45   Porter, T.R., "Evaluation of Flawed Composite Structure Under Static and Cyclic
      Loading," <u>Fatigue of Filamentary Composite Materials</u>, ASTM STP 636, Reifsnider, K.L.
      and Lauraitis, K.N., Editors, ASTM, 1977, p 152-170.

46   Ryder, J.T. and Walker, E.K., "Effects of Compression on Fatigue Properties of a Quasi-
      Isotropic Graphite/Epoxy Compoiste," <u>Fatigue of Filamentary Composite Materials</u>,
      ASTM STP 636, Reifsnider, K.L. and Lauraitis, K.N., Editors, ASTM, 1977.

47   Sendeckyj, G.P., Stalnaker, H.D. and Kleismit, R.A., "Effect of Temperature on Fatigue
      Response on Surface-Notched, $0/+--45/0_{s.3}$ Graphite/Epoxy Laminate," <u>Fatigue of
      Filamentary Composite Materials</u>, ASTM STP 636, Reifsnider, K.L. and Lauraitis, K.N.,
      Editors, ASTM, 1977, p 123-140.

48   Sims, D.F. and Brogdon, V.H., "Fatigue Behavior of Composites Under Different
      Loading Modes," <u>Fatigue of Filamentary Composite Materials</u>, ASTM STP 636,
      Reifsnider, K.L. and Lauraitis, K.N., Editors, ASTM, 1977, p 185-205.

49   Sun, C.T. and Chen J.K., "On the Impact of Initially Stresses Composite Laminates,"
      <u>Journal of Composites Materials</u>, Vol. 19, Nov. 1985.

50   Highsmith, A.L. and Reifsnider, K.L., "Internal Load Distribution Effects During Fatigue
      Loading of Composite Laminates," <u>Composite Materials: Fatigue and Fracture</u>, ASTM
      STP 907, H.T. Hahn, Editor, ASTM Phillidelphia, PA, 1986, p 233-251.

51   Reifsnider, K.L., Stinchcomb, W.W. and O'Brien, T.K., "Frequency Effects on a
      Stiffness-Based Fatigue Failure Criterion in Flawed Composite Specimens," <u>Fatigue of
      Filamentary Composite Materials</u>, ASTM STP 636, Reifsnider, K.L. and Lauraitis, K.N.,
      Editors, ASTM, 1977, p 171-184.

52   Hahn, H.T., "Fatigue of Composites," <u>Composites Guide</u>, University of Delaware, 1981.

53   Kundrat, R.J., Joneja, S.K. and Broutman, L.J., "Fatigue Damage of Hybrid Composite Materials," National Technical Conference on Polymer Alloys, Blands and Composites, The Society of Plastics Engineering, Bal Harbour, FL, Oct. 1982.

54   Kim, R.Y., "Fatigue Strength," <u>Engineered Materials Handbook</u>, Volume 1, Composites, ASM International, Materials Park, OH, 1987.

55   Talreja, R., "Estimation of Weibull Parameters for Composite Material Strength and Fatigue Life Data," <u>Fatigue of Composite Materials</u>, Technomic Publishing, Lancaster, PA, 1987.

56   Burral, et. al., "Cycle Test Evaluation of Various Polyester Types and a Mathematical Model for Projecting Flexural Fatigue Endurance," reprinted from 41st Annual SPI Conference, 1986, Section Marine I, Session 7-D.

57   Konur, O. and Mathews, L., "Effect of the Properties of the Constituents on the Fatigue Performance of Composites: A Review," <u>Composites</u>, Vol. 20 No. 4, July 1989.

58   Jones, David E., "Dynamic Loading Analysis and Advanced Composites," SNAME SE Section, May 1983.

59   Springer, G. S., Environmental Effects on Composite Materials, Volume 1, Technomic Publishing Co. (1981).

60   Burrell, P.P., et al, "A Study of Permeation Barriers to Prevent Blisters in Marine Composites and a Novel Technique for Evaluating Blister Formation", paper 15-E, 42nd Annual Conference, SPI Reinforced Plastics/Composites Institute (1987).

61   Allred, R. E., "The Effect of Temperature and Moisture Content on the Flexural Response of Kevlar®/Epoxy Laminates : Part I. 0/90 Filament Orientation", in Environmental Effects on Composite Materials, Volume 2, Editor G.S. Springer, Technomic Publishing Co. (1984)

62   Lagrange, A., et al, "Aging of E Glass Polyester Laminates and Degradation of Mechanical Properties in Sea Water", paper 8-B, 45th Annual Conference, SPI Composites Institute (1990).

63   Rockett, T. J., et al, "Boat Hull Blisters : Repair Techniques and Long Term Effects on Hull Degradation", final report submitted to USCG/DOT, American Boat Builders and Repairers Association (1988).

64   Shen, C., et al, "Effects of Moisture and Temperature on the Tensile Strength of Composite Materials", in Environmental Effects on Composite Materials, Volume 2, Editor G.S. Springer, Technomic Publishing Co. (1984)

65   Military Standard MIL-STD-2031(SH), <u>Fire and Toxicity Test Methods and Qualification Procedure for Composite Material Systems used in Hull, Machinery and Structural Applications Inside Naval Submarines</u>, Department of the Navy, 26 February, 1991.

66   ASTM E 1317-90, Standard Test Method for Flammability of Marine Surface Finishes, May 1990, ASTM, 100 Barr Harbor Dr., W. Conshohocken, PA 19428-2959.

67   SNAME T & R Bulletin, "Aluminum Fire Protection Guidelines," Pavonia, NJ, 1974.

68   Greene, Eric, "Fire Performance of Composite Materials for Naval Applications," Navy contract N61533-91-C-0017, Structural Composites, Inc, Melbourne, FL 1993.

Figure References

Figure 1-1   Midship Section Structural Design Diagram for Longitudinally Framed Ship, Evans, J.H., Massachusetts Institute of Technology, Ship Structural Design Concepts, published by arrangement with the Ship Structure Commitee, Cornell Maritime Press, Inc., Cambridge, MD, 1975.

Figure 1-2   Comparison of Various Fiber Architectures Using the Hydromat Panel Tester on 3:1 Aspect Ratio Panels, Fabric Handbook, Knytex, New Braunfels, TX, 1994.

Figure 1-3   Specific Strength and Stiffness of Various Construction Material, "Data Manual for Kevlar 49 Aramid," DuPont literature, Wilmington, DE.

Figure 1-4   Overview of Primary (Overall Hull Bending), Secondary (Hydrostatic and Hydrodynamic Forces Normal to Hull Surface) and Tertiary (Local Forces) Loads, orignal graphic.

Figure 1-5   Notation Typically Used to Describe Properties of Unidirectional Reinforcements, original graphic based on notation defined by Camponeschi, E.T, Kadala, E.E. And Wells, B.R, "Three-Dimensional Properties for the MHC-51 Fiberglass/Polyester Material Systems," US Navy CARDEROCKDIV-C-SSM-65-95/22, NAVSEA 03P1, limited distribution, June 1995.

Figure 1-6   Strength and Stiffness for Cored and Solid Construction, Hexcel, "The Basics on Sandwich Construction," TSB 124, 1987 revision, Dublin, CA.

Figure 1-7   Design Flow Chart for Primary Hull Laminate, original graphic.

Figure 1-8   Design Flow Chart for Bottom Panels Subject to Slamming, original graphic.

Figure 1-9   Design Flow Chart for Decks, original graphic.

Figure 1-10   Design Flow Chart for Deckhouses, original graphic.

Figure 1-11   Design Flow Chart for Bulkheads, original graphic.

Figure 1-12   Design Flow Chart for Stringers, original graphic.

Figure 1-13   Design Flow Chart for Joints and Structural Details, original graphic.

Figure 2-1   Reinforcement Fabric Construction Variations, Engineers' Guide to Composite Materials, Metals Park, OH; American Society for Metals, 1987 ed.

Figure 2-2   Comparison of Conventional Woven Roving and a Knitted Biaxial Fabric Showing Theoretical Kink Stress in Woven Roving, Composites Reinforcements, Inc., Walhalla, SC, Dec, 1987.

Figure 2-3   Balsa Cell Geometry, "Why Baltek Core: The Properties of End-Grain Balsa Core Make it Ideal for a Broad Spectrum of Composite Sandwich Structures," Baltek Corporation, data fiel 159, Northvale, NJ.

Figure 3-1   Bending Moment Development of Rectangular Barge in Still Water, Principles of Naval Architecture, by the Society of Naval Architects and Marine Engineers. New York, 1967.

Figure 3-2   Superposition of Static Wave Profile, Principles of Naval Architecture, by the Society of Naval Architects and Marine Engineers. New York, 1967.

Figure 3-3   Principal Axes and Ship Motion Nomenclature, Evans, J.H., Massachusetts Institute of Technology, Ship Structural Design Concepts, published by arrangement with the Ship Structure Commitee, Cornell Maritime Press, Inc., Cambridge, MD, 1975.

Figure 3-4   Pressures Recorded in Five and Six Foot Waves at a Speed of 28 Knots, Heller, S.R. and Jasper, N.H., "On the Structural Design of Planing Craft," Transactions, Royal Institution of Naval Architects, (1960) p 49-65.

Figure 3-5   Dynamic Load factors for Typical Time Varying Impact Loads, Heller, S.R. and

Jasper, N.H., "On the Structural Design of Planing Craft," <u>Transactions</u>, Royal Institution of Naval Architects, (1960) p 49-65.

Figure 3-6   Vertical Acceleration Factor as a Function of Distance from Bow, F_{V1}, Used in ABS Calculations, <u>Guide for Building and Classing High-Speed Craft</u>, ABS, Paramus, NJ, October 1990.

Figure 3-7   Vertical Acceleration Factor as a Function of Distance from Bow, F_{V2}, Used in ABS Calculations, <u>Guide for Building and Classing High-Speed Craft</u>, ABS, Paramus, NJ, October 1990.

Figure 3-8   Longitudinal Impact Coefficient as a Function of Distance from Bow, k_V, Used in Vertical Acceleration Calculations, NAVSEA "High Performance MarineCraft Design Manual Hull Structures," NAVSEACOMBATSYSENGSTA Report 60-204, July 1988. Distribution limited.

Figure 3-9   Design Area Coefficient Used in Design Pressure Calculations, NAVSEA "High Performance MarineCraft Design Manual Hull Structures," NAVSEACOMBATSYSENGSTA Report 60-204, July 1988. Distribution limited.

Figure 3-10   Longitudinal Pressure Distribution Used in Design Pressure Calculations, NAVSEA "High Performance MarineCraft Design Manual Hull Structures," NAVSEACOMBATSYSENGSTA Report 60-204, July 1988. Distribution limited.

Figure 3-11   Theoretical and Measured Stress Distribution for a Cargo Vessel Midship Section, <u>Principles of Naval Architecture</u>, by the Society of Naval Architects and Marine Engineers. New York, 1967.

Figure 3-12   Longitudinal Distribution of Stresses in a Combatant, Hovgaard, <u>Structural Design of Warships</u> (distributed with course notes by J.H. Evans, MIT 1977).

Figure 3-13   Distribution of Longitudinal Strains of a 38.5 Meter GRP Hull (above) and Longitudinal Strain Gage Location (below), X.S. Lu & X.D. Jin, "Structural Design and Tests of a Trial GRP Hull," <u>Marine Structures</u>, Elsever, 1990.

Figure 3-14   Predicted and Measured Vertical Displacements for a 38.5 Meter GRP Hull, X.S. Lu & X.D. Jin, "Structural Design and Tests of a Trial GRP Hull," <u>Marine Structures</u>, Elsever, 1990.

Figure 3-16   Green Water Distribution Factor, K_L, NAVSEA "High Performance MarineCraft Design Manual Hull Structures," NAVSEACOMBATSYSENGSTA Report 60-204, July 1988. Distribution limited.

Figure 4-1   State of Stress and Stress Transfer to Reinforcement, <u>Material Engineering</u>, May, 1978 p. 29.

Figure 4-2   Failure Mode as a Function of Fiber Alignment, <u>Engineers' Guide to Composite Materials</u>, Metals Park, OH; American Society for Metals, 1987 ed.

Figure 4-3   Fiber Composite Geometry, Chamis, <u>Engineers' Guide to Composite Materials</u>, Metals Park, OH; American Society for Metals, 1987 ed.

Figure 4-4   Typical Stress-Strain Behavior of Unidirectional Fiber Composites, Chamis, <u>Engineers' Guide to Composite Materials</u>, Metals Park, OH; American Society for Metals, 1987 ed.

Figure 4-5   Notation Typically Used to Describe Ply Properties, original graphic based on notation defined by Camponeschi, E.T, Kadala, E.E. And Wells, B.R, "Three-Dimensional Properties for the MHC-51 Fiberglass/Polyester Material Systems," US Navy CARDEROCKDIV-C-SSM-65-95/22, NAVSEA 03P1, limited distribution, June 1995.

Figure 4-6   Elastic Properties of Plies within a Laminate, Schwartz, Mel M., <u>Composite Materials Handbook</u>, McGraw Hill, New York, 1984.

Figure 4-7 Carpet Plot Illustrating Laminate Tensile Modulus, Engineered Materials Handbook, Volume 1, Composites, ASM International, Metals park, OH, May 1988.

Figure 4-8 Carpet Plot Illustrating Poisson's Ratio, Engineered Materials Handbook, Volume 1, Composites, ASM International, Metals park, OH, May 1988.

Figure 4-9 Carpet Plot Illustrating Tensile Strength, Engineered Materials Handbook, Volume 1, Composites, ASM International, Metals park, OH, May 1988.

Figure 4-10 Test Specimen Configuration for ASTM D-3039 and D-638 Tensile Tests, graphic developed by Structural Composites, Inc. from test standard.

Figure 4-11 Test Specimen Configuration for ASTM D-695 Compression Test, graphic developed by Structural Composites, Inc. from test standard.

Figure 4-12 Test Specimen Configuration for SACMA SRM-1 Compression Test, graphic developed by Structural Composites, Inc. from test standard.

Figure 4-13 Test Specimen Configuration for ASTM D-790 Flexural Test, Method I, Procedure A, graphic developed by Structural Composites, Inc. from test standard.

Figure 4-14 Test Specimen Configuration for ASTM D-2344 Sort Beam Shear Test, graphic developed by Structural Composites, Inc. from test standard.

Figure 4-15 Test Specimen Configuration for ASTM D-3518 In-Plane Shear Test, graphic developed by Structural Composites, Inc. from test standard.

Figure 4-16 Test Specimen Configuration for ASTM D-3846 In-Plane Shear Test, graphic developed by Structural Composites, Inc. from test standard.

Figure 4-17 Test Specimen Configuration for ASTM D-4255 Rail Shear Test, Method A, graphic developed by Structural Composites, Inc. from test standard.

Figure 4-18 Test Specimen Configuration for ASTM C-297 Core Flatwise Tensile Test, graphic developed by Structural Composites, Inc. from test standard.

Figure 4-19 Test Specimen Configuration for ASTM C-273 Core Shear Test, graphic developed by Structural Composites, Inc. from test standard.

Figure 5-1 h_c as a Function of Edge Stiffener Factor, Department of the Navy, DDS-9110-9, Strength of Glass Reinforced Plastic Structural Members Part I-Single Skin Construction, August, 1969, document subject to export control when published.

Figure 5-2 h_c as a Function of Edge Stiffener Factor, Department of the Navy, DDS-9110-9, Strength of Glass Reinforced Plastic Structural Members Part I-Single Skin Construction, August, 1969, document subject to export control when published.

Figure 5-3 h_c as a Function of Edge Stiffener Factor, Department of the Navy, DDS-9110-9, Strength of Glass Reinforced Plastic Structural Members Part I-Single Skin Construction, August, 1969, document subject to export control when published.

Figure 5-4 H_s as a Function of the Inverse of Edge Stiffener Factor, Department of the Navy, DDS-9110-9, Strength of Glass Reinforced Plastic Structural Members Part I-Single Skin Construction, August, 1969, document subject to export control when published.

Figure 5-5 H_s as a Function of the Inverse of Edge Stiffener Factor, Department of the Navy, DDS-9110-9, Strength of Glass Reinforced Plastic Structural Members Part I-Single Skin Construction, August, 1969, document subject to export control when published.

Figure 5-6 K_8 as a Function of Edge Stiffener Factor, Department of the Navy, DDS-9110-9, Strength of Glass Reinforced Plastic Structural Members Part I-Single Skin Construction, August, 1969, document subject to export control when published.

Figure 5-7 C_f as a Function of m, Department of the Navy, DDS-9110-9, Strength of Glass Reinforced Plastic Structural Members Part I-Single Skin Construction, August, 1969, document subject to export control when published.

Figure 5-8 C_f as a Function of m, Department of the Navy, DDS-9110-9, <u>Strength of Glass Reinforced Plastic Structural Members Part I-Single Skin Construction</u>, August, 1969, document subject to export control when published.

Figure 5-9 C_f as a Function of m, Department of the Navy, DDS-9110-9, <u>Strength of Glass Reinforced Plastic Structural Members Part I-Single Skin Construction</u>, August, 1969, document subject to export control when published.

Figure 5-10 $\frac{\Delta}{t}$ as a Function of $\frac{\delta}{t}$ and C, Department of the Navy, DDS-9110-9, <u>Strength of Glass Reinforced Plastic Structural Members Part I-Single Skin Construction</u>, August, 1969, document subject to export control when published.

Figure 5-11 $\frac{\Delta}{t}$ as a Function of $\frac{\delta}{t}$ and C, Department of the Navy, DDS-9110-9, <u>Strength of Glass Reinforced Plastic Structural Members Part I-Single Skin Construction</u>, August, 1969, document subject to export control when published.

Figure 5-12   Coefficient for Bending Stiffness Factor, Department of the Navy, DDS-9110-9, <u>Strength of Glass Reinforced Plastic Structural Members Part II-Sandwich Panels</u>, August, 1969, document subject to export control when published.

Figure 5-13   Values of K_{MO} for Sandwich Panels in Edgewise Compression, Department of the Navy, DDS-9110-9, <u>Strength of Glass Reinforced Plastic Structural Members Part II-Sandwich Panels</u>, August, 1969, document subject to export control when published.

Figure 5-14 K_M for Sandwich Panels with Ends and Sides Simply Supported and Orthotropic Core (G_{Cb} = 2.5 G_{Ca}), Department of the Navy, DDS-9110-9, <u>Strength of Glass Reinforced Plastic Structural Members Part II-Sandwich Panels</u>, August, 1969, document subject to export control when published.

Figure 5-15 K_M for Sandwich Panels with Ends and Sides Simply Supported and Isotropic Core ($G_{Cb} = G_{Ca}$), Department of the Navy, DDS-9110-9, <u>Strength of Glass Reinforced Plastic Structural Members Part II-Sandwich Panels</u>, August, 1969, document subject to export control when published.

Figure 5-16 K_M for Sandwich Panels with Ends and Sides Simply Supported and Orthotropic Core (G_{Cb} = 0.4 G_{Ca}), Department of the Navy, DDS-9110-9, <u>Strength of Glass Reinforced Plastic Structural Members Part II-Sandwich Panels</u>, August, 1969, document subject to export control when published.

Figure 5-17 K_M for Sandwich Panels with Ends Simply Supported, Sides Clamped and Orthotropic Core (G_{Cb} = 2.5 G_{Ca}), Department of the Navy, DDS-9110-9, <u>Strength of Glass Reinforced Plastic Structural Members Part II-Sandwich Panels</u>, August, 1969, document subject to export control when published.

Figure 5-18 K_M for Sandwich Panels with Ends Simply Supported, Sides Clamped and Isotropic Core ($G_{Cb} = G_{Ca}$), Department of the Navy, DDS-9110-9, <u>Strength of Glass Reinforced Plastic Structural Members Part II-Sandwich Panels</u>, August, 1969, document subject to export control when published.

Figure 5-19 K_M for Sandwich Panels with Ends Simply Supported, Sides Clamped and Orthotropic Core (G_{Cb} = 0.4 G_{Ca}), Department of the Navy, DDS-9110-9, <u>Strength of Glass Reinforced Plastic Structural Members Part II-Sandwich Panels</u>, August, 1969, document subject to export control when published.

Figure 5-20 K_M for Sandwich Panels with Ends Clamped, Sides Simply Supported and Orthotropic Core (G_{Cb} = 2.5 G_{Ca}), Department of the Navy, DDS-9110-9, <u>Strength of Glass Reinforced Plastic Structural Members Part II-Sandwich Panels</u>, August, 1969, document subject to export control when published.

Figure 5-21 K_M for Sandwich Panels with Ends Clamped, Sides Simply Supported and

Isotropic Core ($G_{Cb} = G_{Ca}$), Department of the Navy, DDS-9110-9, <u>Strength of Glass Reinforced Plastic Structural Members Part II-Sandwich Panels</u>, August, 1969, document subject to export control when published.

Figure 5-22 K_M for Sandwich Panels with Ends Clamped, Sides Simply Supported and Orthotropic Core ($G_{Cb} = 0.4\ G_{Ca}$), Department of the Navy, DDS-9110-9, <u>Strength of Glass Reinforced Plastic Structural Members Part II-Sandwich Panels</u>, August, 1969, document subject to export control when published.

Figure 5-23 K_M for Sandwich Panels with Ends and Sides Clamped and Orthotropic Core ($G_{Cb} = 2.5\ G_{Ca}$), Department of the Navy, DDS-9110-9, <u>Strength of Glass Reinforced Plastic Structural Members Part II-Sandwich Panels</u>, August, 1969, document subject to export control when published.

Figure 5-24 K_M for Sandwich Panels with Ends and Sides Clamped and Isotropic Core ($G_{Cb} = G_{Ca}$), Department of the Navy, DDS-9110-9, <u>Strength of Glass Reinforced Plastic Structural Members Part II-Sandwich Panels</u>, August, 1969, document subject to export control when published.

Figure 5-25 K_M for Sandwich Panels with Ends and Sides Clamped and Orthotropic Core ($G_{Cb} = 0.4\ G_{Ca}$), Department of the Navy, DDS-9110-9, <u>Strength of Glass Reinforced Plastic Structural Members Part II-Sandwich Panels</u>, August, 1969, document subject to export control when published.

Figure 5-26 Parameters for Face Wrinkling Formulas, Department of the Navy, DDS-9110-9, <u>Strength of Glass Reinforced Plastic Structural Members Part II-Sandwich Panels</u>, August, 1969, document subject to export control when published.

Figure 5-27 K_M for Sandwich Panels with All Edges Simply Supported and Isotropic Core, Department of the Navy, DDS-9110-9, <u>Strength of Glass Reinforced Plastic Structural Members Part II-Sandwich Panels</u>, August, 1969, document subject to export control when published.

Figure 5-28 K_M for Sandwich Panels with All Edges Simply Supported and Orthotropic Core ($G_{Cb} = 0.4\ G_{Ca}$), Department of the Navy, DDS-9110-9, <u>Strength of Glass Reinforced Plastic Structural Members Part II-Sandwich Panels</u>, August, 1969, document subject to export control when published.

Figure 5-29 K_M for Sandwich Panels with All Edges Simply Supported and Orthotropic Core ($G_{Cb} = 2.5\ G_{Ca}$), Department of the Navy, DDS-9110-9, <u>Strength of Glass Reinforced Plastic Structural Members Part II-Sandwich Panels</u>, August, 1969, document subject to export control when published.

Figure 5-30 K_M for Sandwich Panels with All Edges Clamped, Isotropic Facings and Isotropic Core , DDS 9110-9.Department of the Navy, DDS-9110-9, <u>Strength of Glass Reinforced Plastic Structural Members Part II-Sandwich Panels</u>, August, 1969, document subject to export control when published.

Figure 5-31 K_M for Sandwich Panels with All Edges Clamped, Isotropic Facings and Orthotropic Core ($G_{Cb} = 0.4\ G_{Ca}$), Department of the Navy, DDS-9110-9, <u>Strength of Glass Reinforced Plastic Structural Members Part II-Sandwich Panels</u>, August, 1969, document subject to export control when published.

Figure 5-32 K_M for Sandwich Panels with All Edges Clamped, Isotropic Facings and Orthotropic Core ($G_{Cb} = 2.5\ G_{Ca}$), Department of the Navy, DDS-9110-9, <u>Strength of Glass Reinforced Plastic Structural Members Part II-Sandwich Panels</u>, August, 1969, document subject to export control when published.

Figure 5-33 K_1 for Maximum Deflection,, of Flat, Rectangular Sandwich Panels with Isotropic Facings and Isotropic or Orthotropic Cores Under Uniform Loads, Department of the Navy, DDS-9110-9, <u>Strength of Glass Reinforced Plastic Structural Members Part II-Sandwich Panels</u>, August, 1969, document subject to export control when published.

Figure 5-34 K_2 for Determining Face Stress, F_F of Flat, Rectangular Sandwich Panels with

Isotropic Facings and Isotropic or Orthotropic Cores Under Uniform Loads, Department of the Navy, DDS-9110-9, <u>Strength of Glass Reinforced Plastic Structural Members Part II-Sandwich Panels</u>, August, 1969, document subject to export control when published.

Figure 5-35 K_3 for Determining Maximum Core Shear Stress, F_{Cs}, for Sandwich Panels with Isotropic Facings and Isotropic or Orthotropic Cores Under Uniform Loads, Department of the Navy, DDS-9110-9, <u>Strength of Glass Reinforced Plastic Structural Members Part II-Sandwich Panels</u>, August, 1969, document subject to export control when published.

Figure 5-36 Transversely Stiffened Panel, Smith, C.S., "Buckling Problems in the Design of Fiberglass-Reinforced Plastic Ships," <u>Journal of Ship Research</u>, (Sept., 1972) p. 174-190.

Figure 5-37 Interframe Buckling Modes, Smith, C.S., "Buckling Problems in the Design of Fiberglass-Reinforced Plastic Ships," <u>Journal of Ship Research</u>, (Sept., 1972) p. 174-190.

Figure 5-38 Extraframe Buckling Modes, Smith, C.S., "Buckling Problems in the Design of Fiberglass-Reinforced Plastic Ships," <u>Journal of Ship Research</u>, (Sept., 1972) p. 174-190.

Figure 5-39 Plane Stress Analysis of Hatch Opening, Smith, C.S., "Buckling Problems in the Design of Fiberglass-Reinforced Plastic Ships," <u>Journal of Ship Research</u>, (Sept., 1972) p. 174-190.

Figure 5-40 Deck Grillage Buckling Modes Near Hatch Opening, Smith, C.S., "Buckling Problems in the Design of Fiberglass-Reinforced Plastic Ships," <u>Journal of Ship Research</u>, (Sept., 1972) p. 174-190.

Figure 5-41 Deck Edge Connection - Normal Deck and Shell Loading Produces Tension at the Joint, Gibbs & Cox, Inc., <u>Marine Design Manual for Fiberglass Reinforced Plastics</u>, sponsored by Owens-Corning Fiberglas Corporation, McGraw-Hill, New York, 1960.

Figure 5-42 Improved Hull to Deck Joint for Sandwich Core Production Vessels, original graphic.

Figure 5-43 Connection of Bulkheads and Framing to Shell or Deck, Gibbs & Cox, Inc., <u>Marine Design Manual for Fiberglass Reinforced Plastics</u>, sponsored by Owens-Corning Fiberglas Corporation, McGraw-Hill, New York, 1960.

Figure 5-44 Double Bias and Woven Roving Bulkhead Tape-In, Knytex product literature, Seguin, TX.

Figure 5-45 Reference Stiffener Span Dimensions, Al Horsmon, USCG NVIC No. 8-87, Notes on Design, Construction, Inspection and Repair of Fiber Reinforced Plastic (FRP) Vessels.

Figure 5-46 Stringer Geometry for Sandwich Construction, Al Horsmon, USCG NVIC No. 8-87, Notes on Design, Construction, Inspection and Repair of Fiber Reinforced Plastic (FRP) Vessels.

Figure 5-47 Stringer Geometry including High-Strength Reinforcement (3" wide layer of Kevlar® in the top), Al Horsmon, USCG NVIC No. 8-87, Notes on Design, Construction, Inspection and Repair of Fiber Reinforced Plastic (FRP) Vessels.

Figure 5-48 High Density Insert for Threaded or Bolted fasteners in Sandwich Construction, Gibbs & Cox, Inc., <u>Marine Design Manual for Fiberglass Reinforced Plastics</u>, sponsored by Owens-Corning Fiberglas Corporation, McGraw-Hill, New York, 1960.

Figure 5-49 Through Bolting in Sandwich Construction, Gibbs & Cox, Inc., <u>Marine Design Manual for Fiberglass Reinforced Plastics</u>, sponsored by Owens-Corning Fiberglas Corporation, McGraw-Hill, New York, 1960.

Figure 5-50 Schematic Diagram of Panel Testing Pressure Table, Reichard, Ronnal P., "Pressure Panel Testing of GRP Sandwich Panels,", MACM' 92 Conference, Melbourne, FL, March 24-26, 1992.

Figure 5-51 Computed and Measured Deflections (mils) of PVC Foam Core Panels

Subjected to a 10 psi Load, from Reichard, Ronnal P., "Pressure Panel Testing of GRP Sandwich Panels,", MACM' 92 Conference, Melbourne, FL, March 24-26, 1992.

Figure 5-52 Schematic Diagram of the Hydromat Test System, Bertlesen, W.D and Sikarskie, D.L., "Verification of the Hydromat Test System as a Viable Means of Testing Two-Dimensional Sandwich Panels," project funding request submitted to SNAME T & R panel HS-9, Sep, 1994 and ASTM D30.05.

Figure 6-1 Tensile Failure Modes of Engineered Plastics Defined by ASTM, ASTM D 638-84, ASTM, West Conshohocken, PA.

Figure 6-2 Illustration of Membrane Tension in a Deflected Panel, from personal correspondence with Scott Mattson, OMC Corporation.

Figure 6-3 Compressive Failure Modes of Sandwich Laminates, Giancarlo Caprino Roberto Teti, University of Naples, Sandwich Structures Handbook, Edizioni Il Prato, April, 1989.

Figure 6-4 Critical Length for Euler Buckling Formula Based on End Condition, Giancarlo Caprino Roberto Teti, University of Naples, Sandwich Structures Handbook, Edizioni Il Prato, April, 1989.

Figure 6-5 Nomenclature for Describing Bending Stress in Solid Beam, original graphic.

Figure 6-6 Nomenclature for Describing Shear Stress in Solid Beam, original graphic.

Figure 6-7 Bending and Shear Stress Distribution in Sandwich Beams (2-D) with Relatively Stiff Cores, adapted from Structural Plastics Design Manual, ASCE Manuals and Reports on Engineering Practice number 63, published by the American Society of Civil Engineers, New York, NY, 1984.

Figure 6-8 Bending and Shear Stress Distribution in Sandwich Beams (2-D) with Relatively Soft Cores, Structural Plastics Design Manual, ASCE Manuals and Reports on Engineering Practice number 63, published by the American Society of Civil Engineers, New York, NY, 1984.

Figure 6-9 Stress Distribution with Flexible Cores, adapted from Structural Plastics Design Manual, ASCE Manuals and Reports on Engineering Practice number 63, published by the American Society of Civil Engineers, New York, NY, 1984.

Figure 6-10 Variation in Viscoelastic Modulus with Time, Structural Plastics Design Manual, ASCE Manuals and Reports on Engineering Practice number 63, published by the American Society of Civil Engineers, New York, NY, 1984.

Figure 6-11 Typical Comparison of Metal and Composite Fatigue Damage, Salkind, M.J., "Fatigue of Composites," Composite Materials: Testing and Design (Second Conference), ASTM STP 497, 1972, p. 143-169, ASTM, West Conshohocken, PA.

Figure 6-12 Comparison of Metal and Composite Stiffness Reduction, Salkind, M.J., "Fatigue of Composites," Composite Materials: Testing and Design (Second Conference), ASTM STP 497, 1972, p. 143-169, ASTM, West Conshohocken, PA.

Figure 6-13 Fatigue Failure Modes for Composite Materials, Hahn, H.T., "Fatigue of Composites," Composites Guide, University of Delaware, 1981.

Figure 6-14 Comparison of Fatigue Strengths of Graphite/Epoxy, Steel, Fiberglass/Epoxy and Aluminum, Hercules product literature, Magna, UT.

Figure 6-15 Curve Fit of ASTM D671 Data for Various Types of Unsaturated Polyester Resins, Burral, et. al., "Cycle Test Evaluation of Various Polyester Types and a Mathematical Model for Projecting Flexural Fatigue Endurance," reprinted from 41st Annual SPI Conference, 1986, Section Marine I, Session 7-D.

Figure 6-16 Comparitive Fatigue Strengths of Woven and Nonwoven Unidirectional Glass Fiber Reinforced Plasitc Laminates, Engineers' Guide to Composite Materials, Metals Park, OH; American Society for Metals, 1987 ed.

Figure 6-17   Sketch of the Functional Parts of the Limiting Oxygen Index Apparatus, Rollhauser, C., *Fire Tests of Joiner Bulkhead Panels*, internal Navy report via personal correspondence.

Figure 6-18   Smoke Obscuration Chamber, ASTM E 662, "Standard Test Method for Specific Optical Density of Smoke Generated by Solid Materials, Nov 1983, ASTM, West Conshohocken, PA.

Figure 6-19   Sketch of the Functional Parts of the NBS Radiant Panel Test Configuration, Rollhauser, C., *Fire Tests of Joiner Bulkhead Panels*, internal Navy report via personal correspondence.

Figure 6-20   Sketch of the Functional Parts of a Cone Calorimeter, Rollhauser, C., *Fire Tests of Joiner Bulkhead Panels*, internal Navy report via personal correspondence.

Figure 6-21   Sketch of the DTRC Burn Through Sample and Holder, Rollhauser, C., *Fire Tests of Joiner Bulkhead Panels*, internal Navy report via personal correspondence.

Figure 6-22   LIFT Apparatus Geometry, author photo taken at NIST Building and Fire Research Laboratory.

Figure 6-23   LIFT Test Panel at the Time of Ignition, author photo taken at NIST Building and Fire Research Laboratory.

Figure 6-24   ASTM E 1317 Flame Front Flux vs Time**,** data taken from ASTM E 1317-90, "Standard Test Method for Flammability of Marine Surface Finish," ASTM, Conshohocken, PA.

Figure 6-25   Geometry of E 119 Multiplane Load Jig, graphic developed for SBIR Phase II project, "Fire Performance of Composite Materials for Naval Applications," contract N61533-91-C-0017, Structural Composites, Inc, Melbourne, FL, Nov 1993.

Figure 6-26   Heat Flux from 3-foot Furnace at VTEC using the E 119 (SOLAS) Time/Temperature Curve, original graphic based on VTEC data.

Figure 6-27   Comparison of Three Fire Tests, original graphic based on Rollhauser, C., *Integrated Technology Deckhouse,* internal Navy report via personal correspondence.

Figure 6-28   Fire Test Room Dimensions (in Meters) for ISO 9705 Test, original graphic from International Standard ISO/DIS 9705, Fire tests - Full scale room test for surface products, International Organization for Standardization, 1990

Figure 6-29   Geometry of Sand Burner Used for ISO 9705 Test (dimensions in mm), International Standard ISO/DIS 9705, Fire tests - Full scale room test for surface products, International Organization for Standardization, 1990

Figure 6-30   Coverage for Modified ISO 9705 Test Using (2) 4' x 8' Sheets of Material, original graphic developed for modified ISO-9705 test with reduced material.

Figure 6-31   ISO 9705-Type Test with Reduced Material Quantities at VTEC Laboratories, author photo at VTEC Laboratories.

Figure 6-32   General Arrangement for 3-foot Panels Tested under E-119 Insult with Insulation, graphic developed for SBIR Phase II project, "Fire Performance of Composite Materials for Naval Applications," contract N61533-91-C-0017, Structural Composites, Inc, Melbourne, FL, Nov 1993.

Figure 6-33   Stiffness and Temperature Data for Balsa-Cored E-Glass/Vinyl Ester Panel with 2″ Lo-Con Ceramic Insulation Tested with Multiplane Load Jig and E-119 Fire, data from SBIR Phase II project, "Fire Performance of Composite Materials for Naval Applications," contract N61533-91-C-0017, Structural Composites, Inc, Melbourne, FL, Nov 1993.

Advanced Textiles Reinforcements

Reinforcement Description		Tensile Longitudinal Strength (ksi)	Tensile Longitudinal Modulus (msi)	Tensile Transverse Strength (ksi)	Tensile Transverse Modulus (msi)	Tensile Diagonal Strength (ksi)	Tensile Diagonal Modulus (msi)	Compressive Longitudinal Strength (ksi)	Compressive Longitudinal Modulus (msi)	Compressive Transverse Strength (ksi)	Compressive Transverse Modulus (msi)	Compressive Diagonal Strength (ksi)	Compressive Diagonal Modulus (msi)	Flexural Longitudinal Strength (ksi)	Flexural Longitudinal Modulus (msi)	Flexural Transverse Strength (ksi)	Flexural Transverse Modulus (msi)	Flexural Diagonal Strength (ksi)	Flexural Diagonal Modulus (msi)	Thickness Per Ply (mils)	% Fiber by Weight	Fiber Weight (oz/yd²)
C-1200 (NEWF 120)	0/90 knit	30.54	2.05	21.69	1.43	11.49	0.74	40.66	2.47	30.65	2.02			59.67	1.98	37.07	0.71			24	41.8%	12.2
C-1600 (NEWF 160)	0/90 knit	40.72	2.65	41.00	2.19	11.26	1.31	37.04	2.69	37.08	2.43			47.59	1.39	47.80	1.43			25	58.0%	15.5
C-1800 (NEWF 180)	0/90 knit	42.96	2.90	21.18	1.66	10.99	1.18	47.92	3.06	34.08	2.07			64.57	2.07	30.53	1.00			32	51.2%	17.7
C-2300 (NEWF 230)	0/90 knit	32.62	2.65	31.43	2.55	9.14	0.88	33.65	2.89	35.70	1.95			57.30	2.18	39.08	1.46			37	54.5%	23.2
CM-1208 (NEWFC 1208)	0/90 knit w/mat	36.76	2.17	21.14	1.66	14.13	1.34	42.40	2.81	29.22	1.71			65.62	2.30	34.61	1.26			37	47.4%	18.9
CM-1215 (NEWFC 1215)	0/90 knit w/mat	23.00	1.86	17.00	1.33			18.00	1.89	16.00	1.60			43.00	1.56	29.00	1.14				34.8%	25.6
CM-1608 (NEWFC 1608)	0/90 knit w/mat	24.75	2.13	27.82	2.07	13.17	1.22	29.93	1.92	23.74	1.90			57.08	1.78	42.40	1.39			44	45.2%	22.5
CM-1615 (NEWFC 1615)	0/90 knit w/mat	22.00	1.77	24.21	1.87	13.63	1.22	21.52	2.05	25.07	1.87			51.17	1.88	47.66	1.67			56	44.3%	29.0
CM-1808 (NEWFC 1808)	0/90 knit w/mat	35.27	2.59	21.21	1.74	13.34	1.19	39.28	2.13	24.39	2.90			63.96	2.07	34.61	1.12			43	46.9%	24.4
CM-1815 (NEWFC 1815)	0/90 knit w/mat	28.48	2.20	21.09	1.82	15.00	1.15	37.00	2.72	23.38	2.06			58.14	2.38	39.13	1.61			57	48.4%	31.2
CM-2308 (NEWFC 2308)	0/90 knit w/mat	29.90	2.37	32.13	2.28	13.86	1.36	38.83	3.13	35.59	2.52			55.55	1.90	50.91	1.42			53	48.8%	29.0
CM-2315 (NEWFC 2315)	0/90 knit w/mat	26.33	1.85	25.73	1.79	13.07	1.18	34.99	2.13	31.76	2.52			51.38	2.03	45.72	1.69			73	48.4%	36.7
CM-3308 (NEWFC 3308)	0/90 knit w/mat	41.19	2.38	48.24	2.52			50.13	2.80	50.23	2.77			66.00	1.80	75.39	1.21			61	55.2%	
CM-3415 (NEWFC 3415)	0/90 knit w/mat	25.46	1.98	33.42	2.01	11.65	1.10	39.99	2.48	38.52	3.16	21.33	1.49	50.08	1.74	53.23	1.65	26.13	1.01	80	50.1%	
CM-3610 (NEWFC 3610)	0/90 knit w/mat	29.86	2.17	41.02	2.27			37.44	3.02	39.34	2.77			49.44	1.84	65.76	2.02			76	51.9%	
X-090 (NEMP 090)	+/-45 knit	6.90	0.75	22.65	1.26	23.24	1.68	18.67	0.81	17.80	1.15	41.84	1.74	23.35	0.57	45.33	1.18	48.93	1.56	20	39.0%	9.5
X-120 (NEMP 120)	+/-45 knit	6.70	0.80	23.19	1.24	29.38	1.70	15.07	0.80	15.30	1.20	41.26	2.08	19.31	0.67	27.46	1.08	50.66	1.72	27	38.1%	12.4
X-170 (NEMP 170)	+/-45 knit	7.61	0.70	23.23	1.12	30.10	1.97	15.82	0.85	16.31	1.11	39.69	1.64	25.16	0.76	45.58	1.15	61.13	1.67	34	46.5%	17.6
X-240 (NEMP 240)	+/-45 knit	5.29	1.00	20.35	1.76	26.57	2.08	15.07	0.76	15.44	1.16	42.69	2.03	17.76	0.62	45.62	1.10	61.70	1.88	41	47.8%	24.2
XM-1208 (NEMPC1208)	+/-45 knit w/mat	13.59	1.30	15.94	1.33	27.04	2.03	21.84	1.04	23.36	1.15	37.44	1.83	31.33	0.92	35.97	1.03	48.37	1.40	39	44.1%	19.2
XM-1215 (NEMPC1215)	+/-45 knit w/mat	15.68	1.20	16.25	1.02	27.00	2.19	22.05	1.33	22.63	1.17	31.69	2.09	26.67	1.22	29.93	1.32	45.47	1.80	47	46.1%	26.0
XM-1708 (NEMPC 1708)	+/-45 knit w/mat	14.26	1.31	16.22	1.25	31.82	2.05	20.96	1.22	21.42	1.18	38.76	2.04	38.43	0.88	36.41	1.07	60.96	1.65	44	46.7%	24.4
XM-1715 (NEMPC 1715)	+/-45 knit w/mat	16.20	1.36	16.49	1.35	31.49	2.25	20.28	1.25	21.26	1.21	34.53	2.03	34.45	1.18	35.24	1.32	51.19	1.84	51	50.2%	31.1
XM-2408 (NEMPC 2408)	+/-45 knit w/mat	10.58	1.14	20.48	1.34	31.82	2.05	19.30	0.99	20.53	1.16	39.33	2.07	27.08	1.17	42.91	1.37	55.77	1.77	50	50.3%	31.0
XM-2415 (NEMPC 2415)	+/-45 knit w/mat	13.53	1.22	18.92	1.62	24.99	2.19	16.25	0.92	17.09	1.07	25.65	1.39	28.64	1.17	38.66	1.21	45.71	1.54	66	48.7%	37.8
TV-200 (NEWMP 200)	0, +/-45 knit	36.40	2.14	11.78	0.98	18.15	1.72	32.80	1.97	20.13	1.09	28.38	1.90	70.21	2.06	28.53	0.59	38.65	1.00	34	48.7%	20.2
TV-230 (NEWMP 230)	0, +/-45 knit	30.49	1.67	15.22	0.93	24.64	1.39	29.45	2.48	23.37	1.18	36.70	1.87	63.71	1.85	32.78	0.62	50.71	1.34	39	46.9%	22.8
TV-340 (NEWMP 340)	0, +/-45 knit	31.15	1.71	12.95	1.38	21.76	1.59	29.19	2.78	19.96	1.40	28.67	1.68	70.26	2.22	26.63	0.50	47.92	1.17	49	46.8%	33.1
TVM-2008 (NEWMPC 2008)	0, +/-45 knit w/mat	32.15	2.33	11.73	1.16	17.97	1.39	34.07	2.33	22.60	1.24	26.66	2.11	62.39	1.75	27.65	0.66	40.71	1.03	49	47.6%	27.1
TVM-2308 (NEWMPC 2308)	0, +/-45 knit w/mat	29.46	1.73	13.45	0.94	25.16	1.43	33.14	2.05	23.67	1.13	31.97	1.69	66.71	2.02	31.29	0.84	48.34	1.15	49	50.3%	29.5
TVM-2315 (NEWMPC 2315)	0, +/-45 knit w/mat	29.05	2.79	14.10	1.95	21.77	1.65	26.71	1.98	21.19	1.39	25.70	1.80	54.04	1.84	33.66	0.80	51.04	1.32	59	51.9%	
TVM-3408 (NEWMPC 3408)	0, +/-45 knit w/mat	32.41	1.54	13.28	1.80	24.13	1.84	25.61	2.36	18.76	1.50	30.76	2.16	60.42	2.18	28.23	0.69	46.69	1.38	71	53.5%	40.2
TVM-3415 (NEWMPC 3415)	0, +/-45 knit w/mat	33.86	2.42	12.33	1.42	23.80	1.51	30.61	1.80	20.19	1.35	29.67	2.63	57.46	1.55	40.08	0.68	40.08	1.03	37	53.8%	46.8
TH-200 (NEFMP 200)	90, +/-45 knit	11.60	1.00	34.09	2.23	21.97	1.89	20.08	1.02	41.39	1.80	33.14	1.62	23.85	1.00	54.50	1.81	33.56	1.02	44	47.4%	
TH-230 (NEFMP 230)	90, +/-45 knit	8.86	1.00	33.38	2.11	22.48	1.75	19.60	0.90	38.82	1.96	35.37	1.87	21.86	0.66	56.57	1.75	44.81	1.30	55	46.6%	22.8
TH-340 (NEFMP 340)	90, +/-45 knit	8.02	1.06	37.62	2.80	20.07	1.90	20.74	1.07	47.04	2.45	34.90	1.89	18.44	0.57	63.53	2.26	43.61	1.45	54	50.6%	33.1
THM-2308 (NEFMPC 2308)	90, +/-45 knit & mat	10.85	1.10	29.88	1.83	20.59	1.67	16.12	0.90	30.37	1.50	19.14	1.34	25.63	0.79	51.43	1.82	45.67	1.48	71	46.2%	29.5
THM-3408 (NEFMPC 3408)	90, +/-45 knit & mat	8.41	1.31	37.97	2.45	18.24	1.70	17.70	1.06	40.22	2.36	31.75	1.66	16.44	0.77	63.05	1.83	44.28	1.34	71	48.6%	40.2

BTI Reinforcements

Code	Description	Tensile Str. Long. (ksi)	Tensile Mod. Long. (msi)	Tensile Str. Trans. (ksi)	Tensile Mod. Trans. (msi)	Tensile Str. Diag. (ksi)	Tensile Mod. Diag. (msi)	Compr. Str. Long. (ksi)	Compr. Mod. Long. (msi)	Compr. Str. Trans. (ksi)	Compr. Mod. Trans. (msi)	Compr. Str. Diag. (ksi)	Compr. Mod. Diag. (msi)	Flex. Str. Long. (ksi)	Flex. Mod. Long. (msi)	Flex. Str. Trans. (ksi)	Flex. Mod. Trans. (msi)	Flex. Str. Diag. (ksi)	Flex. Mod. Diag. (msi)	Thickness Per Ply (mils)	% Fiber by Weight (%)	Fiber Weight (oz/yd²)
C-1800	0/90 knit	28.80	1.90					43.09	2.60					52.00	2.18					33	44.8%	18.0
C-2400	0/90 knit	35.00	2.20					37.23	2.80					64.70	2.40					39	49.7%	24.0
CM-1603	0/90 deg w/mat	34.00	2.00					36.00	2.20					56.00	2.10					37	52.0%	
CM-1808	0/90 deg w/mat	29.20	2.00					27.20	1.70					45.00	1.90					48	43.0%	24.8
CM-1810	0/90 deg w/mat	29.10	2.00					31.60	2.60					46.60	1.86					52	42.0%	27.0
CM-1815	0/90 deg w/mat	27.10	2.00					32.80	2.70					42.50	1.90					55	44.0%	31.5
CM-2403	0/90 deg w/mat	32.00	1.90					33.00	2.40					58.00	2.00					45	50.0%	
CM-2408	0/90 deg w/mat	30.10	1.90					30.30	1.80					51.50	2.00					55	46.0%	30.8
CM-2410	0/90 deg w/mat	29.00	1.90					37.00	2.70					50.00	2.00					62	47.0%	33.0
CM-2415	0/90 deg w/mat	36.97	2.25					36.47	2.70					46.00	1.96					70	44.3%	37.5
CM-3205	0/90 deg w/mat	37.00	2.10					36.00	2.20					51.00	2.20					68	52.0%	
CM-3205/7	0/90 deg w/mat	37.00	2.10					36.00	2.20					51.00	2.20					68	52.0%	
CM-3208	0/90 deg w/mat	36.00	2.00					34.88	2.20					49.00	2.10					71	50.0%	
CM-3215	0/90 deg w/mat	36.00	1.95					37.00	2.70					49.00	2.15					81	49.0%	
CM-3610	0/90 deg w/mat	34.75	2.14											54.25	1.60					79	50.0%	
CM-3610UB	0/90 deg w/mat	34.00	1.90	36.00	2.00			36.00	2.60	38.00	2.10			48.00	2.00	50.00	2.20			88	50.0%	
CM-4810	0/90 deg w/mat	38.00	2.00					39.00	2.10					52.00	2.20					95	52.0%	
M-1000	binderless mat	19.00	0.97	19.00	0.97	19.00	0.97	22.00	1.40	22.00	1.40	22.00	1.40	28.00	1.40	28.00	1.40	28.00	1.40	31	26.0%	
M-1500	binderless mat	18.70	0.98	18.70	0.98	18.70	0.98	26.00	1.06	26.00	1.06	26.00	1.06	30.80	1.01	30.80	1.01	30.80	1.01	41	30.0%	
M-1500/7	binderless mat	18.70	0.98	18.70	0.98	18.70	0.98	26.00	1.06	26.00	1.06	26.00	1.06	30.80	1.01	30.80	1.01	30.80	1.01	41	30.0%	
M-2000	binderless mat	19.00	0.98	19.00	0.98	19.00	0.98	24.00	1.20	24.00	1.20	24.00	1.20	30.00	1.40	30.00	1.40	30.00	1.40	52	29.0%	
M-3000	binderless mat	17.00	0.96	17.00	0.96	17.00	0.96	23.00	1.10	23.00	1.10	23.00	1.10	29.00	1.30	29.00	1.30	29.00	1.30	75	28.0%	
THM-2210	horizontal triaxial w/mat			29.20	1.90	32.00	2.10			33.10	2.20	36.30	2.60			48.20	1.90	48.90	2.20	53	49.0%	
TV-2500	vertical triaxial	34.00	2.20			31.00	2.10	38.10	2.50			36.30	2.40	62.00	2.40			57.00	2.20	35	54.0%	
TV-3400	vertical triaxial	35.00	2.20			33.20	2.20	37.20	2.80			36.10	2.80	64.70	2.40			54.10	2.25	51	50.0%	34.0
TVM-3408	vertical triaxial w/mat	33.20	2.25			31.00	2.10	38.10	2.60			36.30	2.60	56.00	2.40			51.00	2.20	68	52.0%	40.8
U-0901	warp unidirectional	32.00	2.10					34.00	2.30					57.00	2.10					19	54.0%	
U-1601	warp unidirectional	36.00	2.00					38.20	1.90					47.00	2.10					31	52.0%	
U-1801	warp unidirectional	38.00	2.00					39.00	2.00					45.00	2.10					35	50.0%	
UM-1608	warp unidirectional w/mat	31.00	1.85					33.20	1.90					45.00	1.90					45	47.0%	
W-16	weft unidirectional			38.00	2.10					40.20	2.20					51.00	2.20			27	54.0%	
X-1500	+/-45 deg					33.00	1.85					37.00	2.30					58.00	2.10	26	55.0%	
X-1800	+/-45 deg					32.00	1.90					36.00	2.60					60.80	2.10	31	55.0%	
X-2400	+/-45 deg	7.15				35.50	1.70	15.80	0.56			26.10	2.80					60.00	2.40	36	44.8%	24.0
X-2800	+/-45 deg	8.00				38.50	1.80	18.00	0.60			28.00	2.80					63.00	2.20	41	50.0%	
XM-1305	+/-45 deg w/mat					35.40	2.00					38.00	2.40					56.80	2.10	29	54.0%	
XM-1308	+/-45 deg w/mat					31.80	2.00					33.20	2.20					51.00	2.10		52.0%	
XM-1708	+/-45 deg w/mat	13.60	1.50			33.20	2.20	23.40	2.10			36.10	3.16	28.30	1.50			54.10	2.25	48	51.4%	24.8
XM-1808	+/-45 deg w/mat	13.60	1.50			33.20	2.20	23.40	2.10			36.10	3.16	28.30	1.50			54.10	2.25	48	51.4%	
XM-1808b	+/-45 deg w/mat	13.60	1.50			33.20	2.20	23.40	2.10			36.10	3.16	28.30	1.50			54.10	2.40	48	51.4%	
XM-2408	+/-45 deg w/mat	14.20	1.55			34.20	2.20	33.20	2.20			38.00	3.25	32.20	1.50			58.10	2.40	56	55.0%	30.8
XM-2415	+/-45 deg w/mat	11.50	1.50			27.70	2.10	39.80	3.10			42.60	3.70	29.10	1.50			52.30	2.30	71	53.5%	37.5

Reinforcement Data — columns grouped as Tensile / Compressive / Flexural, each with Longitudinal, Transverse, Diagonal (Strength in ksi, Modulus in msi), plus Thickness Per Ply (mils), % Fiber by Weight (%), Fiber Weight (oz/yd²).

Reinforcement Description	Tens Long Str (ksi)	Tens Long Mod (msi)	Tens Trans Str (ksi)	Tens Trans Mod (msi)	Tens Diag Str (ksi)	Tens Diag Mod (msi)	Comp Long Str (ksi)	Comp Long Mod (msi)	Comp Trans Str (ksi)	Comp Trans Mod (msi)	Comp Diag Str (ksi)	Comp Diag Mod (msi)	Flex Long Str (ksi)	Flex Long Mod (msi)	Flex Trans Str (ksi)	Flex Trans Mod (msi)	Flex Diag Str (ksi)	Flex Diag Mod (msi)	Thickness Per Ply (mils)	% Fiber by Wt (%)	Fiber Weight (oz/yd²)
1.5 oz chopped mat — random mat	12.50	1.10					22.70	1.04					23.80	0.97					46	30.0%	
A 060 — woven warp unidirectional	70.60	2.60					39.90	2.20					90.60	2.00					10	50.0%	6.1
A 130 Uni — woven warp unidirectional	62.40	3.27					44.80	3.55					82.70	2.46					24	50.0%	13.1
A 260 Uni — woven warp unidirectional	73.70	3.51					44.10	2.80					109.30	3.61					24	50.0%	25.7
A 260-45 H.M. — woven warp unidirectional, high modulus	114.63	5.33																	30	64.4%	25.6
A 260 HBF — woven warp unidirectional	106.54	5.06					72.14	4.99					135.48	4.61					31		25.6
A 260 HBF 1587 — woven warp unidirectional	98.03	4.67																	30	66.5%	25.6
A 260 HBF XP9587 — woven warp unidirectional	99.86	4.96																	28	66.1%	25.6
A 260 Eng Yarn — woven warp unidirectional	113.55	4.96																	32		25.6
A 260 Eng Yarn — woven warp unidirectional	101.08	5.20																	30	63.2%	25.6
Owens Corning Knytex Reinforcements																					
Biply 2415 G — woven roving plus mat	41.19	2.07	35.81	2.01			33.43	2.28	35.29	2.28			55.98	2.21	55.47	2.31			61	50.4%	37.7
CM 1701 Uni/Mat — warp unidirectional & mat	74.70	4.20					54.70	3.39					102.60	2.96					30	50.0%	17.3
CM 2415 Uni/Mat — warp unidirectional & mat	61.40	2.98					44.50	2.28					73.70	2.35					65	50.0%	
CM3205 — warp unidirectional & mat	47.11	2.21					49.95	2.49					68.36	1.70					58	59.0%	
CM3610 — warp unidirectional & mat	52.68	3.07					50.39	2.74					91.39	3.05					55	40.5%	
KA060 — Kevlar® warp unidirectional	96.10	2.74					30.20	2.94					83.70	1.90					13	50.0%	6.3
D155 — stichbonded weft unidirectional			60.40	3.73					48.30	4.00					75.40	3.38			27	50.0%	15.5
D240 — stichbonded weft unidirectional			75.80	3.32					37.90	2.66					88.80	3.05			42	50.0%	24.4
D105 — stichbonded weft unidirectional			71.10	3.56					33.60	3.26					93.80	2.51			18	50.0%	
CD 1850/90 — biaxial 0/90	39.00	1.99	46.00	2.47			16.00	2.36	16.00	2.05			69.00	1.98	49.00	1.66			32	55.0%	19.4
CD 2300/90 — biaxial 0/90	36.00	2.60					33.00	2.22					70.00	1.93					41	55.0%	23.5
CD 2300/90 — biaxial 0/90	41.30	2.39	32.40	2.26			38.80	2.25	35.50	2.18			64.90	2.40	58.10	2.31			41	50.0%	23.5
DB 090+/-45 — double bias +/45					40.40	2.01					39.30	1.94					62.20	2.05	17	50.0%	9.3
DB 090+/-45 — double bias +/45					47.50	2.25					48.70	1.99					76.20	1.90	17	50.0%	9.3
DB 120+/-45 — double bias +/45					44.50	2.13					35.70	1.92					58.70	2.04	21	50.0%	11.6
DB130 — double bias +/45	12.38	1.20	21.26	1.59	31.25	2.08							36.03	1.16	51.89	1.60	62.29	2.14	18	46.1%	
DB 170+/-45 — double bias +/45					39.80	2.18					36.60	2.06					69.90	2.00	31	57.1%	17.6

Owens Corning Knytex Reinforcements

Reinforcement	Description	Tensile Str. Long. (ksi)	Tensile Mod. Long. (msi)	Tensile Str. Trans. (ksi)	Tensile Mod. Trans. (msi)	Tensile Str. Diag. (ksi)	Tensile Mod. Diag. (msi)	Compr. Str. Long. (ksi)	Compr. Mod. Long. (msi)	Compr. Str. Trans. (ksi)	Compr. Mod. Trans. (msi)	Compr. Str. Diag. (ksi)	Compr. Mod. Diag. (msi)	Flex. Str. Long. (ksi)	Flex. Mod. Long. (msi)	Flex. Str. Trans. (ksi)	Flex. Mod. Trans. (msi)	Flex. Str. Diag. (ksi)	Flex. Mod. Diag. (msi)	Thickness Per Ply (mils)	% Fiber by Weight (%)	Fiber Weight (oz/yd²)
1.5 oz chopped mat	random mat	12.50	1.10					22.70	1.04					23.80	0.97					46	30.0%	
A 060	woven warp unidirectional	70.60	2.60					39.90	2.20					90.60	2.00					10	50.0%	6.1
DB 240 +/-45	double bias +/-45					44.90	2.42					37.20	2.34	121.37	4.85			72.50	2.15	44	50.0%	24.7
DB 240 +/-45	double bias +/-45													94.59	4.32					35	53.6%	24.7
DB 240 +/-45	double bias +/-45													144.56	5.22					29	65.4%	24.7
DB400	double bias +/-45, jumbo					41.34	2.73					44.74	2.84					68.72	2.12	45	62.5%	39.8
DB603	double bias +/-45, jumbo					46.93	2.87					51.66	3.06					66.51	2.44	67	62.5%	58.8
DB800	double bias +/-45, jumbo					41.11	2.98					42.61	3.38					71.23	2.61	83	69.2%	
DB803	double bias +/-45, jumbo					45.44	3.04					51.00	3.57					62.62	2.63	87	66.4%	
DBM 1208 +/-45/M	double bias +/-45 plus mat	18.26	1.35	19.56	1.46	40.60	1.95					31.20	1.70	35.29	1.22	44.81	1.41	60.20	1.75	38	45.0%	19.3
DBM 1708 +/-45/M	double bias +/-45 plus mat					36.17	2.21					49.07	2.04					68.98	1.97	39	51.5%	25.3
DBM 1708B 0/+/-45/M	double bias +/-45 plus mat					36.60	1.94					38.80	2.10					63.40	1.85	50	45.0%	25.3
DBM2408A	double bias +/-45 plus mat					33.04	2.15											65.27	1.82	50	53.2%	
XDBM1703	exp. double bias +/-45 & mat					19.15	1.37					34.17	1.78					46.89	1.20	56	39.7%	
XDBM1705	exp. double bias +/-45 & mat					13.57	1.10					20.02	1.55					34.51	1.04	51	35.4%	
XDBM1708F	exp. double bias +/-45 & mat					31.34	1.89					42.38	2.43					61.27	1.79	40	50.1%	
CDB 2000 +/-45	warp triaxial	45.20	2.23			24.30	1.99	36.80	2.16			33.60	1.89	73.20	2.47			43.50	1.98	39	50.0%	22.4
CDB 3400 +/-45	warp triaxial	48.30	2.42			25.50	1.85	40.30	2.22			25.00	1.97	71.50	2.35			34.70	1.88	55	50.0%	31.4
CDB 340B 0/+/-45	warp triaxial, promat stich	36.50	2.45	30.20	1.83	22.50	1.86	33.20	2.28	28.30	1.45	29.10	1.75	71.20	2.10			35.60	1.72	59	50.0%	33.5
CDM 1808 0/90/M	promat (0/90 plus mat)	37.20	2.10					30.20	1.83					61.00	2.30	49.20	1.93			54	45.0%	27.0
CDM 1808 B	promat (0/90 plus mat)	42.90	2.50					59.74	2.58					75.49	2.58					47	55.2%	29.2
CDM 1815 0/90/M	promat (0/90 plus mat)	34.30	2.06	27.60	1.71			28.40	1.74	27.20	1.65			55.90	1.70	53.20	1.45			69	45.0%	32.9
CDM 1815B	promat (0/90 plus mat)	40.59	2.52					54.69	2.33					69.20	2.40					50	55.8%	35.1
CDM 2408 0/90/M	promat (0/90 plus mat)	35.60	2.12	31.20	1.92			35.70	2.03	34.70	1.87			72.00	2.44	61.20	2.01			69	45.0%	33.1
CDM 2408A	promat (0/90 plus mat)	49.08	2.74					63.81	2.08					89.37	2.77					48	56.5%	34.1
CDM 2410 0/90/M	promat (0/90 plus mat)	37.20	2.21	35.20	1.91			30.20	1.87	28.40	1.65			61.60	2.12	50.10	1.88			70	45.0%	34.5
CDM 2415 0/90/M	promat (0/90 plus mat)	35.20	2.06	31.10	1.97			31.30	1.97	27.20	1.80			58.60	1.95	58.40	1.85			83	45.0%	39.0
CDM 2415	promat (0/90 plus mat)	47.74	2.49	49.25	2.40			49.66	2.68	48.48	2.62			72.07	2.06	77.55	2.31			56	54.9%	
CDM 2415A	promat (0/90 plus mat)	33.46	2.21	30.03	1.95			70.48	2.49					73.25	2.36	55.32	1.74			59	54.6%	39.6
CDM 3208	promat (0/90 plus mat)	44.60	2.47					65.95	2.82					84.53	2.57					55	60.2%	40.0
CDM 3610	promat (0/90 plus mat)	52.84	2.88					52.23	3.15					93.29	2.38					56	38.2%	

Owens Corning Knytex Reinforcements

Reinforcement Description		Tensile Strength: Longitudinal (ksi)	Tensile Modulus: Longitudinal (msi)	Tensile Strength: Transverse (ksi)	Tensile Modulus: Transverse (msi)	Tensile Strength: Diagonal (ksi)	Tensile Modulus: Diagonal (msi)	Compressive Strength: Longitudinal (ksi)	Compressive Modulus: Longitudinal (msi)	Compressive Strength: Transverse (ksi)	Compressive Modulus: Transverse (msi)	Compressive Strength: Diagonal (ksi)	Compressive Modulus: Diagonal (msi)	Flexural Strength: Longitudinal (ksi)	Flexural Modulus: Longitudinal (msi)	Flexural Strength: Transverse (ksi)	Flexural Modulus: Transverse (msi)	Flexural Strength: Diagonal (ksi)	Flexural Modulus: Diagonal (msi)	Thickness Per Ply (mils)	% Fiber by Weight (%)	Fiber Weight (oz/yd²)
1.5 oz chopped mat	random mat	12.50	1.10					22.70	1.04					23.80	0.97					46	30.0%	
A060	woven warp unidirectional	70.60	2.60					39.90	2.20					90.60	2.00					10	50.0%	6.1
CDM 3610 ST	promat (0/90 plus mat)	51.54	2.74					47.21	3.24					90.66	2.31					55	39.6%	
CDM 4408	promat (0/90 plus mat)	46.00	2.45	42.59	2.75			50.05	2.45	58.07	2.74			63.78	2.33	84.00	3.05				54.6%	
XCDM 2315	exp promat (0/90 plus mat)	36.54	2.10	36.04	2.10									71.18	2.01	58.72	1.77			60	54.9%	
DDB222	weft triaxial	38.40	2.55			22.40	1.41	33.20	2.04			28.60	1.88	57.50	2.10			42.10	1.77	39	50.0%	22.1
DDB340	weft triaxial	48.00	2.45	71.93	2.88	23.50	1.33	33.90	2.23			27.70	1.93	65.60	2.23	79.56	2.80	49.10	1.83	59	50.0%	33.8
XDDBM2208	exp weft triaxial w/ mat			38.32	2.20	19.65	1.59													51	48.9%	
XDDM2710	exp stichbonded weft triaxial w/ mat			43.68	2.32	22.04	1.58									71.43	2.39	43.06	1.54	55	53.6%	
XDDB222	exp stichbonded weft triaxial	12.48	1.16	54.64	2.69									25.32	1.28	78.41	2.59			30		
XDDB340	exp stichbonded weft triaxial	12.02	1.13	71.08	3.20									25.58	1.31	95.26	3.20			39		
GDB 095 +/-45 carbon	double bias +/-45 carbon					67.00	4.98					52.00	4.55					90.00	2.77		50.0%	9.8
GDB 095 +/-45 carbon	double bias +/-45 carbon					90.20	4.59					58.50	2.97					86.50	2.14	20	50.0%	9.8
GDB 120 +/-45 carbon	double bias +/-45 carbon					67.00	6.19					28.00	5.84					103.00	3.39		50.0%	12.3
GDB 120 +/-45 carbon	double bias +/-45 carbon					76.60	5.28					44.50	2.39					80.40	2.23	25	50.0%	12.3
GDB 200 +/-45 carbon	double bias +/-45 carbon					58.00	6.94					18.00	5.57					78.00	3.04		50.0%	19.8
GDB 200 +/-45 carbon	double bias +/-45 carbon					72.90	5.66					41.20	3.55					95.60	2.65	40	50.0%	19.8
KDB 170 +/-45 Kevlar	double bias +/-45 Kevlar®					51.00	3.23					12.00						34.00			50.0%	15.9
17MPX		59.20	3.60			37.60	2.20	30.00	2.53			32.50	1.71	45.10	1.65			59.80	1.72	31	50.0%	
XH120														67.00	2.06					56	50.0%	
XH120		17.50				17.50	1.43					17.40	1.78	54.00	1.41			22.00	1.20	56	50.0%	
CDDB310	quadraxial	34.02	1.81	31.56	1.93			36.79	1.87	31.12	1.86			57.26	1.49	50.14	1.39			46	55.0%	
CDB 340 0/+/-45	warp triaxial	48.00	2.61					34.00	2.27					67.00	2.06						55.0%	31.4
CDM 2410 0/90/M	promat	37.00	2.31					27.00	1.87					54.00	1.41						45.0%	34.5
GA 045 Uni carbon	woven warp unidirectional, carbon	97.00	9.34					76.00	11.75					195.00	8.98						55.0%	4.6
GA 080 Uni carbon	woven warp unidirectional, carbon	244.40	18.30											135.80	10.90						48.0%	
GA 090 Uni carbon	woven warp unidirectional, carbon	232.90	18.90					45.71	11.49					173.60	14.50					15	58.0%	
GA 130 Uni carbon	woven warp unidirectional, carbon	234.60	18.20					45.94	12.73					150.90	12.20					18	64.0%	9.4

Reinforcement Description		Tensile Strength: Longitudinal (ksi)	Tensile Modulus: Longitudinal (msi)	Tensile Strength: Transverse (ksi)	Tensile Modulus: Transverse (msi)	Tensile Strength: Diagonal (ksi)	Tensile Modulus: Diagonal (msi)	Compressive Strength: Longitudinal (ksi)	Compressive Modulus: Longitudinal (msi)	Compressive Strength: Transverse (ksi)	Compressive Modulus: Transverse (msi)	Compressive Strength: Diagonal (ksi)	Compressive Modulus: Diagonal (msi)	Flexural Strength: Longitudinal (ksi)	Flexural Modulus: Longitudinal (msi)	Flexural Strength: Transverse (ksi)	Flexural Modulus: Transverse (msi)	Flexural Strength: Diagonal (ksi)	Flexural Modulus: Diagonal (msi)	Thickness Per Ply (mils)	% Fiber by Weight (%)	Fiber Weight (oz/yd²)
1.5 oz chopped mat	random mat	12.50	1.10					22.70	1.04					23.80	0.97					46	30.0%	
A060	woven warp unidirectional	70.60	2.60					39.90	2.20					90.60	2.00					10	50.0%	6.1
KBM 1308A	woven Kevlar®/glass hybrid plus mat	48.23	2.48											46.89	2.20					30		
Kevlar/Glass Hybrid		42.45	2.28	37.38	2.15									58.24	2.14					27		

Owens Corning Knytex Reinforcements

Reinforcement Description		Tensile Strength: Longitudinal (ksi)	Tensile Modulus: Longitudinal (msi)	Tensile Strength: Transverse (ksi)	Tensile Modulus: Transverse (msi)	Tensile Strength: Diagonal (ksi)	Tensile Modulus: Diagonal (msi)	Compressive Strength: Longitudinal (ksi)	Compressive Modulus: Longitudinal (msi)	Compressive Strength: Transverse (ksi)	Compressive Modulus: Transverse (msi)	Compressive Strength: Diagonal (ksi)	Compressive Modulus: Diagonal (msi)	Flexural Strength: Longitudinal (ksi)	Flexural Modulus: Longitudinal (msi)	Flexural Strength: Transverse (ksi)	Flexural Modulus: Transverse (msi)	Flexural Strength: Diagonal (ksi)	Flexural Modulus: Diagonal (msi)	Thickness Per Ply (mils)	% Fiber by Weight (%)	Fiber Weight (oz/yd²)
KDB 110 +/-45 Kevlar	double bias, Kevlar®					56.00	3.63					15.00	1.32					49.00	1.11		45.0%	10.4
KDB 110 +/-45 Kevlar	double bias, Kevlar®					73.70	3.00					19.90	1.30					65.70	1.96	23	50.0%	10.4
KB 203 WR E-glass/Kevlar	woven Kevlar®/glass hybrid	66.00	5.48					21.00	3.47					51.00	2.42						45.0%	20.8
SDB 120 S-glass	double bias, S-glass	63.00	3.03					45.00	2.90					70.60	1.88						55.0%	11.4
SDB 120 S-glass	double bias, S-glass	60.00	2.35					46.20	2.10					78.30	2.23					21	50.0%	17.2
B238	starch oil woven roving	31.60	1.91	28.20	1.80			28.50	1.80	26.70	1.76			48.80	1.85	44.30	1.78			57	40.0%	
B238+.75 oz mat	starch oil woven roving w/ mat	27.50	1.78	25.10	1.68			26.80	1.79	24.50	1.73			42.10	1.80	39.70	1.71			86	35.0%	
Spectra 900	Spectra	63.70	2.85	54.10	2.65			18.80	2.04	16.60	1.88			48.40	1.80	44.20	1.72			17	50.0%	
K49/13 Kevlar	Kevlar® 49	51.80	2.89	48.90	2.79			19.70	2.35	17.50	2.10			42.20	1.50	39.10	1.43			27	45.0%	

Reinforcement Description		Tensile Strength: Longitudinal	Tensile Modulus: Longitudinal	Tensile Strength: Transverse	Tensile Modulus: Transverse	Tensile Strength: Diagonal	Tensile Modulus: Diagonal	Compressive Strength: Longitudinal	Compressive Modulus: Longitudinal	Compressive Strength: Transverse	Compressive Modulus: Transverse	Compressive Strength: Diagonal	Compressive Modulus: Diagonal	Flexural Strength: Longitudinal	Flexural Modulus: Longitudinal	Flexural Strength: Transverse	Flexural Modulus: Transverse	Flexural Strength: Diagonal	Flexural Modulus: Diagonal	Thickness Per Ply	% Fiber by Weight	Fiber Weight
		ksi	msi	ksi	msi	ksi	msi	ksi	msi	ksi	msi	ksi	msi	ksi	msi	ksi	msi	ksi	msi	mils	%	oz/yd²
DuPont Kevlar Reinforcements																						
Kevlar 49 243	unidirectional	80.10	5.43											34.60	3.84							6.7
Kevlar 49 243	unidirectional	90.80	6.60											50.40	4.85							6.7
Kevlar 49 281	woven cloth	59.70	3.23											32.10	2.54							5.0
Kevlar 49 281	woven cloth	60.60	3.74											36.60	3.16							5.0
Kevlar 49 285	woven cloth	49.00	2.75											31.50	2.37							5.0
Kevlar 49 285	woven cloth	59.00	3.22											41.00	2.81							5.0
Kevlar 49 328	woven cloth	63.60	3.10											23.50	2.59							6.3
Kevlar 49 500	woven cloth	51.70	2.98											37.80	2.06							5.0
Kevlar 49 500	woven cloth	55.20	3.73											50.60	2.83							5.0
Kevlar 49 1050	woven roving	44.60	3.13											26.90	2.01							10.5
Kevlar 49 1050	woven roving	59.70	2.98											35.40	2.64							10.5
Kevlar 49 1033	woven roving	50.70	3.55											22.50	2.22							15.0
Kevlar 49 1033	woven roving	52.40	3.42											34.40	2.67							15.0
Kevlar 49 1350	woven roving	65.00	7.70											29.30	3.15							13.5
Kevlar 49 118	woven roving	88.80												61.00	6.10							8.0
Kevlar 49/E-glass KBM 1308	woven/mat	34.80	1.79	33.64	1.83			24.65	2.33	25.38	1.94			37.57	1.44	37.13	1.46					18.6
Kevlar 49/E-glass KBM 2808	woven/mat	39.01	2.12	33.79	2.00			22.19	2.19	22.19	2.39			43.51	1.75	36.69	1.76					33.1
Kevlar 49/E-glass C77K/235		39.01	2.12	33.79	2.00									43.51	1.70	36.69	1.76				45.0%	33.2
Anchor Reinforcements																						
Ancaref C160 carbon, 12K	unidirectional	127.00	12.00					90.00	9.00											4	50.0%	4.7
Ancaref C160 carbon, 12K	unidirectional	250.00	21.00					160.00	20.00											3	70.0%	4.7
Ancaref C320 carbon, 12K	unidirectional	125.00	12.00					90.00	9.00											21		9.5
Ancaref C440 carbon, 12K	unidirectional	89.00	5.30					31.00	3.80											14		6.1
Ancaref S275 S-2 glass, O-C	unidirectional	129.00	5.50					62.00												9	60.0%	8.1
Ancaref S275 S-2 glass, O-C	unidirectional	298.00	7.50					119.00	7.80											7	75.0%	8.1
Ancaref S160 S-2 glass, O-C	unidirectional	128.00	5.50					62.00	7.70											7		4.8
Ancaref G230 E-glass	unidirectional	76.00	4.30					79.00	3.10											14		9.5
Unidirectionals																						
High-strength, uni tape carbon	unidirectional	180.00	21.00	8.00	1.70	23.20	2.34	180.00	21.00	30.00	1.70	23.90	2.34									
High-strength, uni tape carbon	unidirectional	180.00	18.70	4.00	0.87	13.20	1.20	70.00	18.70	12.00	0.87	13.70	1.20									
High-modulus, uni tape carbon	unidirectional	110.00	25.00	4.00	1.70	16.90	2.38	100.00	25.00	20.00	1.70	18.00	2.38									
High-modulus, uni tape carbon	unidirectional	96.00	24.10	3.10	0.85	7.20	1.86	60.00	24.10	8.00	0.85	7.20	1.86									
Intermediate-strength, unitapecarbon	unidirectional	160.00	17.00	7.50	1.70			160.00	17.00	25.00	1.70											
Intermediate-strength, unitapecarbon	unidirectional	144.00	16.00	4.00	1.00			65.00	16.00	15.00	1.00											
Unidirectional tape Kevlar	unidirectional	170.00	10.10	4.00	0.80			40.00	10.10	20.00	0.80											

Reinforcement Description	Tensile Str. Long. (ksi)	Tensile Mod. Long. (msi)	Tensile Str. Trans. (ksi)	Tensile Mod. Trans. (msi)	Tensile Str. Diag. (ksi)	Tensile Mod. Diag. (msi)	Compr. Str. Long. (ksi)	Compr. Mod. Long. (msi)	Compr. Str. Trans. (ksi)	Compr. Mod. Trans. (msi)	Compr. Str. Diag. (ksi)	Compr. Mod. Diag. (msi)	Flex. Str. Long. (ksi)	Flex. Mod. Long. (msi)	Flex. Str. Trans. (ksi)	Flex. Mod. Trans. (msi)	Flex. Str. Diag. (ksi)	Flex. Mod. Diag. (msi)	Thickness Per Ply (mils)	% Fiber by Weight (%)	Fiber Weight (oz/yd²)
SCRIMP Process Laminates																					
Cert'teed/Seemann 625 WR	57.10						43.60						70.60						24	73.0%	24.0
Cert'teed/Seemann 625 WR							52.00						79.50						24	73.0%	24.0
Hexcell 8HS, Style 7781	56.90	3.40					58.10						83.60						10	66.0%	8.5
FGI/Seemann 3X1, 10 Twill	53.60	3.40					61.70						76.70						10	70.0%	9.6
8HS, 3K XaSg, 1029 carbon	98.00	8.30					37.00						69.70						16		10.9
8HS, 3K, 1029(UC309) carbon							42.10						68.20						16		10.9
5HS, 12K, 1059(AS4W) carbon		7.90					29.50						60.20						22	64.0%	15.5
Hexcell CD180 stiched biaxial	50.10	3.20					41.50						59.70						26	61.0%	19.4
Chomarat 2 x 2 weave	40.20	2.90					55.00						69.30						31	66.0%	24.0
DF14OO	47.20	3.90	35.00	3.40			39.30		34.70				61.30		46.20				42		40.0
G:Cl029 hybrid E-glass/carbon	71.10	6.40					39.70						96.50						40		
G:Cl059 hybrid E-glass/carbon	64.20	6.10					29.00						99.30						40		
G:K285(60%) hybrid E-glass/Kevlar							23.80						75.40						48		
G:K900(40%) hybrid E-glass/Kevlar							36.70						73.90						33		
G:K900(50%) hybrid E-glass/Kevlar	57.50	3.70					31.80						62.60						38		
G:S985(40%) hybrid E-glass/Spectra	51.50	3.10					35.10						78.50						33		
DuPont 5HS, K49, Kevlar (900)	69.50	4.30					15.80						35.50						17		
Allied-Signal 8HS, S1000, Spectra (985)		2.10					8.50						18.50						10		5.5
Cert'teed/Seemann 625 WR	51.60	3.50					47.80						71.90						24	73.0%	24.0
Cert'teed/Seemann twill, 3X1	51.30	3.10					52.90						79.10						26	71.0%	24.0
Cert'teed/Seemann 625 WR	44.70	3.60					30.80						48.70						24	73.0%	24.0
Cert'teed/Seemann 625 WR	51.50	3.90					32.80						55.00						24	73.0%	24.0
Cert'teed/Seemann 625 WR	48.70	3.90					32.20						58.20						24	73.0%	24.0
5HS, 6K, 1030 carbon	92.00	8.50					57.20						99.20						15		10.2
5HS, 12K, 1059 carbon (AS4W)	89.20	8.30					64.50						100.10						22		15.5
Low-Temperature Cure Prepregs																					
Advanced Comp Grp/LTM21	76.00	4.20					59.90						74.80						9	77.9%	24.0
Advanced Comp Grp/LTM22	63.50	3.40					48.70						69.30						9	65.9%	8.9
Advanced Comp Grp/LTM22	67.80	3.50					51.20						73.60						9	66.9%	8.9
SP Systems/Ampreg75	61.80	3.10					60.70						81.60						9	65.5%	8.9
SP Systems/Ampreg75	66.10	3.30					63.80						90.10						9	62.8%	8.9
DSM Italia/Neoxil	50.10	2.80					68.60						87.20						9	57.0%	8.9
Newport Adhesives/NB-1101	50.60	2.90					57.00						68.50						9	60.3%	8.9
Newport Adhesives/NB-1101	48.30	3.00					62.30						69.60						9	60.3%	8.9
Newport Adhesives/NB-1107	58.30	3.30					59.20						75.20						9	63.3%	8.9
Newport Adhesives/NB-1107	48.20	2.30					48.30						57.80						9	63.3%	8.9
Ciba Composite/M10E	53.60	3.30					52.10						77.10						9	62.8%	8.9
Ciba Composite/M10E	93.50	9.20					44.20						85.80						9		8.9

Reinforcement Description	Tensile Strength: Longitudinal (ksi)	Tensile Modulus: Longitudinal (msi)	Tensile Strength: Transverse (ksi)	Tensile Modulus: Transverse (msi)	Tensile Strength: Diagonal (ksi)	Tensile Modulus: Diagonal (msi)	Compressive Strength: Longitudinal (ksi)	Compressive Modulus: Longitudinal (msi)	Compressive Strength: Transverse (ksi)	Compressive Modulus: Transverse (msi)	Compressive Strength: Diagonal (ksi)	Compressive Modulus: Diagonal (msi)	Flexural Strength: Longitudinal (ksi)	Flexural Modulus: Longitudinal (msi)	Flexural Strength: Transverse (ksi)	Flexural Modulus: Transverse (msi)	Flexural Strength: Diagonal (ksi)	Flexural Modulus: Diagonal (msi)	Thickness Per Ply (mils)	% Fiber by Weight (%)	Fiber Weight (oz/yd²)
YLA, Inc./RS-1	51.80	3.10					51.90						70.80						9	64.7%	8.9
YLA, Inc./RS-1	51.30	3.00					53.60						68.60						9	64.8%	8.9
YLA, Inc./RS-1	55.30	3.00					55.90						71.30						9	63.6%	8.9
3M/SP377	41.90	3.10					56.50						59.70						9	63.1%	8.9
3M/SP377	43.00	3.30					59.40						59.40						9	64.4%	8.9
3M/SP365	35.30						37.50						48.90						16	68.5%	16.1
3M/SP365	47.30						59.20						71.40						16	69.5%	16.1
Fibercote Industries/E-761E	55.30	3.40					63.10						75.90						16	62.4%	16.1
Fibercote Industries/E-761E	58.30	3.50					66.00						78.60						16	62.6%	16.1
Fibercote Industries/P-601	61.30	3.30					64.30						87.50						25	57.0%	18.0
Fibercote Industries/P-601	64.10	3.40					70.20						90.60						25	60.3%	18.0
Fibercote Industries/P-600	54.50	2.90					43.00						66.70						9	62.6%	8.9
Fibercote Industries/P-600	58.70	3.10					50.60						78.70						9	64.7%	8.9
ICI Fiberite/MXB-9420	61.10	2.90					50.40						67.30						9	60.9%	8.9
Fiber Content Study for GLCC																					
Owens-Corning WR	44.50	2.99					45.65	3.31					58.76	2.29					25	52.4%	18.0
ATI NEWF 180 Biaxial	51.92	3.29					51.61	3.55					75.29	2.66					30	47.8%	18.0
Owens-Corning WR	57.58	3.68					46.44	3.57					81.92	2.87					25	61.0%	18.0
ATI NEWF 180 Biaxial	56.38	3.26					61.14	3.54					81.88	2.82					30	53.1%	18.0
Owens-Corning WR	58.40	3.72					46.67	3.64					93.65	3.30					25	66.9%	18.0
ATI NEWF 180 Biaxial	61.06	3.41					55.97	3.56					83.59	2.73					30	61.8%	18.0

Reinforcement Description		Tensile Strength: Longitudinal (MPa)	Tensile Modulus: Longitudinal (GPa)	Tensile Strength: Transverse (MPa)	Tensile Modulus: Transverse (GPa)	Tensile Strength: Diagonal (MPa)	Tensile Modulus: Diagonal (GPa)	Compressive Strength: Longitudinal (MPa)	Compressive Modulus: Longitudinal (GPa)	Compressive Strength: Transverse (MPa)	Compressive Modulus: Transverse (GPa)	Compressive Strength: Diagonal (MPa)	Compressive Modulus: Diagonal (GPa)	Flexural Strength: Longitudinal (MPa)	Flexural Modulus: Longitudinal (GPa)	Flexural Strength: Transverse (MPa)	Flexural Modulus: Transverse (GPa)	Flexural Strength: Diagonal (MPa)	Flexural Modulus: Diagonal (GPa)	Thickness Per Ply (mm)	% Fiber by Weight (%)	Fiber Weight (gms/m²)
C-1200 (NEWF 120)	0/90 knit	211	14.1	150	9.9	79	5.1	280	17.0	211	13.9			411	13.7	256	4.9			0.61	41.8%	412
C-1600 (NEWF 160)	0/90 knit	281	18.3	283	15.1	78	9.0	255	18.5	256	16.8			328	9.6	330	9.8			0.64	58.0%	524
C-1800 (NEWF 180)	0/90 knit	296	20.0	146	11.4	76	8.2	330	21.1	235	14.3			445	14.3	210	6.9			0.81	51.2%	598
C-2300 (NEWF 230)	0/90 knit	225	18.3	217	17.6	63	6.1	232	19.9	246	13.4			395	15.0	269	10.1			0.94	54.5%	784
CM-1208 (NEWFC 1208)	0/90 knit w/mat	253	14.9	146	11.4	97	9.2	292	19.4	201	11.8			452	15.8	239	8.7			0.94	47.4%	639
CM-1215 (NEWFC 1215)	0/90 knit w/mat	159	12.8	117	9.2			124	13.0	110	11.1			296	10.8	200	7.9				34.8%	865
CM-1608 (NEWFC 1608)	0/90 knit w/mat	171	14.7	192	14.3	91	8.4	206	13.2	164	13.1			394	12.3	292	9.6			1.12	45.2%	761
CM-1615 (NEWFC 1615)	0/90 knit w/mat	152	12.2	167	12.9	94	8.4	148	14.1	173	12.9			353	13.0	329	11.5			1.42	44.3%	980
CM-1808 (NEWFC 1808)	0/90 knit w/mat	243	17.8	146	12.0	92	8.2	271	14.7	168	20.0			441	14.3	239	7.7			1.09	46.9%	825
CM-1815 (NEWFC 1815)	0/90 knit w/mat	196	15.2	145	12.6	103	7.9	255	18.8	161	14.2			401	16.4	270	11.1			1.45	48.4%	1055
CM-2308 (NEWFC 2308)	0/90 knit w/mat	206	16.4	222	15.7	96	9.4	268	21.6	245	17.4			383	13.1	351	9.8			1.35	48.8%	980
CM-2315 (NEWFC 2315)	0/90 knit w/mat	182	12.8	177	12.4	90	8.1	241	14.7	219	17.4			354	14.0	315	11.6			1.85	48.4%	1240
CM-3308 (NEWFC 3308)	0/90 knit w/mat	284	16.4	333	17.3			346	19.3	346	19.1			455	12.4	520	8.3			1.55	55.2%	
CM-3415 (NEWFC 3415)	0/90 knit w/mat	176	13.6	230	13.9	80	7.6	276	17.1	266	21.8	147	10.3	345	12.0	367	11.3	180	6.9	2.03	50.1%	
CM-3610 (NEWFC 3610)	0/90 knit w/mat	206	15.0	283	15.6			258	20.8	271	19.1			341	12.7	453	13.9			1.93	51.9%	
Advanced Textiles Reinforcements																						
X-090 (NEMP 090)	+/-45 knit	48	5.2	156	8.7	160	11.6	129	5.6	123	7.9	288	12.0	161	3.9	313	8.1	337	10.8	0.51	39.0%	321
X-120 (NEMP 120)	+/-45 knit	46	5.5	160	8.5	203	11.7	104	5.5	105	8.3	284	14.3	133	4.6	189	7.4	349	11.9	0.69	38.1%	419
X-170 (NEMP 170)	+/-45 knit	52	4.8	160	7.7	208	13.6	109	5.9	112	7.7	274	11.3	173	5.2	314	7.9	421	11.5	0.86	46.5%	595
X-240 (NEMP 240)	+/-45 knit	36	6.9	140	12.1	183	14.3	104	5.2	106	8.0	294	14.0	122	4.3	315	7.6	425	13.0	1.04	47.8%	818
XM-1208 (NEMPC 1208)	+/-45 knit w/mat	94	9.0	110	9.2	186	14.0	151	7.2	161	7.9	258	12.6	216	6.3	248	7.1	333	9.7	0.99	44.1%	649
XM-1215 (NEMPC 1215)	+/-45 knit w/mat	108	8.3	112	7.0	186	15.1	152	9.2	156	8.1	219	14.4	184	8.4	206	9.1	314	12.4	1.19	46.1%	879
XM-1708 (NEMPC 1708)	+/-45 knit w/mat	98	9.0	112	8.6	219	14.1	145	8.4	148	8.1	267	14.1	265	6.1	251	7.4	420	11.4	1.12	46.7%	825
XM-1715 (NEMPC 1715)	+/-45 knit w/mat	112	9.4	114	9.3	217	15.5	140	8.6	147	8.3	238	14.0	238	8.1	243	9.1	353	12.7	1.12	50.2%	1051
XM-2408 (NEMPC 2408)	+/-45 knit w/mat	73	7.9	141	9.2	219	14.1	133	6.8	142	8.0	271	14.3	187	8.1	296	9.4	385	12.2	1.27	50.3%	1048
XM-2415 (NEMPC 2415)	+/-45 knit w/mat	93	8.4	130	11.2	172	15.1	112	6.3	118	7.4	177	9.6	197	8.1	267	8.3	315	10.6	1.68	48.7%	1278
TV-200 (NEWMP 200)	0, +/-45 knit	251	14.8	81	6.8	125	11.9	226	13.6	139	7.5	196	13.1	484	14.2	197	4.1	266	6.9	0.86	48.7%	683
TV-230 (NEWMP 230)	0, +/-45 knit	210	11.5	105	6.4	170	9.6	203	17.1	161	8.1	253	12.9	439	12.8	226	4.3	350	9.2	0.99	46.9%	771
TV-340 (NEWMP 340)	0, +/-45 knit	215	11.8	89	9.5	150	11.0	201	19.2	138	9.7	198	11.6	484	15.3	184	3.4	330	8.1	1.24	46.8%	1119
TVM-2008 (NEWMPC 2008)	0, +/-45 knit w/mat	222	16.1	81	8.0	124	9.6	235	16.1	156	8.5	184	14.5	430	12.1	191	4.6	281	7.1	1.24	47.6%	916
TVM-2308 (NEWMPC 2308)	0, +/-45 knit w/mat	203	11.9	93	6.5	173	9.9	229	14.1	163	7.8	220	11.7	460	13.9	216	5.8	333	7.9	1.24	50.3%	997
TVM-2315 (NEWMPC 2315)	0, +/-45 knit w/mat	200	19.2	97	13.4	150	11.4	184	13.7	146	9.6	177	12.4	373	12.7	232	5.5	352	9.1	1.50	51.9%	
TVM-3408 (NEWMPC 3408)	0, +/-45 knit w/mat	223	10.6	92	12.4	166	12.7	177	16.3	129	10.3	212	14.9	417	15.0	207	4.8	322	9.5	1.52	53.5%	1359
TVM-3415 (NEWMPC 3415)	0, +/-45 knit w/mat	233	16.7	85	9.8	164	10.4	211	12.4	139	9.3	205	18.1	396	10.7	195	4.7	276	7.1	1.80	53.8%	1582
TH-200 (NEFMP 200)	90, +/-45 knit	80	6.9	235	15.4	151	13.0	138	7.0	285	12.4	229	11.2	164	6.9	376	12.5	231	7.0	0.94	47.4%	
TH-230 (NEFMP 230)	90, +/-45 knit	61	6.9	230	14.5	155	12.1	135	6.2	268	13.5	244	12.9	151	4.6	390	12.1	309	9.0	1.12	46.6%	771
TH-340 (NEFMP 340)	90, +/-45 knit	55	7.3	259	19.3	138	13.1	143	7.4	324	16.9	241	13.0	127	3.9	438	15.6	301	10.0	1.40	50.6%	1119
THM-2308 (NEFMPC 2308)	90, +/-45 knit & mat	75	7.6	206	12.6	142	11.5	111	6.2	209	10.3	132	9.2	177	5.4	355	12.5	315	10.2	1.37	46.2%	997
THM-3408 (NEFMPC 3408)	90, +/-45 knit & mat	58	9.0	262	16.9	126	11.7	122	7.3	277	16.3	219	11.4	113	5.3	435	12.6	305	9.2	1.80	48.6%	1359

BTI Reinforcements

Code	Reinforcement Description	Tensile Str. Long. (MPa)	Tensile Mod. Long. (GPa)	Tensile Str. Trans. (MPa)	Tensile Mod. Trans. (GPa)	Tensile Str. Diag. (MPa)	Tensile Mod. Diag. (GPa)	Compr. Str. Long. (MPa)	Compr. Mod. Long. (GPa)	Compr. Str. Trans. (MPa)	Compr. Mod. Trans. (GPa)	Compr. Str. Diag. (MPa)	Compr. Mod. Diag. (GPa)	Flex. Str. Long. (MPa)	Flex. Mod. Long. (GPa)	Flex. Str. Trans. (MPa)	Flex. Mod. Trans. (GPa)	Flex. Str. Diag. (MPa)	Flex. Mod. Diag. (GPa)	Thickness Per Ply (mm)	% Fiber by Weight	Fiber Weight (gms/m²)
C-1800	0/90 knit	199	13.1					297	17.9					359	15.0					0.84	44.8%	608
C-2400	0/90 knit	241	15.2					257	19.3					446	16.5					0.99	49.7%	811
CM-1603	0/90 deg w/mat	234	13.8					248	15.2					386	14.5					0.94	52.0%	
CM-1808	0/90 deg w/mat	201	13.8					188	11.7					310	13.1					1.22	43.0%	838
CM-1810	0/90 deg w/mat	201	13.8					218	17.9					321	12.8					1.32	42.0%	913
CM-1815	0/90 deg w/mat	187	13.8					226	18.6					293	13.1					1.40	44.0%	1065
CM-2403	0/90 deg w/mat	221	13.1					228	16.5					400	13.8					1.14	50.0%	
CM-2408	0/90 deg w/mat	208	13.1					209	12.4					355	13.8					1.40	46.0%	1041
CM-2410	0/90 deg w/mat	200	13.1					255	18.6					345	13.8					1.57	47.0%	1115
CM-2415	0/90 deg w/mat	255	15.5					251	18.6					317	13.5					1.78	44.3%	1268
CM-3205	0/90 deg w/mat	255	14.5					248	15.2					352	15.2					1.73	52.0%	
CM-3205/7	0/90 deg w/mat	255	14.5					248	15.2					352	15.2					1.73	52.0%	
CM-3208	0/90 deg w/mat	248	13.8					240	15.2					338	14.5					1.80	50.0%	
CM-3215	0/90 deg w/mat	248	13.4					255	18.6					338	14.8					2.06	49.0%	
CM-3610	0/90 deg w/mat	240	14.8											374	11.0					2.01	50.0%	
CM-3610UB	0/90 deg w/mat	234	13.1	248	13.8			248	17.9	262	14.5			331	13.8	345	15.2			2.24	50.0%	
CM-4810	0/90 deg w/mat	262	13.8					269	14.5	228	15.2			359	15.2	332	13.1			2.41	52.0%	
M-1000	binderless mat	131	6.7	131	6.7	131	6.7	152	9.7	152	9.7	152	9.7	193	9.7	193	9.7	193	9.7	0.79	26.0%	
M-1500	binderless mat	129	6.8	129	6.8	129	6.8	179	7.3	179	7.3	179	7.3	212	7.0	212	7.0	212	7.0	1.04	30.0%	
M-1500/7	binderless mat	129	6.8	129	6.8	129	6.8	179	7.3	179	7.3	179	7.3	212	7.0	212	7.0	212	7.0	1.04	30.0%	
M-2000	binderless mat	131	6.8	131	6.8	131	6.8	165	8.3	165	8.3	165	8.3	207	9.7	207	9.7	207	9.7	1.32	29.0%	
M-3000	binderless mat	117	6.6	117	6.6	117	6.6	159	7.6	159	7.6	159	7.6	200	9.0	200	9.0	200	9.0	1.91	28.0%	
THM-2210	horizontal triaxial w/mat	234	13.1			221	14.5					250	17.9					337	15.2	1.35	49.0%	
TV-2500	vertical triaxial	234	15.2			214	14.5	263	17.2			250	16.5	427	16.5			393	15.2	0.89	54.0%	
TV-3400	vertical triaxial	241	15.2			229	15.2	256	19.3			249	19.3	446	16.5			373	15.5	1.30	50.0%	1149
TVM-3408	vertical triaxial w/mat	229	15.5			214	14.5	263	17.9			250	17.9	386	16.5			352	15.2	1.73	52.0%	1379
U-0901	warp unidirectional	221	14.5					234	15.9					393	14.5					0.48	54.0%	
U-1601	warp unidirectional	248	13.8					263	13.1					324	14.5					0.79	52.0%	
U-1801	warp unidirectional	262	13.8					269	13.8					310	14.5					0.89	50.0%	
UM-1608	warp unidirectional w/mat	214	12.8					229	13.1					310	13.1					1.14	47.0%	
W-16	weft unidirectional			262	14.5					277	15.2					352	15.2			0.69	54.0%	
X-1500	+/-45 deg					228	12.8					255	15.9					400	14.5	0.66	55.0%	
X-1800	+/-45 deg					221	13.1					248	17.9					419	14.5	0.79	55.0%	
X-2400	+/-45 deg	49				245	11.7	109	3.9			180	19.3					414	16.5	0.91	44.8%	811
X-2800	+/-45 deg	55				265	12.4	124	4.1			193	19.3					434	16.5	1.04	50.0%	
XM-1305	+/-45 deg w/mat					244	13.8					262	16.5					392	15.2	0.66	54.0%	
XM-1308	+/-45 deg w/mat					219	13.8					229	15.2					352	14.5	0.74	52.0%	
XM-1708	+/-45 deg w/mat	94	10.3			229	15.2	161	14.5			249	21.8	195	10.3			373	15.5	1.22	51.4%	
XM-1808	+/-45 deg w/mat	94	10.3			229	15.2	161	14.5			249	21.8	195	10.3			373	15.5	1.22	51.4%	838
XM-1808b	+/-45 deg w/mat	94	10.3			229	15.2	161	14.5			249	21.8	195	10.3			373	15.5	1.22	51.4%	
XM-2408	+/-45 deg w/mat	98	10.7			236	15.2	229	15.2			262	22.4	222	10.3			401	16.5	1.42	55.0%	1041
XM-2415	+/-45 deg w/mat	79	10.3			191	14.5	274	21.4			294	25.5	201	10.3			361	15.9	1.80	53.5%	1268

Owens Corning Knytex Reinforcements

Reinforcement Description		Tensile Strength Longitudinal (MPa)	Tensile Modulus Longitudinal (GPa)	Tensile Strength Transverse (MPa)	Tensile Modulus Transverse (GPa)	Tensile Strength Diagonal (MPa)	Tensile Modulus Diagonal (GPa)	Compressive Strength Longitudinal (MPa)	Compressive Modulus Longitudinal (GPa)	Compressive Strength Transverse (MPa)	Compressive Modulus Transverse (GPa)	Compressive Strength Diagonal (MPa)	Compressive Modulus Diagonal (GPa)	Flexural Strength Longitudinal (MPa)	Flexural Modulus Longitudinal (GPa)	Flexural Strength Transverse (MPa)	Flexural Modulus Transverse (GPa)	Flexural Strength Diagonal (MPa)	Flexural Modulus Diagonal (GPa)	Thickness Per Ply (mm)	% Fiber by Weight (%)	Fiber Weight (gms/m²)
1.5 oz chopped mat	random mat	86	7.6					157	7.2					164	6.7					1.17	30.0%	
A 060	woven warp unidirectional	487	17.9					275	15.2					625	13.8					0.25	50.0%	206
A 130 Uni	woven warp unidirectional	430	22.5					309	24.5					570	17.0					0.61	50.0%	443
A 260 Uni	woven warp unidirectional	508	24.2					304	19.3					754	24.9					0.61	50.0%	869
A 260-45 H.M.	woven warp unidirectional, high modulus	790	36.7																	0.76	64.4%	865
A 260 HBF	woven warp unidirectional	735	34.9					497	34.4					934	31.8					0.79		865
A 260 HBF 1587	woven warp unidirectional	676	32.2																	0.76	66.5%	865
A 260 HBF XP9587	woven warp unidirectional	688	34.2																	0.71	66.1%	865
A 260 Eng Yarn	woven warp unidirectional	783	34.2																	0.81		865
A 260 Eng Yarn	woven warp unidirectional	697	35.9																	0.76	63.2%	865
Biply 2415 G	woven roving plus mat	284	14.3	247	13.9			231	15.7	243	15.7			386	15.2	382	15.9			1.55	50.4%	1274
CM1701 Uni/Mat	warp unidirectional & mat	515	29.0					377	23.4					707	20.4					0.76	50.0%	585
CM2415 Uni/Mat	warp unidirectional & mat	423	20.5					307	15.7					508	16.2					1.65	50.0%	
CM3205	warp unidirectional & mat	325	15.3					344	17.1					471	11.7					1.47	59.0%	
CM3610	warp unidirectional & mat	363	21.1					347	18.9					630	21.0					1.40	40.5%	
KA060	Kevlar® warp unidirectional	663	18.9					208	20.3					577	13.1					0.33	50.0%	213
D155	stichbonded weft unidirectional			416	25.7					333	27.6					520	23.3			0.69	50.0%	524
D240	stichbonded weft unidirectional			523	22.9					261	18.3					612	21.0			1.07	50.0%	825
D105	stichbonded weft unidirectional			490	24.5					232	22.5					647	17.3			0.46	50.0%	
CD185 0/90	biaxial 0/90	269	13.7	317	17.0			110	16.3	110	14.2			476	13.6	338	11.5			0.81	55.0%	656
CD230 0/90	biaxial 0/90	248	18.0					228	15.3					483	13.3					1.04	55.0%	794
CD230 0/90	biaxial 0/90	285	16.5	223	15.6			268	15.5	245	15.0			447	16.5	401	15.9			1.04	50.0%	794
DB 090 +/-45	double bias +/-45					279	13.9					271	13.4					429	14.1	0.43	50.0%	314
DB 090 +/-45	double bias +/-45					328	15.5					336	13.7					525	13.1	0.43	50.0%	314
DB 120 +/-45	double bias +/-45					307	14.7					246	13.2					405	14.1	0.53	50.0%	392
DB130	double bias +/-45	85	8.3	147	11.0	215	14.3							248	8.0	358	11.0	429	14.7	0.46	46.1%	
DB 170 +/-45	double bias +/-45					274	15.0					252	14.2					482	13.8	0.79	57.1%	595
DB 240 +/-45	double bias +/-45					310	16.7					256	16.1					500	14.8	1.12	50.0%	835
DB 240 +/-45	double bias +/-45																			0.89	53.6%	835
DB 240 +/-45	double bias +/-45																			0.74	65.4%	835
DB400	double bias +/-45, jumbo					285	18.8					308	19.6					474	14.6	1.14	62.5%	1345
DB603	double bias +/-45, jumbo					324	19.8					356	21.1					459	16.8	1.70	62.5%	1987
DB800	double bias +/-45, jumbo					283	20.6					294	23.3					491	18.0	2.11	69.2%	
DB803	double bias +/-45, jumbo					313	20.9					352	24.6					432	18.1	2.21	66.4%	
DBM 1208 +/-45/M	double bias +/-45 plus mat	126	9.3	135	10.1	280	13.4					215	11.7	243	8.4	309	9.7	415	12.1	0.97	45.0%	652
DBM 1708 +/-45/M	double bias +/-45 plus mat					249	15.2					338	14.1					476	13.6	0.99	51.5%	855

Owens Corning Knytex Reinforcements

Reinforcement Description		Tensile Strength: Longitudinal	Tensile Modulus: Longitudinal	Tensile Strength: Transverse	Tensile Modulus: Transverse	Tensile Strength: Diagonal	Tensile Modulus: Diagonal	Compressive Strength: Longitudinal	Compressive Modulus: Longitudinal	Compressive Strength: Transverse	Compressive Modulus: Transverse	Compressive Strength: Diagonal	Compressive Modulus: Diagonal	Flexural Strength: Longitudinal	Flexural Modulus: Longitudinal	Flexural Strength: Transverse	Flexural Modulus: Transverse	Flexural Strength: Diagonal	Flexural Modulus: Diagonal	Thickness Per Ply	% Fiber by Weight	Fiber Weight
		MPa	GPa	MPa	GPa	MPa	GPa	MPa	GPa	MPa	GPa	MPa	GPa	MPa	GPa	MPa	GPa	MPa	GPa	mm	%	gms/m²
DBM1708+/-45/M	double bias +/-45 plus mat					252	13.4					268	14.5					437	12.8	1.27	45.0%	855
DBM2408A	double bias +/-45 plus mat					228	14.9											450	12.5	1.27	53.2%	
XDBM1703	exp. double bias +/-45 & mat					132	9.4					236	12.3					323	8.3	1.42	39.7%	
XDBM1705	exp. double bias +/-45 & mat					94	7.6					138	10.7					238	7.2	1.30	35.4%	
XDBM1708F	exp. double bias +/-45 & mat					216	13.1					292	16.8					422	12.4	1.02	50.1%	
CDB 2000/+/-45	warp triaxial	312	15.4			168	13.7	254	14.9			232	13.0	505	17.0			300	13.7	0.99	50.0%	757
CDB 3400/+/-45	warp triaxial	333	16.7			176	12.8	278	15.3			172	13.6	493	16.2			239	13.0	1.40	50.0%	1061
CDB 340B 0/+/-45	warp triaxial, promat stich	252	16.9			155	12.8	229	15.7			201	12.1	491	14.5			245	11.9	1.50	50.0%	1132
CDM 1808 0/90/M	promat (0/90 plus mat)	256	14.5	208	12.6			208	12.6	195	10.0			421	15.9	339	13.3			1.37	45.0%	913
CDM 1808 B	promat (0/90 plus mat)	296	17.2					412	17.8					520	17.8					1.19	55.2%	987
CDM 1815 0/90/M	promat (0/90 plus mat)	236	14.2	190	11.8			196	12.0	188	11.4			385	11.7	367	10.0			1.75	45.0%	1112
CDM 1815B	promat (0/90 plus mat)	280	17.4					377	16.1					477	16.5					1.27	55.8%	1186
CDM 2408 0/90/M	promat (0/90 plus mat)	245	14.6	215	13.2			246	14.0	239	12.9			496	16.8	422	13.9			1.75	45.0%	1119
CDM 2408A	promat (0/90 plus mat)	338	18.9					440	14.3					616	19.1					1.22	56.5%	1153
CDM 24100/90/M	promat (0/90 plus mat)	256	15.2	243	13.2			208	12.9	196	11.4			425	14.6	345	13.0			1.78	45.0%	1166
CDM 24150/90/M	promat (0/90 plus mat)	243	14.2	214	13.6			216	13.6	188	12.4			404	13.4	403	12.8			2.11	45.0%	1318
CDM 2415	promat (0/90 plus mat)	329	17.2	340	16.6			342	18.5	334	18.0			497	14.2	535	15.9			1.42	54.9%	1338
CDM 2415A	promat (0/90 plus mat)	231	15.2					486	17.2					505	16.3	381	12.0			1.50	54.6%	1352
CDM 3208	promat (0/90 plus mat)	308	17.0					455	19.4					583	17.7					1.40	60.2%	
CDM 3610	promat (0/90 plus mat)	364	19.9					360	21.7					643	16.4					1.42	38.2%	
CDM 3610ST	promat (0/90 plus mat)	355	18.9					326	22.3					625	15.9					1.40	39.6%	
CDM 4408	promat (0/90 plus mat)	317	16.9	294	18.9			345	16.9	400	18.9			440	16.1	579	21.0				54.6%	
XCDM 2315	exp promat (0/90 plus mat)	252	14.5	248	14.5									491	13.9	405	12.2			1.52	54.9%	
DDB222	weft triaxial	265	17.6			154	9.7	229	14.1			197	13.0	396	14.5			290	12.2	0.99	50.0%	747
DDB340	weft triaxial	331	16.9			162	9.2	234	15.4			191	13.3	452	15.4			339	12.6	1.50	50.0%	1142
XDDBM2208	exp weft triaxial w/ mat			264	15.1	135	11.0													1.30	48.9%	
XDDM2710	exp stichbonded weft triaxial w/ mat			301	16.0	152	10.9													1.40	53.6%	
XDDB222	exp stichbonded weft triaxial	86	8.0	377	18.6									175	8.8	541	17.8			0.76		
XDDB340	exp stichbonded weft triaxial	83	7.8	490	22.0									176	9.0	657	22.0			0.99		
GDB 095 +/-45 carbon	double bias +/-45 carbon					462	34.3					359	31.3					621	19.1		50.0%	331
GDB 095 +/-45 carbon	double bias +/-45 carbon					622	31.6					403	20.5					596	14.8	0.51	50.0%	331
GDB 120 +/-45 carbon	double bias +/-45 carbon					462	42.7					193	40.3					710	23.4		50.0%	416
GDB 120 +/-45 carbon	double bias +/-45 carbon					528	36.4					307	16.5					554	15.4	0.64	50.0%	416

Reinforcement	Description	Tensile Strength: Longitudinal (MPa)	Tensile Modulus: Longitudinal (GPa)	Tensile Strength: Transverse (MPa)	Tensile Modulus: Transverse (GPa)	Tensile Strength: Diagonal (MPa)	Tensile Modulus: Diagonal (GPa)	Compressive Strength: Longitudinal (MPa)	Compressive Modulus: Longitudinal (GPa)	Compressive Strength: Transverse (MPa)	Compressive Modulus: Transverse (GPa)	Compressive Strength: Diagonal (MPa)	Compressive Modulus: Diagonal (GPa)	Flexural Strength: Longitudinal (MPa)	Flexural Modulus: Longitudinal (GPa)	Flexural Strength: Transverse (MPa)	Flexural Modulus: Transverse (GPa)	Flexural Strength: Diagonal (MPa)	Flexural Modulus: Diagonal (GPa)	Thickness Per Ply (mm)	% Fiber by Weight (%)	Fiber Weight (gms/m²)
Owens Corning Knytex Reinforcements																						
GDB 200 +/-45 carbon	double bias +/-45 carbon					400	47.8					124	38.4					538	21.0		50.0%	669
GDB 200 +/-45 carbon	double bias +/-45 carbon					503	39.0					284	24.5					659	18.3	1.02	50.0%	669
KDB 170 +/-45 Kevlar	double bias +/-45 Kevlar®					352	22.3					83						234	11.9	0.79	50.0%	537
17MPX						259	15.2					224	11.8					412		1.42	50.0%	
XH120		408	24.8					207	17.4					311	11.4					1.42	50.0%	
XH120						121	9.9					120	12.3					152	8.3	1.17	50.0%	
CDDB310	quadraxial	235	12.5	218	13.3			254	12.9	215	12.8			395	10.3	346	9.5				55.0%	
CDB 3400/+/-45	warp triaxial	331	18.0					234	15.6					462	14.2						55.0%	1061
CDM 2410 0/90/M	promat	255	15.9					186	12.9					372	9.7						45.0%	1166
GA 045 Uni carbon	woven warp unidirectional, carbon	669	64.4					524	81.0					1344	61.9						55.0%	155
GA 080 Uni carbon	woven warp unidirectional, carbon	1685	126.2											936	75.2						48.0%	
GA 090 Uni carbon	woven warp unidirectional, carbon	1606	130.3											1197	100.0					0.38	58.0%	318
GA 130 Uni carbon	woven warp unidirectional, carbon	1618	125.5											1040	84.1					0.46	64.0%	
KBM 1308A	woven Kevlar®/glass hybrid plus mat	333	17.1											323	15.1					0.76		
Kevlar/Glass Hybrid		293	15.7	258	14.8									402	14.7					0.69		
KDB 110 +/-45 Kevlar	double bias, Kevlar®					386	25.1					103	9.1					338	7.7		45.0%	352
KDB 110 +/-45 Kevlar	double bias, Kevlar®					508	20.7					137	9.0					453	13.5	0.58	50.0%	352
KB 203 WR E-glass/Kevlar	woven Kevlar®/glass hybrid	455	37.8					145	23.9					352	16.7						45.0%	703
SDB 120 S-glass	double bias, S-glass	434	20.9					310	20.0					487	13.0						55.0%	385
SDB 120 S-glass	double bias, S-glass	414	16.2					319	14.5					540	15.4					0.53	50.0%	581
B238	starch oil woven roving	218	13.2	194	12.4			197	12.4	184	12.1			336	12.8	305	12.3			1.45	40.0%	
B238+.75 oz mat	starch oil woven roving w/ mat	190	12.3	173	11.6			185	12.3	169	11.9			290	12.4	274	11.8			2.18	35.0%	
Spectra 900	Spectra	439	19.7	373	18.3			130	14.1	114	13.0			334	12.4	305	11.9			0.43	50.0%	
K49/13 Kevlar	Kevlar®49	357	19.9	337	19.2			136	16.2	121	14.5			291	10.3	270	9.9			0.69	45.0%	

Reinforcement Description		Tensile Strength: Longitudinal (MPa)	Tensile Modulus: Longitudinal (GPa)	Tensile Strength: Transverse (MPa)	Tensile Modulus: Transverse (GPa)	Tensile Strength: Diagonal (MPa)	Tensile Modulus: Diagonal (GPa)	Compressive Strength: Longitudinal (MPa)	Compressive Modulus: Longitudinal (GPa)	Compressive Strength: Transverse (MPa)	Compressive Modulus: Transverse (GPa)	Compressive Strength: Diagonal (MPa)	Compressive Modulus: Diagonal (GPa)	Flexural Strength: Longitudinal (MPa)	Flexural Modulus: Longitudinal (GPa)	Flexural Strength: Transverse (MPa)	Flexural Modulus: Transverse (GPa)	Flexural Strength: Diagonal (MPa)	Flexural Modulus: Diagonal (GPa)	Thickness Per Ply (mm)	% Fiber by Weight (%)	Fiber Weight (gms/m²)
DuPont Kevlar Reinforcements																						
Kevlar 49 243	unidirectional	552	37.4											239	26.5							226
Kevlar 49 243	unidirectional	626	45.5											347	33.4							226
Kevlar 49 281	woven cloth	412	22.3											221	17.5							169
Kevlar 49 281	woven cloth	418	25.8											252	21.8							169
Kevlar 49 285	woven cloth	338	19.0											217	16.3							169
Kevlar 49 285	woven cloth	407	22.2											283	19.4							169
Kevlar 49 328	woven cloth	439	21.4											162	17.9							213
Kevlar 49 500	woven cloth	356	20.5											261	14.2							169
Kevlar 49 500	woven cloth	381	25.7											349	19.5							169
Kevlar 49 1050	woven roving	308	21.6											185	13.9							355
Kevlar 49 1050	woven roving	412	20.5											244	18.2							355
Kevlar 49 1033	woven roving	350	24.5											155	15.3							507
Kevlar 49 1033	woven roving	361	23.6											237	18.4							507
Kevlar 49 1350	woven roving	448	53.1											202	21.7							456
Kevlar 49 118	woven roving	612												421	42.1							270
Kevlar 49/E-glass KBM 1308	woven/mat	240	12.3	232	12.6			170	16.1	175	13.4			259	9.9	256	10.1					630
Kevlar 49/E-glass KBM 2808	woven/mat	269	14.6	233	13.8			153	15.1	153	16.5			300	12.1	253	12.1					1120
Kevlar 49/E-glass C77K/235		269	14.6	233	13.8									300	11.7	253	12.1				45.0%	1122
Anchor Reinforcements																						
Ancaref C160 carbon, 12K	unidirectional	876	82.7					621	62.1											0.10	50.0%	159
Ancaref C160 carbon, 12K	unidirectional	1724	144.8					1103	137.9											0.08	70.0%	159
Ancaref C320 carbon, 12K	unidirectional	862	82.7					621	62.1											0.53		321
Ancaref C440 carbon, 12K	unidirectional	614	36.5					214	26.2											0.36		206
Ancaref S275 S-2 glass, O-C	unidirectional	889	37.9					427												0.23	60.0%	274
Ancaref S275 S-2 glass, O-C	unidirectional	2055	51.7					820	53.8											0.18	75.0%	274
Ancaref S160 S-2 glass, O-C	unidirectional	883	37.9					427	53.1											0.18		162
Ancaref G230 E-glass	unidirectional	524	29.6					545	21.4											0.36		321
Unidirectionals																						
High-strength, uni tape carbon	unidirectional	1241	144.8	55	11.7	160	16.1	1241	144.8	207	11.7	165	16.1									
High-strength, uni tape carbon	unidirectional	1241	128.9	28	6.0	91	8.3	483	128.9	83	6.0	94	8.3									
High-modulus, uni tape carbon	unidirectional	758	172.4	28	11.7	117	16.4	689	172.4	138	11.7	124	16.4									
High-modulus, uni tape carbon	unidirectional	662	166.2	21	5.9	50	12.8	414	166.2	55	5.9	50	12.8									
Intermediate-strength, unitape carbon	unidirectional	1103	117.2	52	11.7			1103	117.2	172	11.7											
Intermediate-strength, unitape carbon	unidirectional	993	110.3	28	6.9			448	110.3	103	6.9											
Unidirectional tape Kevlar	unidirectional	1172	69.6	28	5.5			276	69.6	138	5.5											

SCRIMP Process Laminates

Reinforcement Description	Tensile Strength: Long. (MPa)	Tensile Modulus: Long. (GPa)	Tensile Strength: Transv. (MPa)	Tensile Modulus: Transv. (GPa)	Compressive Strength: Long. (MPa)	Flexural Strength: Long. (MPa)	Flexural Strength: Transv. (MPa)	Thickness Per Ply (mm)	% Fiber by Weight (%)	Fiber Weight (gm/m²)
Cert'teed/Seemann 625 WR					301	487		0.61	73.0%	811
Cert'teed/Seemann 625 WR	394				359	548		0.61	73.0%	811
Hexcell 8HS, Style 7781	392	23.4			401	576		0.25	66.0%	287
FGl/Seemann 3X1, 10 Twill	370	23.4			425	529		0.25	70.0%	324
8HS, 3K XaSg, 1029 carbon	676	57.2			255	481		0.41		368
8HS, 3K, 1029(UC309) carbon					290	470		0.41		368
5HS, 12K, 1059(AS4W) carbon		54.5			203	415		0.56		524
Hexcell CD180 stiched biaxial	345	22.1			286	412		0.66	64.0%	656
Chomarat 2 x 2 weave	277	20.0			379	478		0.79	61.0%	811
DF14OO	325	26.9	241	23.4	271	423	319	1.07	66.0%	1352
G:Cl029 hybrid E-glass/carbon	490	44.1			274	665		1.02		
G:Cl059 hybrid E-glass/carbon	443	42.1			200	685		1.02		
G:K285(60%) hybrid E-glass/Kevlar					164	520		1.22		
G:K900(40%) hybrid E-glass/Kevlar					253	510		0.84		
G:K900(50%) hybrid E-glass/Kevlar	396	25.5			219	432		0.97		
G:S985(40%) hybrid E-glass/Spectra	355	21.4			242	541		0.84		
DuPont 5HS, K49, Kevlar (900)	479	29.6			109	245		0.43		
Allied-Signal 8HS, S1000, Spectra (985)		14.5			59	128		0.25		186
Cert'teed/Seemann 625 WR	356	24.1			330	496		0.61	73.0%	811
Cert'teed/Seemann twill, 3X1	354	21.4			365	545		0.66	71.0%	811
Cert'teed/Seemann 625 WR	308	24.8			212	336		0.61	73.0%	811
Cert'teed/Seemann 625 WR	355	26.9			226	379		0.61	73.0%	811
Cert'teed/Seemann 625 WR	336	26.9			222	401		0.61	73.0%	811
5HS, 6K, 1030 carbon	634	58.6			394	684		0.38		345
5HS, 12K, 1059 carbon (AS4W)	615	57.2			445	690		0.56		524

Low-Temperature Cure Prepregs

Reinforcement Description	Tensile Strength: Long. (MPa)	Tensile Modulus: Long. (GPa)	Compressive Strength: Long. (MPa)	Flexural Strength: Long. (MPa)	Thickness Per Ply (mm)	% Fiber by Weight (%)	Fiber Weight (gm/m²)
Advanced Comp Grp/LTM21	524	29.0	413	516		77.9%	811
Advanced Comp Grp/LTM22	438	23.4	336	478	0.23	65.9%	301
Advanced Comp Grp/LTM22	467	24.1	353	507	0.23	66.9%	301
SP Systems/Ampreg 75	426	21.4	419	563	0.23	65.5%	301
SP Systems/Ampreg 75	456	22.8	440	621	0.23	62.8%	301
DSM Italia/Neoxil	345	19.3	473	601	0.23	57.0%	301
Newport Adhesives/NB-1101	349	20.0	393	472	0.23	60.3%	301
Newport Adhesives/NB-1101	333	20.7	430	480	0.23	60.3%	301
Newport Adhesives/NB-1107	402	22.8	408	518	0.23	63.3%	301
Newport Adhesives/NB-1107	332	15.9	333	399	0.23	63.3%	301
Ciba Composite/M10E	370	22.8	359	532	0.23	62.8%	301
Ciba Composite/M10E	645	63.4	305	592	0.23		301
YLA, Inc./RS-1	357	21.4	358	488	0.23	64.7%	301

228

Reinforcement Description	Tensile Strength: Longitudinal MPa	Tensile Modulus: Longitudinal GPa	Tensile Strength: Transverse MPa	Tensile Modulus: Transverse GPa	Tensile Strength: Diagonal MPa	Tensile Modulus: Diagonal GPa	Compressive Strength: Longitudinal MPa	Compressive Modulus: Longitudinal GPa	Compressive Strength: Transverse MPa	Compressive Modulus: Transverse GPa	Compressive Strength: Diagonal MPa	Compressive Modulus: Diagonal GPa	Flexural Strength: Longitudinal MPa	Flexural Modulus: Longitudinal GPa	Flexural Strength: Transverse MPa	Flexural Modulus: Transverse GPa	Flexural Strength: Diagonal MPa	Flexural Modulus: Diagonal GPa	Thickness Per Ply mm	% Fiber by Weight %	Fiber Weight gm/m²
YLA, Inc./RS-1	354	20.7					370						473						0.23	64.8%	301
YLA, Inc./RS-1	381	20.7					385						492						0.23	63.6%	301
3M/SP377	289	21.4					390						412						0.23	63.1%	301
3M/SP377	296	22.8					410						410						0.23	64.4%	301
3M/SP365	243						259						337						0.41	68.5%	544
3M/SP365	326						408						492						0.41	69.5%	544
Fibercote Industries/E-761E	381	23.4					435						523						0.41	62.4%	544
Fibercote Industries/E-761E	402	24.1					455						542						0.41	62.6%	544
Fibercote Industries/P-601	423	22.8					443						603						0.64	57.0%	608
Fibercote Industries/P-601	442	23.4					484						625						0.64	60.3%	608
Fibercote Industries/P-600	376	20.0					296						460						0.23	62.6%	301
Fibercote Industries/P-600	405	21.4					349						543						0.23	64.7%	301
ICI Fiberite/MXB-9420	421	20.0					347						464						0.23	60.9%	301
Fiber Content Study for GLCC																					
Owens-Corning WR	307	20.6					315	22.8					405	15.8					0.64	52.4%	608
ATI NEWF 180 Biaxial	358	22.7					356	24.4					519	18.3					0.76	47.8%	608
Owens-Corning WR	397	25.4					320	24.6					565	19.8					0.64	61.0%	608
ATI NEWF 180 Biaxial	389	22.4					422	24.4					565	19.5					0.76	53.1%	608
Owens-Corning WR	403	25.7					322	25.1					646	22.7					0.64	66.9%	608
ATI NEWF 180 Biaxial	421	23.5					386	24.5					576	18.8					0.76	61.8%	608

229

Appendix B Relevant ASTM Test Methods

D-30 Standards as of December 1996

C 613 - 67(1990)		Test Method for Resin Content of Carbon and Graphite Prepregs by Solvent Extraction
D 2344 -84(1989)		Test Method for Apparent Interlaminar Shear Strength of Parallel Fiber Composites by Short-Beam Method
D 2585 - 68(1990)		Test Method for Preparation and Tension Testing of Filament-Wound Pressure Vessels
D 2586 - 68(1990)		Test Method for Hydrostatic Compressive Strength of Glass-Reinforced Plastic Cylinders
D 3039 - 76(1995), 3039M	Test Method for Tensile Properties of Polymer Matrix Composites
D 3171 - 76(1990)		Test Method for Fiber Content of Resin-Matrix Composites by Matrix Digestion
D 3379 - 75(1989)		Test Method for Tensile Strength and Young's Modulus for High-Modulus Single-Filament Materials
D 3410 - 75(1995), 3410M	Test Method for Compressive Properties of Polymer Matrix Composite Materials With Unsupported Gage Section By Shear Loading
D 3479 - 76(1996), 3479M	Test Method for Tension-Tension Fatigue of Polymer Matrix Composite Materials
D 3518 - 76(1994), 3518M	Test Method for Inplane Shear Response of Polymer Matrix Composite Materials by Tensile Test of a +/-45 Laminate
D 3529 - 76(1990), 3529M	Test Method for Resin Solids Content of Epoxy Matrix Prepreg by Matrix Dissolution
D 3530 - 76(1990),3530M	Test Method for Volatiles Content of Epoxy-Matrix Prepreg
D 3531 - 76(1995)		Test Method for Resin Flow of Carbon Fiber-Epoxy Prepreg
D 3532 - 76(1995)		Test Method for Gel Time of Carbon Fiber-Epoxy Prepreg
D 3544 - 76(1989)		Guide for Reporting Test Methods and Results on High Modulus Fibers
D 3552 - 77(1989)		Test Method for Tensile Properties of Fiber Reinforced Metal Matrix Composites
D 3553 - 76(1989)		Test Method for Fiber Content by Digestion of Reinforced Metal Matrix Composites
D 3800 - 79(1990)		Test Method for Density of High-Modulus Fibers
D 3878 - 87(1995)		Terminology of High-Modulus Reinforcing Fibers and Their Composites
D 4018 - 81(1993)		Test Method for Properties of Continuous Filament Carbon and Graphite Fiber Tows
D 4102 - 82(1993)		Test Method for Thermal Oxidative Resistance of Carbon Fibers
D 4255 - 83(1994)		Test Method for In-Plane Shear Properties of Polymer Matrix Composite Materials by the Rail Shear Method
D 4762 - 88(1995)		Guide for Testing of Automotive/Industrial Composite Materials
D 5229 - 92, 5229M		Test Method for Moisture Absorption Properties and Equilibrium Conditioning of Polymer Matrix Composite Materials

D 5300 - 93	Test Method for Measurement of Resin Content and Other Related Properties of Polymer Matrix Thermoset Prepreg by Combined Mechanical and Ultrasonic Methods
D 5379 - 93, 5450M	Test Method for Shear Properties of Composite Materials by the V-Notched Beam Method
D 5448 - 93, 5448M	Test Method for Inplane Shear Properties of Hoop Wound Polymer Matrix Composite Cylinders
D 5449 - 93, 5449M	Test Method for Transverse Compressive Properties of Hoop Wound Polymer Matrix Composite Cylinders
D 5450 - 93, 5450M	Test Method for Transverse Tensile Properties of Hoop Wound Polymer Matrix Composite Cylinders
D 5467 - 93	Test Method for Compressive Properties of Unidirectional Polymer Matrix Composites Using a Sandwich Beam
D 5528 - 94	Test Method for Mode I Interlaminar Fracture Toughness of Unidirectional Fiber-Reinforced Polymer Matrix Composites
D 5687 - 95, 5687M	Guide for Preparation of Flat Composite Panels With Processing Guidelines for Specimen Preparation
D 5766 - 95, 5766M	Test Method for Open Hole Tensile Strength of Polymer Matrix Composite Laminates
D 5961 - 96, 5961M	Test Method for Bearing Response of Polymer Matrix Composite Laminates
E 1309 - 92	Guide for the Identification of Composite Materials in Computerized Material Property Databases
E 1434 - 91 (1995)	Guide for the Development of Standard Data Records for Computerization of Mechanical Test Data for High Modulus Fiber Reinforced Composite Materials
E 1471 - 92	Guide for the Identification of Fibers, Fillers, and Core Materials in Computerized Material Property Databases

Referenced and Related ASTM Standards

B 193-87 (1994)	Test Method for Resistivity of Electrical Conductor Materials
C 271-61 (1994)	Test Method for Density of Sandwich Core Materials
C 272-53 (1996)	Test Method for Water Absorption of Core Materials for Structural Sandwich Constructions
C 273-61 (1994)	Test Method for Shear Properties Sandwich Core Materials
C 274-68 (1994)	Definitions of Terms Relating to Structural Sandwich Constructions
C 297-61 (1994)	Test Method for Flatwise Tensile Strength of Sandwich Constructions
C 363-57 (1994)	Test Method for Delamination Strength of Honeycomb Core Materials
C 364-61 (1994)	Test Method for Edgewise Compressive Strength of Sandwich Constructions
C 365-57 (1994)	Test Methods for Flatwise Compressive Properties of Sandwich Cores
C 366-57 (1994)	Test Methods for Measurement of Thickness of Sandwich Cores
C 393-62 (1994)	Test Method for Flexural Properties of Flat Sandwich Constructions
C 394-62 (1994)	Test Method for Shear Fatigue of Sandwich Core Materials

C	480-62 (1994)	Test Method for Flexure-Creep of Sandwich Constructions
C	481-62 (1994)	Test Method for Laboratory Aging of Sandwich Constructions
C	581-87	Practice for Determining Chemical Resistance for Thermosetting Resins Used in Glass-Fiber-Reinforced Structures Intended for Liquid Service
D	123-93a	Terminology Relating to Textile Materials
D	256-88	Test Methods for Impact Resistance of Plastics and Electrical Insulating Materials
D	543-87	Test Method for Resistance of Plastics to Chemical Reagents
D	618-61 (1981)	Methods of Conditioning Plastics and Electrical insulating Materials for Testing
D	638-89 (1991)	Test Method for Tensile Properties of Plastics
D	638M-89 (1991)	Test Method for Tensile Properties of Plastics, Metric.
D	648-82 (1988)	Test Method for Deflection Temperature of Plastics Under Flexural Load
D	671-87	Test Method for Flexural Fatigue of Plastics by Constant-Amplitude-of-Force
D	695-89 (1991)	Test Method for Compressive Properties of Rigid Plastics
D	695M-89 (1991)	Test Method for Compressive Properties of Rigid Plastics, Metric.
D	696-79 (1991)	Test Method for Coefficient of Linear Thermal Expansion of Plastics
D 756-78 (1983)		Practice for Determination of Weight and Shape Changes of Plastics Under Accelerated Service Conditions
D 790-70 (1992)		Test Methods for Flexural Properties of Unreinforced and Reinforced Plastics and Electrical Insulating Materials
D	79OM-81 (1993)	Test Methods for Flexural Properties of Unreinforced and Reinforced Plastics and Electrical Insulating Materials, Metric.
D	792-44 (1991)	Test Methods for Specific Gravity (Relative Density) and Density of Plastics by Displacement
D	891-89	Test Methods for Specific Gravity, Apparent, of Liquid Industrial Chemicals
D	1423-88	Test Method for Twist in Yams by the Direct-Counting Method
D	1505-85	Test Method for Density of Plastics by the Density-Gradient Technique
D	1781-86	Test Method for Climbing Drum Peel Test for Adhesives
D	1822-89	Test Method for Tensile-Impact Energy to Break Plastics and Electrical Insulating Materials
D	1822M-89	Test Method for Tensile-Impact Energy to Break Plastics and Electrical Insulating Materials, Metric.
D	2289-84	Test Method for Tensile Properties of Plastics at High Speeds
D	2343-67 (1985)	Test Method for Tensile Properties of Glass Fiber Strands, Yarns, and Rovings Used in Reinforced Plastics
D	2584-68 (1994)	Test Method for Ignition Loss of Cured Reinforced Resins
D	2734-70 (1994)	Test Methods for Void Content of Reinforced Plastics
D	2990-77 (1982)	Test Methods for Tensile, Compressive, and Flexural Creep and Creep-Rupture of Plastics

D 3029-84   Test Methods for Impact Resistance of Rigid Plastic Sheeting or Parts by Means of a Tup (Falling Weight)

D 3163-73 (1984)   Test Method for Determining the Strength of Adhesively Bonded Rigid Plastic Lap-Shear Joints in Shear by Tension Loading

D 3418-82 (1988)   Test Method for Transition Temperatures of Polymers by Thermal Analysis

D 3647-84 (1988)   Practice for Classifying Reinforced Plastic Pultruded Shapes According to Composition

D 3846-79 (1985)   Test Method for In-plane Shear Strength of Reinforced Plastics

D 4065-82 (1995)   Practice for Determining and Reporting Dynamic Mechanical Properties of Plastics

E 4-94   Practices for Load Verification of Testing Machines

E 6-89   Terminology Relating to Methods of Mechanical Testing

E 12-70 (1990)   Definitions of Terms Relating to Density and Specific Gravity of Solids, Liquids, and Gases

E 18-93   Test Methods for Rockwell Hardness and Rockwell Superficial Hardness of Metallic Materials

E 83-94   Practice for Verification and Classification of Extensometers

E 467-76 (1982)   Practice for Verification of Constant Amplitude Dynamic Loads in an Axial Load Fatigue Testing Machine

F 1645-96   Test Method for Water Migration in Honeycomb Core Material